ISSN 0003-2670

ANALYTICA CHIMICA ACTA

International monthly devoted to all branches of analytical chemistry
Revue mensuelle internationale consacrée à tous les domaines de la chimie analytique
Internationale Monatsschrift für alle Gebiete der analytischen Chemie

ELSEVIER SCIENTIFIC PUBLISHING COMPANY

AMSTERDAM

Anal. Chim. Acta, Vol. 87, No. 1, 1–258, November 1976

Published monthly

ANALYTICA CHIMICA ACTA

Publication Schedule for 1976

Vol. 81, No. 1	January 1976	
Vol. 81, No. 2	February 1976	**(completing Vol. 81)**
Vol. 82, No. 1	March 1976	
Vol. 82, No. 2	April 1976	**(completing Vol. 82)**
Vol. 83	May 1976	**(complete in one issue)**
Vol. 84, No. 1	June 1976	
Vol. 84, No. 2	July 1976	**(completing Vol. 84)**
Vol. 85, No. 1	August 1976	
Vol. 85, No. 2	September 1976	**(completing Vol. 85)**
Vol. 86	October 1976	**(complete in one issue)**
Vol. 87, No. 1	November 1976	
Vol. 87, No. 2	December 1976	**(completing Vol. 87)**

Subscription price for 1976 (covering November '75/December '76, Vols. 80–87): Dfl. 840.00 plus Dfl. 96.00 postage. Claims for issues not received should be made within three months of publication of the issues; if not, they cannot be honoured free of charge. Subscribers in the U.S.A. and Canada receive their copies by airmail. Additional charges for airmail to other countries are available on request. For advertising rates apply to the publishers.

Subscriptions should be sent to:
Elsevier Scientific Publishing Company, P.O. Box 211, Amsterdam, The Netherlands.

GENERAL INFORMATION

Languages

Papers will be published in English, French or German.

Detailed information

Authors should consult Vol. 73, p. 435 for detailed instructions. Reprints of this information are obtainable from Dr. Macdonald or from: Elsevier Editorial Services Ltd., Mayfield House, 256 Banbury Road, Oxford (Great Britain)

Submission of papers

Papers should be sent to:

Prof. Philip W. West,
Coates Chemical Laboratories,
College of Chemistry and Physics,
Louisiana State University,
Baton Rouge 3,
La. 70803 (U.S.A.)

or to:

Dr. A.M.G. Macdonald,
Department of Chemistry,
The University,
P.O. Box 363
Birmingham B15 2TT (Great Britain)

Reprints

Fifty reprints will be supplied free of charge. Additional reprints (minimum 100) can be ordered at quoted prices. They must be ordered on order forms which are sent together with the proofs.

For your copy of the latest EASTMAN Organic Chemicals Catalog

or to order any of the 6,000 chemicals it contains,

contact one of these laboratory supply houses.

AUSTRALIA
H. B. Selby and Co., Pty., Ltd.
Adelaide
Brisbane
Hobart
Oakleigh
Perth
Sydney
Ramsay Surgical Limited
Victoria

BELGIUM
s.a. Belgolabo N.V.
Overijse

BRAZIL
Atlantida Representaçoes e Importaçoes, Ltda.
Rio de Janeiro
Tennant Quimica S.A.
São Paulo

CANADA
Fisher Scientific Co., Ltd.
Edmonton
Montreal
Ottawa
Don Mills
Vancouver
Dartmouth
Sargent-Welch Scientific of Canada, Ltd.
Weston

CHINA, REPUBLIC OF
San Ho Instrument Co.
Taipei, Taiwan
Teh Ying Co., Ltd.
Taipei, Taiwan

DENMARK
Struers K/S
Copenhagen K

ECUADOR
Rafael Valdez
Guayaquil

FINLAND
Havulinna Oy
Helsinki

FRANCE
Touzart & Matignon
Paris

WEST GERMANY
Serva International
Chemie-Handels GmbH & Co.
Heidelberg

GREECE
P. Bacacos S.A.
Athens

GUATEMALA
F. Krafka and Co., Ltd.
Guatemala City

INDIA
Kodak Limited
Bombay

ISRAEL
Landseas (Israel) Ltd.
Tel Aviv
Yaron Chemicals Ltd.
Tel Aviv

ITALY
Prodotti Gianni, s.r.l.
Milan

JAPAN
Nagase and Co., Ltd.
Tokyo

KOREA
The Sang Chung Commercial Co., Ltd.
Seoul

MEXICO
Alfonso Marhx, S.A.
Mexico 1, D.F.
Hoffman-Pinther and Bosworth, S.A.
Naucalpan de Juarez

MOZAMBIQUE
Baird & Tatlock (S.A.) Pty. Ltd.
Lourenco Marques

NETHERLANDS
N.V. Holland-Indie
Argenturen Mij, HIAM
Amstelveen

NEW ZEALAND
Kempthorne, Prosser & Co. Ltd.
Wellington
Dunedin
Geo. W. Wilton and Co. Ltd.
Wellington

NORWAY
Nerliens Kemisk Tekniske Aktieselskap
Oslo

PORTUGAL
Soquimica, Sociedad de Representaçoes de Quimica
Lisbon

PUERTO RICO
Fisher Scientific Co.
Santurce
Puerto Nuevo

RHODESIA
Baird & Tatlock International Ltd.
Salisbury
Bulawayo

SOUTH AFRICA, REPUBLIC OF
Baird and Tatlock S.A. Pty.
Johannesburg
Durban
Port Elizabeth
Paarden
Eiland
Chemlab (Pty) Ltd.
Transvaal

SOUTHWEST AFRICA
S.W.A. Scientific Services (Pty) Ltd.
Windhoek

SPAIN
Quimigranel S.A.
Barcelona

SWEDEN
KEBO AB
Stockholm 6

SWITZERLAND
Dr. Bender and Dr. Hobein AG
Zurich 6

THAILAND
White & Co., Ltd.
Bangkok

UNITED KINGDOM
Kodak Limited
Kirkby, Liverpool

VENEZUELA
Equipos Cientificos y Educativos, S.A.
Caracas
Reactivos, S.A.
Caracas

ZAMBIA, REPUBLIC OF
Baird and Tatlock (London) Ltd.
Ndola
Lusaka

EASTMAN Organic Chemicals are stocked locally in the continental U.S.A. by:

AMERICAN SCIENTIFIC & CHEMICAL, BECKMAN SCIENCE ESSENTIALS, CURTIN MATHESON SCIENTIFIC, FISHER SCIENTIFIC, GAC LABORATORIES, LABPRODUCTS, INC., NORTH-STRONG, PREISER SCIENTIFIC, SARGENT-WELCH SCIENTIFIC, SCICHEMCO, SCIENTIFIC & INDUSTRIAL SALES & SERVICE, VWR SCIENTIFIC, WARD'S NATURAL SCIENCE ESTABLISHMENT

The catalog may also be obtained from:
Eastman Kodak Company
Dept. 412L
Rochester, N.Y. 14650, U.S.A.

Chemistry and Biochemistry of Natural Waxes

edited by **P.E. KOLATTUKUDY,** Department of Agricultural Chemistry, Washington State University, Pullman, Washington.

1976 xx+460 pages US $49.75/Dfl. 129.00 ISBN 0-444-41470-3 LC 76-18140

In recent years, the development of modern analytical techniques has led to significant advances in the understanding of the components of natural waxes. Since these advances are relevant to those who deal with a variety of biological problems from agriculture to dermatology, it appeared that a research level book on this subject was needed. This book, the first of its kind, fulfills this need, and provides comprehensive information on the chemistry and biochemistry of natural waxes from bacteria, fungi, algae, higher plants, insects, birds, marine organisms, and mammals including man. It will be especially useful as a research level reference book for biologists, biochemists, and lipid chemists.

CONTENTS: Chapters 1. Introduction to Natural Waxes (P.E. Kolattukudy). 2. Mammalian Waxes (D.T. Downing). 3. Marine Waxes (J.R. Sargent, R.F. Lee and J.C. Nevenzel). 4. Bird Waxes (J. Jacob). 5. Biochemistry of Bird Waxes (J.S. Buckner and P.E. Kolattukudy). 6. Insect Waxes (L.L. Jackson and G.J. Blomquist). 7. Chemistry of Waxes of Higher Plants (A.P. Tulloch). 8. Biochemistry of Plant Waxes (P.E. Kolattukudy, R. Croteau and J.S. Buckner). 9. Algal and Fungal Waxes (J.D. Weete). 10. Bacterial Waxes (P.W. Albro). Subject Index.

ELSEVIER SCIENTIFIC PUBLISHING COMPANY

P.O. Box 211, Amsterdam, The Netherlands

Distributor in the U.S.A. and Canada:
ELSEVIER/NORTH-HOLLAND, INC.,
52 Vanderbilt Ave., New York, N.Y. 10017

The Dutch guilder price is definitive. US $ prices are subject to exchange rate fluctuations.

ANALYTICA CHIMICA ACTA
Vol. 87 (1976)

ANALYTICA CHIMICA ACTA

International monthly devoted to all branches of analytical chemistry
Revue mensuelle internationale consacrée à tous les domaines de la chimie analytique
Internationale Monatsschrift für alle Gebiete der analytischen Chemie

ELSEVIER SCIENTIFIC PUBLISHING COMPANY

AMSTERDAM

Anal. Chim. Acta, Vol. 87

PRINTED IN THE NETHERLANDS

Analytica Chimica Acta, 87 (1976) 1—6

COMPARISONS OF SOME SODIUM-SELECTIVE ELECTRODES IN CONCENTRATED SOLUTIONS FOR USE IN AUTOMATIC MONITORING SYSTEMS

K. BERGNER

Department of Analytical Chemistry, University of Umeå, 901 87 Umeå (Sweden)

(Received 1st April 1976)

SUMMARY

Four sodium-selective glass electrodes and a Permaplex ion-exchanger electrode were investigated in strong sodium solutions with and without ammonium carbonate buffer, for potential application in the analysis of pulping liquors. The pretreatment and temperature effects are described. Dilution with ammonium carbonate buffer is necessary to level out differences in ionic strength and composition in the samples. The automated method developed for sodium determination is accurate to about 1 % with a standard deviation of less than 1 % for samples 1—5 M in sodium ions.

In the pulping industry there is a need for measurements of sodium, sulfide and hydroxide ion concentrations in a number of process streams involving black, green and white liquor. In order to control the processes and reduce the waste, the frequency and accuracy of the measurements must be increased. Ion-selective electrodes should be useful for automatic monitoring systems provided that suitable measuring conditions can be found. This paper reports on a study of sodium ion-selective electrodes, and it will be followed by further studies of other electrodes and of a complete automatic system.

Very little information is available in the literature about the use of sodium-selective electrodes in concentrated solutions with high levels of sodium. Lenz and Mold [1] tested various electrode methods for the determination of sodium ions in mill liquors; they used direct potentiometry as well as analate and known addition methods. The electrometric methods compared well with flame spectrophotometry and the uranyl zinc acetate method. Their report gave no details of the electrode performance and the range in which the electrode showed acceptable performance was not defined. Swasey [2] diluted black liquor with 0.2 M ammonium sulphate to a sodium level of 10—100 p.p.m. The electrode performance was not investigated in detail and results were given only for one sample solution. Wilson et al. [3, 4] studied four sodium electrodes in solutions up to 0.1 M in sodium. They also measured the selectivity coefficients for ammonium, silver, potassium and hydrogen ions as well as the response times of the electrodes, but their measure for the response time is unsatisfactory in practical applications.

EXPERIMENTAL

Five electrodes were used, namely Orion 94-11A, Radiometer G502 Na, Beckman 39278, Philips G15, and permaplex electrodes. The permaplex electrode consisted of a cation-exchange membrane, Permaplex C20 (BDH Ltd.), assembled as described by Eriksson and Johansson [5]. One electrode of each was used except for the Orion electrode which was replaced after two months because of an internal short-circuit and then replaced twice again because of malfunction. The Beckman electrode was broken and replaced during the investigation. Between the measurements the electrodes were stored in a 0.1 M sodium chloride solution.

The Orion double-junction reference electrode model 92-02-00 was used throughout. The bridge solution was 10 % potassium nitrate. As the selectivity coefficient for sodium over potassium is 10^{-2}—10^{-4}, the effect of leakage should be negligible in the strong sodium solutions used.

RESULTS AND DISCUSSION

Direct sodium ion measurements

Figure 1 shows the response of four electrodes in some media with varying ionic strength. It can be seen that the anion influence is large at high concentrations. The solutions containing sodium hydroxide and sodium chloride had the same ionic strength but in spite of this there are differences of up to 25 mV for 5 M solutions. In a carbonate solution of corresponding molarity the ionic strength is higher and the deviation from the others is larger. The significance of these results is that direct potentiometry in pulping liquors is impossible. Typical compositions for white liquor are 2.1—2.6 M NaOH, 0.4—0.7 M Na_2S, 0.2—0.5 M Na_2CO_3 and small amounts of $Na_2S_2O_3$ and Na_2SO_4. For green liquor the hydroxide concentration is lower

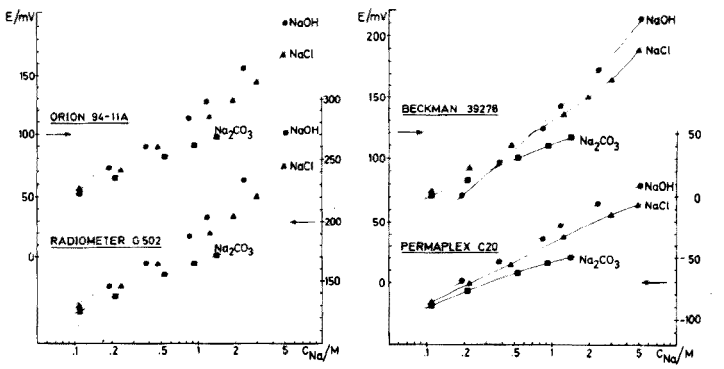

Fig. 1. The response of Orion 94-11A, Radiometer G502, Beckman 39278 and Permaplex C20 sodium-selective electrodes in some sodium solutions of high concentration.

but the carbonate concentration substantially higher. The total sodium concentration is around 4 M. Variation in the type of anion will affect both the activity coefficient and the liquid junction potential and the Figures show that these effects depend on the type of ion to such an extent that direct potentiometry is ruled out.

In a complete monitoring system, the sulfide concentration will be measured and it is also possible to measure a parameter related to the amount of hydroxide. It might then be possible to correct for the specific influence of the respective anions. Attempts were therefore made to derive such a correction procedure. The measurement in sodium hydroxide was fitted to a polynomial by a computer. The measurements in sodium chloride were then fitted to another polynomial and attempts were made to construct a combined polynomial which would describe the electrode behaviour in mixtures of sodium hydroxide and chloride. All attempts were unsuccessful, as well as attempts in which the polynomials were replaced by extended Debye—Hückel formulae with additional terms. Obviously the information which could be derived from measurements in the pure solutions of the two salts was insufficient. Additional information could have been obtained from measurements in mixed solutions, but the number of ions in the liquors is so large that any such procedure becomes impractical.

Figure 1 shows that the response curves for the Orion and Radiometer electrodes are very similar. The Beckman electrode deviates somewhat from the curves shown for the Orion and Radiometer electrodes. It also showed a marked ageing during use. Only the Orion and the Radiometer electrodes had an E^0 which remained within 10 mV of the original value during half a year. The permaplex electrode showed the best linearity and its stability was comparable with the Beckman electrode. About 2 min were required for equilibrium, ± 0.2 mV, which was similar to the other electrodes except the Orion one which was much faster.

Dilution with ammonium buffer

In the selection of a constant ionic strength buffer, various ammonium compounds are judged to be most suitable. The carbonate seems to be the best choice because it gives a higher ionic strength per mole and the solution becomes so alkaline that any hydrogen ion interference is eliminated. Compared with hydroxide the carbonate solution is less corrosive and loses less ammonia. The measurements were therefore made in solutions made up from twenty parts of 1 M ammonium carbonate and one part of sample. Lenz and Mold [1] used ammonium carbonate and Swasey [2] ammonium sulphate.

Figure 2 shows the response of the electrodes in 1 M ammonium carbonate. It can be seen that the Beckman, Radiometer and Philips electrodes give parallel straight lines with a Nernstian slope over the sodium range of interest. At sodium concentrations of somewhat less than millimolar they

level off, because of ammonium interference. This interference was about the same for all three electrodes, which is in some disagreement with the values given by Wilson et al. [4]. They found a lower selectivity for the Beckman electrode at a pH of 7.60. At this pH, however, the Beckman electrode shows a pH-dependence [3].

The Orion electrode gives a very poor sodium response in this medium because of the high interference by ammonium ions. The reason for this low selectivity is not understood. A third electrode was investigated but this gave no response. The fourth electrode from Orion was of the combined type. This showed a response and a selectivity similar to the others shown in Fig. 2.

The permaplex electrode cannot be used with a high ionic strength buffer and it was therefore excluded from further study.

Measuring conditions

Figure 3 shows the response of four sodium electrodes in solutions 0.06 M in sodium ion. The electrodes were previously stored in 0.1 M NaCl, rinsed well with distilled water and immersed in the same solution in a thermostat at 25 °C. All electrodes were measured against the same reference electrode. The first part of the figure shows the drift obtained when a sodium electrode has been rinsed with water. A number of later experiments in alkaline solutions in an automatic system confirmed that flushing with water,

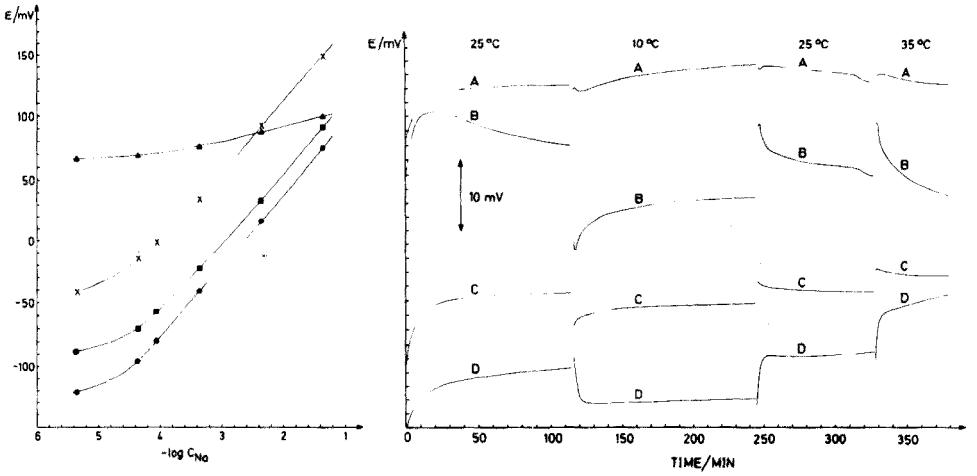

Fig. 2. The response of four sodium-selective electrodes in 1 M ammonium carbonate buffer (pH >9). (▲) Orion 94-11A. (×) Philips G15. (■) Beckman 39278. (●) Radiometer G502.

Fig. 3. The effects of temperature variations on some sodium-selective electrodes in a solution 0.06 M in sodium ion. (A) Philips G15. (B) Beckman 39278. (C) Radiometer G502. (D) Orion 94-11A.

even if it had exactly the right temperature, seriously disturbed the electrode equilibrium.

All the electrodes (including the reference electrode) were then transferred to another thermostat with a solution of the same composition kept at 10 °C. They were later transferred back to the original solution and subsequently to a vessel kept at 35 °C. No washing was done in between. Figure 3 shows that a large temperature transient effect occurs during the first 5 min and that a lower drift continues for a considerable time. The Beckman electrode shows a significant hysteresis and it should also be remembered that the Orion electrode is subject to an ammonium interference, which of course increases with temperature. Similar measurements made in solutions with higher sodium content showed that the temperature effects were also dependent on the sodium level. Even if the Beckman and Orion electrodes are excluded because of poor stability and ammonium interference, respectively, there remains a temperature dependence of about 0.4 mV/ °C (the largest values are not shown in Fig. 3). These effects arise from both the electrodes and changes in the solutions. If voltage readings are to be made to 0.1 mV, the temperature must be controlled to at least 0.2 °C. Experience with an automatic system shows that the solution must have already attained the desired temperature when it is pumped into the electrode chamber. Any temperature difference will cause a heat wave to move inwards towards the internal reference electrodes and stability will not be obtained until equilibrium has been restored. This may take considerable time.

The results shown above indicate that the Radiometer and Philips electrodes should be superior for sodium measurements in pulping liquors. It was found that the Philips electrode showed larger drift in sodium hydroxide solutions and therefore the Radiometer G502 was selected for further study.

Sodium ion measurements

A Radiometer G502 sodium electrode and an Orion double junction reference 90-02-00 were mounted in a flow cell in a water bath at 25.0 °C. The solution was pumped with pneumatically operated syringe pumps, one for the buffer 1 M ammonium carbonate and one for the sample. The volume ratio was 20:1. The pumped liquid passed through 1/16-in. stainless steel heat exchanger tubing immersed in the thermostat before entering the electrode chamber. When the solution had been pumped into the cell the pumps were stopped for 3 min for the electrodes to equilibrate before the potential was read. A pneumatic valve could be switched over, so that a standard solution containing 4.00 M NaOH could be pumped by the sample pump. Every sixth measurement was a standard and the standardization was used in calculating the results from the following five samples. All valve operations as well as the reading and calculations were made with an Alpha 16 minicomputer.

Table 1 shows the results obtained when 41 synthetic samples of sodium

TABLE 1

Measurements with Radiometer G502 Na electrode in sodium hydroxide samples diluted 1:20 with 1 M ammonium carbonate

Sample (M)	Number of measurements	Mean (M)	Deviation (%)	s_r (%)
1.000	10	1.008	+0.8	0.7
2.005	9	1.987	−0.9	0.6
3.00	6	2.98	−0.7	0.5
5.00	16	4.99	−0.2	0.5

hydroxide were analyzed. The samples covered the range 1—5 M sodium ion and they were analyzed in arbitrary order. It can be seen that the standard deviation is well below 1 % and that the mean is accurate to about 1 %. The most accurate values are of course those close to the concentration of the standard (4 M). Two voltage readings, one for the standard and one for the sample, are required in order to compute the results. Table 1 shows that each reading must have been precise to about ± 0.1 mV which sets specifications for the volt-meter, the temperature control and the electrode short-term drift.

I thank Prof. Gillis Johansson for valuable discussions during this work and for suggesting improvements to the manuscript. My thanks are also due to Ulla Lind for typing the manuscript and Dr. Michael Sharp for revising the English text.

REFERENCES

1 B. L. Lenz and J. R. Mold, Tappi, 54 (1971) 2051.
2 C. C. Swasey, Tappi, 53 (1970) 1692.
3 M. F. Wilson, E. Haikala and P. Kivalo, Anal. Chim. Acta, 74 (1975) 395.
4 M. F. Wilson, E. Haikala and P. Kivalo, Anal. Chim. Acta, 74 (1975) 411.
5 T. Eriksson and G. Johansson, Anal. Chim. Acta, 63 (1973) 445.

Analytica Chimica Acta, 87 (1976) 7—17

COMPARISON OF COPPER(II) ION-SELECTIVE ELECTRODES FOR MEASUREMENTS AT MICROMOLAR CONCENTRATIONS

DEREK MIDGLEY

Central Electricity Research Laboratories, Kelvin Avenue, Leatherhead, Surrey KT22 7SE (England)

(Received 28th April 1976)

SUMMARY

Four types of copper ion-selective electrodes have been tested for determining copper at concentrations below 10^{-6} mol l^{-1}. None of the electrodes has a Nernstian response in dilute copper solutions in this concentration range, though their responses are linear in pCu buffer solutions. The causes of the deviations are a direct redox effect in the case of an electrode with a $Cu_{1.8}Se$ single crystal membrane, production of copper ions by oxidation of the membrane itself in Ag_2S—CuS membrane electrodes, and a combination of the two in the case of the Růžička Selectrode. The electrode potentials are affected by the oxygen content and pH of the sample solution and the condition of the membrane surface. Precision tests on two types of electrode are described.

During the commissioning of new power stations, continuous monitoring of copper in the boiler feed-water may be required. As there is a causal relationship between the accumulation of feed system corrosion products in the boiler and corrosion of the boiler itself, the determination of even very low concentrations ($< 10\ \mu g\ l^{-1}$) of copper is very important. The colorimetric zincon method, while being very sensitive, is lengthy, and the possibility of relatively simple analyses with ion-selective electrodes is attractive. Several commercially available copper-selective electrodes of different composition have therefore been investigated.

The Orion 94-29A electrode has a polycrystalline membrane of compressed silver sulphide and copper(II) sulphide, while the membrane of the Radiometer F3002 (Růžička Selectrode [1]) consists of a graphite—Teflon rod impregnated with the same materials. The Tacussel PCU2 electrode has a polycrystalline membrane of silver and copper(II) selenides. The membrane of the Radiometer F1112Cu is a single crystal of composition $Cu_{1.8}Se$. It will be shown that the electrodes differ in their characteristics, especially at copper concentrations below 10^{-6} mol l^{-1}.

EXPERIMENTAL

Apparatus

Potentials were measured on an Orion 801 digital pH meter. A saturated calomel reference electrode (Electronic Instruments Ltd. RJ 23) was used throughout. Plastic beakers and bottles were used for handling the working solutions. The solutions were stirred by a PTFE-coated magnetic stirrer bar.

Reagents

Chemicals were of analytical-reagent grade, except where otherwise indicated. Water was prepared by passing distilled water from a Manesty still through a twin-column mixed-bed de-ionization unit.

For the standard copper solution (0.1 mol l^{-1}), 24.968 ± 0.001 g of copper(II) sulphate pentahydrate or 24.160 ± 0.001 g of copper(II) nitrate trihydrate were dissolved in de-ionized water and made up to 1 l in a calibrated flask. Further standards were prepared by successive dilution and stored in polyethylene bottles.

A series of copper buffer (pCu) solutions [1, 2] was prepared with iminodiacetic acid as the complexing agent to give the concentration range required. A stock solution was prepared by adding 7.20 ± 0.01 g of iminodiacetic acid (Hopkin and Williams Ltd., fine chemical grade) to about 100 ml of de-ionized water. The contents of an ampoule of sodium hydroxide solution (B.D.H. concentrated volumetric solution, to make 500 ml of 0.1 M solution) were added and more water added to make the volume to about 400 ml. The solution was stirred until all the iminodiacetic acid had dissolved and finally made up to 500 ml with water.

The working solutions were prepared by mixing 50 ml of 1.0 mol l^{-1} potassium nitrate, 50 ml of iminodiacetic acid stock solution and 25 ml of 0.1 mol l^{-1} copper(II) nitrate, adding the appropriate volume (0, 2.5, 4.0 and 5.0 ml) of 1.0 mol l^{-1} sodium hydroxide and making up to 500 ml with water. The pH was measured with a Pye E-401 combination glass electrode and pCu = $-\log[Cu]$ calculated from the pH and the stability constant [3]. The final pH values of the above solutions were, in order of increasing sodium hydroxide content, 2.67, 3.53, 5.90 and 7.00, giving pCu values of 3.35, 4.54, 7.00 and 8.10, respectively. A further solution was made with 0.01 mol l^{-1} copper(II) nitrate instead of the 0.1 mol l^{-1} solution and with no added sodium hydroxide; the pH was 3.60 and the pCu was 6.00.

RESULTS

Calibration

The calibration graphs obtained over the concentration range 10^{-3}—10^{-7} mol l^{-1} are shown in Fig. 1; 25-ml portions of solution in a 50-ml polyethylene beaker were used and no other electrolyte was added. The calibrations are shown as functions of concentration and also of activity for

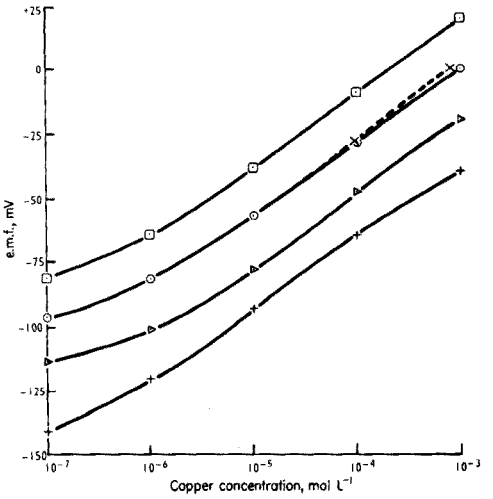

Fig. 1. Calibration of Orion 94-29A (⊙), Radiometer F1112Cu (⊡), Růžička Selectrode (+), Tacussel PCU2 (△). The Orion results are re-plotted as an activity calibration (×),

the Orion 92-29A electrode. The graphs start to curve between 10^{-5} and 10^{-6} mol l^{-1}, as if the real copper concentrations were higher than the nominal ones. Since the solubility products of the various membrane materials are very low (10^{-35}—10^{-50}), there should be no question of the curvature's arising from the equilibrium solubility of the membrane components. The calibrations of the Orion and Radiometer F1112Cu electrodes were checked with the pCu buffers and compared with conventional standards made up to the same ionic strength with potassium nitrate. The calibration graphs (Fig. 2) obtained with the buffer solutions show that the electrodes are capable of responding theoretically at free concentrations as low as 10^{-8} mol l^{-1} in the presence of high total copper concentrations, and possible sources of the apparent increase in copper content in the dilute standard solutions were therefore examined.

(a) Batches of the water used to prepare the standards were evaporated so that any involatile impurities were concentrated five to ten times. There was no change in the apparent copper content of the water (25 μg l^{-1} by a standard addition method with the Radiometer F1112Cu electrode) on evaporation. The copper content of the water indicated by direct potentiometry with the Orion electrode was 5 μg l^{-1} and that determined by flameless atomic absorption spectrometry was less than 0.1 μg l^{-1}.

(b) Instead of being immersed in the copper solution, the reference electrode was joined to it by a 1.0 mol l^{-1} potassium nitrate salt bridge, in case mercury ions from the calomel electrode were reaching the copper electrode and causing an interference. No change in the curvature was observed.

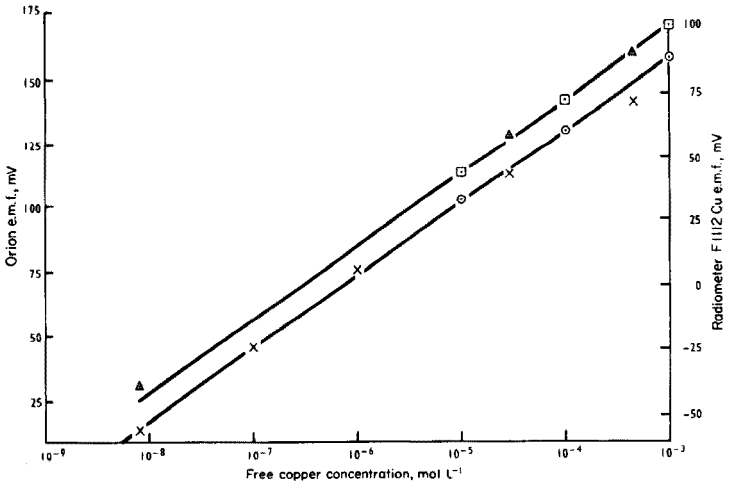

Fig. 2. Calibration of copper electrodes in pCu buffer solutions [x Orion 94-29A, ▲ Radiometer F1112Cu] and in conventional standards at μ = 0.1 (KNO_3) [⊙ Orion 94-29A, ⊡ Radiometer F1112Cu].

(c) Standard solutions prepared from copper nitrate and copper sulphate showed no significant differences in the curvature.

(d) The possibility of contamination by desorption of copper ions from the bodies of the electrodes after previous adsorption by contact with more concentrated solutions was investigated, simultaneously with the dissolution mechanism (e) below.

(e) Work with Orion and Růžička electrodes in acidic solutions [4] indicated that they may be self-contaminating with copper(II) ions through oxidation of the membrane material itself. The reaction (1) has been proposed [5] for oxidation of synthetic copper(II) sulphide in sulphuric acid solution.

$$CuS + \tfrac{1}{2}O_2 + H_2SO_4 \rightarrow CuSO_4\,aq + S + H_2O \qquad (1)$$

At copper concentrations of 10^{-6} mol l^{-1} or more, the Orion and Růžička electrodes soon reach a steady potential, but at a concentration of 10^{-7} mol l^{-1} the potentials tend to increase with time, indicating increasing concentrations of copper. Figure 3(a) shows some response curves obtained when an Orion electrode was transferred from 10^{-6} to 10^{-7} mol l^{-1}copper solutions, with a rinse in de-ionized water before re-immersion. The Růžička electrode gave similar minima in its response curves at 10^{-7} mol l^{-1} copper, but the subsequent rate of increase was slower than with the Orion electrode, provided that the Růžička electrode had been freshly conditioned in disodium—EDTA solution. The Tacussel electrode responded very slowly, but a shallow minimum was observed with 10^{-7} mol l^{-1} solutions. In contrast, the Radiometer F1112Cu electrode reached a steady potential in less than 5 min at all concentrations.

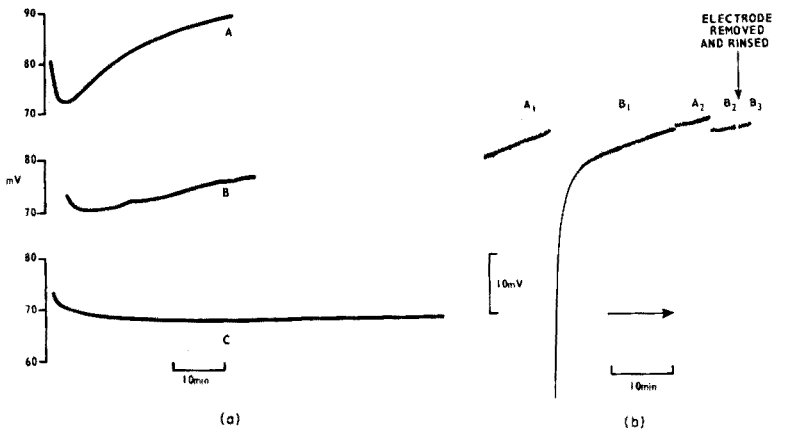

Fig. 3. Recorder traces. (a) For the transfer of an Orion 94-29A electrode from a 10^{-6} mol l^{-1} copper solution, with an intermediate rinse in de-ionized water to (A) 10 ml, (B) 25 ml (C) 100 ml portions of 10^{-7} mol l^{-1} copper solution. (b) Traces obtained on alternating Orion 94-29A electrode between 25-ml portions of de-ionized water.

Response curves of the type found with the Orion, Růžička and Tacussel electrodes in 10^{-7} mol l^{-1} copper solutions could arise from either the desorption or the dissolution process, but when an Orion electrode was successively placed in fresh 10^{-7} mol l^{-1} copper solutions, the same response curve was obtained each time and not the progressively lower minimum potentials and slower subsequent increases expected from a desorption mechanism, where the amount of adsorbed copper should be less in each successive solution.

To confirm that the dissolution mechanism was the more likely, a series of measurements was made in which an Orion electrode was alternately placed in two stirred 25-ml portions of de-ionized water. In Fig. 3(b), curve A_1, shows the potential after several minutes immersion in the first portion of water. Transferring the electrode to a fresh portion produced a large initial drop in e.m.f. before a value in the same region as before was reached (curve B_1). When the electrode was returned to the first portion, the e.m.f. curve (A_2) was a continuation of curve A_1. A similar continuation (B_2) was found when the electrode was re-immersed in the second portion. These continuations occurred whether the intervening solution was higher or lower in apparent copper concentration and also when the electrode was rinsed with fresh water before re-immersion (B_3). These observations showed that little copper was carried over with the electrode and that the measured copper concentrations in the two solutions depended not on each other but on the time of immersion of the electrode, which is in accord with the hypothesis of membrane dissolution.

From the response curves, any copper produced by oxidation in neutral solutions is significant only at added copper concentrations of about

10^{-7} mol l^{-1}, and it would be expected to be negligible in the pCu buffer solutions, which contain $5 \cdot 10^{-3}$ or $5 \cdot 10^{-4}$ mol l^{-1}. All the electrodes gave steady potentials in the pCu buffers, even at lower free copper concentrations than were obtained in the conventional standards. The factors affecting the apparent increases in copper concentration in the very dilute solutions are considered below.

Effect of deoxygenation

Passing oxygen-free nitrogen through the standard copper solutions did not change the potentials of the Orion electrode at concentrations down to 10^{-6} mol l^{-1}. At 10^{-7} mol l^{-1} the increases in potential of Fig. 3(a) were halted when nitrogen was introduced, but there was no reduction in e.m.f. When the solution was deoxygenated before measurements started, the potential in 10^{-7} mol l^{-1} solution was 7—15 mV lower than otherwise. The potential of the Růžička electrode was reduced by 1—3 mV on passing nitrogen through 10^{-3}—10^{-6} mol l^{-1} solutions and by 5—10 mV in 10^{-7} mol l^{-1} solution. The reduction was the same whether the solution was degassed before or during the measurement. With the Radiometer F1112Cu electrode, the potential was reduced by 3 mV in 10^{-5} and 10^{-6} mol l^{-1} solutions and by 8 mV in 10^{-7} mol l^{-1} solutions, and with the Tacussel electrode by 3—4 mV in 10^{-6} and 10^{-7} mol l^{-1} solutions. The potential of the Orion electrode in the pCu buffer solutions was not affected by deoxygenation, but the Radiometer F1112Cu and Růžička electrode potentials were reduced by about 5 mV. It was concluded that while the Radiometer F1112Cu, Růžička and Tacussel electrodes were directly influenced by the redox potential in the solutions being measured, the Orion electrode was affected only through the change in the rate of production of copper(II) ion in the different oxidation conditions. In the pCu buffer solutions the additional copper produced by oxidation of the membrane was insignificant compared with the total copper concentration, and the Orion electrode was unaffected by deoxygenation of those solutions even at very low free copper concentrations.

Effect of surface condition

Johansson and Edström [6] found that the performance of Orion electrodes was improved after treating the surface of the membrane with silicone oil. This was confirmed in the present work: the potentials at 10^{-6} mol l^{-1} and above were unaffected, but the difference in e.m.f. between the 10^{-6} and 10^{-7} mol l^{-1} solutions was extended from 13 to 21 mV. Similar treatment did not change the performance of the Radiometer F1112Cu electrode.

These findings are reinforced by the behaviour of the Orion and Růžička electrodes in acidic solution [4]: response curves similar to those at 10^{-7} mol l^{-1} copper in neutral solutions (Fig. 3(a)) were obtained at all concentrations up to 10^{-3} mol l^{-1} and the performance was improved by the

silicone oil treatment. In contrast, the Radiometer F1112Cu electrodes gave steady potentials in acidic solutions, although the sensitivity was reduced at copper concentrations below 10^{-4} mol l^{-1}.

Effect of sample volume

Corrosion of the membrane materials should proceed at a rate virtually independent of the volume of solution in which the electrode is immersed. In a well-stirred solution the corrosion products are dispersed throughout its volume and the electrode potential should increase more slowly, the greater the volume of the solution in which the electrode is immersed, provided that the response of the electrode is faster than its rate of corrosion. Figure 3 shows the response curves of an Orion electrode on transfer from a 10^{-6} to a 10^{-7} mol l^{-1} solution, with an intermediate rinse with deionized water. In 100 ml of solution, the potential is almost constant, but the rate of increase is much greater as the volume decreases. The minimum potential reached (Table 1) was also lower in the larger volume. At concentrations of 10^{-5} mol l^{-1} and above there was no difference in the readings in different volumes of solution. The Růžička electrode showed similar behaviour but the potential of the Radiometer F1112Cu electrode was independent of the volume of solution.

Orion electrodes were placed in a perspex flow cell (Electronic Instruments Ltd.) so that any decomposition products were continuously removed by the flow of solution (4 ml min^{-1}). In order to reduce the effect of electrical noise, the standard solutions were mixed with 0.5 mol l^{-1} potassium nitrate solution pumped at 0.4 ml min^{-1}. Steady potentials were obtained at copper concentrations of 10^{-7} mol l^{-1} but there was no improvement in sensitivity over that found with 100 ml portions of solution in a beaker. A long time was taken to reach equilibrium (30 min for a change from 10^{-6} to 10^{-7} mol l^{-1}). The Radiometer F1112Cu electrode in the flow cell showed no increase in sensitivity over that obtained in a 25-ml portion of solution in a beaker.

Precision tests

The copper concentrations of interest in the analysis of power station waters are very low and so the precision tests were concentrated on the Orion and Růžička electrodes, since these had a greater sensitivity at low concentrations. For those solutions where no steady potential was reached the

TABLE 1

Variation of electrode readings (in mV) as a function of sample volume

	Orion			Růžička	
Sample volume (ml)	10	25	100	25	100
E.m.f. for 10^{-4} mol Cu l^{-1}	150	150	150	256	256
E.m.f. for 10^{-7} mol Cu l^{-1}	73	70	67	185	180

minimum was recorded. The results are given in Table 2. Duplicate measurements were made in each batch for the Orion electrode, but only single measurements with the Růžička electrode. Each batch was measured on a separate day. The three sets of measurements were made at different times and with different standard solutions. The total standard deviation of the Růžička electrode was less dependent on the concentration than that of the Orion electrode, being smaller at low concentrations but larger at high concentrations. The potential of the Orion electrode varied less between batches than that of the Růžička electrode.

Response time

The times taken for the potential to reach equilibrium after immersion of a rinsed electrode in a stirred 25-ml portion of solution either ten times more dilute or more concentrated than the last one were noted for the various electrodes when new. The Orion 94.29A took less than 2 min at concentrations $\geqslant 10^{-4}$ mol l^{-1} and 5 min or more at lower concentrations. The Radiometer F1112Cu electrode took less than 5 min at all concentrations between 10^{-3} and 10^{-6} mol l^{-1}. The Růžička Selectrode reached

TABLE 2

Precision of measurements with copper-selective electrodes

Copper concn. (mol l^{-1})	$\bar{\Delta}$[a] (mV)	s_w[b] (mV)	s_b[b] (mV)	s_t[b] (mV)
Orion 94-29A 25-ml portions				
10^{-3}	0	0.1	—	(0.1)[c]
10^{-4}	28.1	0.2	N.S.[d]	0.3
10^{-5}	56.7	0.4	N.S.	0.4
10^{-6}	81.9	0.9	N.S.	1.2
10^{-7}	95.9	2.5	N.S.	2.9
100-ml portions				
10^{-3}	0	0.2	—	(0.5)[c]
10^{-4}	26.3	0.3	1.2	1.3
10^{-5}	53.8	0.9	1.6	1.9
10^{-6}	83.0	0.8	1.1	1.4
10^{-7}	108.4	1.9	N.S.	2.0
Růžička Selectrode 25-ml portions				
10^{-3}	0	—	—	(1.4)[c]
10^{-4}	27.1	—	—	0.8
10^{-5}	56.1	—	—	0.6
10^{-6}	80.5	—	—	1.1
10^{-7}	101.6	—	—	0.6

[a] $\bar{\Delta}$ is the mean difference over 5 batches from the reading for the 10^{-3} mol l^{-1} solution.
[b] s_w, s_b, s_t are the within-batch, between-batch and total standard deviations, respectively.
[c] The total standard deviation for the 10^{-3} mol l^{-1} solution is given as the standard deviation of the mean millivolt readings for each batch.
[d] N.S. = not significant.

equilibrium in about 1 min at concentrations above 10^{-5} mol l^{-1} and no more than 5 min at lower concentrations. As the electrodes aged, their response times increased such that the variations in response times between the different types of electrodes were less significant than those found with any given electrode at different times. The history of the Tacussel electrode, which was on loan, was unknown, but it was presumed to be an "old" electrode. Its response times were much longer than those for the other electrodes, extending to 20—30 min at concentrations in the range 10^{-5}—10^{-7} mol l^{-1}. The response times were independent of the direction of the change in concentration.

Consistency of electrode performance

The performance of the Orion electrode was very dependent on its age. With old electrodes the response was slower and the e.m.f. was dependent on the rate of stirring. Even when new, the electrodes had different sensitivities below 10^{-6} mol l^{-1} and their standard potentials differed by up to 20 mV. Interference effects also changed with the age of the electrode [4]. Polishing the surface of the membrane with Radiometer V104 polishing paste largely restored the performance of an old electrode.

The potentials of the Růžička electrode depended on the degree of pre-conditioning in disodium EDTA solution and the subsequent treatment. Before conditioning was complete, the sensitivity of the electrode was sub-Nernstian and the e.m.f. values were lower than those obtained with a fully conditioned electrode, the difference being greater, the higher the concentration. Once an electrode was conditioned, its sensitivity was virtually constant for at least five weeks, depending on how it was stored between use. Storage in air produced a slowly diminishing sensitivity; the e.m.f. difference between 10^{-6} and 10^{-7} mol l^{-1} solutions decreased by about 1 mV for each period of overnight storage. The absolute values of the e.m.f. decreased more sharply but uniformly throughout the range 10^{-3}—10^{-5} mol l^{-1}: on the first period of dry storage by 10 mV, on the second by 4 mV and on the third and fourth by 2 mV. Overnight storage in 10^{-7} mol l^{-1} copper solution gave a very slow change in absolute e.m.f. (6 mV in 4 weeks) and no change in sensitivity. The Růžička electrode would therefore be suitable for continuous monitoring without the need for frequent re-conditioning.

Only one example each of the Tacussel and Radiometer F1112Cu electrodes was tested. As the Radiometer electrode aged, the response time increased and the membrane turned a green-bronze colour. On being polished the performance was restored and colour of the membrane changed to a metallic blue.

DISCUSSION

The limits of detection of the various copper electrodes are much higher than would be predicted from solubility product considerations. In electrodes

with mixed silver sulphide—copper(II) sulphide membranes (Orion 94-29A and the Růžička Selectrode), oxidation of the membrane itself provides the extra copper ions that cause deviations from Nernstian response at low concentrations. This is evident from the shape of the response curves at low concentrations, the effect of deoxygenation of the solution, interference by acids [4] and the Nernstian response obtained in pCu buffer solutions.

The limiting response of the $Cu_{1.8}Se$ single crystal membrane electrode (Radiometer F1112Cu) is determined by a direct redox interference rather than by copper ions dissolved from the membrane. Its response, being stable though non-Nernstian at low concentrations, is affected by deoxygenation and by acids in quite different ways from those of the Orion and Růžička electrodes. In this case the high total copper concentration of the pCu buffer solutions should have no influence on the linearity of the calibration at low levels of free copper, but as the redox potentials in the pCu buffer solutions were about 100 mV less than in the conventional standards, the redox interference was reduced, with the result that a Nernstian response was obtained at pCu values as high as 8.1.

Determination of copper at sub-micromolar concentrations with copper-selective electrodes is more involved than might be expected. The Orion and Růžička electrodes have higher sensitivities than the Radiometer F1112Cu type, but must be used in carefully defined circumstances. Measurements below 10^{-6} mol l^{-1} should be made in at least 100-ml portions of solution. Interference by the redox potential in this concentration range necessitates a close matching of standard and sample solutions with respect to oxygen content and pH, if the non-Nernstian part of the calibration graph is to be used. If a "reagent + electrode blank" is determined, it is valid only for the particular conditions tested, and should be checked for variation with the period of immersion of the electrode. A standard addition technique does not solve the problem of calibration at low levels: by assuming a continuation of the Nernstian slope, the calculated copper concentration merely includes all the interference effects, whatever the source. The Orion electrode is the most affected by pH [4], but in neutral solution it is the least affected by the oxygen content of the solution. A Nernstian calibration obtained with pCu buffer solutions should not be taken as evidence that successful analytical measurements can be made with very dilute copper solutions. The variation between the performances of individual electrodes, and of the same electrode at difference times, is such that the characteristics of analytical measurements near the limits of the response are closely dependent on the individual electrode. In view of the performance of the electrodes at sub-micromolar concentrations, they are not suitable for the routine analysis of highly pure power station waters by direct measurements.

This work was carried out at the Central Electricity Research Laboratories and is published by permission of the Central Electricity Generating Board.

REFERENCES

1 E. H. Hansen, C. G. Lamm and J. Růžička, Anal. Chim. Acta, 59 (1972) 403.
2 R. Blum and H. M. Fog, J. Electroanal. Chem. Interfacial Electrochem., 34 (1972) 485.
3 A. Ringbom, Complexation in Analytical Chemistry, Interscience, New York, 1963.
4 D. Midgley, Anal. Chim. Acta, (1976) 000.
5 A. K. Biswas and N. P. Mohan, J. Appl. Chem. Biotechnol., 21 (1971) 15.
6 G. Johansson and K. Edström, Talanta, 19 (1972) 1623.

Analytica Chimica Acta, 87 (1976) 19—25

HALIDE AND ACID INTERFERENCES WITH SOLID-STATE COPPER(II) ION-SELECTIVE ELECTRODES

DEREK MIDGLEY

Central Electricity Research Laboratories, Kelvin Avenue, Leatherhead, Surrey KT22 7SE (England)

(Received 28th April 1976)

SUMMARY

The responses of copper-selective electrodes with silver sulphide—copper(II) sulphide membranes are modified by the presence of chloride or fluoride ions. Prolonged exposure to these ions produces shifts in the standard potentials of the electrodes. Interferences by mineral acids depend on the anion present. The magnitude of all these effects is very dependent on the surface condition of the electrode membrane.

Chloride interference with copper(II)-selective electrodes of the mixed Ag_2S—CuS precipitate type, such as the Orion 94-29A electrode, has been reported to occur only at such high concentrations of both copper(II) and chloride ions that solid silver chloride was formed [1], but Crombie et al. [2] found effects at lower concentrations, where silver chloride formation would not occur. This additional interference was tentatively ascribed to the formation of copper(II) chloro-complexes causing a tarnish on the membrane, but no evidence was found for such species. Since chloride is such a commonly occurring ion, its interference has been studied as an important factor for the widespread application of the electrode, particularly for determining low ($<10^{-7}$ mol l^{-1}) concentrations of copper in power station waters. Since it is often necessary to treat a sample with acid to dissolve particulate copper before determining total copper, the utility of the electrode at low pH has a bearing on the simplicity of a possible analytical procedure. It is claimed [3] that the electrode can be used in solutions as acidic as pH 1, as is predicted by the influence of protonation of the sulphide ion on the solubility equilibria. However, this claim is not entirely justified and careful consideration must be given to the pH of the solution being analysed.

EXPERIMENTAL

An Orion 94-29A copper ion selective electrode was used in conjunction with an Electronic Instruments RJ23 saturated calomel reference electrode. A Radiometer F3002 copper-selective electrode (Růžička Selectrode) was also used. Potentials were measured on an Orion 801 digital pH meter.

Solutions were made up from analytical reagent-grade chemicals and water that was distilled and then passed through a twin-column mixed bed deionizer. Only plastic bottles and beakers were used. The solutions were stirred with a PTFE-covered magnetic stirrer bar.

RESULTS

Interference by halide ions

The changes in e.m.f. when 1 ml of 1.0 mol l^{-1} potassium chloride solution was added to 100-ml portions of copper(II) sulphate solution were noted for two Orion electrodes, one of which (No. 2) had been used for the first time two days previously and another (No. 1) which had been used intermittently for over a year. The results are shown in Table 1. For response curves that did not reach a steady e.m.f., e.g. Figs. 1(a) and (d), the minimum value was entered in Table 1. The electrodes differ both in the magnitude of the shift in potential and in its dependence on the copper concentration. The 1 % dilution by the potassium chloride solution would account for a shift of only 0.1 mV in all cases and changes in activity coefficients for shifts between 2.3 mV at 10^{-3} mol Cu l^{-1} and 5.2 mV at 10^{-7} mol l^{-1}. Single ion activity coefficients were calculated from the equation

$$-\log f_{Cu} = 2.036 \left(\frac{\sqrt{I}}{1+\sqrt{I}} - 0.3\, I \right)$$

where I is the ionic strength.

If $CuCl^+$ has a stability constant of 10 (estimated from the variety of results reported [4]), the shift in the e.m.f. caused by its formation would be less than 0.25 mV. The redox potentials of the solutions were in the range 250—300 mV (against a saturated calomel electrode) and therefore reduction of the copper(II) ions can be discounted.

TABLE 1

Influence of chloride ion on Orion electrodes

	Electrode No. 1 e.m.f. (mV)		Electrode No. 2 e.m.f. (mV)	
	Vol. of 1.0 mol l^{-1} KCl added (ml)			
	0	1	0	1
Cu (mol l^{-1})				
10^{-3}	175	170	203	200
10^{-4}	—	—	174	170
10^{-5}	119	111	143	138
10^{-6}	95	77	115	110
10^{-7}	71	45	90	85

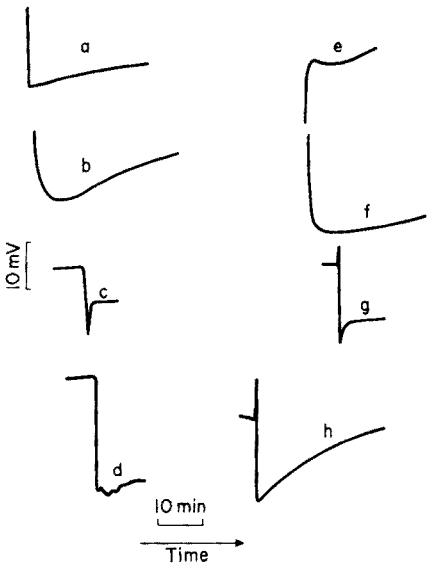

Fig. 1. Response curves for Orion (a—d) and Růžička (e—h) electrodes. (a), (e) electrode rinsed with de-ionized water and placed in 10^{-7} mol l^{-1} copper; (b), (f) electrode immersed in 10^{-5} mol l^{-1} copper in 0.1 mol l^{-1} nitric acid after being rinsed with de-ionized water; (c) injection of 1 ml of 1 mol l^{-1} KCl into 100 ml of 10^{-5} mol l^{-1} copper; injection of 1 ml of 1 mol l^{-1} KCl into 100 ml of 10^{-7} mol l^{-1} copper; (g) injection of 2 ml of 1 mol l^{-1} KCl into 20 ml of 10^{-5} mol l^{-1} copper; (h) injection of 2 ml of 1 mol l^{-1} KCl into 20 ml of 10^{-7} mol l^{-1} copper.

Although the chloride concentration above was lower than that predicted to cause interference by silver chloride formation [1], the tests were repeated with additions of fluoride ion, whose silver salt is quite soluble. The results of adding 1-ml portions of 0.1 mol l^{-1} sodium fluoride solutions to 100 ml of copper sulphate solution are shown in Table 2. Comparison with the chloride results shows the same trends, although the magnitude of the shift was less for the more dilute sodium fluoride solution. After being polished, the older electrode (No. 1) behaved similarly to the new electrode (No. 2). It should be noted that polishing hardly changed the potentials of Electrode No. 1 in the presence of fluoride, but made a marked difference in its absence.

The presence of high (0.1 mol l^{-1}) chloride concentrations produced a cumulative effect on the electrode even at high (10^{-3}—10^{-5} mol l^{-1}) copper concentrations. The e.m.f. corresponding to a given copper concentration was smaller, the later in a batch of solutions it was taken. Over a 90-min period the e.m.f. drifted by about 3 mV for 10^{-3} mol l^{-1} copper solutions. The drift was larger for lower copper concentrations. The rate of change of e.m.f. was sufficiently slow for apparently steady potentials to be observed

TABLE 2

Influence of fluoride ion on Orion electrodes

	Electrode No. 1 e.m.f. (mV)			Electrode No. 1, after polishing e.m.f. (mV)			Electrode No. 2 e.m.f. (mV)		
	Vol. of 0.1 mol l^{-1} NaF added (ml)								
	0	1	2	0	1	2	0	1	2
Cu (mol l^{-1})									
10^{-3}	176	176	—	176	175	175	198	197	196
10^{-4}	—	—	—	147	146	146	167	167	166
10^{-5}	127	120	118	119	117	116	139	136	135
10^{-6}	98	93	92	92	90	89	111	109	108
10^{-7}	77	67	65	71	65	64	86	82	80

in the normal course of measurement (2—5 min), and was only noticeable over long periods. The drift continued in successive solutions, although the electrode was washed between solutions with de-ionized water, and regardless of the concentration of any intervening solution. A similar, but slower, drift was observed with 0.1 mol l^{-1} potassium nitrate in solution. In copper solutions (10^{-3}—10^{-7} mol l^{-1}) without added electrolyte, no such effect occurred. The original performance could be restored by polishing the membrane. The net effect of the interference over a range of copper concentrations was to increase the apparent sensitivity of the electrode beyond that expected from the Nernst equation. Slopes of 50 mV per tenfold change in copper concentration have been found from measurements in sea water [5].

At low copper concentrations (10^{-7} mol l^{-1}) the e.m.f. values were unstable, even in the absence of added electrolyte (Fig. 1), although they could be stabilized by passing oxygen-free nitrogen through the solution.

Interference by acids

From a consideration of the solubility products of silver and copper(II) sulphides and the acid dissociation constants of hydrogen sulphide, displacement of the solubility equilibria by the formation of protonated sulphide species should not cause interferences greater than about 0.1 % in a 10^{-7} mol l^{-1} copper solution at pH 1. The actual interferences in 10^{-3}—10^{-5} mol l^{-1} copper solutions containing 0.1 mol l^{-1} of various acids can be judged by comparing the e.m.f. values in acid and neutral salt solutions (Table 3).

In the oxidizing acids, the potentials indicated incongruously high copper concentrations that were virtually independent of the added concentrations. In hydrochloric acid, the effect was less pronounced. Chloride ion itself tends to reduce the potential and the increase caused by the acidity is partly offset.

TABLE 3

Effect of acids and salts on Orion electrode No. 1

Cu (mol l^{-1})	E.m.f. (mV) in 0.1 mol l^{-1} soln. of					
	KNO_3	HNO_3	KCl	HCl	$HClO_4$	HNO_3[a]
10^{-3}	159	184	157	157	190	165
10^{-4}	131	181	127	132	177	140
10^{-5}	102	180	94	110—140	178	121

[a]Electrode coated with silicone oil.

The effect of nitric acid was reduced by treating the electrode with silicone oil, which improves the stability of the potential in neutral solutions [6].

The potentials in acidic solutions were not very reproducible and the values in Table 3 were obtained from one batch of solutions taken in random order. Acids affected a new electrode (No. 2) slightly less and another (No. 3), whose history was unknown, much more, but the trends were the same in all cases.

Comparison of Orion and Růžička electrodes

The copper-selective 'Selectrode' (Radiometer F3002) [7] has a membrane comprising a mixture of silver and copper(II) sulphides, which is essentially the same as in the Orion electrode, although the membranes are formed by different mechanisms. A Selectrode was tested in standard copper solutions with and without a background concentration of 0.1 mol l^{-1} nitric acid. The results in Table 4 show that the Selectrode is far less affected by acid than the Orion electrode, although some loss of sensitivity is apparent below 10^{-5} mol l^{-1}. The difference in e.m.f. at the higher copper concentrations are typical of changes arising from activity coefficients alone.

With the Růžička electrode, the injection of 2-ml portions of 1.0 mol l^{-1} potassium chloride solution into 20 ml of standard copper sulphate solution

TABLE 4

Effect of nitric acid on the Růžička electrode

	E.m.f. (mV) at Cu concn. (mol l^{-1}) of				
	10^{-3}	10^{-4}	10^{-5}	10^{-6}	10^{-7}
No acid	291	265	235	208	190
In 0.1 mol l^{-1} HNO_3	281	253	227	208	200

(10^{-4}—10^{-7} mol l^{-1}) produced decreases in potential of 10—12 mV, which were predictable from the effect of dilution and activity coefficient changes. Typical response curves are shown in Fig. 1. In all cases, an initial spike in the potential was followed by a sharp decrease, and then a slow increase, which at concentrations of 10^{-5} mol l^{-1} or above levelled off after about 3 min but at 10^{-6} or 10^{-7} mol l^{-1} persisted for over 40 min, sometimes exceeding the original potential. Orion electrodes showed broadly similar behaviour, although there was no initial spike. The slow increase in e.m.f. at low concentrations was also observed when no chloride was added (Fig. 1a, 1e) and its appearance is not necessarily associated with any form of chloride interference. The same shape of response curve could be obtained at higher concentrations by measuring in solutions containing nitric acid (Fig. 1b, 1f) or other mineral acids.

DISCUSSION

Interference by anions with the electrodes must be considered in relation to both long and short-term effects. The results in Tables 1 and 2 show that with a freshly polished membrane surface there was no short-term chloride or fluoride interference that could be distinguished from the effects of changes in ionic strength. With an aged electrode, the addition of halide ions produced much larger changes in e.m.f. than with a new one, but the difference in sensitivity between aged and freshly polished membranes was greatest in the absence of halide ions, i.e. rather than interfering, the halide ions reduced the extent to which the aged electrode deviated from potentials typical of a new electrode. In contrast, nitrate ions had no effect on the sensitivity of an electrode. Prolonged immersion in chloride solutions produced a tarnish on the surface, as reported previously [2], with a resultant general deterioration in performance; the standard potential decreased with time in the chloride solutions and the response became slower. Similar but smaller changes in performance were observed on prolonged exposure to nitrate ions.

The behaviour of the electrodes in acidic solutions also showed a similar difference between the effects of halide ions and oxyanions, i.e. the results in hydrochloric acid deviate less from Nerstian response than those in nitric, perchloric or sulphuric acids, although the deviations occur at much higher copper concentrations than in neutral solutions. The magnitude of any of the effects investigated was found to be individual not only to a particular electrode but to the age of that electrode; nevertheless, the same trends were observed in all cases.

Where the response curves went through a minimum, the increase in e.m.f. was considered to arise from an increase in copper concentration, caused by the oxidation of sulphide ions and the consequent displacement of the solubility equilibria. The rate of increase in copper concentration depends on the condition of the electrode surface, and therefore the increase is probably due

more to direct oxidation of sulphide in the membrane than to oxidation of dissolved sulphide from the membrane. Biswas and Mohan [8] have proposed the reaction (1) for the dissolution of synthetic copper(II) sulphide.

$$CuS + \tfrac{1}{2}O_2 + H_2SO_4 \rightarrow CuSO_4 + S + H_2O \quad (1)$$

Sulphur is deposited on the solid sulphide as a coherent film and at acid concentrations below 1 mol l^{-1}, the rate is controlled by diffusion of hydrogen ions through the sulphur film. Such a reaction is consistent with the present findings, in which the interference is worse if the acid concentration is higher and the acid is an oxidizing acid. The stabilization of the potential on degassing the solutions with oxygen-free nitrogen is also confirmatory. The tarnishing in concentrated chloride solutions could operate through the same reaction catalysed by chloride ion, which has been reported to accelerate the decomposition of copper(II) sulphide [9].

Trace analysis of copper solutions by means of these electrodes is far from straightforward if the sample has a low pH (<4) or contains large concentrations of chloride ion. With frequent polishing of the membrane and restandardisation, analysis of discrete samples should be possible even if chloride is present, but acidic solutions would need to be adjusted to pH 4—5 with sodium hydroxide solution, buffer solutions tending to form complexes with the copper ions, and the standard copper solutions should contain concentrations of chloride comparable to those in the samples. With these restrictions and complications, the attraction of the electrode for the continuous monitoring of copper in sample streams is much reduced.

This work was carried out at the Central Electricity Research Laboratories and is published by permission of the Central Electricity Generating Board.

REFERENCES

1 J. W. Ross, in Ion-Selective Electrodes, R. A. Durst (Ed.), National Bureau of Standards Special Publication 314, U.S. Dept. of Commerce, Washington, 1969, p. 83.
2 D. J. Crombie, G. J. Moody and J. D. R. Thomas, Talanta, 21 (1974) 1094.
3 Orion Research Inc., Cupric Ion Electrode Instruction Manual, Form IM94-29/1721, 1971.
4 A. E. Martell and L. G. Sillén, Stability Constants, Chemical Society Special Publication No. 17, The Chemical Society, London, 1962.
5 R. Jasinski, I. Trachtenberg and D. Andrychuk, Anal. Chem., 46 (1974) 364.
6 G. Johansson and K. Edström, Talanta, 19 (1972) 1623.
7 E. H. Hansen, C. G. Lamm and J. Růžička, Anal. Chim. Acta, 59 (1972) 403.
8 A. K. Biswas and N. P. Mohan, J. Appl. Chem. Biotechnol., 21 (1971) 15.
9 S. I. Tarabaev and N. A. Milyutina, Izv. Akad. Nauk Kazakh. S.S.R., Ser. Gorn. Dela., Met. Stroit. i Stroimat., (1956) 76 (Chem. Abs., 53 (1959) 5000a).

Analytica Chimica Acta, 87 (1976) 27—35

THE DETERMINATION OF COPPER IN SILICON BY ANODIC STRIPPING AND DIFFERENTIAL PULSE VOLTAMMETRY

P. LANZA and M. T. LIPPOLIS

Chemical Institute "G. Ciamician", University of Bologna, Bologna (Italy)

(Received 29th April 1976)

SUMMARY

A critical comparison of the application of differential pulse voltammetry and anodic stripping voltammetry to the determination of micro amounts of copper in silicon is described. The anodic stripping technique offers advantages when a dropping mercury capillary with a long drop time is used. The method recommended allows the determination of copper in silicon with a precision of ± 5 %; the limit of determination is about 1μg g^{-1}. Calibration graphs are linear in the range 0—0.2 μg Cu ml^{-1}. Methods for the dissolution of silicon are also compared.

In connection with a research program on the chemical characterization of semiconductor materials, the determination of microamounts of copper in silicon by electroanalytical techniques was studied. The techniques selected require only relatively simple instrumention, but provide great sensitivity and reliability. The primary aim was to establish simple, rapid procedures that required a minimum of chemical pre-treatment of the silicon samples. On the basis of previous experience [1—3] on the composition of solutions resulting from dissolution procedures for silicon, suitable methods were developed. The two most sensitive electrochemical techniques, anodic stripping and differential pulse voltammetry, were compared for application to the problem of silicon analysis, and anodic stripping polarography was found to be most successful.

EXPERIMENTAL

Reagents

The following reagent-grade chemicals were used: KOH (C. Erba; 1 p.p.m. Cu); H_2O_2 (C. Erba, RSE 120 vol.; 0.02 p.p.m. Cu); HNO_3 (C. Erba, RSE 65 %; 0.005 p.p.m. Cu); HF (J. T. Baker, MOS 48 %; 0.002 p.p.m. Cu); ethylenediamine (C. Erba, RPE); and copper (C. Erba, RS 99.9 %).

A copper(II) stock solution was prepared by dissolving 1.000 g of pure copper with a slight excess of nitric acid and diluting the solution to 1 l. Subsequent dilutions were made as required.

Ethylenediamine was distilled over sodium. All solutions were prepared with twice-distilled water.

Apparatus

When hydrofluoric acid was involved, teflon or polypropylene vessels and volumetric equipment were used. Glass and plastic vessels were washed with a 2 % Contrad 2000 (B.D.H.) detergent solution, then with dilute (1 + 1) nitric acid and then with running distilled water.

Two polarographs were used. An AMEL (Milan) Model 471 multipolarograph was used for the differential pulse polarography and an AMEL Model 448/452 differential cathode ray polarograph for anodic stripping voltammetry. Both instruments were equipped with a Model 460 stand, which holds cells, electrodes and self-levelling mercury containers, and includes the hammers for keeping the capillaries synchronized; this is essential for both pulse voltammetry and anodic stripping voltammetry when a hanging mercury drop is not used. Both polarographs were three-electrode instruments.

The working electrodes were normal dropping mercury electrodes. The reference electrode was a Model 303-NS/5 (Ingold) calomel electrode. The counter electrode was a platinum ring (Model Pt-805/NS/M5; Ingold). When necessary, a salt bridge (Model 305-95-NS/M5; Ingold) with a sintered glass plug and fitted with a SCE was used.

A 5-ml microcell was used in most of the experiments.

The solutions were deaerated with electrolytic hydrogen for 10 min before polarographic analysis. All measurements were carried out at 25.0 ± 0.1 °C.

Sample dissolution

Different dissolution procedures were tested. The following methods were found most suitable.

Dissolution with potassium hydroxide solution. Elemental silicon is readily soluble in potassium hydroxide solution, according to the reaction: $Si + 2\,KOH + H_2O \rightarrow K_2SiO_3 + 2\,H_2$. This reaction has frequently been used for analytical purposes, as well as microanalytical procedures [4, 5]. The following procedure was found most suitable.

Place the pulverized silicon sample (10—100 mg) into a glass or polypropylen test tube, and add 2 ml of 30 % KOH solution. After the first spontaneous reaction, cap the tubes and place them in a water bath at 60—70 °C until dissolution is complete. This treatment may leave some residue, e.g. iron(III) hydroxide, carbon or silicon carbide. Without filtering, quantitatively transfer the mixture to a 25-ml volumetric flask and dilute to volume with water. The copper(II), present as hydroxide complexes, e.g. $HCuO_2^-$, CuO_2^{2-}, can be measured directly. The 1 M NaOH (or KOH) solution is a common supporting electrolyte for polarographic determinations of copper(II) [6]; the copper solubility (as CuO_2^{2-}) is about $1 \cdot 10^{-3}$ mol l^{-1} [6, 7].

Unfortunately, this very simple method cannot be used with high boron-

doped silicon samples, owing to their very low reactivity with the alkaline solution. Moreover, this dissolution cannot be recommended for samples containing very low copper contents, because it is difficult to obtain reproducible results. Adsorption phenomena on the colloidal residues and vessel walls seem to have an important influence on the results. No noticeable improvements were obtained by addition of complexing agents such as ethylenediamine.

Dissolution with hydrofluoric and nitric acid. The reaction of silicon with hydrofluoric and nitric acids has also been used analytically [8, 9]. Sample dissolution is easily achieved without a large excess of reagents, by the reaction: $Si + 6\ HF + 2\ HNO_3 \rightarrow H_2SiF_6 + 2\ HNO_2 + 2\ H_2O$. The following conditions were found suitable.

Treat 10—100 mg of pulverized silicon with 5 ml of 6 M HF solution and 0.5 ml of 65 % HNO_3 in teflon or polypropylene test tubes. For complete dissolution, maintain the test tubes in a water bath at 70—80 °C for about 30 min. The solution, which contains an excess of hydrofluoric acid, is not suitable for polarography with the usual glass capillary and cell. This difficulty is avoided by adding enough potassium hydroxide to neutralize the excess acid and decompose the fluorosilicic acid to fluoride and silicate. For this purpose, transfer the sample solution to a glass vessel containing 7 ml of 30 % KOH solution, and boil until the K_2SiF_6 precipitate is completely dissolved. After cooling, add 2.5 ml of 1 M ethylenediamine, and dilute with water to exactly 25 ml in a volumetric flask. If the silicon sample weighs 100 mg, the composition of the final solution is about 1.2 M KF, 0.14 M K_2SiO_3, 0.1 M KOH, 0.10 M ethylenediamine and contains small quantities of KNO_2.

The solution may contain some residual insoluble hydroxides (essentially $Fe(OH)_3$ and $Ti(OH)_4$) that do not interfere with the polarographic analysis. The copper, present as the ethylenediamine complex, Cu en_2, is in a very suitable form for polarographic testing ($E_{\frac{1}{2}} = -0.45$ V vs. SCE).

Dissolution by means of hydrofluoric acid and hydrogen peroxide with gold(III) as catalyst. A very convenient method for dissolving the silicon is based on the use of hydrofluoric acid and hydrogen peroxide, by the reaction: $Si + 6\ HF + 2\ H_2O_2 \rightarrow H_2SiF_6 + 4\ H_2O$. This reaction occurs only in the presence of catalysts such as Cu(II), Au(III) and Pt(IV). Generally, copper salts are used as catalysts [2, 9—11]; earlier work [1] showed that Au(III) and Pt(IV) can also act as powerful catalysts. The following procedure was chosen.

Place the pulverized silicon samples (10—100 mg) in teflon or polypropylene test tubes. Add 5 drops of ca. 1 % $HAuCl_4 \cdot 3\ H_2O$ solution to each sample and then, successively, 4 ml of 6 M HF and 2 ml of 30 % H_2O_2. The reaction starts spontaneously. Complete the dissolution by keeping the tubes in a thermostat at 100 °C for about 1 h. This solution must undergo alkaline treatment as described above for the HF—HNO_3 mixture, before the polarographic analysis. The composition of the final solution is quoted above.

Elimination of the silicon matrix

In order to reduce the volume of the final sample solution, but principally to allow a greater choice of supporting electrolyte, the silicon matrix must be completely eliminated. This can be easily achieved because of the volatility of fluorosilicic acid which is distilled in an azeotropic mixture with water and hydrofluoric acid (H_2O:HF:H_2SiF_6 = 54:10:36; b.p. 116 °C) [12].

The acid solutions of the samples, obtained by the above procedures, can be taken to dryness with complete elimination of the silicon.

For this purpose, maintain the polypropylene or teflon tubes containing the sample solutions, in a glycerol bath at 120 °C. To accelerate the evaporation, fit the tubes with teflon plugs carrying inlet and outlet tubes, to allow a flow of filtered air. The samples are dry in about 2 h, leaving a very slight residue. The use of nitric acid can cause some trouble when polypropylene tubes are employed in drying the acid solutions; high polarographic residual currents can sometimes be observed. This difficulty does not occur when the HF—H_2O_2 mixture is used.

Differential pulse voltammetry

Sample solutions, obtained by the above acid dissolution procedures, or prepared by dissolving the residue from the evaporation of silicon in a suitable supporting electrolyte, were introduced into the polarographic cell and deaerated with electrolytic hydrogen for 10 min. The voltammogram was then recorded under the following instrumental conditions: instrument sensitivity 4 nA mm^{-1}; pulse level 50 mV; scan rate 2 mV s^{-1}; drop time 2 s. These instrumental parameters, which were used in most of the analyses, gave a sensitivity of 100 mm (peak height) for a concentration of 0.10 μg Cu ml^{-1} ($1.57 \cdot 10^{-6}$ M), with 0.05 M KOH—0.05 M ethylenediamine as supporting electrolyte. The peaks are well shaped with a peak potential, E_p, of —0.45 V vs. SCE. The instrument sensitivity can be increased to 0.80 nA mm^{-1} without excessive noise, solutions of about $1 \cdot 10^{-7}$ M can be analyzed.

This technique is therefore very sensitive, but the shape of the peaks can be strongly influenced by trace quantities of oxygen and hydrogen peroxide, so that very careful removal of the HF—H_2O_2 solution is required.

The capacitance current, which develops at about —0.67 V vs. SCE ("water hump"), is not very reproducible and sometimes hinders the regular growth of the copper peak. The use of 0.1 M nitric acid as the supporting electrolyte does not permit useful peak development, owing to the strongly sloped capacity current of the background. This difficulty has been emphasized previously [13].

Anodic stripping voltammetry

The application of anodic stripping with the hanging mercury drop electrode (HMDE) to the determination of copper in silicon proved successful.

For these analyses, samples were dissolved in the $HF—HNO_3$ or $HF—H_2O_2$ mixtures. It is well known that with this technique the reproducibility of the results depends strongly on constant stirring rate and on the relative positions of the capillary and the stirring bar. In order to ensure the constancy of these parameters, a special cell was designed, and the stirring, at 500 r.p.m. was carried out with a synchronous electric motor.

The experimental conditions were usually as follows: the pre-electrolysis potential was maintained at —1.00 V vs. SCE and the sweep rate was 5.55 mV s^{-1}; the drop surface was about 2.56 mm^2 (corresponding to 5 micrometre divisions of the Metrohm Model E 410 capillary). Stirring was stopped 30 s before the end of the electrolysis period. The cell voltage was then scanned and the voltammogram was recorded with a sensitivity of 4 nA mm^{-1}.

A linear calibration curve was obtained up to the 0.10 μg Cu ml^{-1} level. With the instrumental parameters described, in a supporting electrolyte of the composition indicated for the acid dissolution methods, a peak of 92 mm was obtained with a copper concentration of 0.10 μg ml^{-1}. This technique can be successfully used in either basic or acidic (0.1 M HNO_3) solutions.

Anodic stripping voltammetry with ordinary capillary electrodes

The use of an ordinary capillary electrode in anodic stripping voltammetry can eliminate the most important source of noise characteristics of this technique. The hanging drop electrode is, indeed, a very delicate device and sometimes one encounters difficulties in obtaining sufficiently reproducible results. The use of long drop-time capillaries can make this very valuable analytical technique more practical. However, because of the rather short electrolysis time available in this way, a very sensitive recording apparatus is required. At very high sensitivity, the capacity current becomes comparable with the peak current and must be compensated. At the same time, the growing drop contributes an increasing residual current, and the slope of the voltammogram must be corrected to obtain measurable peaks.

The Model 448/452 AMEL polarograph is very suitable for this type of anodic stripping polarography. This instrument is fitted with a very sensitive $x—y$ recorder, so that voltammograms can be recorded up to a sweep rate of 250 mV s^{-1}. Delay-time (i.e. pre-electrolysis time) and sweep rate can be varied over a wide range, and a device permits compensation for the slope of the residual current (see Fig. 1).

The capillary used in these experiments had a spontaneous drop time of about 40 s dipped in water. The cyclic operation included a pre-electrolysis time (24 s) and a sweep time (10 s). During the sweep time, the voltammogram was recorded at a sweep rate of 40 mV s^{-1}. The amplitude of the sweep ranged from —0.160 V to + 0.240 V (supporting electrolyte 0.1 M HNO_3); and from —1.00 V to —0.30 V (supporting electrolyte 0.05 M KOH—0.05 M ethylenediamine). Most of the measurements were done at 0.20 nA mm^{-1} sensitivity. No stirring was used.

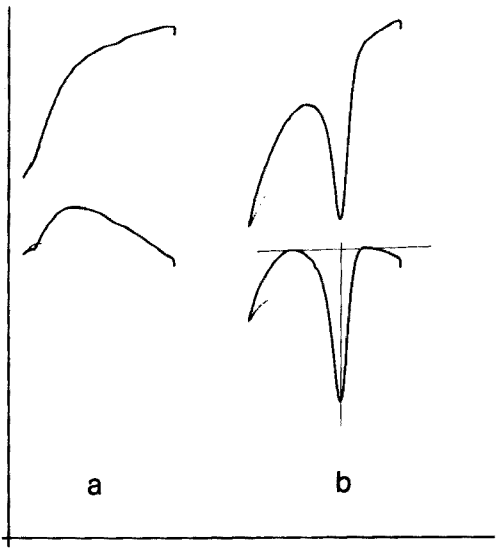

Fig. 1. Effect of the slope correction on the (a) residual current; (b) shape of the peak.

The instrument reproducibility, checked by cyclic recording of several anodic peaks obtained with different successive drops in the same solution, was found to be better than about 0.5 %.

Peak heights were measured as shown in Fig. 1, by drawing a vertical line through the peak and measuring the distance between the peak and the intersection of the vertical line with that of the base-line. To obtain a nearly horizontal base-line the slope control can be used, but a horizontal base-line is not a critical condition for obtaining accurate peak measurements.

The peak heights are a linear function of the copper concentration. In a typical calibration curve, a linear response was obtained for 0—0.20 μg Cu ml^{-1} with peak heights up to 155 mm, in a 0.1 M HNO_3—0.001 % gelatin supporting electrolyte with an electrolysis potential of —0.160 V, under the instrumental conditions given above. The straight line intersected the concentration axis at a slight negative value, probably because of the way the peak heights were measured. The base-line traced does not follow the residual current, but this does not affect the accuracy of the analytical results. For the experimental conditions quoted, the straight line corresponded to the equation $y = 795\,x - 2.2$, where x = μg Cu ml^{-1} and y = peak height (mm). The experimental points on the calibration curve showed an accuracy better than 1 %, related to the corresponding points of the calculated straight line.

In order to increase the sensitivity, some experiments were made with voltage scan rates of 100 and 150 mV s^{-1}. Higher scan rates gave higher peaks, but there was insufficient resolution of the peaks from the anodic oxidation curve of the mercury.

Choice of supporting electrolyte

It is well known that the charging current contribution remains the limiting factor in trace applications of differential pulse polarography. In the absence of faradaic reactions, the differential pulse polarogram is essentially a differential capacity curve, which strongly depends on the composition of the solution being investigated [13, 14]. Accordingly, when this technique is used at high sensitivity, the choice of supporting electrolyte is limited not only by the properties of the test substance, but also by the features of the double-layer capacity curve.

Various supporting electrolytes, including potassium hydroxide, with or without complexing agents (ethylenediamine or EDTA), perchloric, nitric and acetic acids, were investigated in preliminary experiments. In alkaline complexing solutions, e.g. 0.05 M KOH—0.05 M ethylenediamine the copper reduction peak develops approximately at —0.4 V, with a sufficient resolution from the "water hump". In acidic solutions, the peak is strongly affected by the charging current, which causes a high sloping base-line near the copper discharge potential.

The use of the anodic stripping technique greatly reduces these limitations. Well-shaped copper anodic peaks are obtained both in acidic and alkaline solutions. It should be pointed out that with low copper concentrations, strong adsorption can take place on glass walls. This phenomenon, which can often invalidate microanalytical methods, is usually minimized by working in strong acid solutions.

Recommended procedure

After a critical comparison of the above possibilities, the following procedure seems the most suitable. Dissolve 10—100 mg of pulverized silicon sample, containing 0.2—1 μg of copper, in teflon or polypropylene test tubes with hydrofluoric acid and hydrogen peroxide. Evaporate the solution to dryness at 120 °C with the aid of a filtered air flow. Dissolve the residue in 5.00 ml of 0.1 M HNO_3 containing 0.001 % gelatin. Introduce the solution into the cell and, after deaeration, analyze by anodic stripping voltammetry, with a long drop-time capillary as the working electrode. Connect the calomel reference electrode with the test solution through an electrolytic bridge filled with 0.1 M HNO_3. The solution should not be stirred during the pre-electrolysis time.

All operations have been described in detail in previous sections of this paper.

RESULTS AND CONCLUSIONS

Table 1 shows the results obtained with some commercial silicon samples. One can conclude that anodic stripping voltammetry is a very suitable technique for the problem. The possibility of avoiding the use of a hanging mercury drop electrode, by compensating the decreasing sensitivity arising

TABLE 1

Results
(Experimental conditions: electrolysis time, 24 s; electrolysis potential, —0.160 V; scan rate, 40 mV s^{-1}; current sensitivity, 0.2 nA mm^{-1}; supporting electrolyte, 0.1 M HNO_3 + 0.001 % gelatin.)

Silicon type	Average p.p.m. (w)	s p.p.m. (w)	s_r (%)	No. of detns.
B.D.H.	99	± 3.1	3.1	6
Schuchardt SI - 172	10.5	± 0.55	5.2	6
	8.3	± 2.3	28	20[a]
Wacker W/A 10 (Cu doped)	14.9	—	—	2
Wacker W/A 10 (Cu doped)	3.1	—	—	2

[a]Analyses done by differential pulse polarography. Supporting electrolyte 0.05 M KOH—0.05 M ethylenediamine; ΔE = 50 mV; scan rate 2 mV s^{-1}; drop time, 2 s.

from a short pre-electrolysis time with a greater sensitivity of the apparatus, makes this technique especially useful for routine analysis, when high sensitivity, accuracy and rapidity are required.

The use of differential pulse polarography is severely limited for silicon analysis essentially because of the following factors: (1) when acid solutions are used, difficulties are caused by the charge current contribution in the potential range of the copper reduction peak; (2) when alkaline solutions are used, very pronounced adsorption phenomena can cause large systematic errors and erratic results (see the results in parentheses quoted in Table 1).

Anodic stripping with the HMDE provides a high sensitivity similar to that obtained with other more sophisticated apparatus, but in this case it was impossible to obtain a reproducibility better than 10—15 %.

We are grateful to Dr. M. Colombi for his helpful collaboration in the preliminary research, to Prof. L. Grifone (AMEL) for supplying the polarographic apparatus and for technical assistance, to the LAMEL Laboratory, C.N.R., for financial support, and to Prof. G. Semerano, Director of the Chemical Institute "G. Ciamician" for encouragement and interest.

REFERENCES

1 P. Lanza and P. L. Buldini, Anal. Chim. Acta, 70 (1974) 341.
2 P. Lanza and P. L. Buldini, Anal. Chim. Acta, 75 (1975) 149.
3 M. Taddia and P. Lanza, Ann. Chim., 65 (1975) 719.
4 N. Schink, Z. Anal. Chem., 216 (1966) 319.
5 M. Schnoller, Z. Anal. Chem., 259 (1972) 101.
6 J. J. Lingane, Ind. Eng. Chem., Anal. Ed., 15 (1943) 583.

7 M. Pourbaix, Atlas of Electrochemical Equilibria in Aqueous Solutions, Pergamon, Oxford, 1966, p. 389.
8 J. Vivarat-Perrin and E. Bonnier, Chim. Anal. (Paris), 48 (1966) 511.
9 L. V. Myshlyaeva and V. V. Krasnoshchekov, Analytical Chemistry of Silicon, John Wiley, I.P.S.T., New York, 1974.
10 L. Ducret, Anal. Chim. Acta, 17 (1957) 213.
11 L. S. Vasilevskaya, A. I. Kondrashina and G. G. Shifrina, Zavod. Lab., 28 (1962) 674.
12 P. A. Munter, O. T. Aepli and R. A. Kossatr, Ind. Eng. Chem., 39 (1947) 427.
13 D. J. Myers and J. Osteryoung, Anal. Chem., 46 (1974) 356.
14 J. H. Christie and R. A. Osteryoung, J. Electroanal. Chem., 49 (1974) 301.

Analytica Chimica Acta, 87 (1976) 37—50

ELECTROCHEMICAL REDUCTION OF TETRAKETOPIPERAZINE

J. L. OWENS and G. DRYHURST

Department of Chemistry, University of Oklahoma, Norman, Okla. 73019 (U.S.A.)

(Received 9th June 1976)

SUMMARY

Between pH 0 and 2, tetraketopiperazine exhibits three d.c. polarographic reduction waves. Wave I is a quasi-reversible, 2e—2H$^+$ reduction of tetraketopiperazine to 2-hydroxytriketopiperazine, which undergoes loss of water by a reverse Michael reaction to give triketopyrazine, i.e., wave I proceeds by an e.c. reaction. Wave II is due to further electrochemical reduction of triketopyrazine in, overall, a 6e process to give 2,5-diketopiperazine. Since wave II depends on formation of triketopyrazine by a chemical reaction of 2-hydroxytriketopiperazine, it is under kinetic control. Wave III has been shown by potentiostatic experiments to proceed by an e.c.e. mechanism. The first step in this process is a 4e—4H$^+$ reduction of tetraketopiperazine to 2,5-dihydroxydiketopiperazine which then undergoes loss of two molecules of water by reverse Michael reactions to give 2,5-diketopyrazine. This is then reduced in a further 4e—4H$^+$ reaction to give 2,5-diketopiperazine.

Electrochemical oxidation of 6,7-dihydroxypteridine at the pyrolytic graphite electrode (PGE) in acidic solution results in the formation of a number of products [1] including tetraketopiperazine (I),

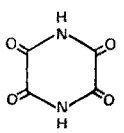

I

the yield of which was measured by a d.c. polarographic method based on the height of the first of its three polarographic reduction waves observed at pH 0—ca. 2.5 [1]. As this appears to give a simple, sensitive, quantitative and qualitative procedure for tetraketopiperazine, a more detailed investigation of the electrochemical reduction mechanism has been carried out, along with an investigation of the limitations of the method.

EXPERIMENTAL

Chemicals

The disodium salt of tetraketopiperazine, synthesized by the method of de Mouilpied and Rule [2], was treated with dilute HCl (e.g., 300 mg of

disodium salt of tetraketopiperazine with 15 ml of 1 M HCl). The precipitated tetraketopiperazine was filtered, washed with cold water, and dried under vacuum. Alternatively, free tetraketopiperazine was obtained by passing a solution of the disodium salt through a column of strong cation-exchange resin (Dowex 50W-X8, H^+ form), followed by lyophilization of the eluent. The purity of tetraketopiperazine, established by elemental analysis and by potentiometric titration with standard 0.1 M sodium hydroxide, was $\geqslant$ 98 %.

2,5-Diketopiperazine (Sigma), oxamide (Matheson, Coleman and Bell) and glyoxylic acid (Aldrich) were used.

Buffer solutions, prepared from reagent-grade chemicals, had ionic strengths of 0.5, except in the case of 1 M acetic acid (pH 2.3) and 1 M H_2SO_4(pH $\approx$ 0).

Thin-layer chromatography was carried out with Brinkmann MN-Polygram Polyamide-6-UV_{254}, Brinkmann Polygram cellulose MN 300 UV_{254}, and Eastman 6060 silica gel precoated sheets, all impregnated with fluorescent indicator. The developing solvents employed were absolute methanol, n-propanol—water (70:30), methanol—glacial acetic acid (90:100), and n-butanol—glacial acetic acid—water (12:3:5). Visualization was accomplished under u.v. light.

The detection of glyoxylic acid was best accomplished by paper chromatography [3] (Whatman No. 1 paper) with ethyl acetate—glacial acetic acid—water (2:1:1) containing bromophenol blue (0.015 %) and sodium acetate (0.05 %); glyoxylic acid gave a yellow spot (r_f 0.37).

2,5-Diketopiperazine was detected by thin-layer chromatography (Brinkmann cellulose t.l.c. plates) with n-butanol—pyridine—water (65:35:65) and visualizing with a spray of starch-iodide reagent (1 % starch; 1 % potassium iodide in water) [4]. A blue-black spot was formed with 2,5-diketopiperazine (r_f 0.58).

Apparatus

Polarography, linear and cyclic sweep voltammetry were carried out with an instrument of conventional operational amplifier design [5] with a function generator [6] patterned after that of Myers and Shain [7]. Polarograms and voltammograms were recorded on a Hewlett-Packard Model 7001A X-Y recorder. Fast-sweep cyclic voltammograms were recorded on a Tektronix Model 5031 Dual Beam Storage Oscilloscope and photographed with a Tektronix Model C-70 Camera.

A.c. polarograms were obtained with a Princeton Applied Research Corporation Model 121 Lock-In Amplifier/Phase Detector both as the source of the alternating signal and as an a.c. voltmeter for detection of the alternating component of the current [8]. A sinusoidal signal having a frequency of 100 Hz or 40 Hz and 10 mV peak-to-peak amplitude was normally employed. A mechanical drop dislodger in conjunction with a dual-channel timing circuit as described by Brown et al. [9] was employed to achieve a reproducible drop time, usually 2.00 s. The second channel of this timing circuit was connected to the remote pen input of the X-Y recorder so that

the current was recorded immediately before the drop was dislodged.

Single and double potential step chronoamperometry was done with a Princeton Applied Research Corporation Model 175 Universal Programmer in conjunction with the electrochemistry system, recorder and oscilloscope described above,

A water-jacketed three compartment cell maintained at a known and constant temperature (±0.1 °C), with each compartment separated by a medium porosity sintered glass disc, was employed for most electrochemical studies. Salt bridges, placed on the counter and reference sides of these discs were prepared by dissolving 4 g of agar (Difco) in 90 ml of water and adding 30 g of KCl. A saturated calomel reference electrode (SCE) and a platinum foil counter electrode were employed. All potentials are referred to the SCE at 25 °C.

The fabrication and preparation of the pyrolitic graphite electrode (PGE) has been described elsewhere [10]. The hanging mercury drop electrode (HMDE) was a Metrohm Model BM5-03 Microburet Electrode of area 2.22 mm^2.

Conventional apparatus was employed for controlled potential electrolysis and coulometry [10] at both mercury pool and pyrolitic graphite electrodes. For large scale electrolyses, each compartment of the electrochemical cell was separated by medium porosity sintered glass frits but acetic acid—agar salt bridges, prepared by dissolving 1.25 g of agar in 20 ml of 1 M acetic acid, were used.

I.r. spectra were recorded on a Beckman IR8 Spectrophotometer (KBr pellets, Barnes Econo-Press), u.v. spectra on a Perkin-Elmer-Hitachi Model 124 Spectrophotometer with 1.00 cm quartz cells, and mass spectra on a Hitachi Model RMU-6E Mass Spectrometer.

Polarographic and voltammetric procedure

Test solutions of tetraketopiperazine were prepared immediately before each study. Solutions were made by dissolving the solid compound in buffer solution of ionic strength 0.5. Deaeration was accomplished by bubbling water-saturated nitrogen through the solution for approximately 10 min. A gentle stream of nitrogen was passed over the surface of the test solution during subsequent experiments.

Isolation and characterization of electrolysis products

For mass electrolysis, typically ca. 160 mg of tetraketopiperazine was dissolved in 160 ml of 1 M acetic acid and electrolyzed at a mercury pool electrode. Acetic acid was selected as the solvent because of its ease of removal by lyophilization.

Electrolysis of Tetraketopiperazine at —0.5 V (Wave I) in 1 M acetic acid. Electrolysis of tetraketopiperazine at —0.5 V on the plateau of wave I in 1 M acetic acid, followed by lyophilization gave a buff-colored solid. Thin-layer chromatography confirmed that all tetraketopiperazine had been reduced.

Attempts to purify this material further were unsuccessful because of its relative instability (see later discussion). It was, however, possible to obtain a mass spectrum of the product (12 eV, 195 °C, *m/e*): 126(M^+, 2.1), 100(2.5), 88(14), 74(3), 60(28), 47(9), 46(35), 45(100) and 44(8). I.r. spectrum (KBr pellet, cm^{-1}): 3300—3400 (strong), 1700 (broad and strong), 1520, 1430, 1410, 1340, 1310, 1230 and 1070. This compound is probably triketopyrazine (see below).

Electrolysis of tetraketopiperazine at —0.95 V (Wave II) or —1.15 V (Wave III) in 1 M acetic acid. Complete electrochemical reduction of tetraketopiperazine on the plateau of wave II or wave III in 1 M acetic acid gave the same products. Thus, after freeze-drying the product solution an off-white fluffy solid was obtained, free of tetraketopiperazine. When this was sublimed at 110 °C and 0.2 mm Hg, a very small amount of white solid collected on the cold finger. D.c. polarography of the sublimate above pH 6 gave two polarographic waves. At pH 10, for example, the $E_{1/2}$ values for the two waves were —1.60 V and —1.25 V, corresponding to that expected for oxamide [11] and glyoxylic acid [12], respectively. Polarography of authentic oxamide and glyoxylic acid gave waves having the same $E_{1/2}$ values as those reported for the product mixture. Further confirmation of the presence of glyoxylic acid was obtained by paper chromatography [3]. Further attempts to separate oxamide and glyoxylic acid were not carried out, but a mass spectrum of the mixture exhibited all of the peaks characteristic of each compound.

The solid remaining after sublimation of the small amount of the glyoxylic acid—oxamide mixture at 110 °C was further sublimed at 170 °C and 0.2 mm Hg pressure. A white solid collected on the cold finger, m.p. = 318 °C (d). Mass spectrum (10 eV, 130 °C, *m/e*): 115(1), 114(M^+, 20), 86(94), 59(27), 44(32), 43(100), 42(11), and 40(17). I.r. spectrum (KBr pellet, cm^{-1}): 3190, 3050, 2990, 2920, 2880, 1690, 1465, 1440, 1335, 1065, 905, 830, and 800. These spectra agreed exactly with those for authentic 2,5-diketopiperazine, and further confirmation was obtained by paper chromatography [4] of the electrolysis product and 2,5-diketopiperazine. The yield of 2,5-diketopiperazine, collected by sublimation at 170 °C, usually corresponded to 0.78—0.80 mole per mole of tetraketopiperazine reduced.

RESULTS AND DISCUSSION

Determination of pK_a values of tetraketopiperazine

Values of the first and second pK_a of tetraketopiperazine were determined by potentiometric titration with standard sodium hydroxide solution. The value of pK_{a_1} was 4.8 and pK_{a_2} was 8.2. The first pK_a corresponds to a neutral molecule-anion equilibrium; pK_{a_2} corresponds to monoanion—dianion equilibrium [2].

D.c. polarography

Tetraketopiperazine hydrolyzes to oxamide, oxalic acid and oxamic acid

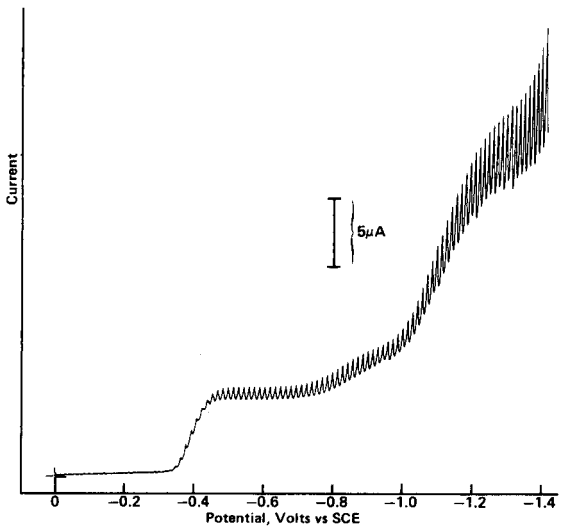

Fig. 1. Typical d.c. polarogram of ca. 1 mM tetraketopiperazine in pH 2.0 McIlvaine buffer.

in neutral aqueous solution [1, 13]. The stability of tetraketopiperazine was therefore studied, as a function of pH and time, by d.c. polarography. Polarograms were run at intervals of ca. 30 min between pH 0 and 7. Below pH 2 the polarographic waves of tetraketopiperazine decreased by less than 10 % over 24 h. At pH 2, the wave heights decreased by only 15—20 % over 24 h. However, at pH 3, hydrolysis was complete in about 4—5 h (i.e., all polarographic waves had disappeared). At pH 4 and above, complete hydrolysis occurred within a few minutes. Accordingly, detailed electrochemical studies of tetraketopiperazine were confined to pH values of 3 and below.

A typical d.c. polarogram of tetraketopiperazine is shown in Fig. 1. Between pH 0 and 6, tetraketopiperazine exhibits three polarographic reduction waves, the $E_{1/2}$ values for which shift linearly to more negative values with increasing pH as given by the following equations:

Wave I (pH 0—6); $E_{1/2} = -0.275 - 0.054$ pH

Wave II (pH 0—6); $E_{1/2} = -0.60 - 0.069$ pH

Wave III (pH 0—6); $E_{1/2} = -0.89 - 0.059$ pH

The diffusion current constant ($I = i_l/Cm^{2/3}\ t^{1/6}$) for wave I is essentially constant between pH 1 and 4 and has an average value of 2.8, which is close to the expected value of 3.2 for a 2e process.* Below pH 1, wave I becomes distorted by a large maximum.

The diffusion current constant for wave II was always appreciably smaller than that for wave I and had an average value of 1.6. In contrast, wave III

*This is the theoretical value calculated for a 2e process for a molecule having a diffusion coefficient of $7.24 \cdot 10^{-6}$ cm^2 s^{-1}. The latter value is that obtained for 5,6-diaminouracil [14], a molecule of similar size to tetraketopiperazine.

generally had a larger diffusion current constant than wave I. Because of the closeness of this wave to background discharge, particularly at higher pH values, it was difficult to obtain a precise value of the diffusion current constant. However, typical values of the diffusion current constant for wave III ranged from about 5 to 7.

The ratio of the limiting current for wave I to the corrected mercury column height (h_{corr}) generally decreased slightly with increasing h_{corr}, indicating that the electrode process was probably not entirely under diffusion control [15], although the temperature coefficient for wave I, 1.5 % per °C at pH 2, was close to that expected for a diffusion controlled process [15]. Subsequent voltammetric and potentiostatic results will indicate that the process responsible for polarographic wave I is partially under kinetic control.

Polarographic wave II of tetraketopiperazine is also at least partially under kinetic control as shown by its large temperature coefficient (6.3 % per °C at pH 2). In addition, at pH 0.5, for example, the limiting current for wave II is independent of h_{corr} as expected for a kinetically controlled process [15].

Because of the rather close proximity of wave III to background discharge, it was not possible by means of i_l vs. h_{corr} and temperature studies to deduce the nature of the process controlling this wave with any real confidence, but potentiostatic methods were of help (see below).

The wave I process of tetraketopiperazine exhibited many of the characteristics of a reversible polarographic reaction, i.e., $dE_{1/2}/d(pH)$ is close to the 59 mV expected for a reversible process involving an equal number of electrons and protons. In addition, the $E_{1/2}$ for wave I is independent of the mercury droptime [15]. However, a plot of E_{DME} vs. $\log i/(i_l - i)$ yielded a slope of 42.7 mV which is larger than the predicted value of 30 mV for a perfectly reversible, uncomplicated 2e reaction.

A.c. polarography

A.c. polarography of tetraketopiperazine solutions was carried out primarily to discover if the compound was adsorbed at the DME. Over the pH range 0.5—2, a.c. polarograms of tetraketopiperazine exhibited no base current depression, compared with solutions of supporting electrolyte, indicating that the compound is not adsorbed to any significant extent [16].

Linear and cyclic sweep voltammetry

At both the PGE and HMDE, tetraketopiperazine exhibits three voltammetric reduction peaks (I_c, II_c and III_c) corresponding to polarographic waves I, II and III, respectively. Oxidation peaks are not observed on the initial sweep towards positive potentials at a clean PGE. Cyclic voltammetry, however, shows that once reduction peak I_c has been scanned, an oxidation peak (peak I_a) is observed on the reverse sweep. Peaks I_c and I_a form an almost reversible couple. A typical cyclic voltammogram of tetraketopiperazin is presented in Fig. 2.

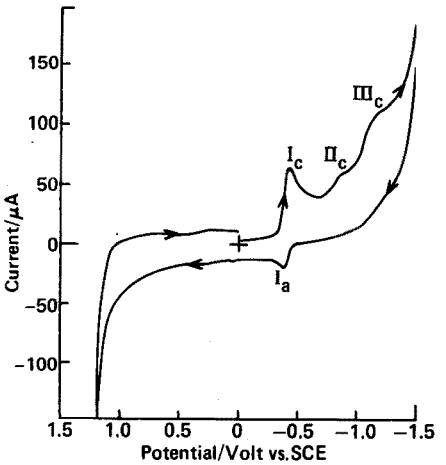

Fig. 2. Cyclic voltammogram of 1 mM tetraketopiperazine in pH 2.0 McIlvaine buffer. Sweep rate 0.2 V s^{-1}. Initial potential 0.0 V; initial sweep towards negative potentials.

The experimentally determined peak current function ($i_p/AC\nu^{1/2}$) for peak I_c of tetraketopiperazine at the HMDE, was compared with that calculated theoretically [17] (1801 μA $cm^{-2}mM^{-1}V^{-1/2}s^{1/2}$) for an uncomplicated, 2e, reversible electrode reaction from eqn. (1):

$$i_p = 2.69 \cdot 10^5 AD^{1/2}\nu^{1/2}n^{3/2}C \qquad (1)$$

where all terms have their usual electrochemical significance. The experimental peak current function for peak I decreased from 2180 μA $cm^{-2}mM^{-1}V^{-1/2}s^{1/2}$ at a sweep rate of 5 mV s^{-1} to ca. 1740 μA $cm^{-2}mM^{-1}lV^{-1/2}s^{1/2}$ at a sweep rate of 50 V s^{-1}. The fact that the experimental peak current function for peak I_c decreases with increasing sweep rate suggests that a chemical reaction follows or precedes the electron-transfer step (i.e., an e.c. or c.e. mechanism) [17]. The additional fact that at sweep rates exceeding 50 mV s^{-1} the experimental peak current function is somewhat smaller than predicted theoretically for an uncomplicated linear diffusion-controlled process also suggests that the overall electrode process may contain a small contribution from a preceding chemical reaction [17].

That an irreversible chemical reaction follows the initial electron-transfer reaction of peak I_c is quite clear from the cyclic voltammetry of tetraketopiperazine. For example, at pH 2.0 at a sweep rate of 0.2 V s^{-1} (Fig. 2) it is clear that peak I_a is appreciably smaller than peak I_c, typical of an e.c. process. With increasing sweep rate peak I_a grows relative to peak I_c as would be expected for an e.c. process.

For an uncomplicated reversible system, the potential increment (ΔE_p) between the reduction and oxidation peaks observed by cyclic voltammetry should be $59/n$ mV [18], where n is the number of electrons involved in the

electrode reaction. In the case of peak I_c and I_a of tetraketopiperazine, ΔE_p is 80 mV at a sweep rate of 0.02 V s^{-1} and decreases to 40 mV at sweep rates of 0.5 V s^{-1}. This decrease of ΔE_p with increasing sweep rate also suggests the involvement of complicating chemical processes in the overall peak I_c—I_a electrode reactions. The effect of sweep rate on ΔE_p for a variety of electrode reaction schemes has been discussed by Nicholson and Shain [17]. The behavior noted for peaks I_c and I_a of tetraketopiperazine corresponds to the behavior expected for an e.c.-type reaction or an electrode reaction where the electron-transfer process is complicated by both preceding and follow-up reactions (i.e., c.e. and e.c. processes). At no sweep rate did ΔE_p become smaller than 40 mV, indicating that the peak I_c process is probably quasi-reversible.

Peaks II_c and III_c of tetraketopiperazine gave no evidence for any reverse peaks on cyclic voltammetry at sweep rates up to 50 V s^{-1}.

Controlled potential electrolysis and coulometry

Wave 1. Electrochemical reduction of tetraketopiperazine on the plateau of wave I at pH 0.5 and 2.0 at both mercury pool and pyrolitic graphite electrodes yielded a faradaic *n*-value of 2 ± 0.2 (Table 1). After completion of the electrolysis, d.c. polarography and voltammetry at the PGE showed the presence of only wave II or peak II_c. Wave II, however, was about three times as high as the initial wave I height. The fact that only wave II remains after electrolysis at wave I suggests that the wave III and peak III_c process represents an alternative pathway to wave I or peak I_c for the reduction of tetraketopiperazine. After electrolysis at pH 0.5, the u.v. spectrum of the product solution exhibited a small, broad peak (λ_{max} = ca. 260 nm) and a further peak at 215—220 nm. At pH 2, the electroreduction product showed a single, small broad peak at ca. 260 nm.

By monitoring the height of polarographic wave II, formed after complete electrochemical reduction of tetraketopiperazine at wave I potentials, it became clear that the compound responsible for wave II was rather unstable; the limiting current for wave II under the latter conditions decreased by ca. 23 % in 24 h, and the wave disappeared completely in 4—5 d. Examination of the solution after complete disappearance of wave II showed the presence of oxamide and glyoxylic acid (see Experimental). Quantitative analysis proved that the species responsible for wave II decomposes almost quantitatively to oxamide and glyoxylic acid.

Wave II. Electrochemical reduction of tetraketopiperazine at wave II without first removing wave I gave a faradaic *n*-value of 7.8 ± 1.2 (Table 1). Since wave I is a 2e process under coulometric conditions, wave II appears to be a ca. 6e process. If tetraketopiperazine is first electrolyzed at wave I then, as mentioned previously, only wave II remains. However, after removal of wave I, wave II is about three times the original height of wave I. Coulometry at wave II potentials immediately after electrolysis at wave I, gives *n*-values between 5—6 in agreement with the above polarographic observations. After

TABLE 1

Coulometric *n*-values for the electrochemical reduction of tetraketopiperazine

pH	Electrode	Controlled potential (V)	Initial concn. of tetraketopiperazine (mM)	*n*-value[f]
			Wave I	
0.5[a]	Hg[b]	−0.40	1.0	1.91
2.0[c]	Hg[b]	−0.48	1.0	1.90
2.0[c]	PGE	−0.50	1.0	2.2
			Wave II	
2.0[c]	Hg[b]	−0.95	0.1	8.6[d]
2.0[c]	Hg	−0.95	0.2	8.5[d]
2.0[c]	Hg	−0.95	0.3	7.1[d]
2.0[c]	Hg	−0.95	0.5	7.2[d]
2.0[c]	Hg	−0.95	1.0	6.6[d]
2.0[c]	Hg	−0.95	2.0	6.9[d]
2.0[c]	Hg	−0.95	5.0	7.4[d]
2.0[c]	Hg	−0.95	0.2	5.5[e]
0.5[a]	Hg	−0.80	0.2	5.4[e]
0.5[a]	Hg	−0.80	0.1	6.0[e]
			Wave III	
0.5[a]	Hg	−0.95	1.0	8.0[g]
2.0[c]	Hg	−1.20	1.0	7.8[g]

[a]Chloride supporting electrolyte (KCl + HCl). [b]Stirred mercury pool electrode. [c]McIlvaine buffer. [d]Direct electrolysis of tetraketopiperazine at wave II potentials. [e]Electrolysis first at wave I then, when complete, further electrolysis at wave II. *n*-Value refers to value obtained only at wave II potentials. [f]Average of at least two replicate values. [g]Direct electrolysis of tetraketopiperazine on wave III.

complete removal of wave II by electrolysis, no polarographic reduction waves remained and the product solution gave no u.v. spectrum.

Wave III. Controlled potential electrolysis and coulometry of tetraketopiperazine at wave III potentials gave faradaic *n*-values close to 8 (Table 1).

Mass electrolysis, product isolation and characterization

To prepare a sufficient amount of material for product characterization, solutions of up to 5 mM concentration were electrolyzed at a mercury pool electrode; normally 1 M acetic acid (pH 2.3) medium was used. The behavior of tetraketopiperazine in this medium was representative of its behavior at lower and higher pH.

The product of wave I could not be identified unequivocably because of its relative instability. It decomposed slowly in aqueous solution to oxamide and glyoxylic acid (see Experimental). The crude wave I product gave a fairly characteristic mass spectrum with an apparent molecular ion at m/e = 126. A compound with this molecular weight which could decompose to glyoxylic acid and oxamide is triketopyrazine (III). This could be formed by a $2e—2H^+$ reduction of tetraketopiperazine (see below). Compound III has not previously

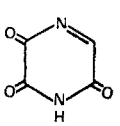
III

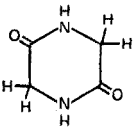
VIII

been reported in the literature. The major product of electrochemical reduction of tetraketopiperazine at wave II and wave III potentials is 2,5-diketopiperazine (VIII) (see Experimental).

Potentiostatic studies

The evidence presented above suggests that tetraketopiperazine is reduced electrochemically in the wave I process by a 2e reaction to give triketopyrazine (III), which further decomposes slowly to oxamide and glyoxylic acid. In order to form III, it seems reasonable that an e.c. reaction occurs (see below). Cyclic voltammetry of the peak I_c—I_a couple at both the HMDE and PGE also supports the fact that polarographic wave I or voltammetric peak I_c is an e.c. reaction. However, d.c. polarographic mercury column height studies, and cyclic voltammetric peak height and peak potential studies, suggest that wave I/peak I_c is not completely under diffusion control but might have a small kinetic contribution. To verify the latter observation, potentiostatic current-time curves were measured over the pH range 0—2 for 0.05—5 mM solutions of tetraketopiperazine. Potentials were selected which were sufficiently negative of peak I_c that the surface concentration of tetraketopiperazine would be zero, yet not sufficiently negative to cause overlap with peak II_c. All potentiostatic experiments were carried out at the HMDE for periods up to 6—8 s and showed that the product $i_t t^{1/2}$ increased somewhat with increasing time. The Cottrell equation

$$i_t t^{1/2} = \frac{nFAD^{1/2}C}{\pi^{1/2}} \qquad (2)$$

predicts that for a linear diffusion-controlled electrode reaction, $i_t t^{1/2}$ should be constant [19]. An increase of $i_t t^{1/2}$ with time is an indication that the electrode process is under some degree of kinetic control. Because of this small but significant kinetic contribution to the wave I/peak I_c process, it was not possible to investigate the heterogeneous kinetics of the electron transfer process by, for example, cyclic voltammetric methods, or to employ double potential step chronoamperometry to investigate the mechanism and kinetics of the chemical reaction that clearly follows the initial electron-transfer process.

Potentiostatic current time curves, however, could be employed to investigate the wave III/peak III_c process; the potential of a stationary HMDE was stepped to a value corresponding to the plateau of polarographic wave III of tetraketopiperazine and the resultant current was measured as a function of time. Some typical normalized current ($i_t/FAD^{1/2}C$, where i_t is the current at

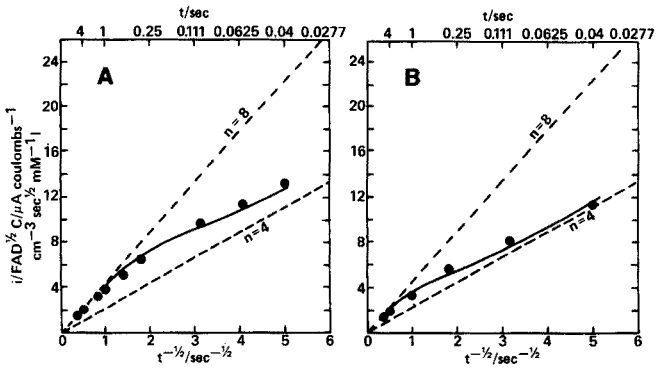

Fig. 3. Comparison of experimental and theoretical current—time curves for the electrochemical reduction of tetraketopiperazine at polarographic wave III potentials at the HMDE. (A) pH 0.5 KCl/HCl supporting electrolyte, $k_f = 4\ s^{-1}$; (B) pH 2.0 McIlvaine buffer, $k_f = 1\ s^{-1}$. (•) Experimental values, (—) theoretical curve for the given rate constants calculated from eqn. (4); (---) theoretical curves for uncomplicated 4e and 8e transfer processes.

time t(s) after application of the potential step) versus time (or $t^{-1/2}$) curves are presented in Fig. 3. The variation of current with time in these plots suggested an e.c.e.-type of electrode reaction which may be represented as:

$$\mathrm{A} \xrightarrow{n_1 e} \mathrm{B} \xrightarrow{k_f} \mathrm{C} \xrightarrow{n_2 e} \mathrm{D} \qquad (3)$$

Regardless of the reversibility of the chemical reaction interposed between the two electron-transfer steps, the normalized current is given by

$$i_t/\mathrm{FA}D^{1/2}C = \frac{n_1 + n_2\,(1-e^{-k_f t})}{t^{1/2}\pi^{1/2}} \qquad (4)$$

where n_1 is the number of electrons in the first charge transfer step; n_2 is the number of electrons in the second charge transfer step; and k_f is the rate constant for the interposed chemical reaction [20]. All other terms have their usual electrochemical significance. There are clearly two limiting cases of eqn. (4): when $k_f = \infty$ and when $k_f = 0$. When $k_f = \infty$, the interposed chemical reaction is so rapid that an $n_1 + n_2$ electron process occurs. When $k_f = 0$, only an n_1 electron process takes place. For each limiting case, eqn. (4) reduces to the Cottrell equation [19] for $(n_1 + n_2)$e and n_1e processes, respectively. The normalized current—time relationships for 4e and 8e processes calculated by the Cottrell equation are shown in Fig. 3A and B. At short times the current response for the wave III/peak III_c process of tetraketopiperazine is close to that expected for a 4e reaction; at longer times it shifts to that expected for an 8e process. Such a transition is expected for an e.c.e. electrode reaction [20]. The value of k_f at each pH shown in Fig. 3 was obtained by the working curves prepared by Alberts and Shain [20].

The theoretical curves shown in Fig. 3 were calculated from the computed value of k_f along with eqn. (4). It is clear from Fig. 3A and B that the transition from the 4e to 8e reaction takes longer at pH 2 than at pH 0.5. This implies that the value of k_f decreases with increasing pH. The results presented in Fig. 3 reveal that at pH 2, $k_f = 1\ s^{-1}$ and at pH 0.5, $k_f = 4\ s^{-1}$.

Reaction scheme

Wave I/peak I_c. The height of the d.c. polarographic wave I, voltammetric peak I_c and coulometry all indicate that the electrode reaction involves 2e. Polarography, voltammetry and potentiostatic experiments suggest that the electrode process is predominantly, but not entirely under diffusion control. The evidence also suggests that the electrode reaction has a minor component of kinetic control. The peak I_c (wave I) process is quasi-reversible as shown by the appearance of peak I_a on cyclic voltammetry. In addition, the peak I_c process is clearly an e.c. mechanism as shown by the increase of wave I_a with respect to peak I_c with increasing sweep rate. The product of the wave I/peak I process appears to be triketopyrazine; this decomposes to oxamide and glyoxylic acid, which have been identified. Accordingly, the wave I/peak I_c process is proposed to be a $2e—2H^+$ reduction of tetraketopiperazine (I, Fig. 4) to 2-hydroxytriketopiperazine (II, Fig. 4). This then undergoes a reverse Michael reaction to give triketopyrazine (III). This reaction is essentiall

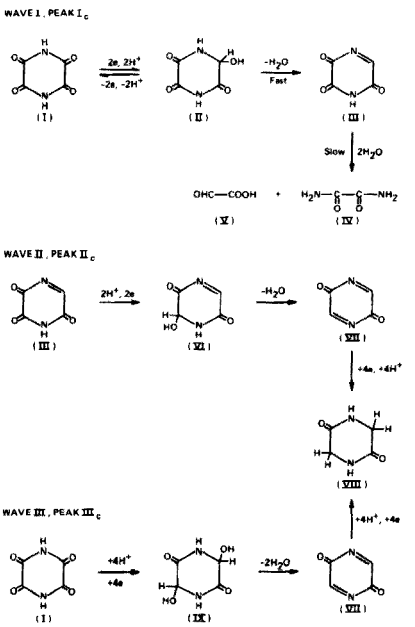

Fig. 4. Proposed reaction scheme for the three polarographic/voltammetric waves of tetraketopiperazine.

identical to that proposed by Furlani [21] for the electrochemical reduction of 2,3-dihydroxyquinoxaline.

The exact nature of the process contributing to the partial kinetic control of the wave I/peak I_c process is not known. Probably, some hydration of tetraketopiperazine occurs, and dehydration of the hydrated species imparts some kinetic control to the electrode process in much the same way as is observed for alloxan, a similar molecule [22].

Hydrolysis of III (Fig. 4) would readily give oxamide (IV) and glyoxylic acid (V).

Wave II/peak II_c. Elimination of wave I of tetraketopiperazine by controlled potential electrolysis leaves only wave II which is totally irreversible and about three times the original height of wave I. The height of the polarographic wave II (after elimination of wave I) and coulometry clearly indicate that it is a 6e process. The product of the electrolysis is 2,5-diketopiperazine. Accordingly, the kinetically controlled wave II electrode reaction must involve the reduction of triketopyrazine (III, Fig. 4). By analogy with the wave I process it is proposed that a similar $2e-2H^+$ reduction of the 1,2-dione grouping occurs to give 2,5-diketo-6-hydro-6-hydroxypyrazine (VI). A reverse Michael reaction on VI gives 2,5-diketopyrazine (VII). Further $4e-4H^+$ reduction of VII gives 2,5-diketopiperazine (VIII). The fact that polarographic wave II is three times the height of original wave I after removal of the latter indicates that the entire 6e wave II process can occur within polarographic droptimes (i.e., 2s). This indicates that the reverse Michael reaction (VI→VII) is very rapid. Because of this fact, and the tendency for III to decompose to oxamide and glyoxylic acid, no attempt was made to measure the kinetics of the dehydration step.

Wave III/peak III_c. The wave III process is totally irreversible and, as indicated by potentiostatic studies, is an e.c.e. reaction. Under potentiostatic conditions an initial 4e reduction of tetraketopiperazine occurs, followed by a chemical reaction to give a product which is reduced in a further 4e reaction to give 2,5-diketopiperazine. The proposed reaction scheme therefore involves an initial $4e-4H^+$ reduction of two carbonyl groups of tetraketopiperazine (I, Fig. 4) to give 2,5-dihydroxydiketopiperazine (IX). By analogy with reactions proposed for waves I and II, compound IX undergoes a reverse Michael reaction, losing two molecules of water to form 2,5-diketopyrazine (VII). Further $4e-4H^+$ reduction of VII gives 2,5-diketopiperazine (VIII). It is likely that the loss of water from IX to give VII proceeds in two steps, each step involving loss of one molecule of water. In view of the fact that the reaction VI→VII of wave II is very fast, it seems reasonable to assume that the k_f value computed for the chemical reaction involved in wave III refers to the loss of the first molecule of water to form VI.

Analytical utility of d.c. polarography

Linear limiting current vs. concentration curves were obtained for the first wave (wave I) of tetraketopiperazine in solutions of pH 1—2.5. For practical

purposes, pH 2 is probably the pH of choice, since tetraketopiperazine is reasonably stable at this pH and wave I is well defined and free of any complicating maxima. Linear concentration curves at pH 1—2.5 could be obtained between 10^{-5} M and $>2 \cdot 10^{-3}$ M, which was the concentration range of interest in these investigations [1]. However, much lower concentration levels of tetraketopiperazine may be determined by pulse or differential pulse polarography.

The authors thank the National Science Foundation for partial support of this work.

REFERENCES

1 D. L. McAllister and G. Dryhurst, J. Electroanal. Chem. Interfacial Electrochem., 55 (1974) 69.
2 A. T. de Mouilpied and A. Rule, J. Chem. Soc., 91 (1907) 176.
3 R. D. Hartley and G. J. Lawson, J. Chromatogr., 4 (1960) 410.
4 H. N. Rydon and P. W. G. Smith, Nature, 169 (1952) 922.
5 G. Dryhurst, M. Rosen and P. J. Elving, Anal. Chim. Acta, 42 (1968) 143.
6 D. L. McAllister and G. Dryhurst, Anal. Chim. Acta, 64 (1973) 121.
7 R. L. Myers and I. Shain, Chem. Instrum., 2 (1969) 203.
8 D. L. McAllister and G. Dryhurst, Anal. Chim. Acta, 58 (1972) 273.
9 E. R. Brown, T. E. McCord, D. E. Smith and D. D. DeFord, Anal. Chem., 38 (1966) 1119.
10 D. L. McAllister and G. Dryhurst, J. Electroanal. Chem. Interfacial Electrochem., 47 (1973) 479.
11 D. L. McAllister, J. Pinson and G. Dryhurst, Anal. Chim. Acta, 67 (1973) 415.
12 M. Takagi, S. Ono and T. Wasa, Rev. Polarogr., 11 (1963) 210.
13 Y. T. Pratt, in Heterocyclic Compounds, Vol. 6, R. C. Elderfield (Ed.), Wiley, New York, 1957, p. 454.
14 B. M. Visinski and G. Dryhurst, J. Electroanal. Chem. Interfacial Electrochem., 70 (1976) 199.
15 L. Meites, Polarographic Techniques, 2nd edn., Wiley, New York, 1965.
16 B. Breyer and H. H. Bauer, Alternating Current Polarography and Tensammetry, Interscience, New York, 1963, pp. 267—269.
17 R. S. Nicholson and I. Shain, Anal. Chem., 36 (1964) 706.
18 R. N. Adams, Electrochemistry at Solid Electrodes, Marcel Dekker, New York, 1969, pp. 145—147.
19 P. Delahay, New Instrumental Methods in Electrochemistry, Interscience, New York, 1954, p. 51.
20 G. S. Alberts and I. Shain, Anal. Chem., 35 (1963) 1859.
21 C. Furlani, Gazz. Chim. Ital., 85 (1955) 1646.
22 B. H. Hansen and G. Dryhurst, J. Electrochem. Soc., 118 (1971) 1747.

Analytica Chimica Acta, 87 (1976) 51—57

VOLTAMMETRIC BEHAVIOUR OF HYPONITRITE ION AND ITS ANALYTICAL APPLICATIONS

A. CINQUANTINI, G. RASPI and P. ZANELLO

Istituto di Chimica Generale, Università di Siena, 53100-Siena (Italy)

(Received 14th April 1976)

SUMMARY

Hyponitrite is electrochemically oxidized at a platinized platinum microelectrode. The overall process is characterized by an appreciable overvoltage; in alkaline solution nitrite and nitrous oxide are the ultimate products. The wave is well shaped and diffusion-controlled, and can be used for the voltammetric determination of microamounts of hyponitrite. Alternatively, the oxidation of hyponitrite by hypochlorite in basic solution can be used for the direct determination of hyponitrite with amperometric end-point detection. The limits of determination of the voltammetric and amperometric methods are about 10^{-4} M and $5 \cdot 10^{-4}$ M, respectively.

More than a hundred years ago Divers [1] first identified hyponitrites among the reduction products of nitrite with sodium amalgam, but comparatively little attention has been paid to these compounds, although several authors have demonstrated their potential interest. The elucidation of the structure [2—6] and the decomposition pathways [7—10] of hyponitrite at different pH values have been studied, and the rôle played by this ion as an intermediate in the Nitrogen Cycle has been emphasized [11, 12]. The reducing properties of hyponitrites were established long ago [1, 13—15], and in 1914 Oesterheld [16] reported data on electrolysis of alkaline solutions of hyponitrite. However, the voltammetric behaviour of hyponitrite has not been examined previously. In the work described here the voltammetric behaviour of hyponitrite ion in aqueous solutions at different pH values was investigated at a platinum microelectrode for which the diffusion layer was periodically renewed. Analytical applications of the work are: (a) an amperometric method for the standardization of alkaline hyponitrite solution, even in the presence of an excess of nitrite and carbonate ions, which represents a convenient alternative to the existing techniques; and (b) a voltammetric determination of micro amounts of hyponitrite in the presence of different ions in hydroxide media. Both methods are sensitive, reproducible and accurate, and are generally preferable to earlier methods [13—21].

EXPERIMENTAL

Reagents

All reagents were of analytical grade. Anhydrous sodium hyponitrite was prepared by reduction of nitrite with sodium amalgam by a modification [2] of Diver's method [1]. The product was purified by precipitation as the silver salt, which was reconverted to the sodium salt by treatment with sodium iodide [22]. Alternatively, sodium hyponitrite was prepared by the method of Jones and Scott [23], who used a condensation reaction between hydroxylamine and ethyl nitrite in the presence of sodium ethoxide in ethanolic solution. Both methods gave products of similar characteristics, with low yields (about 13 %); the sodium hyponitrite, tested by direct titration with standard hydrochloric acid [19], was found to be 100 % pure. Unfortunately, this titration cannot show the presence of sodium carbonate in the sample, since the molecular weights of the two salts are identical and the pK_2 values of carbonic and hyponitrous acids are very close. Attempts to determine the hyponitrite content gravimetrically as $Ag_2N_2O_2$ [13, 17] gave erratic and unacceptable results, probably because of coprecipitation of silver carbonate and silver nitrite. For these reasons, the analyses of samples of sodium hyponitrite were based on the reaction between hypochlorite and hyponitrite in alkaline solution, as suggested by Raschig [14].

$$N_2O_2^{2-} + OCl^- + H_2O \rightarrow Cl^- + 2\,NO + 2\,OH^-$$

As this reaction is slow in alkaline solution at room temperature, its analytical use involves adding an excess of reagent and back-titrating the excess with an appropriate reducing agent, e.g. arsenic(III) oxide. On the basis of the results obtained, the following procedure is suggested. Weighed amounts (25—40 mg) of sodium hyponitrite are added to a known excess of carefully deaerated standard hypochlorite solution, buffered at pH 13. The nitric oxide produced is removed by bubbling pure nitrogen through the solution for about 10 min, and then standard arsenic(III) oxide solution is added to a potentiometric end-point. This method showed the sodium hyponitrite to be 90—95 % pure, the major impurity being sodium carbonate, which arises from atmospheric carbon dioxide absorbed by the alkaline liquor during the preparation and cannot be removed, as unreacted sodium nitrite is, by recrystallization of sodium hyponitrite from ethanolic solution.

The sodium hyponitrite was kept in a vacuum desiccator over P_2O_5; its solutions were prepared and standardized immediately before use.

Apparatus

Voltammetry. A cell with a platinum electrode with periodical renewal of the diffusion layer was used [24]. The measurements were made with the three-electrode technique at 25 ± 0.1 °C with a Princeton Applied Research (PAR) Electrochemistry System Model 170. A platinized electrode was used because the process is characterized by a very high degree of irreversibility on

bright platinum electrodes. The conditions for the platinization were: cleaning of the electrode with nitric acid, electrolytic hydrogen development on its surface for 1—2 min in a dilute sulphuric acid solution and platinizing for 7 s with a current density of about 1.1 A cm^{-2} in a 3 % chloroplatinic acid—0.025 % lead acetate solution. Between any two treatments, the electrode was washed carefully with distilled water. Before each set of measurements, the electrode was platinized freshly, after the previous layer had been dissolved in boiling dilute aqua regia. Both the reference and the auxiliary electrodes were saturated mercury(I) sulphate electrodes, connected to the cell by bridges of silica gel and sodium sulphate in the ratio 3:2. The solution was deoxygenated by passing pure nitrogen gas for 10 min. All the potential values reported here are referred to the saturated calomel electrode.

The pH values of the supporting electrolytes were measured with a Metrohm E388 potentiometer and a glass electrode, except for the 1 M and 0.1 M KOH solutions. In these cases the pH was taken as 14.0 and 13.0, respectively. The ionic strength was kept at unity by adding potassium nitrate, whenever necessary.

Coulometric measurements and controlled potential electrolysis. For controlled potential coulometry, 50 ml of a 5.0 mM solution of sodium hyponitrite in 0.1 M KOH were placed in the above-mentioned cell, equipped with a platinized platinum working electrode (area, 4 cm^2) polarized at + 0.450 V; the nitrogen flow was continued during the electrolysis in order to stir the solution efficiently. For macroscale electrolysis, a cell equipped with a magnetic stirrer was used; the working electrode compartment was filled with deaerated 0.1 M KOH solution containing about 350 mg of sodium hyponitrite. This compartment was sealed with a rubber stopper which held a stopcock connected to a gas buret into which the nitrous oxide produced was flushed with nitrogen gas.

Identification and determination of electrolysis products. Nitrite ion produced by electrolysis was identified from the u.v. spectra; then solid NaH_2PO_4 was added to buffer the solution at pH 8 and nitrite was determined voltammetrically [25] by the standard addition method. The only other product of electrolysis was nitrous oxide, which was detected by gas chromatography on silica gel at room temperature, as suggested by Szulczewski and Higuchi [26]. These results agree with the data obtained by Oesterheld [16] on the electrolysis of alkaline solutions of hyponitrite.

RESULTS AND DISCUSSION

Figure 1 shows the current—voltage curves obtained by changing the voltage applied to the platinum microelectrode towards more positive values, in the intervals 0 to + 0.5 V (curve a) and + 0.4 to + 1.1 V (curve b), in deaerated solutions containing 1.5 mM sodium hyponitrite buffered at pH 13.0 and 1.3, respectively. Reproducible measurements are impossible in the pH range 4—12, where the decomposition rate of hyponitrite solutions is too

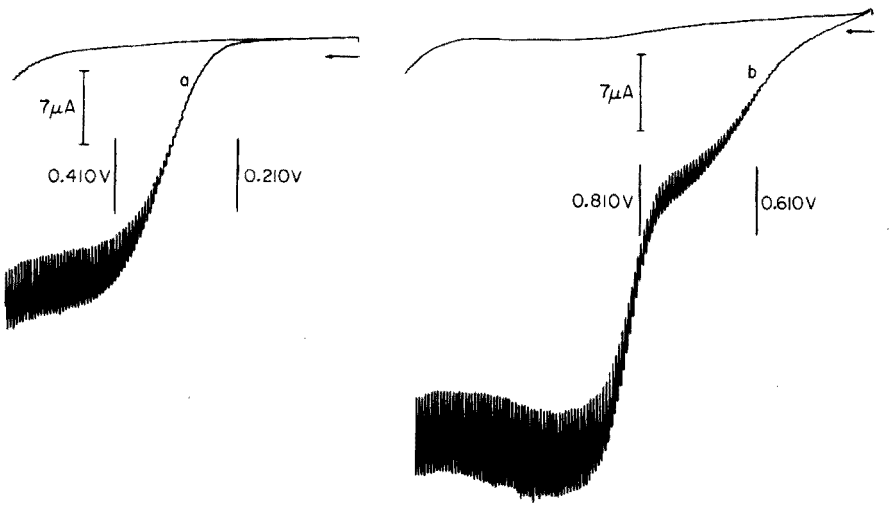

Fig. 1. Voltammetric curves obtained with $1.5 \cdot 10^{-3}$ M $Na_2N_2O_2$ in (a) 0.1 M KOH + 0.9 M KNO_3 solution, (b) 0.25 M $KHSO_4$ + 0.25 M K_2SO_4 solution.

large, as shown by many workers [7—10]. The electrooxidation of hyponitrite ion in acid solution gives rise to two polarographic steps (curve b); the amplitude of the two waves is about the same, suggesting that the same number of electrons is involved in the two processes. Since the more anodic wave corresponds to the oxidation of nitrite to nitrate [25], the less anodic wave must correspond to the oxidation of hyponitrite to nitrite.

Since nitrite reacts with hyponitrite in acidic solution [7, 8] to give nitrate and nitrogen as the final products, it seemed better from the analytical viewpoint to study the electrooxidation of hyponitrite in strongly alkaline solutions (pH 12—14), where it is fairly stable and there is no interaction between these ions.

The electrooxidation of strongly alkaline solutions of sodium hyponitrite is characterized by a well shaped wave (curve a), which is independent of the direction of recording, and whose mean limiting current is proportional to the concentration in the range 0.1—1.5 mM (Table 1). The $E_{\frac{1}{2}}$ value depends on the pH of the solution changing from + 0.306 V at pH 12.2 to + 0.333 at pH 14; increase of alkalinity causes a half-wave potential displacement towards more positive values of about 14 mV/pH unit. Consequently, the wave is obscured by oxygen discharge when the hydroxide activity exceeds unity. Coulometric measurements in alkaline solution are complicated by the slow auto-decomposition of hyponitrite to nitrous oxide and hydroxide, so that the correlation between the total number of Faradays and moles of sodium hyponitrite used is erratic or unacceptable (Table 2). However, more meaningful data can be achieved by determining the nitrite ion produced by exhaustive electrooxidation of sodium hyponitrite at controlled potential: it was found that 1 Faraday yields about 0.5 mol of nitrite ion. Since the only

TABLE 1

Effect of hyponitrite ion concentration on wave amplitude at pH 13.0

$C_{N_2O_2^{2-}}$ (mM)	$\bar{i}_d$ (μA)	$\bar{i}_d/C$ (μA mmol^{-1} l)	$C_{N_2O_2^{2-}}$ (mM)	$\bar{i}_d$ (μA)	$\bar{i}_d/C$ (μA mmol^{-1} l)
0.100	0.71	7.1	0.666	4.81	7.2
0.141	1.01	7.2	0.789	5.59	7.1
0.200	1.40	7.0	0.909	6.46	7.1
0.278	2.01	7.2	1.02	7.38	7.2
0.411	2.92	7.1	1.25	9.06	7.2
0.540	3.79	7.0	1.50	10.50	7.0

TABLE 2

Coulometry of hyponitrite in 0.1 M KOH at a platinized platinum anode (4 cm^2) with a controlled potential of + 0.450 V vs. SCE

$Na_2N_2O_2$ taken (mmol)	Faradays consumed	$NaNO_2$ found (mmol)	Faradays mol $NaNO_2$
0.185	$1.7 \cdot 10^{-4}$	0.092	1.85
0.242	$2.5 \cdot 10^{-4}$	0.132	1.89
0.580	$5.9 \cdot 10^{-4}$	0.317	1.86

other product of electrooxidation is nitrous oxide, the overall electrode process is most probably represented by the equation

$$2\ N_2O_2^{2-} + 2\ OH^- \rightarrow 2\ NO_2^- + N_2O + H_2O + 4\ e^-$$

The process is characterized by an appreciable overvoltage: logarithmic analysis of the curve shows that the ratio $\Delta E/\Delta\log[(i_d - i)/i]$ is 72 mV, which is well above the theoretical value of 30 mV for a reversible process. The mean limiting current, $\bar{i}_d$, is related to the diffusion coefficient, D, by the equation $\bar{i}_d = a + (b/t_{tot})\ (2t_{tot}^{\frac{1}{2}} - 1.5t_p^{\frac{1}{2}})$, where $a = nFADC/r$, $b = nFAD^{\frac{1}{2}}C/\pi^{\frac{1}{2}}$; n, r, C and A have their usual meanings, t_p is the washing period of the electrode (0.025 s) and t_{tot} is the period between two subsequent washings (5 s). When the measured values of $\bar{i}_d$, A and r were inserted in this expression, the diffusion coefficient for hyponitrite was found to be $0.58 \cdot 10^{-5}$ cm^2 s^{-1} at 25 °C.

Voltammetric curves were also recorded in the temperature range 5—40 °C: the half-wave potential shifts to less positive values with a mean variation of 1.7 mV/degree ($E_{\frac{1}{2}}$ decreases from + 0.337 V at 5 °C to + 0.278 V at 40 °C in 0.1 M potassium hydroxide). The mean limiting current increases by 1.4 % per degree.

ANALYTICAL APPLICATIONS

Amperometric titrations of hyponitrite solutions

Several methods have been proposed for the determination of hyponitrite ion — gravimetric [13, 17], acidimetric [14, 15, 18, 19], oxidimetric [15, 18] and potentiometric [2, 20, 21] — but they are generally laborious and time-consuming. Moreover, hyponitrite is usually contaminated by nitrite and carbonate: carbonate especially makes the argentimetric and acidimetric methods inapplicable. As shown in the Experimental, alkaline solutions of recrystallized sodium hyponitrite can be standardized by oxidizing with an excess of hypochlorite [14] and back-titrating with arsenite to a potentiometric end-point; but this procedure is subject to large errors when nitrite is present, because nitrite reacts slowly with hypochlorite in alkaline solution.

The platinum microelectrode allows the oxidation of hyponitrite to be studied in hydroxide solutions. The corresponding wave is fairly well shaped and its limiting current, which is diffusion-controlled, can be used to follow the decrease in the hyponitrite concentration during its direct titration with hypochlorite. Hydroxylamine and α-hyponitrate interfere seriously. The reaction rate between hyponitrite and hypochlorite is sufficiently high to make the titration feasible even in presence of large (5-fold) quantities of nitrite. The results of some titrations are shown in Table 3. On the basis of the results obtained, the following procedure is suggested.

Procedure. Place 40 ml of 0.1 M potassium or sodium hydroxide solution in a polarographic cell thermostatted at 25 °C. Remove oxygen by bubbling purified nitrogen and add 3—20 mg of sodium hyponitrite. Titrate with 0.04 M calcium hypochlorite solution at + 0.450 V (SCE), bubbling nitrogen through the solution after each addition of the reagent. After correction for dilution, plot the results of the mean limiting diffusion current observed, after stabilization, against the volume of the reagent added. Determine the end-point from the intersection of these points with the zero line which corresponds to the residual current of the supporting electrolyte at + 0.450 V.

Voltammetric determination of micro amounts of hyponitrite

The anodic wave at the platinized platinum electrode is well shaped and the limiting current is strictly proportional to the hyponitrite concentration, so that a voltammetric determination of hyponitrite is possible: the proposed method gives reproducible results for hyponitrite concentrations down to $1 \cdot 10^{-4}$ M.

The effects of foreign anions on the determination of hyponitrite were established. Reducing anions and hydroxylamine interfered strongly. When 40 ml of a 0.1 M KOH—0.9 M KNO_3 solution containing 2.0 mg of $Na_2N_2O_2$ was analyzed, there were no interferences from 1000 mg of carbonate, sulphate or phosphate, 500 mg of chloride, 250 mg of arsenate, chromate or nitrite, 100 mg of molybdate or 1.0 mg of arsenite. The concentration of hyponitrite in a sample can be determined by a calibration curve or by the standard addition method.

TABLE 3

Amperometric titration of hyponitrite in 0.1 M KOH with 0.04 M hypochlorite solution at an applied voltage of + 0.450 V vs. SCE

$Na_2N_2O_2$ (mg)		No. of detns.	Relative error (%)	s	s_r (%)
Taken	Found				
3.34	3.42	8	+2.39	0.05	1.5
3.97	4.02	4	+1.26	0.17	4.2
7.45	7.46	4	+0.13	0.07	0.9
9.03	8.90	4	−1.44	0.19	2.1
12.62	12.50	4	−0.95	0.04	0.3
4.02[a]	3.99	2	−0.75	—	—
4.19[b]	4.15	2	−0.95	—	—

[a]10 mg $NaNO_2$ added. [b]20 mg $NaNO_2$ added.

We are grateful to the Consiglio Nazionale delle Ricerche of Italy for financial support (Cont. n. CT 74.00731.03).

REFERENCES

1 E. Divers, Proc. Roy. Soc., 19 (1871) 425.
2 C. C. Addison, G. A. Gamlen and R. Thompson, J. Chem. Soc., (1952) 338.
3 D. J. Millen, C. N. Polydoropoulos and D. Watson, J. Chem. Soc., (1960) 687.
4 J. E. Rauch and J. C. Decius, Spectrochim. Acta, 22 (1966) 1963.
5 M. N. Hughes, J. Inorg. Nucl. Chem., 29 (1967) 1376.
6 G. E. McGraw, D. L. Bernitt and I. C. Hisatsune, Spectrochim. Acta, 23 (1967) 25.
7 J. R. Buchholz and R. E. Powell, J. Am. Chem. Soc., 85 (1963) 509; 87 (1965) 2350.
8 M. N. Hughes and G. Stedman, J. Chem. Soc., (1963) 1239; (1964) 163.
9 J. H. Anderson, Analyst (London), 88 (1963) 494.
10 C. N. Polydoropoulos and M. Pippinis, Z. Phys. Chem. (Frankfurt am Main), 40 (1964) 322.
11 A. S. Corbet, Biochem. J., 28 (1928) 1575.
12 A. Medina and D. J. Nicholas, Nature (London), 179 (1957) 533; Biochim. et Biophys. Acta, 25 (1957) 138.
13 E. Divers, J. Chem. Soc., (1899) 113.
14 F. Raschig, Schwefel- und Stickstoffstudien, Leipzig-Berlin, 1924, 106.
15 L. Cambi, Gazz. Chim. Ital., 59 (1929) 770.
16 G. Oesterheld, Z. Anorg. Chem., 86 (1914) 132.
17 J. R. Partington and C. C. Shah, J. Chem. Soc., (1931) 2071; (1932) 2589.
18 A. Thum, Monatsh. Chem., 14 (1893) 309.
19 T. M. Oza, N. L. Dipali and V. T. Oza, J. Indian Chem. Soc., 27 (1950) 409.
20 H. Holzapfel and O. Gürtler, J. Prakt. Chem., 4 (1957) 59.
21 G. Ferrani, Ann. Chim. (Rome), 48 (1958) 322.
22 C. N. Polydoropoulos, Chem. Chron. A, 24 (1959) 147.
23 L. W. Jones and A. W. Scott, J. Am. Chem. Soc., 46 (1924) 2174.
24 D. Cozzi, G. Raspi and L. Nucci, J. Electroanal. Chem., 12 (1966) 36.
25 G. Raspi and F. Pergola, Chim. Ind. (Milan), 45 (1963) 1398.
26 D. H. Szulczewski and T. Higuchi, Anal. Chem., 29 (1957) 1541.

Analytica Chimica Acta, 87 (1976) 59—65

THE COULOMETRIC DETERMINATION OF SALICYLATE IN SERUM*

H. C. NIPPER** and W. C. PURDY***

Department of Chemistry, University of Maryland, College Park, Maryland 20742 (U.S.A.)

(Received 22nd April 1976)

SUMMARY

Constant-current coulometry can be used for the determination of salicylate in 100 μg of blood serum. The titration is preceded by extraction of acidified serum with ethylene dichloride followed by removal of the salicylate to an aqueous solution of pH 7.5 tris(hydroxymethyl)aminomethane buffer which also contains copper(II) sulfate to enhance recovery. A residual titration with bromine as titrant followed by addition of potassium thiocyanate is used because of the slow bromination of salicylate. Serum samples containing salicylate in the range 4—60 mg/100 ml were analyzed. Recoveries of about 90 % were obtained.

Because derivatives of salicylic acid are important pharmaceuticals and industrial chemicals, measurement of salicylate concentration in blood serum is useful for toxicological and pharmacological applications. Although salicylic acid has been titrated coulometrically [1—3], no coulometric method of analysis has been developed for its measurement in serum. Other methods for the determination of this class of compounds in body fluids include reaction with iron(III) nitrate under conditions developed by Brodie et al. [4] and modified by Trinder [5] to eliminate a prior solvent extraction step. Fluorimetry [6] and gas—liquid chromatography [7] have also been found to be important techniques for the measurement of the concentration of salicylates in body fluids.

Salicylates were titrated coulometrically by Nikolic and Volaservic [1], who used hydrogen ion as the titrant. A phenolphthalein end-point was observed visually. Kawamura et al. [2] chose electrogenerated bromine in excess, followed by back-titration with copper(II) ion, for their study of the titration of aqueous solutions of sodium salicylate. A procedure which permitted "direct" titration of salicylate with bromine was proposed by Delgado [3], but required that small increments of bromine be generated,

---

*Taken in part from the Ph.D. Dissertation of Henry C. Nipper, University of Maryland, 1971.

**Present address: Clinical Laboratories, V. A. Hospital, Baltimore, Maryland 21218.

***Present address: Department of Chemistry, McGill University, Montreal, Quebec H3C 3G1 Canada.

each increment being followed by a reaction period. Analytical throughput with this method cannot be very large.

This study was undertaken as a part of a continuing study of the application of coulometric titrations to the analysis in body fluids of substances of clinical importance [8, 9].

EXPERIMENTAL

Apparatus

The titration equipment used is essentially that described by Ladenson and Purdy [10], and was constructed from component parts in this laboratory. Equivalent equipment which can precisely maintain the current at the desired value may be substituted. The cell employed for the titrations was a modification of the design of Meyers and Swift [11] and held four platinum electrodes, including the isolated cathode, which was in a compartment formed from a sintered-glass disc of fine porosity sealed in a glass tube. Each electrode was approximately 0.5 cm^2 in area. Usable cell volumes were 25—50 ml. The contents of the cell were stirred with a magnetic stirring bar.

Biamperometric end-point currents were produced through application of a 200-mV potential across the indicator electrodes and detected by measuring the *iR* drop across a precision 10 Kohm resistor with a recording potentiometer.

Reagents

All chemicals used were reagent grade wherever possible and were used without further purification except that ethylene dichloride was redistilled and washed with concentrated NaOH. Solutions of salicylate used for standardization were prepared from the sodium salt. Serum based controls were bought from General Diagnostics. Bromine was generated from a solution of 0.2 M KBr in 0.1 M H_2SO_4. The buffer containing copper(II) used to extract salicylate from the ethylene dichloride was prepared from tris(hydroxymethyl)aminomethane (Tris), 0.2 M, which was also 0.01 M in $CuSO_4$, and made pH 7.5 with (1 + 1) HCl.

Procedures

Extraction of salicylate from serum. Pipette a 100-μl sample of serum into a 125-ml conical separatory funnel equipped with a Teflon stopcock. Dilute with 4 ml of 2 M HCl. Add 10 ml of ethylene dichloride, stopper and agitate for approximately 15 min on a wrist-action shaker. Break any emulsion formed with centrifugation. Remove the organic layer into a clean separatory funnel. Add a 5-ml aliquot of the Tris buffer containing copper(II) and agitate again for 15 min. Allow the layers to separate and add the blue aqueous layer to the titration vessel.

Coulometric titration of salicylate. Add a 25-ml aliquot of the electrolyte used for bromine generation to the cell, begin agitation and activate the

indicator circuit. When the indicator current as measured on the recorder chart has decreased in value from its initial pulse to a point very near the baseline, activate the generating circuit and generate bromine to an indicator current of 0.75 μA. Immediately and simultaneously, shut off the indicator circuit and place the generating circuit in the standby mode. Reset all times to zero on the timers. Deliver sample to the cell and activate the generating circuit for 240 s, generating bromine at the rate of approximately 0.01 μeq s^{-1}. At the end of 240 s, again place the generating circuit on standby and begin the timing of the reaction period using a second timer. After 120 s, add 2.00 ml of KSCN working solution (0.2 gl^{-1}) to the titration vessel to reduce the remaining bromine. Then activate the indicating and generating circuits simultaneously and allow the titration to proceed until the indicator current is 0.75 μA. Record the total titration time in seconds, which corresponds to the total time bromine was generated, as well as the titration current measured during the titration with a slidewire potentiometer.

Before titrations are done on actual samples, the KSCN solution must be titrated to determine a "working" concentration by performing the above procedure without addition of salicylate. This "working" concentration of the KSCN solution includes the required corrections for bromine loss and for titration efficiency less than 100 %. Titrations of standard solutions of salicylates should also be performed so that a standard curve can be constructed.

Calculations. Calculations are based on Faraday's Law; $\mu eq = i\ t\ 10^{-6}/F$, where i is the titration current (A), t is the net titration time (s), F is the Faraday constant (96,493), and μeq is the number of microequivalents of analyte titrated. For a stable current source, i can be measured and found constant to at least three significant figures; thus for a given titration current, a calculation factor may be easily derived. For example, a titration current of 0.961 mA results in a titration rate of 0.009959 ueq s^{-1}. Calculations of the amount of titrant generated during a titration are given by the equation: $0.009959\ (t_{total} - t_{KSCN}) = \mu eq$ of Br_2 generated, where t_{total} is the time in (s) required to titrate sample plus the KSCN which remains in the titration mixture, and t_{KSCN} represents the time required to titrate the total amount of KSCN added to the mixture. Once the number of microequivalents of bromine is obtained, reference to the standard curve is made to obtain the concentration of salicylate in serum.

RESULTS AND DISCUSSION

Choice of analytical variables

Titration efficiency for the electrogeneration of bromine in the cell used was studied by the method of Lingane [12]. In this method, direct titration of potassium thiocyanate was compared to an indirect titration where bromine was pre-generated at a rate of $0.94 \cdot 10^3$ $\mu eq\ s^{-1}$ to approximately 95 % of the direct value, then 2.00 ml of $7.85 \cdot 10^{-5}$ N thiocyanate was added and the titration completed.

The mean direct titration time was 288.9 ± 1.2 s (1 s.d.) and mean indirect titration time was 303.4 ± 0.67 s. Titration efficiency is 95.2 %. Also, data on titration efficiency were obtained under conditions which included a 120-s incubation period in order that volatilization of bromine could occur. The mean titration time for this back-titration was 301.6 ± s, which yields an efficiency of 95.8 %. Titration efficiency was not 100 % because current densities were not optimal and because bromine was lost through volatilization during the titration.

Bromine loss as a function of generation time and length of reaction period before the back-titration step is shown in Fig. 1. In choosing other conditions for the titration, loss of bromine was a limiting factor because more bromine was lost during the long reaction times required for complete reaction. If larger excesses of bromine had been generated to force the reaction to completion sooner, proportionately more bromine would have been lost than when a smaller excess was used.

A generation rate of approximately 0.01 μeq s^{-1} was chosen to allow a titration time of slightly more than 100 s for a serum sample of 100 μl which contained approximately 30 mg of salicylate per 100 ml. The KSCN concentration ($7.85 \cdot 10^{-5}$ M) was chosen because a conveniently titratable excess would remain after reaction with the residual bromine in the cell. This excess could be pipetted with a volumetric pipette rather than with less accurate devices. Other conditions are more or less conventional for this type of titration: a generating electrolyte of 0.2 M KBr—0.1 M H_2SO_4 and a polarizing voltage for the biamperometric indicating system of 200 mV.

The variables, excess of bromine generated and the length of reaction period, were studied for a salicylate concentration of 30 mg/100 ml. In a sample of 100 μl, this concentration would have 0.224 μmol of salicylate. Results are shown in Table 1. Study of the amount of generated excess indicates that generation of bromine for more than 8 min — roughly a three-

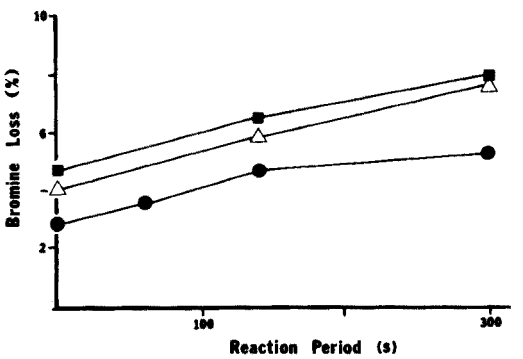

Fig. 1. Bromine loss as a function of reaction period for generation times of: 60 sec (•), 180 sec (△) and 300 sec (■).

TABLE 1

Bromine consumption in the titration of salicylate as a function of excess bromine and length of reaction period[a]

A. Amount of excess bromine		(Reaction period, 120 s)			
Sample (μmol)	Gen. time of excess (s)	Titn. time, mean (s)	Net time (s)	Br used (μeq)	Br/SA ratio
0[b]	240	304.5	—	—	—
0.2243[b]	240	413.4	108.9	1.082	4.8:1
0[c]	300	453.6	—	—	—
0.2243[c]	300	574.6	121.0	1.202	5.4:1
0[d]	500	614.3	—	—	—
0.2243[d]	500	732.9	118.6	1.357	6.0:1
B. Length of reaction period[b]		(Generation time, 240 s)			
Sample (μmol)	Reaction time (s)	Titn. time, mean (s)	Net time (s)	Br used (μeq)	Br/SA ratio
0	0	300.3	—	—	—
0.2243	0	397.2	96.9	0.963	4.3:1
0	120	304.5	—	—	—
0.2243	120	413.4	108.9	1.082	4.8:1
0	300	309.6	—	—	—
0.2243	300	423.5	113.9	1.132	5.1:1

[a]Generation rate: $9.938 \cdot 10^{-3}$ μeq s^{-1} except for the 500-s time of excess where a rate of $1.44 \cdot 10^{-2}$ μeq s^{-1} was used.
[b]Titration done with 2.00 ml KSCN working solution.
[c]Titration done with 3.00 ml KSCN working solution.
[d]Titration done with 4.00 ml KSCN working solution.

fold excess — is required for completion of the reaction. This would result in an unacceptable loss of precision owing to volatilization of the titrant, and would require that the titration times be too long for adequate throughput. Use of a standard curve shortens the time of analysis and permits correction for the loss of bromine. A standard curve obtained on aqueous solutions is shown in Fig. 2.

Extraction conditions for salicylates

Bromine reacts with many chemical species found in blood serum. For it to be used as a titrant for serum salicylate requires that salicylate be isolated from possible interferences. Ethylene dichloride, diethyl ether and ethyl acetate have been employed in solvent extraction of salicylate from serum. Diethyl ether and ethyl acetate react with bromine. Ethylene dichloride is unreactive with bromine but yields poor recoveries of salicylate, unless some means is found to promote higher extraction efficiencies. In one method [4] the presence of iron(III) in the aqueous layer to complex salicylate enhanced

recovery. Iron(III) reacts with bromine, but copper(II) also complexes salicylate and does not react with the titrant. Results of a recovery study showing the effect of copper(II) in the extraction buffer are shown in Table 2. Recoveries are not quantitative from serum, possibly because of coprecipitation with protein in the organic solvent extraction step, but they are reproducible at approximately the 90 % level.

Analysis of serum samples

Serum samples for analysis were prepared by reconstituting lyophilized human serum controls (Verstol, General Diagnostics) according to package directions, except that the diluent was spiked with sodium salicylate. Two groups of sera were prepared and analyzed by coulometric titration and by the colorimetric method of Trinder [5] on several different days. Results of the coulometric analysis are shown in Fig. 3. Mean values at all levels except the 4 mg/100 ml obtained on different days with different standards were judged to be not significantly different at the 95 % confidence level by the Student *t* test. Additional recovery data indicate that losses occurred in the solvent extraction step. Precision of analysis is also limited by this separation method and is acceptable, except at clinically low levels of salicylate where imprecision can be better tolerated than at critical decision levels which are in the mid-range of the concentrations studied. In comparison to the coulometric method, the colorimetric method yields somewhat higher recoveries, but on different days with different lots of sera, the mean absorbance value of the two sets of sera used differed significantly at the 95 % level by the Student *t* test. Precision was similar to that of the coulometric method.

TABLE 2

Recoveries for the extraction of salicylates from aqueous solution and serum in the presence of copper(II) (Sample size: $2.243 \cdot 10^{-1}$ μmol.)

Sample and extraction type	Mean net titn. time (s)	Recovery (%)
Aqueous: no extraction	111.8	—
Aqueous: Tris, no Cu(II)	72.7	65.1
Aqueous: Tris—Cu(II)	109.0	97.6
Serum: Tris, no Cu(II)	98.9	64.0[a]
Serum: Tris—Cu(II)	129.9	91.7[a]
Serum blank	27.4	—

[a]Corrected for serum blank value.

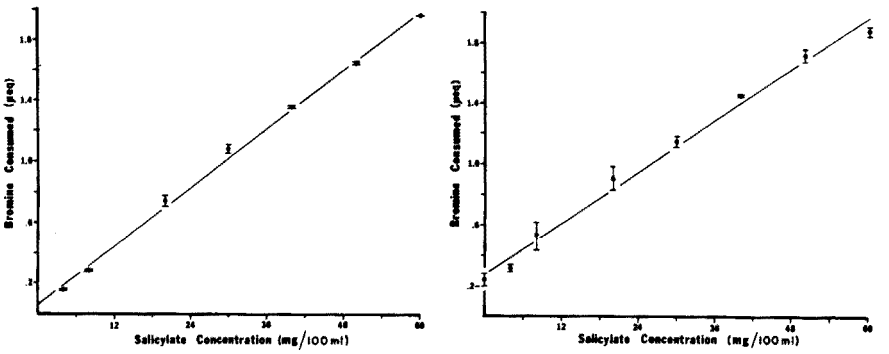

Fig. 2. Coulometric titration of standard aqueous solutions of sodium salicylate, without extraction, showing standard deviations. (Regression equation: Y = 0.061 + 0.032X; r = 0.997.)

Fig. 3. Coulometric titration of extracts of spiked serum, showing standard deviations. (Regression equation: Y = 0.275 + 0.028X; r = 0.991.)

REFERENCES

1 K. Nikolic and K. Volaservic, Acta Pharm. Jugosl., 14 (1964) 25.
2 F. Kawamura, K. Momoki and S. Suzuki, Bunseki Kagaku, 3 (1954) 29.
3 O. A. Delgado, Rev. Fac. Ing. Quim. Univ. Nac. Litoral., 30 (1961) 85.
4 B. B. Brodie, S. Udenfriend and A. F. Colburn, J. Pharmacol. Exp. Ther., 80 (1944) 114.
5 P. Trinder, Biochem. J., 57 (1954) 301.
6 D. Schachter and J. G. Manis, J. Clin. Invest., 37 (1958) 800.
7 M. Rowland and S. Riegelman, J. Pharm. Sci., 56 (1967) 717.
8 M. A. Brooks and W. C. Purdy, Clin. Chem., 18 (1972) 503.
9 S. W. McClean and W. C. Purdy, Anal. Chim. Acta, 69 (1974) 425.
10 J. H. Ladenson and W. C. Purdy, Clin. Chem., 17 (1971) 908.
11 R. J. Meyers and E. H. Swift, J. Am. Chem. Soc., 70 (1948) 1047.
12 J. J. Lingane, Electroanalytical Chemistry, 2nd edn. Interscience, New York, 1958, p. 280.

Analytica Chimica Acta, 87 (1976) 67—78

EIN VERBUNDVERFAHREN ZUR BESTIMMUNG VON BERYLLIUM IN BIOLOGISCHEN MATRICES DURCH FLAMMENLOSE ATOMABSORPTIONSSPEKTROMETRIE

TH. STIEFEL, K. SCHULZE und G. TÖLG

Laboratorium für Reinststoffe des Instituts für Werkstoffwissenschaften am Max-Planck-Institut für Metallforschung, Stuttgart (B.R.D.)

H. ZORN

Institut für Organische Chemie, Biochemie und Isotopenforschung der Universität Stuttgart (B.R.D.)

(Eingegangen den 7. Juni 1976)

ZUSAMMENFASSUNG

Es wird ein hinsichtlich systematischer Fehler optimiertes Verbundverfahren zur Bestimmung von ng-Mengen Beryllium in biologischen Matrices (z.B. Urin, Blut, Muskelgewebe) durch flammenlose Atomabsorptionsspektrometrie beschrieben. Beim Einsatz von z.B. 1 ml Urin liegt der Variationskoeffizient für den Gehaltsbereich von 0,8 bis 4,6 p.p.b. Be zwischen 20 und 4 %. Die Nachweisgrenze beträgt c = 0,6 p.p.b., bezogen auf die Analysenprobe. Die Probe wird mit Salpetersäure in einem PTFE-Gefäß unter Druck mineralisiert, das Beryllium anschließend im gleichen Gefäß als $Be(acac)_2$-Komplex mit Benzol ausgeschüttelt und in einem mit einer $ZrOCl_2$-Lösung behandelten Graphitofen atomisiert. Durch die Zr-Beschichtung konnte das Beryllium-Signal gegenüber unbeschichteten Öfen um das 3- (Benzolphase) bzw. 9-fache (wässrige Lösungen) verbessert werden. Es wurde nachgewiesen, daß vereinfachte Vorschriften (z.B. eine direkte Vorgabe von Urin in den Graphitofen) mit erheblichen systematischen Fehlern durch Interelementeffekte behaftet sind.

SUMMARY

A combined method for the determination of beryllium in the nanogram range in biological matrices (e.g. urine, blood, muscle) by flameless a.a.s. is described. For a 1-ml sample of urine, the relative standard deviation decreases from 20 to 4 % for contents of 0.8 to 4.6 p.p.b. Be, and a limit of detection of 0.6 p.p.b. Be can be obtained. To avoid severe interferences from foreign ions, the sample is decomposed with nitric acid in a PTFE-tube under pressure, and beryllium is separated in the same vessel by liquid—liquid extraction of the $Be(acac)_2$ complex with benzene. The separated beryllium is then atomized in a graphite tube treated with a solution of $ZrOCl_2$. This preparation increases the beryllium signal by a factor of 3 for benzene phases and 9 for aqueous solutions. Simplification of the given procedure at any step leads to large systematic errors, which are especially high, if the urine sample is measured directly by flameless excitation.

Beryllium und seine Legierungen sind durch eine Reihe besonderer Eigenschaften für zahlreiche technische Anwendungen prädestiniert [1]. Ihrer weiteren Verbreitung als Werkstoffe steht jedoch die wenig geklärte toxische und eventuell cancerogene Wirkung gegenüber [2—5]. Hinzu kommt, daß der an sich schon niedrige MAK-Wert in Höhe von 2 μg Be m^{-3} Luft von der für die Bundesrepublik Deutschland zuständigen DFG-Kommission seit 1973 nicht weitergeführt wurde, und Beryllium nun in der Gruppe IIIa der "beim Menschen erfahrungsgemäß bösartige Geschwülste" verursachenden Substanzer ohne Literaturnachweis aufgezählt wird [6]. Daraus ergibt sich die Notwendigkeit, den pathophysiologischen Effekt des Berylliums durch Untersuchung des Xenometabolismus zu klären und so den fundierten Grenzwert der ungefährlichen Dosis aufzufinden. Da es sich um Konzentrationen im p.p.m.- und p.p.b. Bereich handelt, ist die Entwicklung einer zuverlässigen spurenanalytischen Methode ein erster Schritt.

Für die Überwachung von Berylliumgehalten (>10 p.p.b.) an gefährdeten Arbeitsplätzen bewährte sich vor allem die AAS mit Anregung durch die Lachgas—Acetylenflamme [7, 8]. Für eine zusätzliche Kontrolle der Berylliumgehalte in Blut und Urin von berylliumexponierten Personen existieren jedoch für den arbeitsmedizinisch relevanten Bereich (<10 p.p.b.) nur unbefriedigende Analysenmethoden hinsichtlich des Nachweisvermögens, der Richtigkeit und der Wirtschaftlichkeit. Ein äußerst nachweisstarkes und zuverlässiges chelatgaschromatographisches Verbundverfahren (Nachweisgrenze: 10^{-13} g Be) [9] erfordert eine unübliche instrumentelle Ausstattung sowie sehr qualifiziertes Personal. Deshalb war es Ziel dieser Arbeit, die gaschromatographische durch eine atomabsorptiometrische Endbestimmung mit flammenloser Anregung zu ersetzen, die bei vergleichbarer Nachweisstärke ($5 \cdot 10^{-12}$ g Be) die Be-Anreicherung wesentlich vereinfacht. Bei vergleichenden Untersuchungen an Luftproben fanden Pilz und Monkmann [10] für die Atomisierung mit der Flamme eine Nachweisgrenze (NWG) von 10 p.p.b., für das Graphitrohr entsprechend 0,2 p.p.b. Durch Einengen von Mineralwasser-Proben erreichten Janoušková et al. [11] eine NWG von 0,05 p.p.b. Mit Hilfe einer Direktfiltratio von Luft durch das Graphitrohr gelangten Siemer et al. [12] zu einer Nachweisgrenze von 2 μg m^{-3} Luft mit einer relativen Standardabweichung von 15 %. Von Welz und Wiedeking [13] wurde die Bestimmung von Be-Spuren in biologischen Matrices ohne jede Probenvorbehandlung direkt im Graphitrohr durchgeführt und eine Nachweisgrenze von 20 pg gefunden. Hurlbut [14] beschreibt ein Direktverfahren zur Spurenbestimmung von Be in Urin mit flammenloser AAS. Nach diesen Untersuchungen liefert ein mit Beryllium aufgestockter Urin eine nahezu gleiche Eichgerade wie eine wäßrige Vergleichslösung. Bei einer NWG von 0,1 p.p.m. wird eine relative Standardabweichung von 10 % angegeben. Gegen Direktverfahren sprechen jedoch die Beobachtunge von erheblichen Störeinflüssen, verursacht durch andere Probenbestandteile. Zum Beispiel beobachteten Janoušková et al. [11] eine Signaldepression von 14 % bei Anwesenheit von Sulfat, aber einen Signalanstieg von 11 % bei Magnesium. Findlay et al. [15] registrierten bei der Messung eines mit einem $HF—HNO_3$-Gemisch mineralisierten Glasfiberfilters einen totalen Signalverlust.

Eine signifikante Signalerhöhung bei der Be-Analyse im Graphitrohr wird von Runnels et al. [16] beschrieben. Durch eine Beschichtung mit $ZrOCl_2$ erhöht sich das Nachweisvermögen der Be-Bestimmung um den Faktor 3 bis 13 je nach verwendeter Graphitsorte.

In Tab. 1 sind die Daten einiger Methoden der Be-Bestimmung in organischen Matrices zusammengestellt. Zum Vergleich werden auch die Verfahren mit fluorimetrischer und chelatgaschromatischer Endbestimmung aufgeführt. Wie aus den Angaben ersichtlich ist, kann eine zuverlässige Bestimmung durch AAS mit hohem Nachweisvermögen nur durch ein Verbundverfahren erzielt werden, das die vielseitigen Störmöglichkeiten durch Mineralisieren der Probe und Abtrennung des Berylliums vor seiner Bestimmung eliminiert. Dies bestätigten auch weitere Untersuchungen [22], bei denen wäßrige Be-haltige Lösungen, die jeweils mit Fremdionen in physiologisch orientierten Konzentrationen versetzt waren, erheblich differierende Signalhöhen ergaben. Zur Mineralisierung der organischen Begleitstoffe lagen bereits beste Erfahrungen über einen Aufschluß mit konzentrierter Salpetersäure unter Druck im PTFE-Gefäß [23] vor. Zur Komplexbildung mit anschließender Flüssig—Flüssig-Extraktion des Be wurde Acetylaceton (Pentan-2,4-dion) als Komplexbildner und Benzol als Extraktionsmittel gewählt.

Zur Beurteilung der Eignung der Be-Abtrennung wurde zuerst das Verhalten reiner benzolischer Be—Komplex-Lösungen im Graphitrohr untersucht. Dann wurde die Verteilung des Be—Acetylacetonats zwischen wäßriger und organischer Phase in Abhängigkeit vom pH-Wert und von Fremdionen ermittelt und optimiert.

Zur Eliminierung systematischer Fehlerquellen war es unumgänglich, bei allen Schritten spezielle spurenanalytische Regeln zu beachten, wie z.B. die Verwendung von Gefäßmaterial mit geringer Adsorptionswirkung, die Konditionierung dieser Gefäße zur Verringerung von Blindwerten und die Durchführung des gesamten Verfahrens im gleichen Gefäß. Das daraus resultierende Verbundverfahren wurde nach [24] statistisch untersucht.

Beschichtung des Graphitrohrs (GR)

Durch eine Beschichtung des Graphitrohrs mit Zirkon konnte das Nachweisvermögen der AAS-Bestimmung gesteigert werden. Für das verwendete GR (Perkin-Elmer HGA-72) betrug die optimale Zirkon-Menge 40 mg/GR. Während die Signalhöhe einer wäßrigen $BeCl_2$-Lösung um das 9,4 fache gesteigert wurde, ergab sich für eine benzolische Berylliumacetylacetonat-Lösung ein Steigerungsfaktor von ca. 3 (Abb. 1). Dieses Ergebnis ist mit dem von Runnels [16] angegebenen Befund vergleichbar. Die Signalerhöhung wird vermutlich durch die Bildung einer Diffusionsbarriere für Be-Atome durch die Wandung des GR verursacht. Die $ZrOCl_2$-Lösung kann beim Erhitzen auf Atomisierungstemperatur eine stabile ZrC-Schicht bilden [25]. Die unterschiedliche Empfindlichkeitssteigerung wäßriger und benzolischer Lösungen kann mit dem Benetzungsverhalten im GR erklärt werden. Durch die breitere Ausdehnung der Benzolphase ist die im Gasstrom entweichende Menge größer.

TABELLE 1

Literaturübersicht über Methoden zur Be-Analytik in organischen Matrices

Endbestimmung	Matrix	Probenvorbereitung	Aufschluß	Anreicherung	Bestimmungsber./ Nachweisgrenze	rel. Standardabweichung	Zitat
AAS mit Graphitrohr	Urin	Zugabe von $HClO_4$	—	—	0,5—10 p.p.b./ 0,1 p.p.b.	10—20 %	14
AAS mit Graphitrohr	Urin/ Blutserum	Zugabe von $HClO_4$	—	—	—/0,02 ng	—	13
AAS mit N_2O—Acetylen-Flamme	Urin	HNO_3-Zugabe	$HNO_3/HCl/HClO_4$	Acetylaceton/MIBK	—/3 p.p.b.	—	17
Emission/AAS mit N_2O—Acetylen-Flamme	Gemüse	Waschen mit H_2O	Soda/$LiBO_2$ O_2 unter Druck	—	—/AAS: 10 p.p.m.	—	18
Chelat-GC mit ECD	org. Matrices	—	Verbrennung im angeregten Sauerstoff/ Druckaufschluß im Teflongefäß mit HF/HNO_3	TFA/Benzol	0,01—100 p.p.b./ 0,01 p.p.b.	3—25 %	9
Fluorimetrie mit Morin	Urin, Gewebe	Eindampfen $CaSO_4$-Fällung, Elektrolyse mit Hg-Kathode	HNO_3	Acetylaceton/Benzol, anschliessend rückschütteln in HCl	—/0,4 p.p.b.	—	19
Fluorimetrie mit Morin	Fettproben Urin, Knochen	Urin: $CaSO_4$-Fällung $Ca_3(PO_4)_2$ Mitfäll.	$HClO_4/HNO_3$	Acetylaceton/CCl_4, Rückschutteln in $HNO_3/HClO_4$	20—100 p.p.b./ 20 p.p.b.	0,2—0,4 %(?)	20
Feststoff-Fluorimetrie	Blätter	—	$HClO_4/HNO_3$	Dinaphtoylmethan-Fällung	20—200 p.p.b./ 20 p.p.b.	3,5—7 %	21

Einfluß des Temperaturprogramms

Der Verlauf des Temperaturprogramms wurde so gewählt, daß die Ausbeute im Atomisierungsschritt einen maximalen Wert erreichte. Dies erfordert eine optimale thermische Vorbehandlung der Proben, die sich neben der Art der Probe auch nach der Bauart des GR richtet (Graphitsorte, Abmessungen, elektr. Kenngrößen, Art und Strömungsgeschwindigkeit des Schutzgases).

Die im GR durchgeführten Untersuchungen mit reinen wäßrigen Lösungen ($BeCl_2$, $BeSO_4$, $Be(NO_3)_2$) und reinen benzolischen Komplexlösungen ($Be(TFA)_2$, $Be(acac)_2$) ergaben eine signifikante Abhängigkeit der Höhe des Meßsignals von Verlauf des Trocknungs- und Verkokungsprozesses (Zwischenprogramm).

In den Abb. 2—4 sind einige Beispiele aufgeführt, die bei Anwendung der optimalen Atomisierungstemperaturen erhalten wurden. Während für die $BeCl_2$-Lösung die ab 500 °C auftretenden Verluste mit dem Beginn der Verflüchtung der $BeCl_2$-Molekel zusammenfallen, ergibt sich die Temperatur der maximalen Ausbeute bei den $BeSO_4$-, $Be(NO_3)_2$-, $Be(TFA)_2$- und $Be(acac)_2$-Lösungen durch ein komplexes Zusammenwirken von Verflüchtigung und Dissoziation der Verbindungen. Messungen, die mit dem jeweils als optimal ermittelten Temperaturprogramm durchgeführt wurden, ergaben bei übereinstimmenden Be-Gehalten der Probelösung vergleichbare Signalhöhen für wäßrige und benzolische Lösungen. Die Nachweisgrenzen für wäßrige und benzolische Lösungen sind in Tab. 2 angegeben.

Einfluß von Fremdionen

Unter dem Aspekt der Minimalisierung der Verfahrensschritte wurde das Verhalten reiner wäßriger Be-Lösungen bei Anwesenheit von Fremdionen

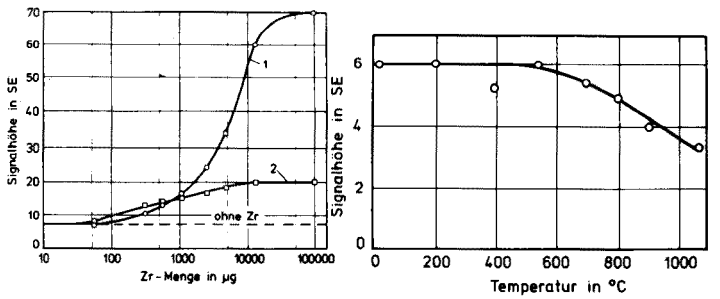

Abb. 1. Abhängigkeit der Signalhöhe der AAS von der Beschichtungsmenge an Zirkon des GR: (1) $BeCl_2$ (0,1 ng Be/10 µl), (2) Be(acac) (0,1 ng Be/10 µl); Temperaturprogramm: Trocknen: 39 °C, 1 min, 138 °C, 0,5 min; Temperaturgleitprogramm bis auf 1490 °C mit Anstiegsrate 8; Atomisieren: 2660 °C, 15 S; Skalendehnung 3, Rauschunterdrückung 1.

Abb. 2. Abhängigkeit der Signalhöhe von der Zwischentemperatur für eine $BeCl_2$-Lösung (0,02 ng Be/20 µl). Temperaturprogramm: Trocknen: 100 °C, 0,5 min; Zwischentemperatur: 20—1080 °C, 1 min; Atomisieren: 2660 °C, 15 S; Skelendehnung 3; Rauschunterdrückung 1, unbehandeltes GR.

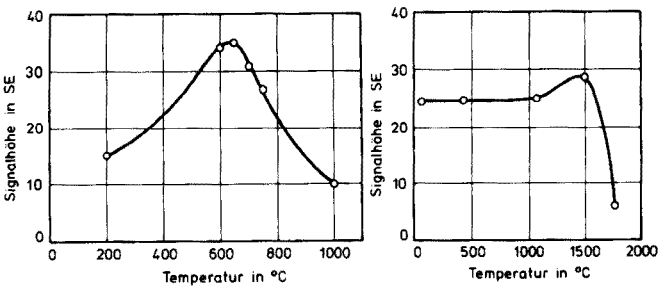

Abb. 3. Abhängigkeit der Signalhöhe von der Zwischentemperatur für eine $BeSO_4$-Lösung (0,05 ng Be/50 µl). Temperaturprogramm: Trocknen: 100 °C, 30 S; Zwischentemperatur: 20—1000 °C, 2 Min; Atomisieren: 2660 °C, 20 S; Skalendehnung 10, Rauschunterdrückung 2, unbehandeltes GR.

Abb. 4. Abhängigkeit der Signalhöhe von der Zwischentemperatur für eine benzol. $Be(acac)_2$-Lösung (wäßrige Ausgangslösung: 10 ng Be ml^{-1}); Einspritzvolumen 20 µl; Temperaturprogramm: Trocknen: 39 °C, 1 Min; 139 °C, 0,5 Min; Zwischentemperatur: 20—1800 °C, 10 S; Atomisieren: 2660 °C, 15 S; Skalendehnung 3, Rauschunterdrückung 1, Zr-beschichtetes GR.

TABELLE 2

Nachweisgrenzen der AAS in g Be für reine wäßrige und benzolische Be-Lösungen

Be-Verbindung	Zr-beschichtetes GR [g]	Unbehandeltes GR [g]
$BeCl_2$	$6{,}6 \cdot 10^{-12}$	—
$BeSO_4$		$2 \cdot 10^{-11}$
$Be(NO_3)_2$		—
$Be(TFA)_2$	$3 \cdot 10^{-11}$	—
$Be(acac)_2$		—

untersucht. Dazu wurden die Lösungen unter Konstanthaltung aller weiteren Einflußgrößen vermessen. Die Ergebnisse sind in Abb. 5 dargestellt. Während die Mehrzahl der Fremdionen das Signal nur im Bereich von ± 10 % beeinflussen, verursachen Kalzium- und Fluor-Ionen eine Depression von 50 % bzw. 90 %. Bei Anwesenheit von Magnesium steigt das Signal um etwa 30 % seines ursprünglichen Wertes an. Die Signalerhöhung durch Mg bestätigt die Messungen von Findlay et al. [15]. Dieser Befund weist darauf hin, daß bei einem Überschuß an Fremdionen nicht ihre Konzentration, sondern die Art der Fremdionen das Verhalten des Be im GR beeinflußt.

Aus den unterschiedlichen Signalhöhen geht hervor, daß eine Direktbestimmung des Berylliums mit dem GR bereits aus anorganischen Matrices mit Fremdionen wechselnder Konzentration zu fehlerhaften Ergebnissen führen kann. Eine Isolierung des Berylliums ist unter diesen Umständen erforderlich.

Aufschluß

Der Isolierung des Berylliums muß eine Mineralisierung zur Zerstörung organischer Bestandteile vorgeschaltet werden, um eventuell vorhandene Beryllium—Proteinkörper-Komplexe zu zerstören. Der Aufschluß erfolgt im PTFE-Gefäß mit 70 % iger HNO_3 bei 170 °C unter Druck in einer speziellen Aufschlußapparatur [23]. Die Verwendung von PTFE als Gefäßmaterial hat außerdem den Vorteil geringer Adsorptionswirkung gegenüber Beryllium [8].

Flüssig—Flüssig-Verteilung

Wie mehrere Autoren [19, 26, 27] bereits gezeigt haben, ist es bei der Be-Extraktion mit Acetylaceton zweckmäßig, zunächst in wäßriger Phase die $Be(acac)_2$-Chelatbildung durchzuführen und anschließend mit Benzol den Komplex auszuschütteln. Als optimale Komplexbildungs- und Ausschuttelzeit wurde bei Verwendung eines Intensivschüttlers je 5 Min ermittelt. Der Einfluß des pH-Wertes auf die Extraktion des Berylliums aus der wäßrigen Lösung macht sich zwischen pH 1 und pH 5 stark bemerkbar, jedoch ist der Übergang in die Benzolphase zwischen pH 5 und pH 7 praktisch konstant und vollständig (Abb. 6). Da eine Reihe von Fremdionen in der wäßrigen Lösung mit dem Beryllium ausgeschüttelt werden kann, wurde ihr Einfluß auf das Be-Signal nach dem Ausschütteln untersucht. Die Ergebnisse dieser Meßreihe sind in Abb. 5 zusammengestellt. Durch Fe- bzw. Cu-Zugabe zeigten sich im Vergleich zu einer reinen Be-Lösung

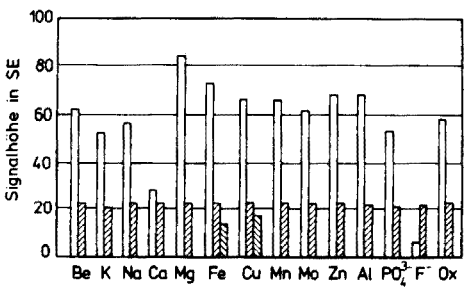

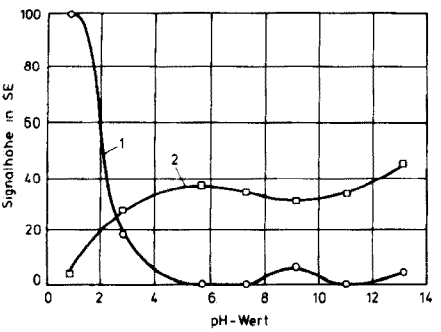

Abb. 5. Einfluß von Fremdionen auf die Signalhöhen wäßriger (□) und benzolischer Be-haltiger Phasen mit (■) und ohne (▪) ÄDTA-Zugabe. Bezugslösung: 0,1 ng Be/10 µl als $BeCl_2$. Konzentration der Fremdionen: K, Na, Phosphat, Oxalat 5 g l^{-1}; Ca, Mg, Fluorid 0,5 g l^{-1}; Fe, Cu $1 \cdot 10^{-3}$ g l^{-1}; Mn, Mo, Zn, Al $1 \cdot 10^{-3}$ g l^{-1}. Temperaturprogramm: Trocknen: 39 °C, 1 Min; 138 °C, 0,5 Min. Zwischentemperatur: Gleitprogramm von 20 bis 1490 °C mit Anstiegsrate 8. Atomisieren: 2660 °C, 15 S; Skalendehnung 3, Rauschunterdrückung 1, (Zr-beschichtetes GR).

Abb. 6. pH-Wert-Abhängigkeit der Be-Verteilung als $Be(acac)_2$, zwischen wäßriger (1) und benzolischer (2) Phase; wäßrige Ausgangslösung 10 ng Be/ml; Temperaturprogramm: Trocknen: 39 °C, 1 Min; 138 °C, 0,5 Min; Zwischentemperatur: Gleitprogramm von 20 bis 1490 °C mit Anstiegsrate 8. Atomisieren: 2660 °C, 15 S; Skalendehnung 3, Rauschunterdrückung 1, (Zr-beschichtetes GR), Einspritzvolumen: 20 µl.

Signaldepressionen, die auf Acetylacetonkomplexe dieser Elemente zurückgeführt werden können. Durch ihre Maskierung mit ÄDTA konnte die Störung eliminiert werden. Alle restlichen Lösungen wurden daraufhin mit ÄDTA-Zugabe vermessen. Unter diesen Bedingungen wurden bei allen untersuchten Fremdionen nur innerhalb der Standardabweichung schwankende Peakhöhen beobachtet. Die gegenüber den wäßrigen Lösungen kleineren Signalhöhen der Benzolphasen beruhen auf der geringeren Wirksamkeit der Zirkon-Beschichtung (Abb. 1).

EXPERIMENTELLER TEIL

Geräte

Aufschlußvorrichtung: PTFE-Gefäß (10 ml) in Edelstahlbombe mit Heizung [23]; Knick-pH-Meter, mit Jenaer Glas Mikro-pH-Einstabmeßkette N59; Intensivschüttler REAX I der Heidolph-Elektro KG; Perkin-Elmer Atom-Absorptions-Spektrophotometer 303 mit GR HGA-72; Kompensations-Schreiber; Mikrobüretten Metrohm E 457 mit 5 ml-Wechselaufsatz, Beckman-Ultramikrobüretten mit PTFE-Verdrängungskolben; Ausdämpfapparate zur Reinigung von Quarz- und PTFE-Gefäßen.

Konditionierung der Gefäße. Zur Reduzierung der Blindwerte und von Adsorptionseffekten müssen Quarz- und PTFE-Gefäße ca. 4h über siedender HNO_3 oder HCl und 10h über siedendem H_2O ausgedämpft werden. Die PTFE-Gefäße werden zuvor 2h in konz. HNO_3 ausgekocht.

Be-Standardlösungen

Die Gebrauchslösungen (1 μg Be ml^{-1}) werden durch Verdünnen mit bidest. H_2O (Quarz-Destillierapparat) hergestellt und durch Ansäuern stabilisiert. In einer konditionierten Polyäthylenflasche sind sie längere Zeit haltbar. Verdünntere Probelösungen müssen täglich frisch hergestellt werden.

Präparation des Graphitrohrs (GR)

Das GR in bidest. H_2O mit einigen Tropfen Triton X-100 mehrere Stunden einlegen. Dann wird es in einem PTFE-Gefäß in der Druckbombe mit gesättigter $ZrOCl_2$-Lösung etwa 6h auf 170 °C erhitzt. Nach dem Trocknen bei 110 °C wird das bereits angegebene Temperaturprogramm (Abb. 1) mehrmals durchlaufen.

AAS-Bestimmungen

Die Messungen werden bei der Resonanzwellenlänge 234,9 nm bei Spaltstellung 4 (1 mm) durchgeführt. Ausgewertet werden die Peakhöhen. Eine Integration der Peakflächen verbesserte die Standardabweichung nur unwesentlich. Die Probelösung wurde mit einer Metrohm-Mikrobürette in das Graphitrohr einpipettiert. Zur Einstellung reproduzierbarer Bedingungen wurde die Bürette mechanisch fixiert. Die Einspritz-Volumina lagen zwischen 5 und 50 μl. Als

Schutzgas wurde N_2 verwendet. Die Spülung der Küvette mit Argon führt bei organischen Lösungen zu einer Steigerung des Nachweisvermögens.

Optimierung der Temperaturprogramme. Die Temperaturprogramme müssen für jeden Geräte- und Graphitrohrtyp folgendermaßen bestimmt werden:

1. Aufstellung eines Fiktivprogramms, orientiert an den Siede-oder Zerset zungspunkten der zu erwartenden Verbindungen mit Trocknung und thermischer Dissoziation der Matrix.
2. Variation von Zeit und Temperatur jedes Teilschrittes unter Konstanthaltung der anderen Parameter.
3. Zusammenstellung der jeweils optimalen Teilschritte zum Temperaturprogramm.

Vorschrift für Urinproben

Das Verbundverfahren zur Be-Bestimmung in organischen Matrices wurde von uns lediglich für Urinproben eingesetzt. Nach unserer Erfahrung kann es jedoch auf Grund des Aufschlusses in der Druckbombe auf andere organische Matrices (Vollblut, Serum, Gewebe u.a.) übertragen werden, da hierdurch eine vollständige Mineralisierung der Probe erfolgt.

Die Probe (1 ml) wird im konditionierten PTFE-Gefäß für 1,5h (170 °C) mit 0,5 ml HNO_3 (70 % ig Suprapur) aufgeschlossen und anschließend mit NaOH (8 M und 1 M) ein pH-Wert zwischen 5 und 7 eingestellt. Die Komplexbildung erfolgt durch Zugabe von 50 µl Acetylaceton (p.a.), nachdem die Maskierung der Störelemente mit 0,5 ml 1 M Natriumacetatlösung, gesättigt an ÄDTA, erfolgte. Ausgeschüttelt wird für 5 Min mit 200 µl Benzol ("für die Spektroskopie", dest.). Aliquote Teile von 10 µl der Benzolphase werden in das Graphitrohr eingespritzt und atomisiert.

Trocknen: 39 °C, 1 Min; 138 °C, 0,5 Min; Zwischentemperatur: Temperaturgleitprogramm von 20 auf 1490 °C mit Anstiegsrate 8; Atomisieren: 2660 °C, 15 S.

Die Eichung des Verfahrens erfolgt durch Ausschütteln von Eichlösungen (1—50 p.p.b.) in analoger Weise. Zur Kontrolle wurden pro Meßreihe ein Reagentienblindwert und eine Standardprobe durch alle Analysenschritte mitgeführt.

Die statistischen Kenngrößen des Verfahrens [24] stellen nur ein Maß für die Reproduzierbarkeit der Ergebnisse dar und erlauben keine Aussage über die Richtigkeit. In Tab. 3 sind die Ergebnisse aus jeweils $n = 6$ Einzelmessungen eingetragen. Wie aus den Angaben hervorgeht, ist der Absolutwert der Standardabweichungen s_x vergleichbar mit dem Reagentienblindwert x_0 und in seiner Höhe praktisch unabhängig vom Be-Gehalt der Probelösungen. Gleichzeitig liefert das Verbundverfahren mit und ohne Aufschluß bei reinen Be-Lösungen fast übereinstimmende Analysenwerte. Dieser Befund deutet auf geringe systematische Fehler bei der Probenaufbereitung hin. Die Analysen von reinen und Be-dotiertem Urin zeigen hohe Wiederfindungsraten.

Das beschriebene Verfahren läßt sich gegenüber den bisher angewandten Methoden leicht handhaben. Seine Durchführung erfordert dennoch — gemessen

TABELLE 3

Statistische Kenngrößen des Verbundverfahrens zum Nachweis von Beryllium im ng-Bereich durch AAS

Methode	Be-Konz. der Ausgangsprobe [p.p.b.]	$\bar{x}$ [SE]	s_n [SE] $n = 6$	s_r [%]	T [SE] für $P = 99$ %	c^a und $c^{a,b}$ [p.p.b.]
Mit Aufschluß: leerlaufendes Verfahren	—	1,6	1,4	—	—	0,6
Ohne Aufschluß reine Be-Lösungen	2[c]	19,2	1,3	7,0	5,2	2[c]
Mit Aufschluß reine Be-Lösungen	2[c]	18,7	1,6	8,6	6,4	1,9
Reiner Urin	—	7,5	1,5	20	6,0	0,8
Urin um 2 p.p.b. Be aufgestockt	+2	24,7	2,0	8,1	8,0	2,6
Urin um 4 p.p.b. aufgestockt	+4	44,2	1,8	4,1	7,3	4,6

[a] Die p.p.b.-Angabe ist auf die wäßrige Ausgangslösung und eine Einspritzmenge von 10 μl Benzolphase bezogen.
[b] Aus Eichfunktion ermittelt.
[c] Vorgegeben.

an "Direktverfahren" — einen relativ hohen zeit- und kostenmäßigen Aufwand. Daher haben wir seine Leistungsfähigkeit mit einigen vereinfachten Varianten verglichen. Dazu wurde reiner und um 10 p.p.b. aufgestockter Urin nach den in Tab. 4 angegebenen Verfahren analysiert und bei den Methoden ohne Isolierung des Berylliums zusätzlich die Deuterium-Untergrundkompensation eingesetzt, um Störsignale zu reduzieren. Es zeigte sich, daß bei der Anregung im Graphitrohr unspezifische Lichtschwächungen auftreten, und die Beryllium-Signale selbst Minderbefunde aufweisen. Das Ergebnis bei Direktextraktion (ohne Aufschluß) von 4,8 p.p.b. läßt auf eine teilweise Bindung des Berylliums an organische Bestandteile des Urins schließen. Ergänzend wurden einige Analysen mit Flammenanregung (N_2O—C_2H_2) durchgeführt. Die vorgegebenen Be-Gehalte liegen im Bereich der Nachweisgrenze. Deshalb können diese Analysenwerte nur als Richtwerte angesehen werden. Ein Vergleich der verschiedenen Methoden untereinander zeigt, daß im Spurenbereich (< 10 p.p.b.) sowohl die Direktmessung in der Flamme als auch im GR mit Deuterium-Untergrundkompensation eine größenordnungsmäßige Abschätzung zuläßt. Ist man hingegen auf exakte Daten angewiesen, so ist der Einsatz des beschriebenen Verbundverfahrens unbedingt vorzuziehen.

Die Untersuchungen wurden im Pulvermetallurgischen Laboratorium des Instituts für Werkstoffwissenschaften durchgeführt. Herrn Prof. Dr. G. Petzow danken wir für seine Unterstützung durch Bereitstellung der Arbeitsmöglich-

TABELLE 4

Vergleichsbestimmungen des Be-Gehaltes von Urinproben durch AAS für verschiedene Probenvorbereitungen

Verfahren	Urinmenge [ml]	Be-Gehalt [p.p.b.]	Be-Gehalt nach Aufstockung um 10 p.p.b. [p.p.b.]	Wiederfindungsrate [%]	Zahl der Wiederholmessungen *n*
Graphitrohr direkt					
mit Komp.[a]	0,15	1,1	5,0	39	5
ohne Komp.	0,15	4,1	11,5	74	5
Graphitrohr mit Aufschluß					
mit Komp.	0,2	—	2,0	—	5
ohne Komp.	0,2	4,1	6,7	26	2
Graphitrohr mit Direktextraktion (ohne Komp.)	1,0	—	4,8	—	5
Graphitrohr mit Aufschluß und Extraktion Verbundverfahren (ohne Komp.)	1,0	0,8	10,7	99	10
Flamme direkt					
mit Komp.	5	(12)	(25)	—	5
ohne Komp.	5	(7)	(20)	—	5

[a]Zur Kompensation unspezifischer Lichtverluste wurde eine Deuteriumlampe eingesetzt.

keiten. Das Laboratorium verfügt über einen Bereich, der für das Arbeiten mit Beryllium konzipiert ist und der einer ständigen analytischen und arbeitshygienischen [28] Kontrolle unterliegt.

LITERATUR

1 G. Petzow und F. Aldinger, Ullmanns Enzyklopädie der Technischen Chemie, 4. Aufl., Bd. 8, Verlag Chemie GmbH Weinheim, 1974.
2 G. Petzow und H. Zorn, Chem. Z., 98 (1974) 236.
3 A. L. Reeves, Zbl. Arbeitsmed., 24 (1974) 46.
4 L. B. Tepper, CRC Critical Reviews in Toxicology, (1972) 235.
5 H. Zorn und H. Diem, Zbl. Arbeitsmed., 24 (1974) 3.
6 Deutsche Forschungsgemeinschaft: Kommission zur Prüfung gesundheitsschädlicher Arbeitsstoffe, Mitteilung IX, 1973.
7 B. Welz, Atomabsorptionsspektrometrie, 2. Aufl., Verlag Chemie GmbH, Weinheim, 1975.
8 D. L. Bokowski, Am. Ind. Hyg. Ass. J., 29 (1968) 474.
9 G. Kaiser, E. Grallath, P. Tschöpel und G. Tölg, Z. Anal. Chem., 259 (1972) 257.

10 W. Pilz und M. Monkmann, (Farbenfabriken Bayer AG, Leverkusen), M.S. Nr. 36/72 (1972).
11 J. Janoušková, Z. Sulcek und V. Sychra, Chem. Listy, 68 (1974) 969.
12 D. Siemer, J. F. Lech und R. Woodriff, Spectrochim. Acta Part B, 28 (1973) 469.
13 B. Welz und E. Wiedeking, Z. Anal. Chem., 252 (1970) 111.
14 J. A. Hurlbut, Rep. Atom. Energy Comm. US, RFP-2151 (1974).
15 W. J. Findlay, A. Zdrojewski und N. Quickert, Spectrosc. Lett., 7 (1974) 355.
16 J. H. Runnels, R. Merryfield und H. B. Fischer, Anal. Chem., 47 (1975) 1258.
17 H. Massmann und S. Gücer, Spectrochim. Acta Part B, 29 (1974) 283.
18 F. Ecrément und F. P. Burelli, Analusis, 2 (1973) 306.
19 T. Y. Toribara und R. E. Sherman, Anal. Chem., 25 (1953) 1594.
20 C. W. Sill und C. P. Willis, Anal. Chem., 31 (1959) 598.
21 D. E. Ryan, M. Granda und M. Janmohammed, Anal. Chim. Acta, 76 (1975) 467.
22 Th. Stiefel, Diplomarbeit, Universität Stuttgart und MPI für Metallforschung Stuttgart, 1976.
23 L. Kotz, G. Kaiser, P. Tschöpel und G. Tölg, Z. Anal. Chem., 260 (1972) 207.
24 R. Kaiser und G. Gottschalk, Elementare Tests zur Beurteilung von Meßdaten, Bibliographisches Institut, Mannheim, Wien, Zürich, 1972.
25 B. Zmbova und M. Marinković, Talanta, 20 (1973) 647.
26 T. Y. Toribara und P. S. Chen, Anal. Chem., 24 (1952) 539.
27 I. P. Alimarin und I. M. Gibalo, Z. Anal. Chem., 156 (1956) 435.
28 Hauptverband der gewerblichen Berufsgenossenschaften, Nr. VGB 1a, 35—47 (1969) S.31.

Analytica Chimica Acta, 87 (1976) 79—90

DETERMINATION OF SILICATE, PHOSPHATE, AND SULFATE BY CALCIUM ATOMIZATION INHIBITION TITRATION

J. R. SAND,* J. H. LIU, AND C. O. HUBER

Department of Chemistry and Center for Great Lakes Studies, University of Wisconsin-Milwaukee, Milwaukee, Wisconsin 53201 (U.S.A.)

(Received 17th February 1976)

SUMMARY

The anion-inhibition effects on calcium flame emission can be employed to allow the determination of silicate, phosphate, and sulfate and their mixtures by a simple titration procedure. Direct correlations are made between features of the titration curves and sample anion concentrations. These correlations are used to analyze a variety of samples for the anions mentioned. Refractory particulates produced during these inhibition titration are collected and analyzed. The compositional changes of the particles collected from different regions of the titration are correlated with observed signals to describe a mechanism for the flame droplet chemical processes.

In addition to direct flame spectrometric techniques for nonmetallic elements, several indirect methods have been developed. These methods can be classified on the basis of the chemistry involved: (1) precipitation methods; (2) formation of extractable metal chelates; (3) formation of extractable heteropoly complexes; (4) utilization of flame atomization inhibition. The apparent stoichiometry and the initial linear depression of signal for flame atomization inhibition by sulfate and phosphate on alkaline earths prompted early investigations into the use of these suppression effects as a means of indirect determination of the respective anion [1, 2].

A titration procedure based on adding a monitor metal to a sample solution while monitoring the metal signal [3—6] yields several important advantages. There is a continuous increase in the metal/anion ratio in the droplets during the titration. The rapid concentration, precipitation, dehydration, etc., processes occurring in the approximately millisecond life of the droplet in the flame depend on the metal/anion ratio, thus the signals obtained expose some of the necessarily intricate chemistry occurring during the life of the droplets. The resulting titration curves are therefore useful and, often yield specific analytical signals for the inhibiting anions. In addition, the analytical measurement does not depend on the absolute magnitude of the instrumental response. By use of an infusion pump, titration procedures

*Present address: The Trane Company, LaCrosse, Wisconsin 54601.

can be arranged so that the most concentrated samples require about 4 min to reach the equivalence point.

Calcium is important as a monitor metal in atomization inhibition titration (a.i.t.), as it produces relatively sensitive flame emission signals. Emission signals require simple spectrometric apparatus, especially when monitoring a titration curve rather than for quantitative measurement of signal intensity. Calcium forms stable refractories with many anions. Fortunately, some of the anions important in water quality control, silicate, phosphate, and sulfate, are predominant among the anions forming refractory compounds. The use of calcium flame photometric measurements for many years has resulted in a large literature on anion inhibition for this system.

EXPERIMENTAL

Apparatus and solutions

The Jarrell-Ash model 82-516 spectrometer with an infusion pump for titrant insertion was used for flame emission measurement. For increased signal intensity, a 620-nm interference filter replaced the monochromator and a solid-state d.c. amplifier was used [4, 6]. All glassware and polyethylene used, was acid-hardened by soaking in 3 M hydrochloric acid overnight. Flame temperature for the a.i.t. titrations was 1790 °C. The temperature measurement was carried out by a line reversal technique as described by Craig et al. [7]. A standard deviation of 6 °C was estimated for a series of five independent measurements on a flame of fixed composition.

All solutions were prepared from reagent-grade materials with deionized distilled water. Stock solutions of silicate, phosphate, and sulfate were made up as previously described [6]. Interfering cations were removed from samples by treatment in a batch process with the hydrogen form of Rexyn 101, (16-50 mesh) cation-exchange resin.

Procedure

A 100-ml beaker containing 50 ml of sample serves as titration vessel; it is placed on a magnetic stirrer. Immediately after aspiration has started, titrant flow and recording are initiated simultaneously by a common switch. Titrant delivery is continued until well past the end-points so that appropriate linear extrapolations can be made on the recorded titration curves.

RESULTS AND DISCUSSION

Atomization inhibition titration (a.i.t.) curves

When calcium is titrated into a mixture of silicate and sulafte or of silicate, phosphate, and sulfate with a flame temperature of about 1790 °C an a.i.t. curve such as that shown in Fig. 1 is obtained. The curve shape shown requires that the total molar concentration of silicate plus phosphate must not

be more than half that of the sulfate, a condition ordinarily applying to supply, surface, and waste waters.

Variations in the horizontal positions of points A, B, and C, corresponding to changes in the SiO_2, PO_4^{3-}, and SO_4^{2-} content of the titrated solutions are summarized by Figs. 2—4. These results show that the relationships are linear and somewhat selective. Point A, for example, is insensitive to either phosphate or sulfate. Figure 2 shows that points A and B have much greater linear sensitivity to silicate concentration than does point C. Phosphate variation (Fig. 3) shows a distinct linear relationship to point B and a smaller linear relationship to point C, but importantly, none to point A. The increase seen with phosphate is only one-half or one-third of that seen with increasing silica on a molar basis. The linear increase in the position of B with increasing orthophosphate drops off at concentrations larger than 6 p.p.m. Higher flame temperatures increase the sensitivity of B to phosphate. Unfortunately, increased flame temperatures decrease the sensitivity of C to sulfate. A flame

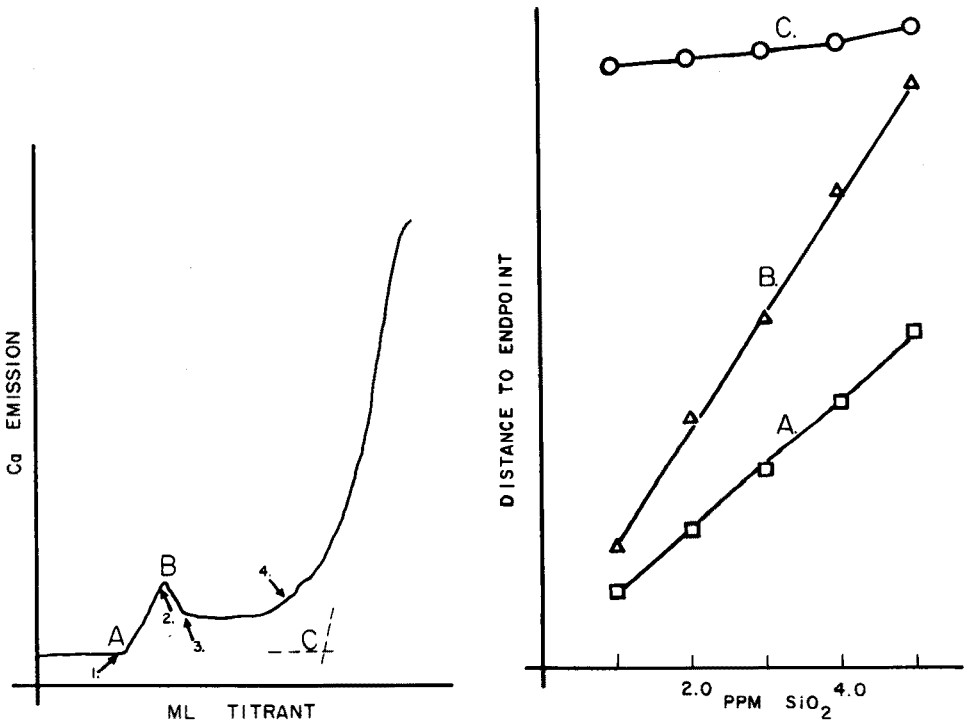

Fig. 1. Atomization inhibition titration (a.i.t.) curve, showing A, B, and C points. 2 p.p.m. SiO_2, 2 p.p.m. PO_4^{3-}, 20 p.p.m. SO_4^{2-}. 1, 2, 3, 4 are the points on the curve where refractory particulates were collected.

Fig. 2. Variations in A, B, and C points with SiO_2 concentration.

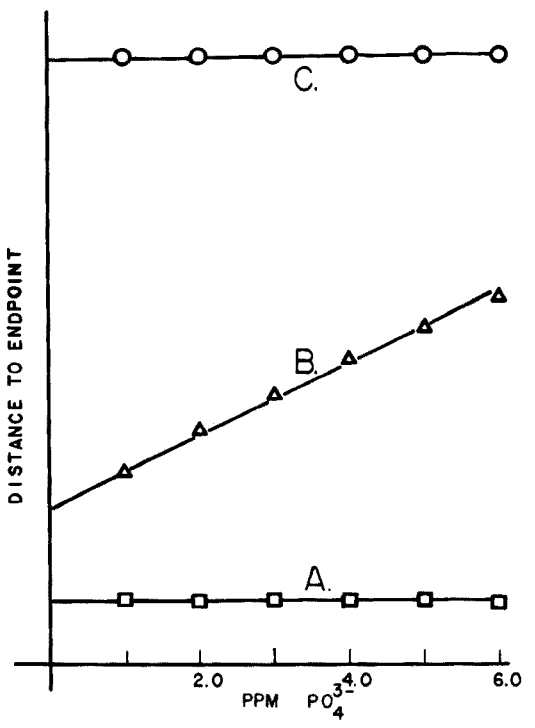

Fig. 3. Variations in A, B, and C points with PO_4^{3-} concentration.

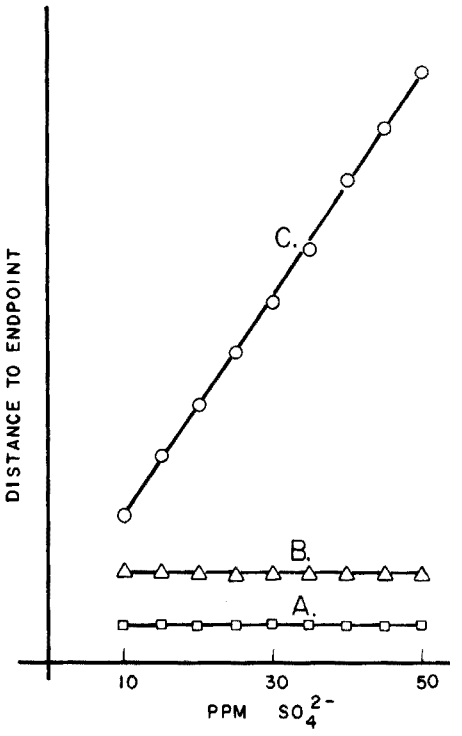

Fig. 4. Variations in A, B, and C points with SO_4^{2-} concentration.

temperature of 1790 °C represents a compromise yielding reasonable phosphate and sulfate sensitivities.

Figure 4 indicates that only C is dependent on the sulfate concentration. The slope of this plot indicates a $[Ca]/[SO_4]$ ion ratio near 1.0 at the point where C occurs. This apparent stoichiometry is somewhat dependent on the flame temperature. Higher temperatures result in a smaller ion ratio.

It has previously been shown [5] that such inhibition properties can be described by a set of linear equations

$$[SiO_2] = k_1\,(A) - k_2 \tag{1}$$

$$[PO_4^{3-}] = k_3\,(B) - k_4\,(A) - k_5 \tag{2}$$

$$[SO_4^{2-}] = k_6\,(C) - k_7\,(B) + k_8\,(A) + k_9 \tag{3}$$

Prepared standards containing known amounts of silicate, phosphate and sulfate are first titrated. With the A, B, and C, end-point data from these titrations, a multiple linear regression analysis provides k_1—k_9 in eqns. (1)—(3) These solutions make it possible to calculate silica, orthophosphate, and

sulfate levels in an unknown from the positions of the A, B, and C points in its titration curve. The technique is equally applicable to water samples which contain very low (less than 0.5 p.p.m.) concentrations of phosphate. For such samples, simple linear calibration plots from the standardizations rather than multiple linear regression can be used.

Linear calibration plots were obtained for titrations of silicate solutions by means of point A over the silica range 0.5—100 $\mu g\ ml^{-1}$. Blanks are necessary to compensate for the presence of silicate in the solvent and the time lag between initiation of titrant flow and the appearance of titrant in the flame (about 2.0 s). Mole ratios of calcium to silicate at the end-point of the titration are somewhat dependent on flame temperature, with hotter flames resulting in a larger calcium to silicate ratio. Under the conditions studied this ratio ranged from 1.3 to 2.0.

A.i.t. mechanisms

Flame particulates representing various points on the a.i.t. titration curves were collected and analyzed by scanning electron microscopy and energy-dispersive x-ray analysis (x.r.a.) to determine the relative amounts of anions in the particles [6]. To simplify the interpretation of the results sample solutions contained silicate and sulfate only. The processed x.r.a. data are summarized in Table 1. These data indicate four regions where the composition of the collected particles undergoes a transition, and that these composition changes correlate with the shape of the a.i.t. curves (Fig. 1). Before the A point the particles are composed entirely of calcium and silicate. Between points A and B, the Si/Ca ratio has decreased indicating the incorporation of more calcium into the particles. The change in the Si/Ca ratio observed between the A and B points is 1.6 and compares well with the change of 1.72 calculated from SiO_2 and calcium concentration data. Results from this region also show the presence of a small but reproducible amount of sulfur in the refractory particulates. After point B in the titration, the Si/Ca composition in the samples appears to change only slightly, but no sulfur is detected. Just before the C point of the curve, particles are collected which again contain sulfur in the lattice. The change in the Si/Ca ratio from just after B to just before C is so small that it may not be significant. The most striking compositional features discernible

TABLE 1

Results of x.r.a. refractory particulate analysis

Location	Si Counts/Ca Counts	S Counts/Ca Counts
Before A	0.65 ± 0.10[a]	0.00 ± 0.01[a]
Between A and B	0.38 ± 0.05[a]	0.05 ± 0.01[a]
Just after B	0.23 ± 0.01[b]	0.00 ± 0.05[b]
Just before C	0.20 ± 0.01[b]	0.09 ± 0.05[b]

[a]Average of four results (± *s*). [b]Average of two results (± range/2).

from these data are the change in Si/Ca ratio between A and B and the alternate exclusion and incorporation of sulfur in the particulate matrixes.

To interpret the titration curve shapes, it must be noted that the aqueous droplets containing dilute solutions of calcium and refractory anions are carried into a flame of nearly 2000 °C with a residence time of approximately 1 ms. Loss of solvent, complexation, precipitation, and pyrochemical reactions between the chemical components of the droplet must occur on that time scale. The extreme temperature conditions, the large number of reactions possible, and the rate at which these reactions have to occur all contribute to the complexity of the chemical system and its interpretation. The titration curve data and the particulate composition data reported here are not inconsistent with a mechanistic scheme reported earlier for magnesium based on kinetic effects [5, 8, 9].

The reversal at point B is probably the most remarkable feature of this titration curve, because it indicates that the signal from the metal atom or molecular bond emission in the flame is decreasing while the concentration of metal in the titrated solution and in the aspirated droplets is increasing. This suggests the formation of a more refractory compound (i.e., less likely to release calcium after the B point).

The horizontal plateau region of the titration curve before C indicates nearly total inhibition or, at least, an extent of inhibition independent of the total calcium concentration. This is the portion of the curve that is sensitive to the sulfate concentration, and it is assumed that calcium and sulfate form a refractory compound which does not dissociate at the flame temperature used. This probably occurs coincidently with silica and phosphate inhibition reactions.

The linear increase in signal observed after point C is attributed to the addition of calcium in excess of that needed for the formation of refractory compounds. Discrepancies seen in the end-points as a result of changing flame temperatures may imply temperature-dependent variations in the net stoichiometries of some of these compounds or variations in the extent of formation of volatile products of the anions, e.g., SiO_2, P_2O_5, SO_3, etc.

A parallel mechanistic explanation to that presented above can be expressed by means of equilibrium arguments. The essential argument is the same in that the characteristic regions of the a.i.t. curves are ascribed to changes in the metal:anion ratios of refractory particulates formed in the flame. Regions in Fig. 1 where increasing or decreasing signals are observed (between A and B, just after B, and possibly after C) can result from changes in the form or composition of the compound produced which make it more or less susceptible to decomposition by the flame. The rate of this signal change, i.e. the slope of the titration curve, can be attributed to several causes. Slowly changing signals may result from a gradual changeover from one stoichiometry or crystalline form to another, representing a region where both the refractory and slightly labile material are formed. Slowly rising or decreasing titration signals could also be attributed to size variations

in the nebulized droplets and dried aerosol clotlets of the sample. These mass discrepancies could be expected to cause selective decomposition of one size extreme and survival of the other while a change in metal:anion ratio occurs.

The high flame temperatures used in these reactions should aid the rapid attainment of equilibrium, but the rapid removal of solvent suggests the importance of mass transport and chemical kinetics in interpreting the results. The possibility of a mixture of rate and equilibrium mechanisms cannot be excluded.

The x.r.a. data (Table 1) show the expected change in the Si/Ca ratio for particulates collected before and after A on the titration curve (see above). X.r.a. data on particulates from after B and before C on the a.i.t. curves indicate an increase in the S/Ca ratio, as would be expected since the position of C is responsive to sulfate. Precisely how these compositional variations change the shape of the titration curve cannot be ascertained from these data.

Flame temperatures affect the shapes of the anion inhibition curves and, to a certain extent, influence the positions of the end-points for these titrations [5]. A changeover from a.i.t. to "sulfate peak" titrations [6] is found with repetitive titrations at increasing temperature. Such data indicate the importance of maintaining reproducible flame gas flow rates in order to acquire consistent data from these titrations.

The titration curves described were obtained for the calcium atomic emission line at 422.7 nm, the CaOH band at 554 nm, and the CaO band at 622 nm. This would seem to indicate an equilibrium distribution between Ca, CaOH, and CaO in flames [10] and that the peaks and reversals seen in these flame photometric titrations correspond to rapid increases or decreases of all of these species in the flame.

Interference effects

Ordinarily, all cations in the sample are removed by an ion-exchange sample pretreatment. Some investigations, however, were made of metals as interferences for the titration step. Sodium, potassium, and lithium concentrations up to 25 p.p.m. did not interfere. Barium concentrations up to 5 p.p.m. had no significant effect on the curves for SiO_2, PO_4^{3-}, and SO_4^{2-}, probably because barium does not compete effectively with calcium for the formation of refractory compounds in the flame. Since the barium salts are more insoluble and thermally stable than the corresponding calcium salts, this suggests that the inhibition effects are due to rate processes.

Small amounts of both Mg^{2+} and Fe^{3+} interfered significantly, although the manner of interference was quite different. Magnesium concentrations as low as 3 p.p.m. resulted in a.i.t. curves with no A and B reversal points. The effect of small amounts of iron(III) was minimal through point A but a marked and relatively featureless signal enhancement occurred where the B and C points were usually observed. This may indicate that iron(III) interferes with the PO_4^{3-} and/or the SO_4^{2-} inhibition of calcium, but not

with the stronger SiO_2 inhibition. Investigations into applications based on such a specific release were unsuccessful, however.

Anions which did not interfere at the 1000 p.p.m. level are Cl^-, Br^-, NO_3^-, and HCO_3^-.

Concentration measurements

Application to water samples gave the data shown in Table 2. The accuracy and precision of the method compares well with existing slower methods for these anions. The a.i.t. method was also used in the simultaneous determination of silica and phosphate in simulated drinking water [5] (Table 3). Boiler water contains relatively high concentrations of phosphate. For such samples, titration of phosphate can be performed with simple linear calibration based on end-point B. Samples were diluted to about 5 p.p.m. for analysis. Results are shown in Table 4. This technique was also applied to the determination of phosphate in commercial detergent products without previous hydrolysis of polyphosphates (Table 4). A sample equivalent to about 5 p.p.m. of orthophosphates was dissolved in water; about 20 p.p.m. sulfuric acid was added. The phosphate concentration for

TABLE 2

Simultaneous determination of silicate and sulfate in raw and treated municipal water

Sample	A.i.t.		Independent[a]	
	SiO_2 (p.p.m.)	SO_4 (p.p.m.)	SiO_2 (p.p.m.)	SO_4 (p.p.m.)
Raw H_2O	1.37	20.7	≃1.4	≃20.2
Treated H_2O	1.22	24.1	≃1.2	≃25.7

[a]Gravimetric as reported by municipal water purification plant.

TABLE 3

Simultaneous determination of silicate and phosphate in simulated drinking water

Added (p.p.m.)		Found[a] (p.p.m.)	
SiO_2	PO_4	SiO_2	PO_4
1.00	4.00	0.97 ± 0.00	3.94 ± 0.00
1.00	0.00	0.93 ± 0.00	0.20 ± 0.05
2.00	1.00	2.15 ± 0.07	0.67 ± 0.11
4.00	2.00	3.58 ± 0.07	2.36 ± 0.22
4.00	4.00	4.45 ± 0.07	3.79 ± 0.28

[a]Triplicate determinations (± *s*).

TABLE 4

Determination of phosphate

Sample	PO_4 Concn.	
	A.i.t.	Independent
Boiler H_2O no. 1	120 p.p.m.	119.5[a]
Boiler H_2O no. 2	28.0 p.p.m.	26.6[a]
Boiler H_2O no. 3	31.5 p.p.m.	33.0[a]
Detergent A	22.0 ± 0.5 %[b]	22.0[c]
Detergent B	32.8 ± 0.0 %[b]	34[c]
Detergent C	18.0 ± 0.5 %[b]	19[c]
Detergent D	30.2 ± 1.7 %[b]	28[d]

[a]As reported by power plant. [b]Estimated s.d. based on triplicate determinations. [c]Heteropoly blue method. [d]Label value.

Detergent A determined by the standard heteropoly method, was used as the basis of standardization.

Point A on the a.i.t. curve can be used for convenient determination of silicate in water. The result of a standard addition analysis on a tap water sample containing 1.2 p.p.m. SiO_2 was 1.16, when three additions in the range 1.00—4.00 p.p.m. SiO_2 were made. The data showed good linearity, excellent percentage recovery, and adequate sensitivity to resolve sub-p.p.m. levels of silica.

Precision and determination limits

Repeated (5) runs on 0.50 p.p.m. SiO_2 provided a standard deviation of 0.026 and a relative standard deviation of 4.8 %. Larger samples tended to increase the relative precision. The detection and determination limits were calculated by a method outlined by Parsons [11] for a 95 % confidence interval and a 5 % relative standard deviation. The detection limit was 0.014 p.p.m. (range 0.034 p.p.m.) and the determination limit 0.10 p.p.m. (range 0.22 p.p.m.). The analytical signal measured in these determinations is the amount of titrant or, because a constant-rate infusion pump is used for titrant delivery, the time needed to reach the end-point. The associated noise is some measure of the scatter of the end-point measurement for repeated runs on the same sample. The detection and determination limits given above were calculated by using either the estimated standard deviation or the range from a series of runs as an estimate of the noise. The precision of both methods is good enough for detection limits of less than 0.1 p.p.m. and determination limits near 0.1 p.p.m. to be expected. However, the practical problem in realizing these low levels experimentally is that the magnitude of the titration curve end-points decreases rapidly with decreasing sample concentration. The net result is that the actual determination limits were about twice those predicted.

These techniques allow titrations of anions at concentration levels one or two orders of magnitude less than is common for other titration methods. The sensitivity can be attributed to the inherent sensitivity of flame emission and the complete utilization of discrete portions of the titration solution.

An interesting consequence of attempts to increase the optical efficiency of the detection system showed that the optimum wavelength for observing calcium emission depends on the bandpass of the resolving system used. With 100-μm slits in the monochromator, the 422.7-nm calcium atomic emission line yielded greater sensitivity than the CaOH (554 nm) or the CaO (622 nm) bands. With 1-mm slits, the calcium sensitivity increased at each of the wavelengths listed, but the increase was most dramatic at the 554-nm band. When a narrow-line interference filter is used the 622-nm CaO emission band provides the most sensitive wavelength for observation. This shift in relative sensitivity is due to the molecular emission bands being less intense but much broader than the atomic emission lines. Wider bandpasses permit integration of the emission intensity over a wider wavelength region [12].

Burners other than the pre-mix laminar-flow type were briefly examined. Several titrations were attempted with the total consumption burner of a Coleman 51Ca flame photometer and a burner from an Instrumentation Laboratory (IL) model 143 flame photometer. Discontinuities and slope changes which could be related to the silicate and the sulfate content of the samples were observed. Figure 5 represents a tracing of some titration curves obtained on a Coleman 51Ca filter flame photometer. Some clearly definable points are evident, and the positions of these points were used to prepare linear calibration curves for silica concentrations up to 10 p.p.m. and sulfate concentrations to 60 p.p.m. Table 5 lists some analytical results obtained with the Coleman Instrument for solutions containing silica and sulfate. The accuracy, precision, range, and selectivity seem suitable for analysis of potable waters. The slope of the sulfate calibration plot was used to calculate a Ca/S ratio.

The discrepancy between the titration curve shapes obtained with these burners compared to those described earlier can be attributed to several factors. The total consumption burner on the Coleman, and to a lesser extent the Instrumentation Laboratory burner, produce an aspirated aerosol containing a large range of droplet sizes [13]. Crawford et al. [8] have compared total consumption and premix flames and have demonstrated that the smaller range of droplet sizes resulting from a laminar flow burner gives a significant difference in the inhibition effects of anions. Apparently some size discrimination is necessary for observation of the reversal phenomena. The titration curve comparisons are complicated by differences in flame temperature. The Coleman and IL burners use methane as fuel, so that higher temperatures are obtained. These anion effects have been shown to be very dependent on flame temperature [4, 5]. Exact flame temperatures were not measured for either of these burners, but the Ca/S ratio results described earlier indicate higher flame temperatures.

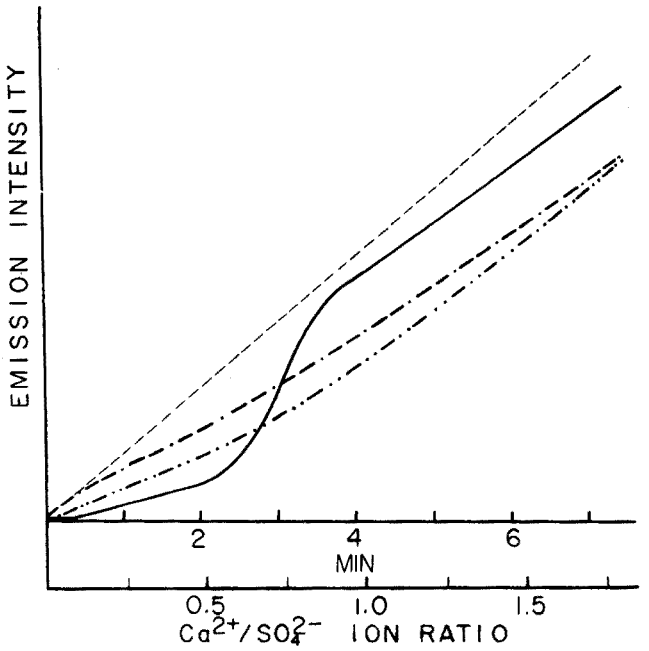

Fig. 5. Anion inhibition titration with the Coleman 51Ca flame photometer. ——— Blank. ——·—— 20 p.p.m. SO_4^{2-}. ··—··— 6 p.p.m. SiO_2. —— 20 p.p.m. SO_4^{2-} + 6 p.p.m. SiO_2.

TABLE 5

A.i.t. results with a Coleman flame photometer

	SO_4^{2-} Found[a] p.p.m.	SiO_2 Found[a] p.p.m.	SO_4^{2-} Present p.p.m.	SiO_2 Present p.p.m.
No. 1	8.7 ± 1.1	0.75 ± 0.20	10.0[b]	1.0[b]
No. 2	31.1 ± 0.7	4.1 ± 0.06	30.0[b]	4.0[b]
No. 3	49.5 ± 0.5	5.9 ± 0.10	50.0[b]	6.0[b]
Milw. Tap H_2O	25.6 ± 0.3	1.3 ± 0.20	25.7[c]	1.2[c]

[a]Results (± s). [b]Added as pure SO_4^{2-} or SiO_2. [c]Gravimetric as reported by municipal water purification plant.

In addition to providing useful analytical methods, these studies of flame inhibition titration yield information on the mechanisms of anion inhibition and enhancement in flame spectrometry. The technique provides a convenient method of looking at pyrochemical reaction products as a function of the concentration of one of the reactants. The dynamic nature of this titration approach represents a substantial improvement over a series of individual experiments at different concentration levels.

The authors are grateful for the assistance of the Linnwood Water Purification Plant and the Wisconsin Electric Power Co. of Milwaukee, Wisconsin, for samples, and to Instrumentation Laboratories, Inc., Wilmington, Massachusetts for a burner.

REFERENCES

1 D. J. Currough, in J. Jordan (Ed.), Treatise on Titrimetry: New Developments in Titrimetry, Vol. 2, M. Dekker, New York, 1974, pp. 172—178.
2 W. A. Dippel, C. E. Bricker, and N. H. Furman, Anal. Chem., 26 (1954) 553.
3 K. C. Singhal, T. P. C. Sinha, and B. K. Banerjee, Technology (Sindri, India), 6 (1969) 219.
4 R. M. Looyenga and C. O. Huber, Anal. Chem., 43 (1971) 498.
5 C. I. Lin and C. O. Huber, Anal. Chem., 44 (1972) 2200.
6 J. R. Sand and C. O. Huber, Anal. Chem., 48 (1976) 1331.
7 M. C. Craig, T. S. Carlton, and R. C. Schoonmacker, J. Chem. Educ., 51 (1974) 54.
8 M. E. Crawford, C. I. Lin, and C. O. Huber, Anal. Chim. Acta, 64 (1973) 387.
9 R. W. Looyenga and C. O. Huber, Anal. Chim. Acta, 55 (1971) 179.
10 D. R. Jenkins and T. M. Sugden, in J. A. Dean and T. C. Rains (Eds.), Flame emission and Atomic Absorption Spectrometry, Vol. 1, Dekker, New York, 1969, Chapter 5.
11 M. L. Parsons, J. Chem. Educ., 46 (1969) 290.
12 J. Duorak, I. Rubeska, and Z. Razac, Flame Photometry: Laboratory Practice, Chemical Rubber Co. Press, Cleveland, Ohio, 1971, Chapter 14.
13 R. Herrmann, in J. A. Dean and T. C. Rains (Eds.), Flame Emission and Atomic Absorption Spectroscopy, Vol. 2, M. Dekker Inc., New York, 1971, Chapter 3.

Analytica Chimica Acta, 87 (1976) 91—95

THE DETERMINATION OF LITHIUM ISOTOPE ABUNDANCES WITH A DUAL-BEAM ATOMIC ABSORPTION SPECTROMETER

J. F. CHAPMAN and L. S. DALE

Chemical Technology Division, Australian Atomic Energy Commission, Research Establishment, Lucas Heights, New South Wales 2232 (Australia)

(Received 17th May 1976)

SUMMARY

The direct determination of lithium isotope abundances by atomic absorption spectrometry with a dual-beam instrument is described. A natural lithium hollow-cathode lamp and an enriched lithium-6 hollow-cathode lamp are both aligned on the optical axis. When a solution of lithium is nebulized into an air-acetylene flame, the difference in absorbance of the outputs of the two lamps, obtained in a single measurement and computed electronically, is proportional to the isotopic abundance. This relationship has been used as a basis for carrying out abundance measurements of 0—100 atom % lithium-6. The method is simple and rapid and compares favourably with the atomic absorption procedure based on absorbance ratios. The precision is ± 0.5 atom % lithium-6. The method is dependent on concentration with respect to total lithium content.

The potential of atomic absorption spectrometry for isotopic analysis was first recognised by Walsh [1]. When low-resolution spectrometers are used, the emission line widths of the primary source must be less than the isotopic wavelength shift. The absorption line widths of the isotopic components in the flame should also be sufficiently separated to allow peak absorbance measurements to be a function of concentration.

For lithium, the isotopic shift in the 670.8-nm resonance line is 0.015 nm and the fine structure for each isotope consists of a doublet with 0.015-nm separation. The spectrum emitted by a mixture of lithium isotopes thus appears as a triplet (Fig. 1). Because of the overlap it is not possible to measure one isotope independently of the other. Zaidel' and Korennoi [2] determined lithium isotope abundances by atomic absorption with an enriched lithium-7 lamp. Their method required a prior total lithium determination by flame emission since the slope of the calibration curve was concentration-dependent. For emission sources, Manning and Slavin [3] used open flames into which lithium-6 and lithium-7 solutions were nebulized. Analyses were based on the ratio of the absorbances for the lithium-6 and lithium-7 sources. Line broadening in the emission sources increased the overlap of the isotopic components which limited the precision to about ± 10 %.

The absorbance ratio technique was further investigated by Wheat [4] who

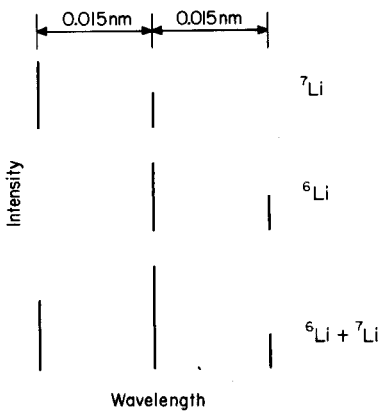

Fig. 1. Fine structure and isotopic separation in lithium 670.8-nm line.

used hollow-cathode lamps as emission sources. He showed that the use of pure isotopic sources was unnecessary as long as the sources were sufficiently different. This method represented a significant improvement on previous techniques since isotopic analysis could be carried out rapidly from two absorbance measurements on the one sample. The method also did not rely on intimate matching of the total lithium concentration. For optimum results by this technique, flame conditions must be stabilized because of the time interval between the two absorbance measurements. Even small changes in flame conditions during a run of standards and samples lead to significant variations in the absorbance ratio, and this affects the precision of the analysis. Simultaneous measurement of both absorbances would overcome the problem of flame fluctuations and allow the absorbance ratio to be independent of flame fluctuations. The introduction of dual-beam atomic absorption spectrometers designed for background correction offered the possibility of carrying out such a measurement. Accordingly, an attachment described by Dick et al. [5] was used to investigate the feasibility of direct abundance measurement.

Basis of the method

The optical arrangement of the dual-beam attachment consists of a hollow-cathode lamp (the analysis lamp) aligned in the optical axis of the instrument, and a hydrogen hollow-cathode lamp (the continuum lamp) set at right angles to the axis. The beam of the hydrogen lamp is aligned on the optical axis with a 45° half-aluminized mirror situated in front of the analysis lamp. By triggering the continuum lamp 180° out of phase with the analysis lamp, an effective subtraction of the two absorbances is obtained. For true background correction, the two light beams should be matched as closely as possible on the optical axis.

If, in this system, the continuum lamp is replaced by a lithium lamp having

different isotopic abundance to the analysis lamp (in this case a natural lithium lamp), the net output from the amplifier will be the difference between the absorbances.

EXPERIMENTAL

All measurements were made on a Varian-Techtron Model AA5 atomic absorption spectrometer with an air-acetylene flame. The dual-beam attachment was built at these laboratories and incorporated a separate gain control on the logarithmic preamplifier which permitted operation of the main amplifier in the normal gain mode. An enriched lithium-6 (93 atom %) hollow-cathode lamp was specially manufactured by Varian Pty Ltd, Springvale, Victoria. This lamp was used in the dual-beam attachment and a natural lithium hollow-cathode lamp was used in the normal turret position. The lamps were operated at around 3 mA. A R446 photomultiplier (Hamamatsu Co., Japan) was used for increased sensitivity at the lithium resonance line. The slits were set at 100 μm. The monochromator was peaked on the 670.8-nm resonance line by masking the natural lamp from the slit and monitoring the radiation from the enriched lithium lamp.

Lithium carbonate isotope standards (99.3 ± 0.2 atom % lithium-6, 99.992 atom % lithium-7) were obtained from Oak Ridge National Laboratory. Stock solutions (100 mg l^{-1}) of total lithium were prepared by dissolving the lithium carbonate in distilled water and neutralizing with a minimum volume of A.R. hydrochloric acid. Isotopic standards were prepared by diluting combinations of the stock solutions to 2.0 mg l^{-1} of total lithium. Samples of lithium carbonate were similarly processed to give a solution of 2.0 mg l^{-1}. The solutions were nebulized into an air-acetylene flame in which the fuel-oxidant ratio was set to give optimum stability and sensitivity.

In setting up the calibration, with matched intensities of the two lamps, it was found that the response of the amplifier had a null point around 50 atom % which corresponded to the zero of the amplifier meter. This was to be expected since the average abundance of the two lamps was 50 atom %. Solutions containing less than 50 atom % lithium-6 gave a negative response. It was therefore necessary to displace the recorder zero to mid-scale to cover the range 0—100 atom % lithium-6 and record both positive and negative readings with respect to the recorder zero. Since it is not necessary to match the intensities of the two beams, it was decided to run the standards with the intensity from the natural lamp varied. Calibrations were obtained with the natural lamp output set at the 30, 50 and 80 % points on the amplifier meter. (These points are a measure of the difference in the logarithms of the intensities of the two lamps.) The resultant calibrations were all parallel to the matched (100 %) intensity calibration. At the 50 % setting, all standards gave a negative response and this calibration was chosen as the most suitable.

RESULTS AND DISCUSSION

A typical calibration over the range 0—99.3 atom % lithium-6 is shown in Fig. 2. The slight curvature is probably due to the fact that, for each isotope, the measured absorbance results from the combination of the different absorption coefficients of the two fine-structure components. Under normal operating conditions a much smaller dynamic range is used and the calibration may be considered linear over smaller concentration ranges. Under these conditions, a precision of ± 0.5 atom % ^{6}Li is obtainable.

Although it is not necessary to match the intensities of the two lamps, it is essential to maintain a constant intensity at the level chosen. For this reason, an adequate warm-up period must be selected for the lamps to give the desired stability. To obtain adequate sensitivity in the calibration, it was necessary to run the preamplifier at a high gain and to set the photomultiplier voltage two ranges above that required for full-scale peaking of the lamp. Under these conditions high stability of the hollow-cathode lamp output is essential to minimize drift and obtain optimum precision.

To assess the suitability of the method, a set of lithium carbonate samples previously analyzed by thermal ionization mass spectrometry was analyzed using the conditions described. Table 1 compares the values obtained by this method with those obtained by the absorbance ratio method. It should be pointed out that high precision was not required for the mass spectrometric results when the analysis was originally requested. The agreement between the atomic absorption results by the dual-beam method and by the ratio method is very good and is within the experimental error. From this, it cannot be ascertained whether one method is superior to the other. However, from experience in the use of both methods, the dual-beam method is slightly faster and is independent of flame fluctuations, unlike the ratio method. A disadvantage is the requirement for constant total lithium concentration.

The samples used in this test were approximately stoichiometric lithium

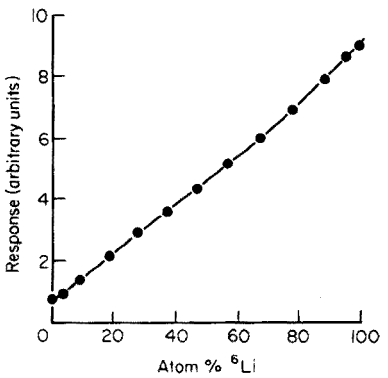

Fig. 2. Typical calibration for the measurement of ^{6}Li abundance.

TABLE 1

Comparison of lithium isotope abundances by atomic absorption by the dual-beam absorbance difference method and the absorbance ratio method (All results are given as atom % lithium-6.)

Sample No.	Dual-beam method	Absorbance ratio method	Mass spectrometry
1	47.6	46.6	47.8
2	47.0	46.3	45.8
3	41.3	39.0	40.0
4	46.8	46.1	47.0
5	93.4	92.8	93.0
6	40.0	39.0	38.7
7	41.8	41.7	41.1
8	47.2	47.5	47.0

carbonate which facilitated the dilution to the appropriate concentration range. For solutions of unknown lithium content it is necessary to carry out a total lithium determination so that the correct concentration level may be selected. However, it should be possible to modify the electronics of the dual-beam arrangement so that absorbance ratios can be read directly. This would make the technique independent of total lithium concentration, at least to the extent of that obtained in the absorbance ratio technique. This aspect is presently being investigated.

Conclusion

The use of a dual-beam atomic absorption spectrometer is suitable for direct determination of lithium isotope abundances when hollow-cathode lamps of different isotopic composition are used. The simultaneous measurement of absorbances eliminates problems with flame fluctuations but it is necessary to standardize the total lithium concentration. The method is rapid and adequate for control purposes, and the technique should be applicable to isotopic analysis for other elements amenable to atomic absorption analysis and which have suitable isotopic separations in their spectral lines.

REFERENCES

1 A. Walsh, Spectrochim. Acta, 7 (1955) 108.
2 A. N. Zaidel' and E. P. Korennoi, Opt. Spectrosc., 10 (1961) 299.
3 D. C. Manning and W. Slavin, At. Absorpt. Newsl., 1 (1962) 1.
4 J. A. Wheat, Appl. Spectrosc., 25 (1971) 328; Paper presented to 11th Conference on Analytical Chemistry in Nuclear Technology, Gatlinburg, Tenn., USA, October 10—12, 1967. CONF-671012-7, DP-MS-67-62.
5 D. L. Dick, S. J. Urtamo, F. E. Lichte and R. K. Skogerboe, Appl. Spectrosc., 27 (1973) 467.

Analytica Chimica Acta, 87 (1976) 97—101

THE DETERMINATION OF ANIONIC DETERGENTS AT p.p.b. LEVELS BY GRAPHITE FURNACE ATOMIC ABSORPTION SPECTROMETRY

P. T. CRISP, J. M. ECKERT and N. A. GIBSON

Department of Inorganic Chemistry, University of Sydney, Sydney, N.S.W. 2006 (Australia)

G. F. KIRKBRIGHT and T. S. WEST*

Department of Chemistry, Imperial College, London SW7 2AY (England)

(Received 3rd May 1976)

SUMMARY

A method is described for the determination of anionic detergents at levels below 50 $\mu g\ l^{-1}$. The detergent anions are extracted into chloroform as an ion-association compound with the bis(ethylenediamine)copper(II) cation and determinations are completed by atomic absorption spectrometry with a graphite furnace atomizer. With a 750-ml water sample, the limit of detection is 2 $\mu g\ l^{-1}$ (as linear alkyl sulphonic acids). The method requires a single extraction and is highly selective. It is applicable without modification to fresh, estuarine and sea-water samples.

Few methods are available for the determination of anionic detergents at levels below 50 $\mu g\ l^{-1}$. The widely used methylene blue active substances test is not adequate in this concentration range, having a detection limit of 25 $\mu g\ l^{-1}$, as linear alkyl sulphonic acids, in fresh water and still poorer sensitivity with marine and estuarine waters [1].

In 1970, Le Bihan and Courtot-Coupez reported procedures for the determination of anionic detergents in sea water [2] and, in 1974, procedures applicable to fresh-water samples [3]. The detergent anions are extracted into methyl isobutyl ketone (MIBK) as an ion-association compound with the tris(1,10-phenanthroline)copper(II) cation. The limit of detection is 3 $\mu g\ l^{-1}$ (as Manoxol O.T. and sodium dodecyl sulphate) in sea water and 1.5 $\mu g\ l^{-1}$ in fresh water. The high sensitivity follows partly from the use of large (1 l) samples and partly from the method chosen by these authors to complete the analysis, i.e., the determination of copper in the MIBK extract by flame a.a.s. A total of five procedures were described, the selection of which depends on the detergent concentration and salinity of the sample.

The literature also contains a radiometric method, developed by Taylor and Waters [4], which has a detection limit of 5 $\mu g\ l^{-1}$ (as sodium dodecyl

*Present address: The Macaulay Institute for Soil Research, Craigiebuckler, Aberdeen AB9 2QJ (Scotland).

sulphate) in potable and ground waters. The extracting cation is tris(1,10-phenanthroline)iron(II), labelled with iron-59.

This paper describes a new method for the determination of anionic detergents at very low levels. The basis of the method is the same as that of a method reported in an earlier paper [5], namely the extraction of detergent anions into chloroform as an ion-association compound with the bis(ethylenediamine)copper(II) cation.

The procedure outlined here retains the simplicity and high selectivity of the earlier method. It requires a single extraction, regardless of the salinity of the sample, and is applicable without modification to fresh, estuarine and marine waters. By the use of larger sample volumes and an a.a.s. finish with graphite furnace atomization, the limit of detection is reduced to 2 $\mu g\ l^{-1}$ (as linear alkyl sulphonic acids).

EXPERIMENTAL

Apparatus and reagents

A Perkin-Elmer 300S atomic absorption spectrophotometer, fitted with a deuterium background compensator and an HGA 74 graphite furnace atomizer, was used.

Standard reference anionic detergent solution. A solution containing 5.55 % active linear alkyl sulphonic acids (LAS), of mean molecular weight 318, was obtained from the U.S. Environment Protection Agency. This solution was used to prepare a stock standard solution containing 750 μg LAS l^{-1}, which was diluted further as required.

Bis(ethylenediamine)copper (II) reagent. Dissolve 124.6 g of copper sulphate pentahydrate and 99.2 g of ammonium sulphate in warm water. Add 90.2 g (100 ml) of ethylenediamine and dilute to 1 l with water. The reagent is stable for at least a month.

Capillary siphons. Bend 30-cm lengths of 0.5-mm bore capillary glass tubing through a 300° angle 12 cm from one end.

Recommended procedure

Place a 750-ml water sample, containing not more than 50 μg LAS l^{-1}, in a 1-l separating funnel and, if necessary, adjust the pH to 5—9. Add 25.0 ml of bis(ethylenediamine)copper(II) reagent and 20.00 ml of chloroform. Shake for 1 min and allow to stand until the phases separate.

Run about 13 ml of the chloroform layer into a 15-ml graduated centrifuge tube and add 1 ml of the aqueous phase (to prevent evaporation of the chloroform). Stopper the tube and centrifuge at 2000 r.p.m. for 30 min.

Fill a capillary siphon with chloroform and insert the short arm through the aqueous layer into the chloroform extract, keeping the long arm closed. Allow the chloroform to siphon, discard the first ml of liquid and then collect about 10 ml of clear extract in a small flask fitted with a ground-glass stopper.

Complete the determination by injecting 50-μl aliquots of the chloroform

extract into the carbon tube of the atomic absorption spectrometer, using the following temperature programme: 100 °C for 30 s (solvent evaporation), 950 °C for 30 s (ashing), 2500 °C for 10 s (atomization) and 3000 °C for 10 s (burn off). The lamp current was 15 mA, the wavelength 324.7 nm and the spectral band pass 0.2 nm.

Carry out a blank determination with 750 ml of distilled water and calculate the detergent concentration in the sample by comparison with standards run simultaneously.

RESULTS AND DISCUSSION

The proposed method was designed as a low concentration complement to the earlier method [5]. The extraction conditions are similar but greater sensitivity is achieved by the use of a larger sample volume, clarification of the extract by centrifugation, and the direct determination of copper in the chloroform extract by a.a.s. with graphite furnace atomization.

Calibration

Since the working conditions of an atomic absorption spectrometer are optimized at the beginning of a run, standards must be measured with the unknowns. The calibration graphs showed slight curvature in the range 0—50 μg LAS l^{-1} and marked curvature beyond 50 μg l^{-1}. To determine anionic detergent in the concentration range 50—500 μg l^{-1} and so overlap with the earlier method [5], it is recommended that 10-μl aliquots of the chloroform extract be substituted for the 50-μl aliquots.

Precision, limit of detection and accuracy

The precision of the proposed method was assessed by carrying out repeated determinations of standard solutions containing between 5 and 200 μg LAS l^{-1}. The results are shown in Table 1.

The limit of detection, taken to be the detergent concentration which gave an absorbance equal to twice the standard deviation of a set of 16

TABLE 1

Precision of proposed method

LAS taken[a] (μg l^{-1})	s (μg l^{-1})	s_r (%)
5	1	20
10	0.5	5
50	1.5	3
100	3	3
200	4	2

[a] 14 determinations were carried out at each level.

TABLE 2

Recovery of linear alkyl sulphonic acids from sea water

LAS added ($\mu g\ l^{-1}$)	Mean LAS found[a] ($\mu g\ l^{-1}$)	s ($\mu g\ l^{-1}$)	Mean recovery (%)
0	<2	—	—
10	9	0.5	90
100	94	3	94

[a]Mean of 8 determinations.

TABLE 3

Allowable concentrations of foreign ions[a]

Concentration	Ion
0.5 M	Cl^-, F^-, NO_3^-, SO_4^{2-}
1000 mg l^{-1}	SCN^-, ClO_4^-, NO_2^-, CH_3COO^-, Br^-, I^-, $P_2O_7^{4-}$, Mg^{2+}, Ca^{2+}, $C_6H_5O_7^{3-}$ (citrate)
100 mg l^{-1}	Cu^{2+}, Ni^{2+}
10 mg l^{-1}	Al^{3+}, Cr^{3+}, Mn^{2+}, Zn^{2+}, Co^{2+}
1 mg l^{-1}	Fe^{3+}
0.1 mg l^{-1}	S^{2-}

[a]95—100 % recovery of 100 μg LAS l^{-1} (0.100 mg l^{-1}) was obtained in the presence of the stated concentration.

absorbance readings at or near blank level, was found to be 2 $\mu g\ l^{-1}$ (as linear alkyl sulphonic acids). The accuracy of the method was evaluated by determining the recovery of different concentrations of linear alkyl sulphonic acids added to sea water (Table 2).

Interferences

The effects of various ions on the recovery of 100 μg LAS l^{-1} are summarized in Table 3. No recovery greater than 100 % was observed, i.e., there were no positive interferences. The pattern of interferences was similar to that found with the method of Crisp et al. [5].

Only sulphide and iron(III) ions interfere at concentrations likely to be found in polluted waters. There is, however, no interference from 100 mg $S^{2-}\ l^{-1}$ if the water sample is treated with 2 ml of 30 % hydrogen peroxide for 5 min before the addition of the bis(ethylenediamine)copper(II) reagent. The addition of 10 ml of 2 % EDTA (disodium salt) solution suppresses interference by 100 mg $Fe^{3+}\ l^{-1}$. Hydrated iron(III) oxide interferences much less than iron(III) ions and, if the iron is mostly present in this form, the addition of EDTA can be omitted.

The non-ionic detergent Triton X100 does not interfere with the recovery

of 100 μg LAS l^{-1} when present at the same concentration.

The proposed method, in combination with that of Crisp et al. [5] permits the determination of anionic detergents over the concentration range of 2—15,000 μg l^{-1} (as linear alkyl sulphonic acids), with a precision of 5 % or better for concentrations above 10 μg l^{-1}. Both methods are insensitive to ionic interference and can be used directly with fresh, estuarine and seawater samples.

One of us (P. T. C.) received support during this work from an Australian Government Post-Graduate Research Award.

REFERENCES

1 Standard Methods for the Examination of Water and Wastewater, American Public Health Association, Washington, D.C., 13th edn., 1971, p. 340.
2 A. Le Bihan and J. Courtot-Coupez, Bull. Soc. Chim. Fr., (1970) 406.
3 A. Le Bihan and J. Courtot-Coupez, Analusis, 2 (1974) 695.
4 C. G. Taylor and J. Waters, Analyst (London), 97 (1972) 533.
5 P. T. Crisp, J. M. Eckert and N. A. Gibson, Anal. Chim. Acta, 78 (1975) 391.

Analytica Chimica Acta, 87 (1976) 103—112

HIGH RESOLUTION FIELD DESORPTION MASS SPECTROMETRY PART VI. ORGANIC SULPHATES AND SULPHATE ESTERS*

H.-R. SCHULTEN and W. D. LEHMANN

Institute of Physical Chemistry, University of Bonn, 5300 Bonn, Wegelerstr, 12 (West Germany)

(Received 8th June 1976)

SUMMARY

Sulphate esters and sulphate salts of biochemicals and pharmacologically active compounds have been investigated by field desorption mass spectrometry. The underivatized substances gave high cation and cluster ion intensities. Low, but structurally significant, fragmentation was observed. The field desorption mass spectra were characterized by intense doubly charged as well as some triply charged cluster ions. In general the information obtained allowed the molecular weight of the intact salt (cation + anion) to be determined.

The use of field desorption mass spectrometry (f.d.m.s.) for the analysis of nonvolatile compounds has been demonstrated for a wide variety of substances [1]. The basic advantages of the f.d. technique are small sample consumption, high sensitivity, and strongly reduced thermal degradation (no evaporation is required). Although analytical applications of the method to inorganic [2—4] and organic [5] salts have been reported, few results on f.d.m.s. of alkali salts of sulphate esters have been published [6] and no f.d. spectra of large organic sulphate salts have been reported.

The formation of conjugates with carbohydrates, amino acids, peptides, and sulphuric acid is an important metabolite excretion mechanism. The f.d. spectra of hormone glucuronides [7, 8] and the glycyl, *N*-acetyl-*S*-cysteinyl, and glutathionyl conjugates of a drug have been described [9]. Therefore it was of interest to explore the behaviour of sulphate conjugates under the conditions of field desorption. In addition, sulphate salts of pharmacologically active substances were examined by f.d.m.s. since the intact salts as well as the sulphate esters are not amenable to conventional ionization techniques, such as electron impact, chemical ionization, and field ionization. A particular difficulty in the analysis for these compounds by m.s. is that a convenient derivatization method is not available.

The main objectives of this study were the molecular weight determination of the intact, underivatized sulphate esters and salts, and the description of the characteristic features of these compounds in f.d.m.s.

*Part V. H.-R. Schulten and B. Wittmann-Liebold. Anal. Biochem., in press.

EXPERIMENTAL

The f.d. spectra were produced on a modified CEC 21-110B instrument [10] by the photographic detection system with vacuum evaporated AgBr plates (Ionomet, Waban, Mass., USA). The resolution obtained was better than 15000 (at half peak width), and the average accuracy in the mass determination was ± 2 millimass units. For accurate mass measurements (in the text the theoretical masses are given) reference masses were taken from the field ionization mass spectrum of perfluorotributylamine. Field desorption emitters, used in all experiments, were prepared by high temperature activation of 10 μm diameter tungsten wires [11]. The distribution and morphology of the microneedles produced were as shown previously [12]. F.d. emitters with an average length of 30 μm for the carbon microneedles were used as standards. The ionization efficiency and the adjustment of the f.d. emitter were determined by means of *m/e* 58 of acetone in the field ionization mode. In general, $1 \cdot 10^{-7}$ g was applied as sample to the standard emitter via the syringe technique [13]. All f.d. spectra were produced by emission-controlled f.d. [14] at a threshold of $1 \cdot 10^{-8}$ *A* measured between the field anode and the slotted cathode plate at 2 mm distance and at +10 to −2 kV accelerating voltage. The recorded mass range extended from *m/e* 17 to *m/e* 560. Water was normally used as solvent, but strychnine sulphate, quinine sulphate, and atropine sulphate were dissolved in methanol.

RESULTS AND DISCUSSION

Inorganic sulphate salts

Under f.d. conditions simple inorganic salts such as sodium sulphate show large cation intensities [3] and exhibit a series of cluster ions with the composition $[(Na_2SO_4)_n + Na]^+$ where $n = 1$ and 2. In the f.d. spectrum of $(NH_4)_2SO_4$ the ions $[NH_4]^+$, $[(NH_4)_2SO_4 + H]^+$, and $[(NH_4)_2SO_4 + NH_4]^+$ are recorded. In contrast to the behaviour of sodium sulphate, the tendency for the formation of higher clusters is not observed. Since intense ions that result from an exchange of $[NH_4]^+$-ions for $[H]^+$-ions are found, it is assumed that thermal elimination of NH_3 occurs. This is confirmed by an intense ion for $[NH_4HSO_4 + H]^+$ and a pronounced series of clusters of sulphuric acid $[(H_2SO_4)_n + H]^+$, where n is 1, 2, and 3. The types of ion occurring in the f.d.m.s. of inorganic salts and the energetically and kinetically favoured process of cluster formation have been discussed previously [2].

Organic sulphate esters

Figure 1 shows the f.d. spectrum of the potassium salt of α-naphthyl-sulphate ester. The organic part of the salt is a stable aromatic system and the behaviour of the salt under field desorption is similar to that described

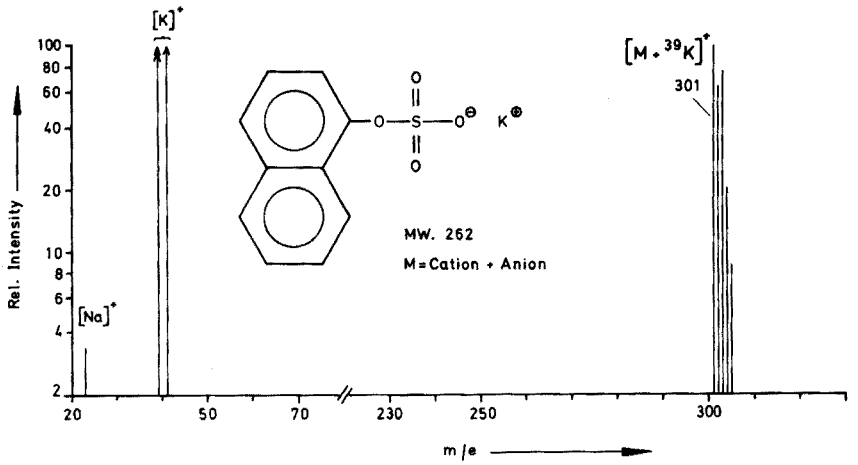

Fig. 1. F.d. spectrum of α-naphthyl sulphate ester, potassium salt.

for the inorganic sulphate salts. The spectrum is characterized by intense cluster ions for $[M + K]^+$. As expected, intense signals for potassium at *m/e* 39 and *m/e* 41 are displayed. Neither the molecular ion nor fragment ions are observed.

The f.d. spectrum of the sodium salt of dodecylsulphate (Fig. 2) similarly shows a very intense signal for the cation (at *m/e* 23) and a prominent $[M + Na]^+$ cluster ion. From a knowledge of the *m/e* values for the cation and cluster ion, the mass of the anion can be calculated, and thus the molecular unit (cation + anion) is easily derived. This molecular weight determination is strongly supported by the occurrence of an intense doubly charged cluster ion $[M + 2Na]^{2+}$. This type of ion has already been found in the f.d. spectra of sulphonates [15, 16], bile acids [6], and dinucleotides [17] and appears to be a significant type of ion in the f.d. spectra of large organic alkali salts. In addition, a series of inorganic cluster ions of sodium sulphate is found in the spectrum in Fig. 2. Gravimetric analysis revealed no detectable free sulphate and elemental analysis gave agreement within 0.1 % for C, H, S, O. The sodium sulphate is thereby shown to be negligible. Therefore the inorganic cluster ions at *m/e* 93.955 $[Na_2SO_4 + 2Na]^{2+}$, *m/e* 164.921 $[Na_2SO_4 + Na]^+$ and *m/e* 306.852 $[(Na_2SO_4)_2 + Na]^+$ are generated by a thermally induced f.d. process. Surprisingly only one fragment ion of the aliphatic chain is found at *m/e* 43.055 for $[C_3H_7]^+$ with 10 % relative abundance.

Among the conjugates of dopamine found in human urine the dopamine-*O*-sulphates play an important rôle [18]. As part of a programme of qualitative and quantitative analysis of dopamine and some of its metabolites in urine samples by electron impact and f.d.m.s. [19] dopamine-4-*O*-sulphate has been investigated. The f.d. spectrum of the synthetic compound [20] is displayed in Fig. 3. By far the most intense signal is recorded at *m/e* 234.044

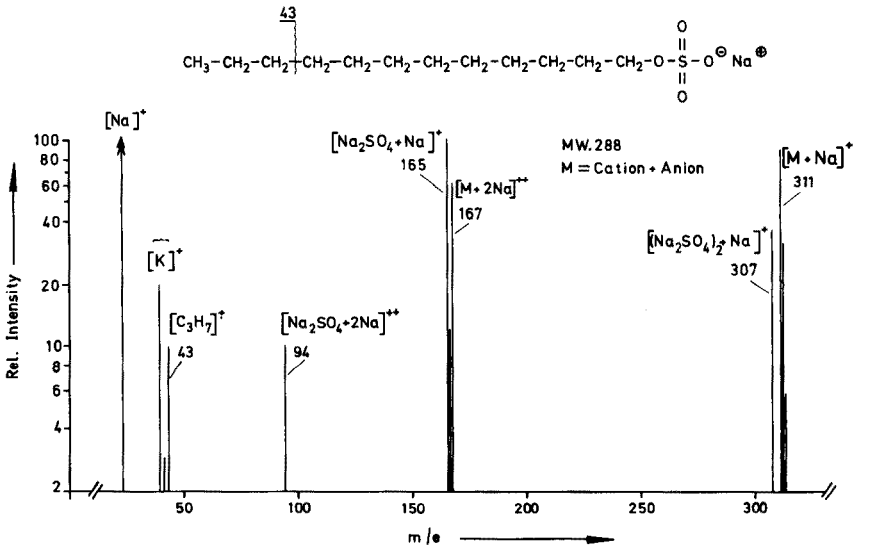

Fig. 2. F.d. spectrum of n-dodecyl sulphate ester, sodium salt.

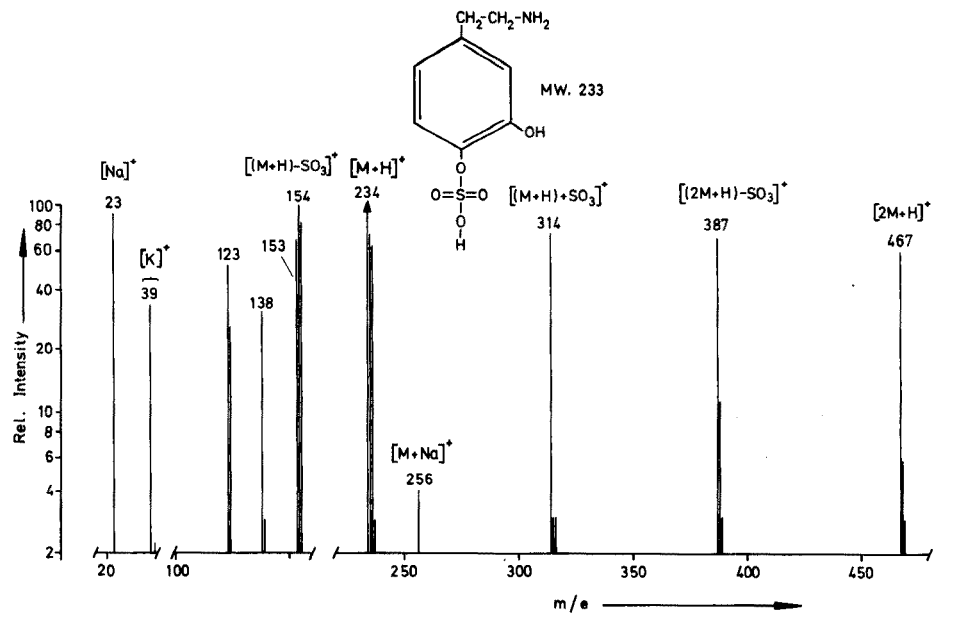

Fig. 3. F.d. spectrum of dopamine-4-*O*-sulphate.

for the protonated molecule which is recorded with saturated blackening of the photoplate. Although the molecular ion is not detected, the correct assignment for the molecular weight is confirmed by a $[M + Na]^+$ signal of medium intensity at *m/e* 256.026 produced by cationisation [21]. Since

inorganic cluster ions are not found alkali salts are only present in trace amounts in the sample. The high relative abundances of the sodium and potassium ions are explained by the high sensitivity of the f.d. method for the detection of these cations. The signal with the second highest relative intensity at *m/e* 154.087 was chosen as base peak and is formed by loss of SO_3 from the protonated molecule. In addition the loss of SO_4 from the $[M + H]^+$ ion leads to an ion at *m/e* 138.092. On the basis of the high resolution data the elemental composition of the ion at *m/e* 123.045 was determined to be $C_7H_7O_2$. This ion is probably generated by loss of SO_3 and β-cleavage in the aliphatic side chain of dopamine-4-*O*-sulphate. This is supported by the occurrence of analogue cleavages in the f.d. spectra of unprotected D-adrenaline and L-Dopa [22]. The $[2M + H]^+$ ion, generally found in the f.d. spectra of polar compounds, is recorded at *m/e* 467 with 58 % relative abundance. From the results of accurate mass measurements the two intense organic cluster ions at *m/e* 314.000 and *m/e* 387.123 were identified as $[(M + H) + SO_3]^+$ and $[(2M + H) - SO_3]^+$, respectively. Above a threshold of 2 % relative intensity, no multiply charged ions were found. Since dopamine-4-*O*-sulphate is present as free acid (or inner salt) the formation of multiply charged ions apparently is not favoured. In contrast, large organic salts show intense multiply charged ions in their f.d. mass spectra. This has been described above for the sodium salt of dodecyl sulphate and will be discussed below for organic sulphates in more detail.

Organic sulphate salts

The f.d. spectra of the following seven organic sulphate salts (Fig. 4) with large organic cations have been recorded. In Table 1 characteristic singly charged ions of compounds I—VII are listed. All sulphate salts showed very intense cation $[C]^+$ and $[C—H]^+$ ion signals. In all cases one of these ions is the base peak of the f.d. mass spectrum. Obviously the f.d. method is a suitable technique for the determination of cations of large organic amines which are present as sulphate salts. In all cases elimination of water from the $[C]^+$ and/or $[C—H]^+$ ion is observed. With the exception of compounds V and VI which show a loss of the isopropylamine moiety, virtually no fragmentation of the organic cations is observed under the experimental conditions selected. At *m/e* values considerably above the nominal mass of the cation, intense cluster ions are observed. One fraction of these cluster ions is organic; the other fraction is purely inorganic. Table 1 shows that the latter cluster ions are useful analytically to show that the compound under investigation is a sulphate salt; some cluster ions (e.g. $[C + H_2SO_4]^+$) also enable the molecular weight (2 C + anion) to be determined.

As mentioned above, the f.d. spectra of the sulphate salts showed intense doubly charged ions and it appears that this is a typical feature in f.d.m.s. of large organic salts of polyvalent acids, such as sulphuric acid and phosphoric acid [23]. Table 2 lists the prominent multiply charged ions in the f.d. mass spectrum of isoprenaline sulphate. Accurate mass measurements enabled the

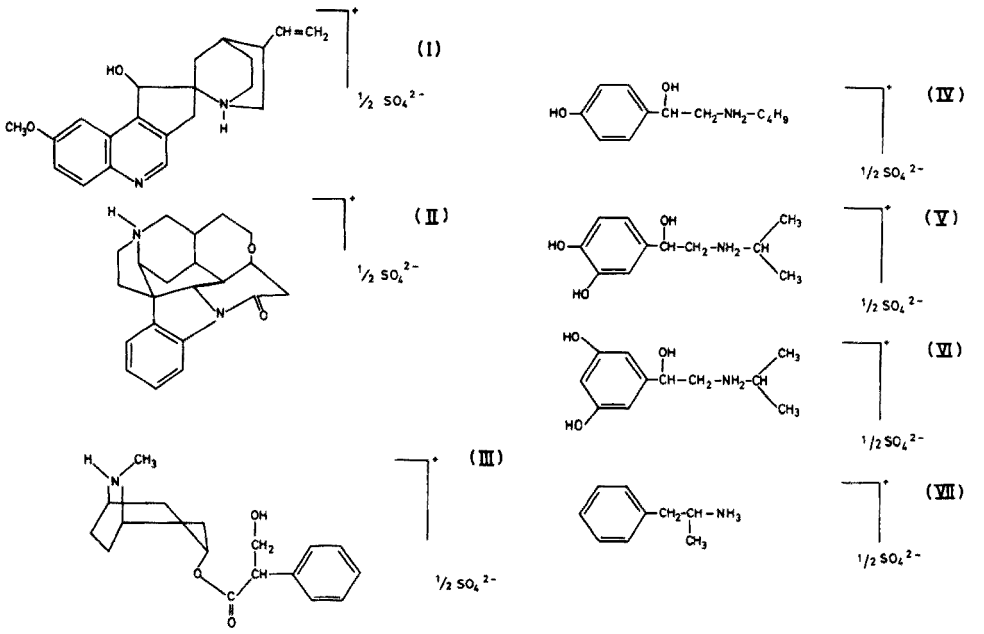

Fig. 4. Structures of the investigated organic sulphate salts: (I) quinine sulphate, (II) strychnine sulphate, (III) atropine sulphate, (IV) bamethane sulphate, (V) isoprenaline sulphate, (VI) orciprenaline sulphate, (VII) amphetamine sulphate.

tentative assignment of the elemental composition to be made. On the basis of these data an abbreviated description of the cluster ions using the cation and fragments as building blocks was employed. It is noteworthy that the intense triply charged ions recorded, a novel type of ion in f.d.m.s., have not been reported previously. The utility of doubly charged ions as an additional information for the interpretation of f.d. mass spectra has been described previously [24].

It is remarkable that all building blocks of the multiply charged cluster ions formulated in Table 2 are also observed as very intense singly charged ions. In field ionization, the formation of doubly charged ions is explained by ionization of singly charged species, which are bound intermediately to the emitter surface [25]. It is assumed that multiply charged cluster ions of large organic sulphate salts are generated under f.d. conditions via aggregation of singly charged ions bound in the adsorbed layer of the emitter surface.

In the investigation of the organic sulphate salts I—VII by f.d.m.s. it was found that the intensities of fragment- and cluster-ions were strongly dependent on the selected programme for emission-controlled desorption. This technique allows a threshold for the total emission — measured between the anode and the cathode plate — to be chosen. This threshold value (a measure of the f.d. ion currents produced) is automatically stabilized by control of the emitter heating current. Simple f.d. spectra with few but

TABLE 1

Characteristic ions in the f.d. spectra of the organic sulphate salts I—VII
(The relative intensities of the signals are given as high ++++, medium +++, low ++, weak +.)

	C—H—H_2O	C—H_2O	C—2H	C—H	C
(I) Quinine sulphate				++	++++
(II) Strychnine sulphate	+			++++	+++
(III) Atropine sulphate	+++	+		++++	+++
(IV) Bamethane sulphate	+++	++		+++	++++
(V) Isoprenaline sulphate		+++	+++	+++	++++
(VI) Orciprenaline sulphate		+++	+++	+++	++++
(VII) Amphetamine sulphate			+++	+++	++++

	C—H—H_2O + H_2SO_4	C—H_2O + H_2SO_4	C + H_2SO_4	C + $2H_2SO_4$	2C—H + H_2SO_4
(I) Quinine sulphate			+++	++	
(II) Strychnine sulphate	+++		++		+
(III) Atropine sulphate			+		
(IV) Bamethane sulphate			++		
(V) Isoprenaline sulphate		+++	++		
(VI) Orciprenaline sulphate		+++	++		
(VII) Amphetamine sulphate			+++		+++

TABLE 2

Doubly and triply charged ions in the f.d. spectrum of isoprenaline sulphate (V)
(The relative intensities are given in four degrees as in Table 1.)

Doubly charged ions	Rel. int.	Triply charged ions	Rel. int.
$[2\,C—H_2O]^{2+}$	++	$[2(C—H_2O) + C]^{3+}$	+++
$[2\,C—H]^{2+}$	+++	$[3(C—H_2O) + (C—H) + H_2SO_4]^{3+}$	++
$[2(C—H_2O) + H_2SO_4]^{2+}$	+++		
$[(2\,C—H_2O) + H_2SO_4]^{2+}$	++		
$[2(C—H) + H_2SO_4]^{2+}$	++		
$[2\,C + H_2SO_4]^{2+}$	++		

significant ions and cluster ions were observed during the beginning of the emission controlled desorption process (especially when a low threshold for the total emission, e.g. $5 \cdot 10^{-9}$ *A*, was set). Integrating ion detection over the complete desorption period, which included higher anode wire currents at the end of the desorption process, yielded a higher amount of fragment ion and cluster ion formation. This phenomenon is illustrated in Figs. 5 and 6 for amphetamine sulphate (compound VII). In Fig. 5 the f.d. spectrum of this compound generated by photographic detection during the first half of the total desorption period is shown. Few intense ions and cluster ions that are easily interpreted are found. Figure 6 displays the f.d. spectrum of the same compound obtained by integrating detection over the total desorption period. In comparison with the f.d. spectrum in Fig. 5 the number of cluster ions is increased and a pronounced series of inorganic cluster ions is observed. Since ammonium sulphate was not present in the sample under investigation, as confirmed by C, H, S, O, and $[SO_4]^{2-}$ analysis, these inorganic cluster ions are generated by a thermally induced degradation during f.d. This observation corresponds with the occurrence of inorganic cluster ions in the f.d. mass spectrum of n-dodecylsulphate ester sodium salt (Fig. 2).

A comparison of Figs. 5 and 6 shows that complex f.d. spectra of large organic sulphate salts obtained by integrating detection over the complete desorption process can be greatly simplified by fractionated desorption [15].

The authors thank Prof. H. D. Beckey for his continuous support and interest in these investigations. This work was supported by grants from the Deutsche Forschungsgemeinschaft, Ministerium für wissenschaft und

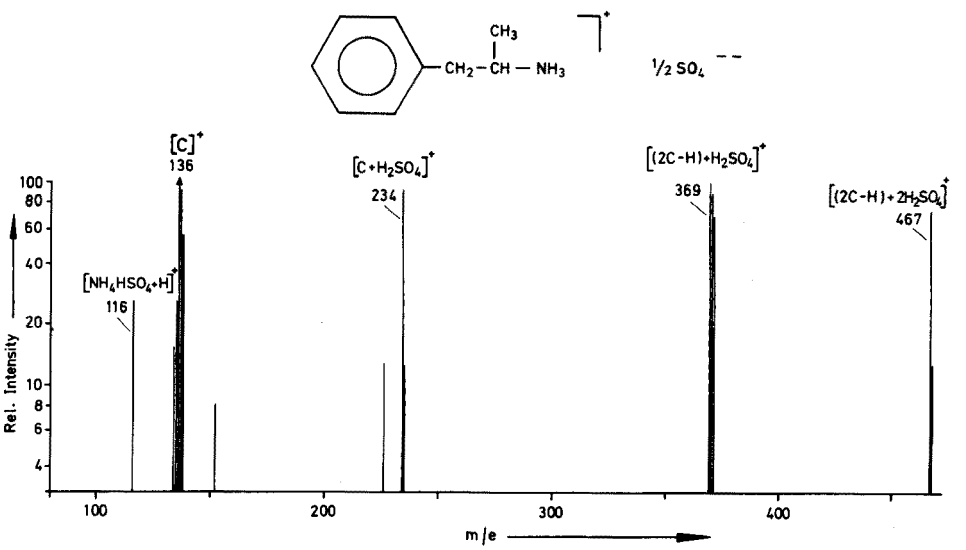

Fig. 5. F.d. spectrum of amphetamine sulphate. Exposure time of the photoplate, 6 min; emitter heating current, 18—21 mA; threshold, $2 \cdot 10^{-8}$ *A*; recorded mass range, *m/e* 17 to *m/e* 560.

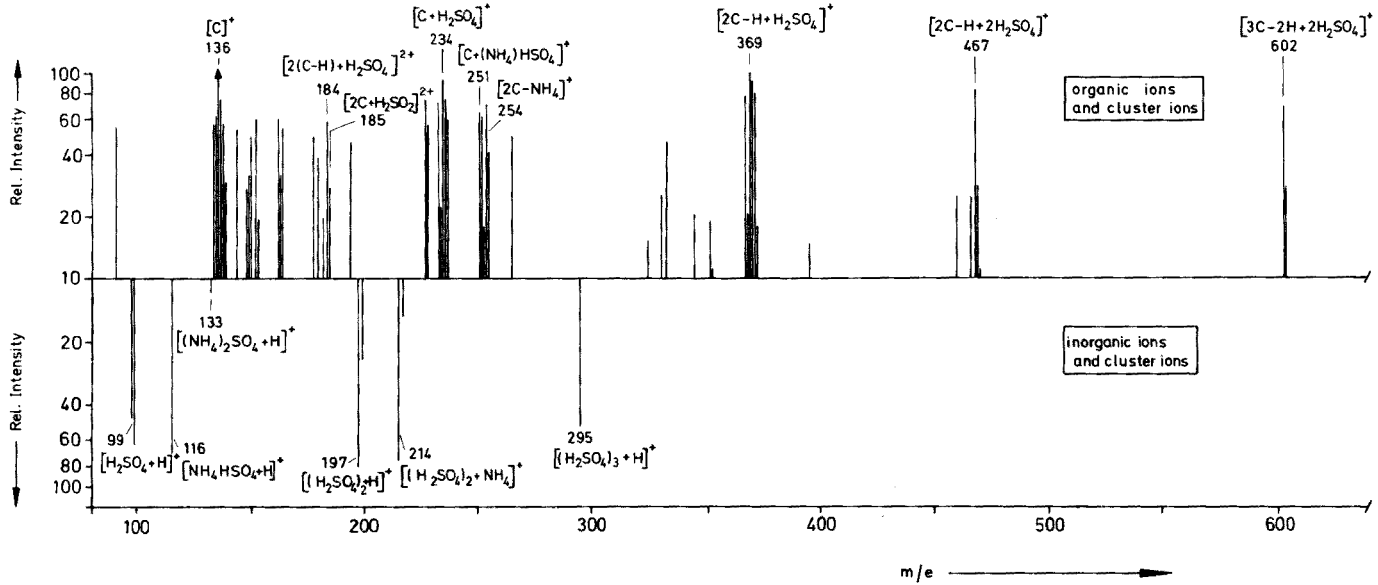

Fig. 6. F.d. spectrum of amphetamine sulphate. Exposure time of the photoplate, 11 min; emitter heating current, 18—30 mA; threshold, $6 \cdot 10^{-8}$ *A*; recorded mass range, *m/e* 30—*m/e* 960.

Forschung des Landes Nordrhein-Westfalen, and Fonds der Deutschen Chemischen Industrie.

REFERENCES

1 H. D. Beckey and H.-R. Schulten, Angew. Chem., 87 (1975) 425; Angew. Chem. Int. Ed. Eng., 14 (1975) 403.
2 H.-R. Schulten and F. W. Röllgen, Org. Mass Spectrom., 10 (1975) 649.
3 H.-R. Schulten and F. W. Röllgen, Angew. Chem., 87 (1975) 544; Angew. Chem. Int. Ed. Eng., 14 (1975) 561.
4 M. Anbar and G. A. St. John, J. Am. Chem. Soc., 97 (1975) 7195; Anal. Chem., 48 (1976) 198.
5 H.-R. Schulten and H. D. Beckey, Org. Mass Spectrom., 6 (1972) 885; H.-R. Schulten and H. D. Beckey, in A. R. West (Ed.), Advances in Mass Spectrometry, Applied Science Publications, London, Vol. VI, 1974, p. 499; H.-R. Schulten, H. D. Beckey, E. M. Bessel, A. B. Foster, M. Jarman and J. H. Westwood, Chem. Commun., 13 (1973) 416; W. D. Lehmann and H.-R. Schulten, in Mass Spectrometry in Drug Metabolism, A. Frigerio and E. L. Ghisalberti (Eds.), Spectrum Publications, New York, in press. H.-R. Schulten, Biomed. Mass Spectrom., 1 (1974) 223; D. A. Brent, D. J. Rouse, M. C. Sammons and M. M. Bursey, Tetrahedron Lett., (1973) 4127; R. Large and H. Knof, Chem. Commun., (1974) 935; D. E. Games, A. H. Jackson, L. A. P. Kane-Maguire and K. Taylor, J. Organomet. Chem., (1975) 345; U. Schurath and H.-R. Schult Atmos. Environ., 9 (1975) 1107; H. U. Winkler and H. D. Beckey, Org. Mass Spectrom., 6 (1972) 655; M. C. Sammons, M. M. Bursey and D. A. Brent, Biomed. Mass Spectrom., 1 (1974) 169; M. C. Sammons, M. M. Bursey and C. K. White, Anal. Chem., 47 (1975) 1165; G. W. Wood, J. M. McIntosh and P.-Y. Lau, J. Org. Chem., 40 (1975) 636; H.-R. Schulten, J. Agric. Food Chem., 24 (1976) 743.
6 D. E. Games, M. P. Games, A. H. Jackson, A. H. Olavesen, M. Rossiter and P. J. Winterburn, Tetrahedron Lett., (1974) 2377.
7 H. Aldercreutz, B. Soltmann and M. J. Tikkanen, J. Steroid Biochem., 5 (1974) 163.
8 H.-R. Schulten and D. E. Games, Biomed. Mass Spectrom., 1 (1974) 120.
9 D. A. Brent, P. de Miranda and H.-R. Schulten, J. Pharm. Sci., 63 (1974) 1370.
10 H.-R. Schulten and H. D. Beckey, Org. Mass Spectrom., 7 (1973) 861.
11 H. D. Beckey, E. Hilt and H.-R. Schulten, J. Sci. Instrum., 6 (1973) 1043.
12 H.-R. Schulten and H. D. Beckey, Org. Mass Spectrom., 6 (1972) 885.
13 H. D. Beckey, A. Heindrichs and H. U. Winkler, Int. J. Mass Spectrom. Ion Phys., 3 (1970) App. 9 p. 11.
14a H.-R. Schulten and H. D. Beckey, Proc. of the Twenty-Third Annual Conference on Mass Spectrometry and Allied Topics, Houston, Texas, May 25—30, 1975, No. B-1.
b H.-R. Schulten, Cancer Treat. Rep., 60 (1976) 501.
15 H.-R. Schulten and D. Kümmler, Z. Anal. Chem., 278 (1976) 13.
16 A. Mathias, A. E. Williams, D. E. Games and A. H. Jackson, Org. Mass Spectrom., 11 (1976) 266.
17 H.-R. Schulten and H. M. Schiebel, Z. Anal. Chem., 280 (1976) 139.
18 McC. Goodall and H. Alton, Biochem. Pharmacol., 17 (1968) 905; Biochem. Pharmacol. 21 (1972) 2401.
19 W. D. Lehmann, H. D. Beckey and H.-R. Schulten, Anal. Chem., 48 (1976).
20 W. N. Jenner and F. A. Rose, Biochem. J., 135 (1973) 109.
21 F. W. Röllgen and H.-R. Schulten, Org. Mass Spectrom., 10 (1975) 660.
22 H.-R. Schulten, in D. Glick (Ed.), Methods of Biochemical Analysis, Vol. 24, Interscience-Wiley, New York, in press.
23 H.-R. Schulten, H. D. Beckey, A. J. H. Boerboom and H. L. C. Meuzelaar, Anal. Chem., 45 (1973) 2358.
24 H.-R. Schulten, H. D. Beckey, G. Eckardt and S. H. Doss, Tetrahedron, 29 (1973) 3861.
25 F. W. Röllgen and H. D. Beckey, Z. Physik. Chem. N.F., 82 (1972) 161.

Analytica Chimica Acta, 87 (1976) 113—117

NEUTRON ACTIVATION ANALYSIS FOR HEAVY METALS IN CAUSTIC SODA

M. H. YANG, P. Y. CHEN, S. J. YEH and S. TANAKA*

Institute of Nuclear Science, National Tsing Hua University, Hsinchu (Taiwan)

(Received 30th March 1976)

SUMMARY

A neutron activation method has been developed for the simultaneous determination of eight heavy metals in caustic soda. The heavy metals are pre-concentrated by complexing with cyanide and anion exchange. A further removal of ^{24}Na by HAP is applied after irradiation, and the γ-rays from the nuclides of interest are assayed with a Ge(Li) detector.

In recent years there has been increased concern over trace metals in processed foodstuffs. Of the possible sources of heavy metals, caustic soda and hydrochloric acid may be of importance; they are used widely in large amounts in food processing industries in Taiwan.

In this study, the simultaneous determination of eight trace metals (Cr, Fe, Co, Cu, Zn, La, Au and Hg) in caustic soda by a neutron activation analysis technique has been developed. Since the metals of interest may be present at low concentrations (p.p.m. to p.p.b. ranges) and sodium is a composite element in the matrix, the resulting ^{24}Na may completely obscure the activity of the product nuclides of interest in the γ-ray measurement. To obviate this difficulty, an efficient way of isolating the trace metals from the matrix before and after irradiation has been developed; the technique involves complexing with cyanide and anion-exchange separation for the pre-concentration of heavy metals in caustic soda samples, and the HAP (Hydrated Antimony Pentoxide) separation [1] for the post-irradiation removal of ^{24}Na. Great care has been taken to avoid introducing impurities during the pre-concentration procedure. Recovery experiments have been made, under various conditions, with radioactive tracers.

Investigations have already been made into the application of pre-concentration techniques to trace analysis by neutron activation [2]. In this study the matrix involves caustic soda made in Taiwan; the combination of complexing with cyanide and anion exchange separation applied to a pre-

*Permanent address: Institute for Nuclear Study, University of Tokyo, Tanashi, Tokyo 188, Japan.

concentration procedure was applied [3] to the concentration of mercury in irradiated water samples.

EXPERIMENTAL

Preconcentration

Great care was taken to avoid introducing impurities from reagents, distilled water and glassware during the pre-concentration procedure. All the reagents used were Suprapur grade (E. Merck Co.). Redistilled water (from a quartz still) was used throughout.

The anion-exchange resin Bio-Rad AG2 X 10 (100—200 mesh), pre-treated successively with 8 M HCl, 20 ml of re-distilled water, 10 ml of 1 M $HClO_4$, 10 ml of re-distilled water, and a mixture of 0.1 ml of 10 % NaCl and 1 ml of 1 % NaOH, was packed into a column (0.7 cm diam., 2.5 cm deep). The optimal length of the column was determined with a ^{60}Co tracer.

The caustic soda sample (10 ml) was diluted to 100 ml with redistilled water, and neutralized to pH 12 with HCl; 1 ml of 10 % NaCN was added to form complexes of heavy metals. After the volume had been adjusted to 200 ml and the pH to 12, the solution was passed through the anion-exchange column, which was then washed with 50 ml of re-distilled water. The heavy metals retained on the column were eluted with 20 ml of nitric acid (1 + 1). An aliquot (5 ml) of the effluent, sealed in a quartz ampoule, was used for neutron irradiation.

Contamination during the pre-concentration procedure was examined by a blank run carried through the entire experiment. The blank started without any NaOH present and consequently did not require neutralization with HCl; tests for impurities in the amount of HCl used were made separately. Only 0.002 μg of copper and 0.003 μg of antimony were detected in the blank sample; the amounts of other impurities were so low that no corrections were necessary.

Neutron irradiation

Two samples and one reference standard were packed in a polyethylene bag and irradiated simultaneously for 30 h in the Open-pool Reactor (THOR), National Tsing Hua University, Taiwan, in a vertical facility with a thermal neutron flux of ca. $2 \cdot 10^{12}$ n cm^{-2} s^{-1}.

Separation and measurement

After irradiation, and a cooling period of 1 d, the sample was transferred from the quartz ampoule and passed through a HAP [1] column to remove the ^{24}Na produced. After the column had been washed with 20 ml of 12 M HCl, the effluent and the wash solution were transferred to a polyethylene tube for γ-ray counting.

The activity in the samples was assayed by measuring prominent γ-rays from the nuclides of interest with a 38-cm^3 Ge(Li) detector coupled with a

TABLE 1

Nuclear data

Target nuclide	Abundance (%)	Neutron capture cross-section (b)	Radioactive product	Half-life	γ-peak used (keV)
^{50}Cr	4.31	15.9	^{51}Cr	27.8 d	320
^{58}Fe	0.33	1.2	^{59}Fe	45 d	1095, 1292
^{59}Co	100	37	^{60}Co	5.26 y	1173, 1332
^{63}Cu	69.1	4.5	^{64}Cu	12.8 h	511
^{64}Zn	48.9	0.47	^{65}Zn	245 d	1115
^{68}Zn	18.6	0.10	^{69m}Zn	13.8 h	439
^{139}La	99.9	9.6	^{140}La	40.2 h	329, 487
^{197}Au	100	98.8	^{198}Au	64.8 h	412
^{196}Hg	0.15	3092	^{197}Hg	64.1 h	68[a], 77
^{202}Hg	29.8	5.0	^{203}Hg	46.9 d	279

[a] Au, K-x ray.

4096-channel pulse-height analyzer. The detector had a high resolution of 2.2 keV (FWHM) for the 1332-keV ^{60}Co γ-ray and a peak-to-Compton ratio of 27. Constant geometry was assured by counting samples and standards at the same position relative to the detector. A Hewlett-Packard 2116C computer program was used. The nuclear data used are summarized in Table 1. For copper determination, the 511-keV annihilation peak of ^{64}Cu was used after the contribution of ^{65}Zn had been deducted by referring to its 1115-keV photo-peak. In order to raise the sensitivity of γ-ray measurement, the 439-keV γ-ray from ^{69m}Zn was measured instead of the 1115-keV γ-ray from ^{65}Zn for zinc, the 68-keV x-ray from gold and the 77-keV γ-ray from ^{197}Hg were measured instead of the 279-keV γ-ray from ^{203}Hg for mercury.

RESULTS AND DISCUSSION

Recovery test for pre-concentration

To establish the pre-concentration procedure recommended above, a recovery test for the heavy metals of interest was made with radioactive tracers. The percentage adsorption of cobalt and mercury on the resin from the solution of pH 12 was first examined in a variety of concentrations of NaCl and NaCN. Table 2 shows that 99 % of both cobalt and mercury are retained by the resin from the solution containing 3 % NaCl and 0.05 % NaCN at pH = 12. At higher chloride and lower cyanide concentration, cobalt is not retained sufficiently by the resin. Thus, it is necessary to dilute the neutralized solution to give a NaCl concentration of 3 %, and then add the required amount of NaCN.

The effect of cyanide complexing on the anion-exchange separation of heavy metals from sodium chloride solution is presented in Table 3, together

TABLE 2

Percentage adsorption of Co and Hg on Bio-Rad AG2x10 (100—200 mesh) resin in a variety of concentrations of NaCl and NaCN at pH 12

NaCN 0.05 %			NaCl 3 %		
NaCl (%)	Adsorption (%)		NaCN (%)	Adsorption (%)	
	Co	Hg		Co	Hg
33.0	10.8	93.7	0.05	98.7	98.5
20.0	18.5	94.3	0.005	97.6	98.3
10.0	37.4	94.5	0.0005	60.4	96.4
5.0	90.4	95.1	0.00005	40.6	93.9
3.0	98.7	98.5	0	36.9	91.9
1.0	98.5	98.5			
0.1	98.9	99.0			
0	99.0	99.4			

TABLE 3

Effect of cyanide complexing and pH on percentage adsorption of heavy metals from 3 % NaCl solution on Bio-Rad AG2x10 (100—200 mesh) resin

pH	Cr	Fe	Co	Cu	Zn	La	Au	Hg
With NaCN (0.05 %)								
12	98.6	98.5	98.7	96.5	100	97.3	98.8	98.5
7	97.1	92.3	94.0	95.7	91.5	91.6	95.7	89.8
3	74.9	82.1	92.1	92.4	8.0	9.5	82.7	83.7
Without NaCN								
12	67.1	88.4	36.9	60.7	69.1	81.1	72.5	91.9
7	48.8	82.9	0.1	14.4	2.0	14.3	81.0	89.9
3	0.6	0.4	0.5	0.5	0.5	0.8	79.4	96.4

with the effect of the pH of the solution. Without NaCN, elements such as Cr, Co, Cu and Zn are not retained sufficiently by the resin even at pH 12.

Analysis of caustic soda

The caustic soda samples analysed were one laboratory reagent (R) (pro analysi grade, E. Merck Co.), two products manufactured by the diaphragm cell (D-1 and 2), and five by the flowing mercury cathode cell (M-1 to 5) in different factories in Taiwan.

The results are presented in Table 4. Mercury concentrations in the mercury cell samples are in the range 0.6—3.8 p.p.m., while the diaphragm cell samples contain 0.010 and 0.043 p.p.m. In contrast, copper concentrations in the diaphragm cell samples are an order of magnitude higher than in the mercury cell samples. The concentration of iron in the diaphragm cell samples is consistently higher than that in the mercury cell samples.

TABLE 4

Heavy metals in caustic soda products (Concentrations are given as p.p.m. except for Au which is p.p.b.)

Sample number	Cr	Fe	Co	Cu	Zn	La	Au	Hg
R	0.012	ND[a]	0.003	0.23	0.63	0.0013	ND	0.034
D-1	0.042	15.1	0.062	14.6	0.67	ND	0.018	0.043
D-2	0.014	16.6	0.007	4.0	1.00	ND	ND	0.010
M-1	0.015	5.4	ND	0.29	1.46	0.0060	0.001	3.15
M-2	0.35	5.5	ND	0.11	0.74	0.0053	0.001	0.99
M-3	0.057	3.3	0.006	0.28	1.11	0.0015	0.052	0.67
M-4	0.042	1.7	0.003	0.10	0.55	0.0012	0.040	0.63
M-5	0.21	4.0	0.042	0.76	0.37	0.0007	0.014	3.82

[a]Not detected.

S. J. Yeh and P. Y. Chen wish to thank the National Science Council for financial support.

REFERENCES

1 F. Girardi and E. Sabbioni, J. Radioanal. Chem., 1 (1968) 169.
2 e.g., J. M. Rottschafer, R. J. Boczkowski and H. B. Mark, Jr., Talanta, 19 (1972) 163.
3 A. Kolaczkowski and W. A. Jester, J. Radioanal. Chem., 16 (1973) 21.

Analytica Chimica Acta, 87 (1976) 119—124

NEUTRON ACTIVATION ANALYSIS FOR TRACE ELEMENTS IN UNPOLISHED RICE

S. J. YEH, P. Y. CHEN, C. N. KE, S. T. HSU and S. TANAKA*

Institute of Nuclear Science, National Tsing Hua University, Hsinchu (Taiwan)

(Received 30th March 1976)

SUMMARY

Twenty-two elements in 19 unpolished rice samples harvested in Taiwan during 1973 have been determined by a neutron activation analysis technique, consisting of both non-destructive and destructive methods. After the removal of ^{24}Na and ^{32}P, chemical separation into three groups is achieved by anion exchange and distillation. The concentrations of heavy metals in different rice samples vary widely.

Since there has been increased concern over the presence of trace elements in foodstuffs, an effective method of monitoring these in biological materials by simple and reliable techniques must be developed. Rice is the most important foodstuff in daily use in the East. In this study 22 elements in unpolished rice have been determined by neutron activation analysis, consisting of both non-destructive and destructive methods. Biological materials usually contain a large amount of potassium, sodium and phosphorus; consequently the prevailing radionuclides ^{42}K, ^{24}Na and ^{32}P produced may completely obscure the minor activities of interest in γ-spectrometry; radiochemical separations are necessary after irradiation to remove these interfering radionuclides. The separation techniques employed are the selective removal of ^{24}Na by hydrated antimony pentoxide [1], the removal of ^{32}P by acidic aluminum oxide [2], and separation into three groups by anion exchange and distillation.

EXPERIMENTAL

Samples and standards

Nineteen unpolished rice samples harvested in 1973 in ten different prefectures in Taiwan were collected by the Bureau of Food Administration. Two different kinds of rice (Fen-Lai and Tsai-Lai) are represented by suffix numbers 1 and 2, respectively, in the sample notation in Table 4. Each

*Permanent address: Institute for Nuclear Study, University of Tokyo, Tansaki, Tokyo 188, Japan.

sample (20 g) was washed three times with redistilled water and once with acetone, dried at 40 °C, pulverized in an agate mortar and stored in a desiccator. Portions (0.5 and 1 g) of each rice sample were sealed in a polyethylene bag and a quartz ampoule, respectively, for non-destructive and destructive analysis.

Standard solutions were prepared by dissolving the pure metals or compounds of the elements of interest in redistilled water or nitric acid to give appropriate concentrations. The standard reference for non-destructive analysis was prepared by adding 100 μl of each standard solution to a filter paper, and allowing it to air-dry before sealing in a polyethylene bag. The standard reference for destructive analysis was prepared by adding known amounts of each standard solution to a quartz ampoule and adjusting the volume to 2 ml with redistilled water before sealing.

Neutron irradiation

Two samples and one standard were packed in a polyethylene bag and irradiated simultaneously in the Open-pool Reactor (THOR), National Tsing Hua University, Taiwan. Irradiation conditions for non-destructive and destructive analysis are shown in Table 1, together with the cooling and counting times.

Chemical separation after irradiation

After irradiation, and cooling for 1 d, the sample was transferred from the quartz ampoule to a Sjöstrand type wet-ashing reflux apparatus [3]. After appropriate carriers had been added, the sample was digested with a mixture of 14 M HNO_3 and 30 % H_2O_2. The digestion was repeated three times before the sample solution was distilled twice, after adding 5 ml of water, to expel free nitrogen and bromide. After the residue was dissolved in 8 M HCl, the chemical separation scheme shown in Fig. 1 gave a separation into three groups. The hydrated antimony pentachloride (HAP) was air-dried at 270 °C for 5 h, pulverized and sieved (60—100 mesh). Then 1 g of the powder was added to a column (1 cm diameter, 3 cm in depth) and pretreated with 8 M HCl. The anion-exchange resin was Dowex 1—X8 (100—200 mesh) (column dimensions 0.7 cm diameter, 15 cm deep). The acidic aluminum oxide was chromatographic-grade acid alumina (E. Merck, W. Germany) (5 g in a column of 1 cm diameter, 7 cm in depth).

γ-Ray measurement

Prominent γ-peaks from nuclides of interest were measured with a 38-cm^3 Ge(Li) detector coupled with a 4096-channel pulse-height analyser. The detector had a high resolution (2.2 keV (FWHM) for the 1332-keV ^{60}Co γ-ray) and a peak-to-Compton ratio of 27. Peak analysis was done with the Hewlett-Packard 2116 C computer program. The nuclear data are summarized in Table 2. Special care was given to the determination of the following nuclides. Since the 844-keV peak from ^{27}Mg and the 847-keV peak from ^{56}Mn were superimposed on each other, the attenuated 1014-keV and

TABLE 1

Experimental conditions with thermal neutrons

Sample (g)	Flux (n cm^{-2} s^{-1})	Irradn. time	Cooling time	Counting time	Elements determined
Non-destructive					
0.5[a]	$\sim 1 \cdot 10^{12}$	1 m	2 m	5 m	Mg, Al, Cl, Ca, Mn
0.5[b]	$\sim 2 \cdot 10^{12}$	2 h	2 d	5 m	Na, K, Br
Destructive					
1.0[c]	$\sim 2 \cdot 10^{12}$	30 h	1.5 d	50 m	As
			2.5 d	50 m	Fe, Co, Cu, Zn Mo, Cd, Sb, Hg
			6.5 d	50 m	Sc, Cr, Rb, Cs, Sm

[a]Fast shuttle rabbit. [b]Pneumatic transfer tube. [c]Vertical tube.

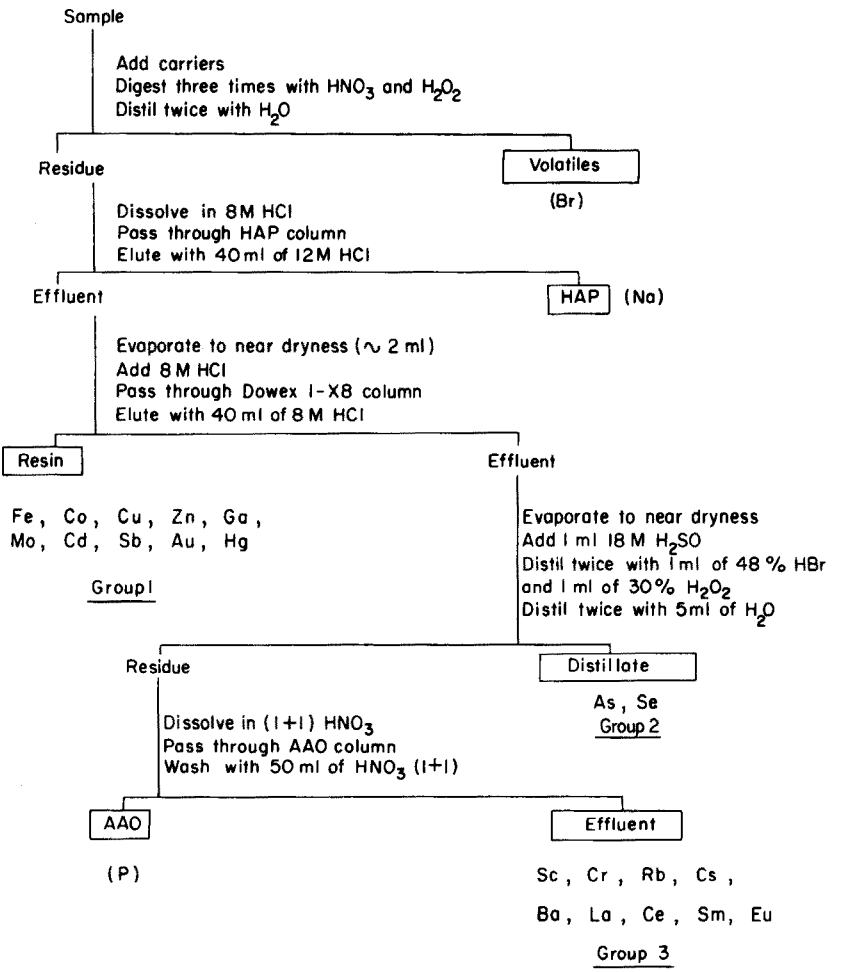

Fig. 1. Radiochemical group separation scheme.

TABLE 2

Nuclear data

Target nuclide	Abundance (%)	Neutron capture cross-section (barn)	Radioactive product	Half-life	γ-peak used (keV)
^{23}Na	100	0.53[a]	^{24}Na	15.0 h	1369
^{26}Mg	11.3	0.034	^{27}Mg	9.5 m	1014
^{27}Al	100	0.24	^{28}Al	2.31 m	1779
^{37}Cl	24.5	0.43	^{38}Cl	37 m	1642, 2168
^{41}K	6.9	1.2	^{42}K	12.5 h	1525
^{48}Ca	0.185	1.1	^{49}Ca	8.8 m	3083
^{45}Sc	100	23[a]	^{46}Sc	83.9 d	889, 1120
^{50}Cr	4.31	16	^{51}Cr	27.8 d	320
^{55}Mn	100	13.3	^{56}Mn	2.57 h	1811
^{58}Fe	0.33	1.2	^{59}Fe	45 d	1095, 1292
^{59}Co	100	37	^{60}Co	5.26 y	1173, 1332
^{63}Cu	69.1	4.5	^{64}Cu	12.8 h	511
^{64}Zn	48.9	0.47	^{65}Zn	245 d	1115
^{75}As	100	4.5	^{76}As	26.5 h	559, 657
^{81}Br	49.5	2.7[a]	^{82}Br	35.3 h	555, 777
^{85}Rb	72.2	0.8[a]	^{86}Rb	18.7 d	1076
^{98}Mo	23.8	0.13	^{99}Mo	67 h	141[b]
^{114}Cd	28.9	0.30	^{115}Cd	53 h	337[c]; 528
^{121}Sb	57.3	6.6	^{122}Sb	67.2 h	564, 693
^{133}Cs	100	30	^{134}Cs	2.07 y	605, 796
^{152}Sm	26.7	204	^{153}Sm	47 h	103
^{196}Hg	0.146	3092	^{197}Hg	65 h	68[d]; 77

[a]Sum of the cross-sections for the formation of metastable and ground state (for ^{81m}Br, 83 % IT). [b]From the daughter ^{99m}Tc. [c]From the daughter ^{115m}In. [d]K-x ray from Au.

TABLE 3

Chemical yield and reproducibility

Element	Chemical yield %	R.s.d.[a] (%)	Element	Chemical yield %	R.s.d.[a] (%)
Sc	97	1.6	Rb	69	4.5
Cr	98	2.0	Mo	92	3.2
Fe	98	2.7	Cd	99	3.6
Co	99	1.5	Sb	99	4.0
Cu	100	0.4	Cs	94	1.1
Zn	99	2.6	Sm	98	2.2
As	92	0.6	Hg	82	0.4

[a]Relative standard deviation from the mean of three measurements.

TABLE 4

Analytical data for unpolished rice harvested in Taiwan, 1973

Sample	Concentrations (p.p.m.)																		Concentrations (%)			
	Na	Al	Sc	Cr	Mn	Fe	Co	Cu	Zn	As	Br	Rb	Mo	Cd	Sb	Cs	Sm	Hg	Mg	Cl	K	Ca
A-1	75	12	0.010	0.27	70	56	0.10	3.3	24	0.10	2.4	4	0.18	0.50	0.075	0.03	0.0013	0.008	0.19	0.058	0.40	0.012
A-2	16	21	0.012	0.20	44	21	0.07	3.6	25	0.10	0.7	8	0.27	0.10	0.003	0.04	0.0011	0.038	0.31	0.047	0.42	0.010
B-1	62	17	0.004	0.22	65	47	0.07	4.7	15	0.27	2.7	33	0.41	0.22	0.006	0.16	0.0015	0.012	0.20	0.032	0.35	0.019
B-2	79	28	0.004	0.25	33	12	0.07	3.0	17	0.17	2.0	18	0.42	0.20	0.005	0.08	0.0015	0.019	0.21	0.045	0.32	0.016
C-1	86	10	0.004	0.45	37	11	0.11	3.5	29	0.12	3.7	7	0.31	0.11	0.084	0.03	0.0019	0.016	0.21	0.078	0.39	0.012
C-2	13	11	0.003	0.24	25	13	0.04	3.2	24	0.11	1.3	6	0.39	0.88	0.030	0.02	0.0013	0.028	0.23	0.027	0.39	0.010
D-1	44	16	0.004	0.24	52	17	0.04	3.2	30	0.26	2.9	22	0.40	0.15	0.040	0.03	0.0030	0.031	0.21	0.055	0.48	0.023
D-2	15	13	0.004	0.33	34	15	0.06	4.4	24	0.12	1.5	7	0.34	0.23	0.026	0.03	0.0033	0.031	0.24	0.050	0.52	0.013
E-1	81	30	0.013	0.17	32	16	0.05	4.0	11	0.16	1.8	8	0.48	0.11	0.012	0.02	0.0072	0.014	0.14	0.069	0.41	0.013
E-2	30	19	0.003	0.20	44	16	0.05	3.5	13	0.46	1.8	9	0.90	0.36	0.023	0.02	0.0036	0.035	0.20	0.063	0.33	0.017
F-1	22	19	0.001	0.25	47	9	0.02	3.0	12	0.09	1.7	9	0.55	0.12	0.002	0.02	0.0022	0.032	0.16	0.049	0.43	0.009
F-2	13	22	0.002	0.23	34	13	0.03	2.6	15	0.14	1.9	28	0.52	0.12	0.005	0.02	0.0037	0.040	0.19	0.027	0.42	0.009
G-1	26	14	0.005	0.28	42	49	0.07	4.2	13	0.11	1.3	4	0.34	0.09	0.018	0.05	0.0021	0.022	0.26	0.036	0.38	0.014
G-2	10	21	0.005	0.49	39	19	0.14	3.6	15	0.16	1.2	2	0.25	0.27	0.015	0.26	0.0026	0.039	0.30	0.032	0.40	0.022
H-1	12	9	0.004	0.24	30	31	0.10	5.0	18	0.11	0.9	3	0.52	0.24	0.009	0.05	0.0007	0.047	0.21	0.024	0.33	0.009
H-2	6	10	0.007	0.31	32	13	0.08	4.0	21	0.16	0.8	4	0.29	0.37	0.004	0.02	0.0010	0.017	0.21	0.023	0.35	0.011
I-1	14	16	0.001	0.15	30	15	0.02	4.0	9	0.17	1.9	7	0.37	0.11	0.004	0.02	0.0030	0.021	0.19	0.079	0.47	0.014
I-2	10	14	0.002	0.17	34	16	0.01	3.7	8	0.27	1.4	8	0.17	0.08	0.002	0.02	0.0026	0.024	0.21	0.034	0.52	0.009
J-2	47	17	0.005	0.40	24	94	0.08	3.4	19	0.04	0.6	8	0.23	0.13	0.034	0.02	0.0012	0.023	0.31	0.042	0.32	0.010
D.L.[a]	1	1	0.001	0.03	0.6	4	0.005	0.05	0.5	0.002	0.5	0.3	0.01	0.01	0.002	0.02	0.0001	0.004	0.004	0.003	0.002	0.004

[a]D.L. = detection limit.

1811-keV peaks were used respectively. For ^{64}Cu determination, the 511-keV annihilation peak was used after subtracting the contribution from ^{65}Zn by reference to the 1115-keV photopeak [4]. For ^{82}Br, the 777-keV peak was used, because the 555-keV peak was coincident with the 559-keV ^{76}As peak. For ^{99}Mo, the 141-keV peak from the daughter nuclide ^{99m}Tc was used after subtracting the contribution from ^{59}Fe by reference to the 1095-keV photopeak [4]. For ^{115}Cd, the 337-keV peak from the daughter ^{115m}In was used instead of the 528-keV peak from ^{115}Cd to raise the sensitivity by an order of magnitude [5]. The sensitivity was also increased by measuring the 564-keV ^{122}Sb peak instead of the 621-keV ^{124}Sb peak, and the 68-keV x-ray and 77-keV γ-peak from ^{197}Hg were used instead of the 279-keV ^{203}Hg peak.

RESULTS AND DISCUSSION

Chemical recovery and reproducibility of experiment

The percentage recoveries of 14 elements from the chemical separation procedure were measured by means of radioactive tracers; the results are presented in Table 3. Only Rb and Hg are not recovered almost quantitatively; a considerable part of the rubidium may be adsorbed on the HAP column and some mercury may be lost during the distillation procedure. The reproducibility of the analytical results was checked by irradiating three solution standards in one pack and applying the procedure used for samples (Table 3).

Analysis of rice

The data for 22 elements in 19 unpolished rice samples are summarized in Table 4, together with the detection limits of this method.

The concentrations of most of the elements vary widely in the different rice samples. The differences exceed a factor of 10 for Na, Sc, Co, As, Rb, Cd, Cs and Sm, and there are no clear correlations between different elements. The rice harvested in mountainous districts, I and J, contains low heavy metal concentrations in general, and relatively high concentrations of As and Br may reflect the use of agricultural chemicals in some districts. More detailed investigations are required.

Comparison of the present results with those for unpolished rice harvested [6] in Fuchu city (Tokyo) reveals that Taiwan rice contains more Mn and As and less Cr and Sb than Fuchu rice.

S. J. Yeh and P. Y. Chen thank the National Science Council for financial support.

REFERENCES

1 F. Girardi and E. Sabbioni, J. Radioanal. Chem., 1 (1968) 169.
2 E. Sabbioni, R. Pietra and F. Girardi, J. Radioanal. Chem., 4 (1970) 289.
3 B. Sjöstrand, Anal. Chem., 815 (1964) 36.
4 H. Al-Shahristani and M. J. Al-Atyia, J. Radioanal. Chem., 14 (1973) 401.
5 G. H. Morrison and W. M. Potter, Anal. Chem., 839 (1972) 44.
6 S. Nagatsuka and Y. Tanizaki, Radioisotopes, 22 (1973) 234.

Analytica Chimica Acta, 87 (1976) 125—140

ÉTUDE D'ÉQUILIBRES EN SOLUTION À L'AIDE DES ÉCHANGEURS D'IONS
I DISSOCIATION DU PERCHLORATE D'ARGENT ET DE L'ACIDE NITRIQUE DANS LES MÉLANGES EAU—ACIDE ACÉTIQUE—ACIDE PERCHLORIQUE OU ACIDE NITRIQUE

A. R. RODRIGUEZ et C. POITRENAUD

Institut National des Sciences et Techniques Nucléaires de Saclay, B.P. n° 6, 91190 Gif-sur-Yvette (France)

(Reçu le 26 mars 1976)

RÉSUMÉ

Une relation théorique entre le coefficient de partage d'un élément monovalent et les paramètres dont il dépend (concentration de l'acide en solution, constantes de dissociation de l'acide et du sel, coefficient de sélectivité des ions échangés) a été établie. Cette relation a été vérifiée dans le cas de la dissociation du perchlorate d'argent dans les mélanges eau—acide acétique—acide perchlorique, en comparant les valeurs de constantes de dissociation trouvées aux valeurs expérimentales obtenues par potentiométrie. La relation établie a été utilisée pour déterminer les constantes de dissociation de l'acide nitrique dans les mélanges eau—acide acétique—acide nitrique de teneur en eau inférieure à 25 % en poids. La valeur du pK de dissociation de l'acide nitrique dans l'acide acétique pur a été évaluée par extrapolation. On prévoit que la relation théorique du coefficient de partage pourra être utilisée pour déterminer les constantes de dissociation d'un acide lorsque l'on connaît les constantes de dissociation d'un sel et réciproquement.

SUMMARY

A theoretical relationship postulated between the distribution coefficient of a monovalent element and the parameters upon which it depends (acid concentration in solution, dissociation constants of the acid and the salt, selectivity coefficient of exchanged ions) has been verified for the dissociation of silver perchlorate in water—acetic acid—perchloric acid mixtures. The dissociation constants found have been compared with the experimental values obtained by potentiometric measurements. The relationship established has been employed for the determination of nitric acid dissociation constants in water—acetic acid—nitric acid mixtures containing less than 25 % by weight of water. From the results the pK value for nitric acid in pure acetic acid has been evaluated by extrapolation. The theoretical relationship might be used to determine an acid dissociation constant when the dissociation constant of a salt is known and vice versa.

L'étude des équilibres dans les systèmes formés par des solvants non aqueux ou des mélanges hydro-organiques en contact avec une résine échangeuse d'ions permet d'obtenir des renseignements sur les propriétés de ces solvants et sur les interactions des espèces qui y sont dissoutes.

Le comportement des échangeurs d'ions dans les solvants purs et dans les mélanges hydro-organiques a fait l'objet de plusieurs revues bibliographiques [1—4]. Depuis la publication de la plus récente mise au point, de nombreux travaux ont été effectués dans ce domaine. En ce qui concerne les coefficients de partage et les constantes d'échange d'éléments métalliques entre une résine échangeuse de cations et des mélanges eau—solvant organique variés, plusieurs études ont été réalisées dans les mélanges eau—alcools [5—26], eau—acétone [9, 11—13, 16, 18, 26—34], eau—dioxane [5, 9, 35—37], eau—acide acétique [5, 8, 22—24, 26, 36, 38, 39], eau—acide formique [26, 36, 39—41], eau—diméthylsulfoxide [42—44], eau—éthanolamine [45], eau—hexaméthylphosphorotriamide [46, 47].

Les courbes de variation des coefficients de partage ou des constantes d'échange d'ions en fonction de la composition du mélange hydro-organique présentent souvent des formes caractéristiques avec un maximum ou un minimum qui ne peuvent être expliquées qu'en admettant que d'autres phénomènes se superposent à l'équilibre d'échange d'ions.

Dans ce même domaine, peu d'études [4, 36] ont été faites pour expliquer quantitativement l'influence exercée par les solvants sur les coefficients de partage. La description des différents phénomènes par des relations faisant intervenir des paramètres mesurables ou connus aurait un double intérêt: cela permettrait de calculer les coefficients de partage de différents éléments métalliques dans un milieu donné et de prévoir leur variation en fonction du pouvoir dissociant des mélanges hydro-organiques. On pourrait en déduire des possibilités de séparation. Cela permettrait aussi, par des mesures de coefficients de partage, de déterminer certains paramètres et d'atteindre ainsi des renseignements sur les propriétés des espèces en solution.

Pour répondre à ce besoin, nous avons établi l'expression du coefficient de partage d'un élément métallique entre une résine échangeuse de cations et un mélange hydro-organique en fonction des différents paramètres dont il dépend. Pour vérifier la validité de la relation établie, nous l'avons utilisée pour déterminer la constante de dissociation d'un sel et nous avons comparé la valeur trouvée à une valeur expérimentale obtenue à l'aide d'une autre méthode. Ce test a été effectué dans le cas de la dissociation du perchlorate d'argent dans les mélanges eau—acide acétique—acide perchlorique.

Nous avons ensuite appliqué la méthode d'échange d'ions à la détermination de la constante de dissociation de l'acide nitrique dans les mélanges eau—acide acétique—acide nitrique.

PARTIE THEORIQUE

Le coefficient de partage d'un élément entre une solution acide de ses sels et une résine échangeuse d'ions est défini par le rapport de ses concentrations totales dans les deux phases en présence.

Dans une solution contenant un acide HX à la concentration C_0 et une faible quantité d'un sel MX dans un mélange donné d'eau et de solvant

organique existent les espèces suivantes

$$HX \rightleftharpoons H^+ + X^-$$

$$K_{0_D}^{HX} = \frac{[H^+]_{(S)}\,[X^-]_{(S)}}{[HX]_{(S)}}\,\frac{y_{H^+(S)}\,y_{X^-(S)}}{y_{HX(S)}} \qquad (1)$$

$$MX \rightleftharpoons M^+ + X^-$$

$$K_{0_D}^{MX} = \frac{[M^+]_{(S)}\,[X^-]_{(S)}}{[MX]_{(S)}}\,\frac{y_{M^+(S)}\,y_{X^-(S)}}{y_{MX(S)}} \qquad (2)$$

(Une quantité entre crochets représente une concentration et y un coefficient d'activité dans le même système d'unités. Dans tout ce qui suit nous supposerons que les coefficients d'activité des espèces non dissociées, $y_{HX(S)}$ et $y_{MX(S)}$, sont égaux à l'unité.)

L'élément métallique existe en solution sous deux formes: M^+ et MX (nous négligerons l'espèce MOAc car le milieu est acide et les ions AcO^- sont peu concentrés).

Lorsque la solution est mise en contact avec la résine acide il peut y avoir pénétration de l'élément métallique dans la résine par équilibre d'échange des ions M^+ et H^+ ou simple équilibre de partage du sel MX. Dans la résine et en particulier lorsque le liquide qui l'imbibe est riche en solvant organique, les groupements fonctionnels R^- peuvent donner des paires d'ions avec les cations M^+ et H^+. Finalement, le partage de l'élément métallique entre la résine et la solution peut être décrit par les équilibres suivants

$$M^+_{(S)} + H^+_{(R)} \overset{K_{0_{H^+}}^{M^+}}{\rightleftharpoons} M^+_{(R)} + H^+_{(S)}$$

$$M^+_{(S)} + RH \overset{K_{0_{RH}}^{RM}}{\rightleftharpoons} RM + H^+_{(S)}$$

$$M^+_{(S)} + X^-_{(S)} \overset{K_{0_{DR}}}{\rightleftharpoons} XM_{(R)}$$

(Les indices R et S indiquent respectivement, les phases résine et solution. On peut admettre que dans la résine les coefficients d'activité des espèces neutres RM et RH sont voisins: $y_{RM} = y_{RH}$.)

Le coefficient de partage de l'élément M a pour expression

$$D = \frac{[M]_{(R)}}{[M]_{(S)}} = \frac{K_{0_{H^+}}^{M^+}\,[H^+]_{(R)}\,\dfrac{y_{H^+(R)}}{y_{M^+(R)}} + K_{0_{RH}}^{RM}\,[RH]}{[H^+]_{(S)}\left[1 + \dfrac{[X^-]_{(S)}}{K_{0_D}^{MX}}\,y_{M^+(S)}\,y_{X^-(S)}\right]}\,\frac{y_{M^+(S)}}{y_{H^+(S)}}$$

$$+ \frac{\dfrac{[X^-]_{(S)}}{K_{0_{DR}}} y_{X^-(S)}\, y_{M^+(S)}}{1 + \dfrac{[X^-]_{(S)}}{K_{0_D^{MX}}} y_{M^+(S)}\, y_{X^-(S)}} \qquad (3)$$

Posons $[H^+]_{(R)} = \alpha\, c_E$ soit $[RH] = (1 - \alpha)\, c_E$ (c_E étant la capacité d'échange de la résine).

On peut admettre que: α est constant pour un mélange hydro-organique donné, quelle que soit C_0 car il ne dépend que du pouvoir dissociant du mélange; et que $y_{H^+(R)}/y_{M^+(R)}$ est constant car la force ionique dans la résine est grande et varie peu quand C_0 varie de 0,1 à 0,01 M.

Dans ces conditions

$$K_{0_{H^+}^{M^+}} \frac{y_{H^+(R)}}{y_{M^+(R)}} [H^+]_{(R)} + K_{0_{RH}^{RM}} [RH] = K^\star\, c_E = \text{cte} \qquad (4)$$

avec

$$K^\star = K_{0_{H^+}^{M^+}} \frac{y_{H^+(R)}}{y_{M^+(R)}} \alpha + K_{0_{RH}^{RM}} (1 - \alpha) \qquad (5)$$

où $K^\star$ peut être considéré comme un coefficient de sélectivité caractéristique des ions M^+ et H^+ dans le mélange étudié et indépendant de la concentration C_0 de l'acide en solution.

L'expérience montre qu'une résine en équilibre avec un mélange hydro-organique contient une phase liquide plus riche en eau que le mélange extérieur. Nous admettrons que dans ce milieu riche en eau, contenant en outre peu d'ions X^-, on peut négliger la concentration de MX devant celles de M^+ et RM. Nous négligerons donc $[X^-]_{(S)}/K_{0_{DR}}$ au numérateur de l'expression de D.

Les concentrations $[H^+]_{(S)}$ et $[X^-]_{(S)}$ qui interviennent dans l'expression de D sont liées à la concentration totale C_0 de l'acide en solution. Les ions X^- résultent de la dissociation de HX et de MX. Dans nos expériences la concentration totale de l'acide était toujours supérieure à 10^{-2} M tandis que celle de l'élément M était, à l'équilibre, de l'ordre de 10^{-5} M. Dans ces conditions, tant que $K_{0_D^{MX}}/K_{0_D^{HX}}$ est inférieur à 100, on peut négliger les ions X^- provenant de la dissociation du sel devant ceux produits par la dissociation de l'acide.

Donc, si $pK_{0_D^{MX}} > pK_{0_D^{HX}} - 2$ on peut écrire

$$[X^-]_{(S)} \approx C_0 - [HX]_{(S)} \qquad (6)$$

Pour la même raison, $[M^+]_{(S)}$ est dans ce cas petit devant $[H^+]_{(S)}$ et le bilan ionique en solution peut s'écrire

$$[H^+]_{(S)} \approx [X^-]_{(S)} + [AcO^-]_{(S)} \qquad (7)$$

Compte tenu du produit ionique des mélanges eau—acide acétique (K_{0i}), on

trouve finalement

$$[X^-]_{(S)} = [H^+]_{(S)} - \frac{K_{0_i}}{[H^+]_{(S)}} \frac{1}{y_{H^+(S)}\, y_{AcO^-(S)}} \tag{8}$$

D'où l'expression du coefficient de partage

$$D = \frac{K^* c_E \dfrac{y_{M^+(S)}}{y_{H^+(S)}}}{[H^+]_{(S)}\left[1 + \dfrac{[H^+]_{(S)} - \dfrac{K_{0_i}}{[H^+]_{(S)}} \dfrac{1}{y_{H^+(S)}\, y_{AcO^-(S)}}}{K_{0_D}^{MX}}\, y_{M^+(S)}\, y_{X^-(S)}\right]} \tag{9}$$

où $[H^+]_{(S)}$ à l'équilibre dépend de C_0, K_{0_i} et $K_{0_D}^{HX}$ et peut être calculée en résolvant l'équation de 3ème degré

$$[H^+]^3_{(S)} + \frac{K_{0_D}^{HX}}{y_{H^+(S)} y_{X^-(S)}} [H^+]^2_{(S)} - \left[\frac{K_{0_i}}{y_{H^+(S)} y_{AcO^-(S)}} + \frac{K_{0_D}^{HX}}{y_{H^+(S)} y_{X^-(S)}}\right][H^+]_{(S)}$$

$$- \frac{K_{0_i} K_{0_D}^{HX}}{y_{X^-(S)} y_{AcO^-(S)} y^2_{H^+(S)}} = 0 \tag{10}$$

En milieu suffisamment acide on peut négliger les ions H^+ dus à l'ionisation du solvant devant ceux résultant de la dissociation de l'acide.

Dans ce cas, $[H^+]_{(S)} \approx [X^-]_{(S)}$ et, parmi les différentes expressions de D que l'on peut trouver, nous utiliserons la suivante

$$D = K^* \frac{c_E\, y_{M^+(S)}}{C_0\, y_{H^+(S)}} \frac{1 + \dfrac{[X^-]_{(S)}}{K_{0_D}^{HX}} y_{H^+(S)}\, y_{X^-(S)}}{1 + \dfrac{[X^-]_{(S)}}{K_{0_D}^{MX}} y_{M^+(S)}\, y_{X^-(S)}} \tag{11}$$

$$\text{avec } [X^-]_{(S)} = \frac{K_{0_D}^{HX}}{2 y_{H^+(S)}\, y_{X^-(S)}} \left[\left(1 + \frac{4\, C_0\, y_{H^+(S)}\, y_{X^-(S)}}{K_{0_D}^{HX}}\right)^{\frac{1}{2}} - 1\right] \tag{12}$$

qui n'est valable que si $pK_{0_D}^{MX} > pK_{0_D}^{HX} - 2$ et $[H^+]_{(S)} \gg (K_{0_i}/y_{H^+(S)} y_{AcO^-(S)})^{\frac{1}{2}}$

Suivant la composition du mélange hydro-organique on peut envisager trois cas.

1. Milieu très peu dissociant. Dans les mélanges très riches en solvant organique (% $H_2O < 5$) on peut négliger la concentration des ions libres devant celle des paires d'ions. Les constantes de dissociation de HX et MX sont très petites. Dans l'expression du coefficient de partage, les termes $[X^-]_{(S)}\, y_{H^+(S)}\, y_{X^-(S)}/K_{0_D}^{HX}$ et $[X^-]_{(S)}\, y_{M^+(S)}\, y_{X^-(S)}/K_{0_D}^{MX}$ sont grands devant 1 et

$$D \approx K^{\star} \frac{c_E}{C_0} \frac{K_{0_D}^{MX}}{K_{0_D}^{HX}} \tag{13}$$

Dans un mélange de composition fixée le coefficient de partage varie comme l'inverse de la concentration totale de l'acide en solution.

2. Milieu très dissociant. Dans les mélanges riches en eau (> 40 %) l'acide et le sel sont entièrement dissociés en ions. Dans ce cas $[X^-]_{(S)}\, y_{H^+(S)}\, y_{X^-(S)}/K_{0_D}^{HX}$ et $[X^-]_{(S)} y_{M^+(S)}\, y_{X^-(S)}/K_{0_D}^{MX}$ sont toujours négligeables devant 1 et

$$D \approx K^{\star} \frac{c_E}{C_0} \frac{y_{M^+(S)}}{y_{H^+(S)}} \tag{14}$$

D varie linéairement avec $y_{M^+(S)}/C_0\, y_{H^+(S)}$.

3. Milieu moyennement dissociant. Ce sont des milieux intermédiaires caractérisés par la présence d'ions libres et de paires d'ions. D dépend de C_0 et de $[X^-]_{(S)}$. Dans ce cas D varie avec C_0 suivant la relation générale

$$D = K^{\star} \frac{y_{M^+(S)}}{y_{H^+(S)}} \frac{c_E}{C_0} \frac{1 + \dfrac{2}{\left(1 + \dfrac{4C_0\, y_{H^+(S)} y_{X^-(S)}}{K_{0_D}^{HX}}\right)^{\frac{1}{2}} - 1}}{\dfrac{K_{0_D}^{HX}}{K_{0_D}^{MX}} \dfrac{y_{M^+(S)}}{y_{H^+(S)}} + \dfrac{2}{\left(1 + \dfrac{4C_0\, y_{H^+(S)} y_{X^-(S)}}{K_{0_D}^{HX}}\right)^{\frac{1}{2}} - 1}} \tag{15}$$

L'allure que l'on prévoit pour la courbe $D = f(1/C_0)$ est représentée sur la Fig. 1 dans les différents cas possibles. Elle présente plusieurs parties caractéristiques. Aux grandes valeurs de C_0 l'équation de la tangente à l'origine est

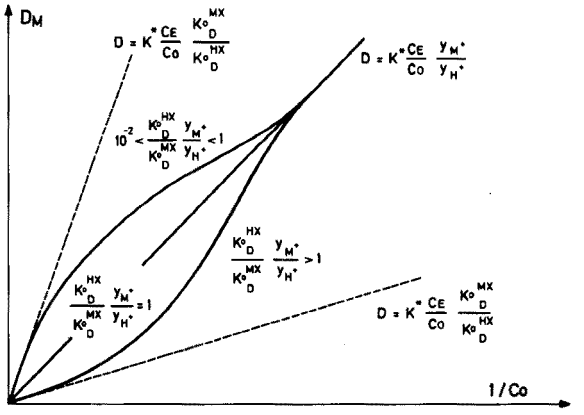

Fig. 1. Variation théorique de D_M en fonction de $1/C_0$.

$$D = K^{\star} \frac{c_E}{C_0} \frac{K_{0_D}^{MX}}{K_{0_D}^{HX}}$$

On retrouve l'expression correspondant aux milieux peu dissociants. En effet, plus la concentration de l'acide est grande moins celui-ci est dissocié.

Si C_0 diminue, le terme $2/(1 + 4C_0 y_{H^+(S)} y_{X^-(S)}/K_{0_D}^{HX})^{\frac{1}{2}} - 1)$ qui a été négligé au numératuer et au dénominateur dans le cas précédent devient non négligeable. La courbe s'écarte de la tangente à l'origine

vers le bas, si $\frac{K_{0_D}^{HX}}{K_{0_D}^{MX}} \frac{y_{M^+(S)}}{y_{H^+(S)}} < 1$; et vers le haut, si $\frac{K_{0_D}^{HX}}{K_{0_D}^{MX}} \frac{y_{M^+(S)}}{y_{H^+(S)}} > 1$.

Dans le cas particulier où les deux constantes $K_{0_D}^{HX}$ et $K_{0_D}^{MX}$ sont voisines, la courbe reste linéaire même pour des valeurs de C_0 où la dissociation de l'acide n'est pas négligeable.

Aux faibles valeurs de C_0 le terme $2/(1 + 4C_0 y_{H^+(S)} y_{X^-(S)}/K_{0_D}^{HX})^{\frac{1}{2}} - 1)$ devient grand devant 1 et devant $K_{0_D}^{HX} y_{M^+(S)}/K_{0_D}^{MX} y_{H^+(S)}$ et la courbe tend vers l'asymptote

$$D = K^{\star} \frac{c_E}{C_0} \frac{y_{M^+(S)}}{y_{H^+(S)}}$$

On retrouve l'équation obtenue en milieu très dissociant. En effet, aux très faibles concentrations, l'acide est complètement dissocié.

Méthode d'exploitation des courbes expérimentales

Théoriquement la détermination expérimentale de la variation de D avec $1/C_0$ et la comparaison des résultats avec les courbes théoriques doit permettre le calcul des paramètres $K^{\star}$, $K_{0_D}^{HX}$ et $K_{0_D}^{MX}$ qui interviennent dans ces équations. Toutefois, étant donné la complexité des expressions de D, une telle exploitation des résultats serait difficile et nécessiterait des mesures précises et nombreuses du coefficient de partage.

Nous nous sommes fixé le but de déterminer, à partir de la courbe $D = f(1/C_0)$, l'une des constantes de dissociation ($K_{0_D}^{HX}$ ou $K_{0_D}^{MX}$) lorsque l'autre est connue.

1. Dans le cas où K_0 n'est pas négligeable, on utilise l'equation générale (9). Si $K_{0_D}^{HX}$ est connu, $[H^+]_{(S)}$ peut être calculé à toute valeur de C_0 (équation de 3ème degré (10)). Si D est mesuré on peut calculer Z et w définis par

$$Z = \frac{c_E}{D[H^+]_{(S)}} \frac{y_{M^+(S)}}{y_{H^+(S)}} = \frac{1}{K^{\star}} + \frac{[H^+]_{(S)} - \frac{K_{0_i}}{[H^+]_{(S)}} \frac{1}{y_{H^+(S)} y_{AcO^-(S)}}}{K^{\star} K_{0_D}^{MX}} y_{M^+(S)} y_{X^-(S)} \tag{16}$$

$$w = \left[[H^+]_{(S)} - \frac{K_{0_i}}{[H^+]_{(S)}} \frac{1}{y_{H^+(S)} y_{AcO^-(S)}} \right] y_{M^+(S)} y_{X^-(S)} \tag{17}$$

Les coefficients d'activité y_{M^+} et y_{H^+}, peuvent être calculés par la relation

$\log y_{i^+} = (AI^{\frac{1}{2}}/1 + BaI^{\frac{1}{2}}) - dI$ déduite de la théorie de Debye et Hückel, où d est un paramètre empirique déterminé dans chaque mélange hydro-acétique [48]. On peut tracer les courbes de variation $Z = f(w)$; ce sont des droites dont l'ordonnée à l'origine $1/K^*$ et la pente $1/K_{0_D}^{MX}K^*$ permettent de déterminer le coefficient de sélectivité K^* et la constante thermodynamique de dissociation $K_{0_D}^{MX}$.

Si $K_{0_D}^{MX}$ est le paramètre connu, $K_{0_D}^{HX}$ ne peut pas être déduit de façon simple de la courbe $D = f(1/C_0)$.

2. Dans le cas où K_{0_i} est négligeable, on utilise l'équation (15). Si $K_{0_D}^{HX}$ est connu, à chaque valeur de C_0 où D a été mesuré, on peut calculer

$$u = \frac{2}{\left(1 + \frac{4C_0\, y_{H^+(S)}\, y_{X^-(S)}}{K_{0_D}^{HX}}\right)^{\frac{1}{2}} - 1}$$

$$\text{et } Z' = \frac{1+u}{DC_0}\, c_E \qquad (18)$$

D'après l'expression (15) Z' varie avec u suivant

$$Z' = \frac{1+u}{DC_0}\, c_E = \frac{1}{K^*}\left[\frac{K_{0_D}^{HX}}{K_{0_D}^{MX}} + \frac{y_{H^+(S)}}{y_{M^+(S)}}\, u\right] \qquad (19)$$

En portant $Z' = f(u\, y_{H^+(S)}/y_{M^+(S)})$ on doit obtenir des droites qui permettent de déterminer K^* (pente $1/K^*$) et $K_{0_D}^{HX}/K_{0_D}^{MX}$ (ordonnée à l'origine $K_{0_D}^{HX}/K^* K_{0_D}^{MX}$) et donc $K_{0_D}^{MX}$ puisque $K_{0_D}^{HX}$ est connu.

Dans le cas où $K_{0_D}^{MX}$ est le paramètre connu, on ne peut pas faire une exploitation simple des résultats. Il est toutefois possible de déterminer K^* et $K_{0_D}^{HX}$ par approximations successives. Pour cela on donne à K^* et $K_{0_D}^{HX}$ différentes valeurs à partir desquelles on calcule par itération la force ionique et les coefficients d'activité des espèces ioniques. On trace les courbes théoriques $D = f(1/C_0)$ correspondantes. On considère comme valables les valeurs trouvées du coefficient de sélectivité (K^*) et de la constante de dissociation de l'acide $K_{0_D}^{HX}$ pour lesquelles la courbe théorique $D = f(1/C_0)$ est la plus proche de la courbe expérimentale.

PARTIE EXPERIMENTALE

L'échangeur d'ions utilisé était la résine Bio-Rad AG50W-X8, 50—100 mesh, mise sous forme H^+ après plusieurs cycles d'échange H^+—Na^+.

L'acide acétique (R. P. Prolabo) contenait entre 0,05 et 0,3 % d'eau. Les acides perchlorique et nitrique étaient des produits R. P. Prolabo, le perchlorate d'argent était un produit Touzart et Matignon et le nitrate d'argent un produit Merck. Les mélanges hydro-acétiques ont été préparés par pesée.

Les expériences effectuées par simple équilibre en flacon, consistent à mettre en présence une solution d'un sel d'argent de titre connu dans un mélange hydro-organique et un échantillon de résine sous forme acide préalablement mis en équilibre avec le même mélange.

Avant et après l'équilibre l'argent en solution a été dosé par volumétrie à l'aide d'une solution titrée d'iodure de potassium avec détermination potentiométrique du point équivalent (pH mètre Beckman de recherche). Le coefficient de partage a été déduit de la variation de la concentration de l'argent en solution.

Pour chaque mélange hydro-organique nous avons fait deux essais parallèles sur deux échantillons de résine et nous avons adopté comme résultat la moyenne de deux valeurs obtenues.

RESULTATS EXPERIMENTAUX ET DISCUSSION

Nous avons étudié la variation du coefficient de partage de l'argent avec la proportion d'eau et d'acide acétique. La Fig. 2 montre les courbes expérimentales obtenues dans les mélanges eau—acide acétique—acide perchlorique 0,1 M et eau—acide acétique—acide nitrique 0,1 M.

Dans les mélanges riches en eau, le coefficient de partage de l'argent ne dépend pas de l'anion commun à l'acide et au sel. Ceci pouvait être prévu puisque dans ces milieux, les acides nitrique et perchlorique et leurs sels sont complètement dissociés et les équilibres d'échange sont, quelque soit l'anion: $Ag^+_{(S)} + H^+_{(R)} \rightleftharpoons Ag^+_{(R)} + H^+_{(S)}$. Les deux courbes tendent vers la même valeur qui représente le coefficient de partage de l'argent dans une solution aqueuse 0,1 M en acide. Cette valeur est du même ordre de grandeur que celle que l'on trouve dans la littérature [49].

Dans les mélanges riches en acide acétique, on voit que D_{Ag} est beaucoup plus grand en milieu nitrique qu'en milieu perchlorique. Or, dans ces mélanges peu dissociants, nous avons vu que D_{Ag} variait avec C_0 suivant l'expression (13). c_E et C_0 ayant les mêmes valeurs sur les deux courbes et les constantes de dissociation des nitrate et perchlorate d'argent étant voisines [48], les résultats obtenus indiquent que les constantes de dissociation des acides nitrique et perchlorique doivent être très différents. Ceci est en accord avec les résultats déjà obtenus dans l'acide acétique pur [50—53].

Nous avons aussi étudié la variation du coefficient de partage de l'argent avec la concentration totale de l'acide HX dans plusieurs mélanges hydro-acétiques de teneur en eau constante et inférieure à 20 %.

La variation du coefficient de partage de l'argent en fonction de l'inverse de la concentration C_0 de l'acide est représentée sur les Figs. 3 et 4, en milieu perchlorique dans des mélanges eau—acide acétique à 3,7; 7,0; 10,5; 14,3 et 19,1 % d'eau et en milieu nitrique à 8,6 et 14,4 % d'eau dans les mêmes mélanges.

Dans les mélanges eau—acide acétique—acide perchlorique on remarque que D_{Ag} varie linéairement avec $1/C_0$ à tous les pourcentages d'eau, à l'exception du plus élevé: 19,1 %.

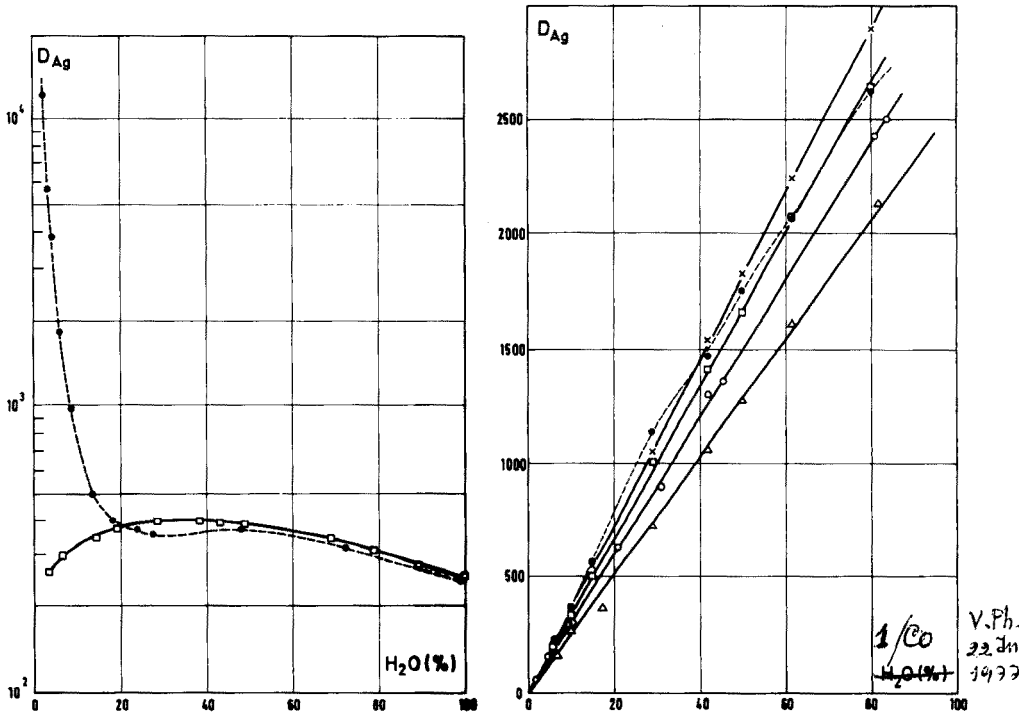

Fig. 2. Variation de D_{Ag} en fonction du pourcentage d'eau des solutions. □ Mélanges eau—acide acétique—acide perchlorique 0,1 M. • Mélanges eau—acide acétique—acide nitrique 0,1 M.

Fig. 3. Variation de D_{Ag} en fonction de $1/C_0$. Mélanges eau—acide acétique—acide perchlorique: △ 3,7 % H_2O; ○ 7,0 % H_2O; □ 10,5 % H_2O; x 14,3 % H_2O; • 19,1 % H_2O.

Si l'on examine les valeurs de la constante de dissociation de l'acide perchlorique dans les mélanges eau—acide acétique [48, 54], on s'aperçoit que dans les mélanges que nous avons étudiés, la dissociation de l'acide perchlorique ne peut pas être négligée. Donc dans l'expression (15) u ne peut pas être négligé devant 1 et devant $K_{0_D}^{HX} y_{Ag^+}/K_{0_D}^{AgX} y_{H^+}$. Dans ces conditions, on ne peut trouver une variation lineaire de D avec $1/C_0$ que si $K_{0_D}^{HX} y_{Ag^+}/K_{0_D}^{AgX} y_{H^+}$ est voisin de l'unité. Comme le rapport des coefficients d'activité d'ions de même charge, pour un mélange donné, est proche de l'unité, les résultats obtenus nous permettent donc de prévoir que dans tous les mélanges étudiés (sauf 19,1 % d'eau), les constantes de dissociation de l'acide perchlorique et du perchlorate d'argent sont voisines.

En milieu nitrique, au contraire, les variations de D_{Ag} avec l'inverse de la concentration C_0 de l'acide nitrique ne sont pas linéaires (Fig. 4) et d'après les concavités des courbes obtenues on prévoit que $K_{0_D}^{AgNO_3} > K_{0_D}^{HNO_3}$

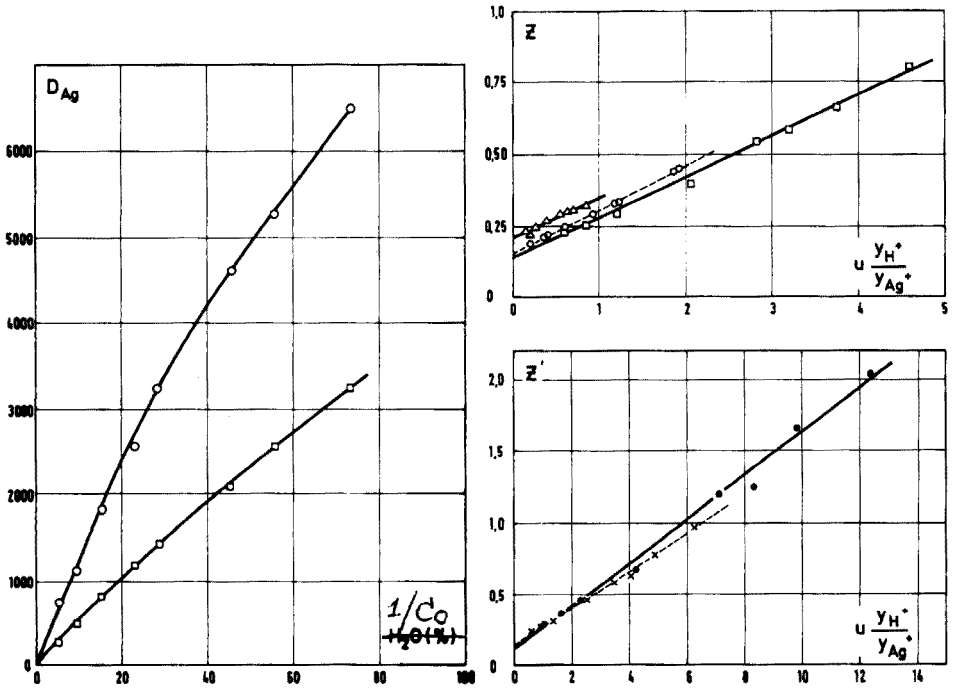

V.Ph.
22 June
1977

Fig. 4. Variation de D_{Ag} en fonction de $1/C_0$. Mélanges eau—acide acétique—acide nitrique: ○ 8,6 % H_2O; □ 14,4 % H_2O.

Fig. 5. Variation de Z' en fonction de $u\ y_{H^+}/y_{Ag^+}$. Mélanges eau—acide acétique—acide perchlorique: △ 3,7 % H_2O; ○ 7,0 % H_2O; □ 10,5 % H_2O; x 14,3 % H_2O; • 19,1 % H_2O.

Exploitation des résultats

Milieu perchlorique. Nous avons exploité les résultats obtenus dans les mélanges eau—acide acétique—acide perchlorique selon les méthodes que nous avons décrites précédemment afin de déterminer la constante de dissociation du perchlorate d'argent et, par comparaison des valeurs trouvées avec celles obtenues par potentiométrie [48], de vérifier la validité de l'expression du coefficient de partage.

D'après les valeurs du produit ionique des mélanges eau—acide acétique trouvées dans la littérature [54, 55], nous avons pu montrer que dans les mélanges eau—acide acétique—acide perchlorique étudiés, il est possible de négliger les ions H^+ apportés par l'ionisation du solvant devant ceux dus à la dissociation de l'acide perchlorique. Dans ces conditions, nous avons exploité nos résultats à l'aide de l'expression (19) dans laquelle D est mesuré et $K_{0_D}^{HX}$, c_E et C_0 sont connus. On se propose de déterminer K^* et $K_{0_D}^{AgX}$.

Expérimentalement, nous avons bien trouvé des variations linéaires de Z' en fonction de $u\ y_{H^+}/y_{Ag^+}$ comme le montrent les courbes représentées sur la Fig. 5. Des valeurs de la pente et de l'ordonnée à l'origine nous avons

déduit les valeurs de K^* et du $pK_{0_D}^{AgX}$ dans les différents mélanges eau—acide acétique. Les résultats obtenus sont rassemblés dans le Tableau 1.

Le coefficient de sélectivité peut être considéré comme constant, compte tenu des erreurs dues aux mesures, et ne dépend pas du pourcentage d'eau des mélanges. La valeur moyenne obtenue (6,8) est très proche de celle mesurée dans l'eau pure par Bonner et Smith [56] et trouvée égale à 6,70.

La variation de $pK_{0_D}^{AgClO_4}$ en fonction de la teneur en eau des mélanges est représentée sur la Fig. 6 sur laquelle nous avons fait aussi figurer les valeurs de $pK_{0_D}^{AgClO_4}$ obtenues par potentiométrie. On remarque qu'il y a un bon accord entre les valeurs obtenues à l'aide de la méthode d'échange d'ions et celles trouvées par potentiométrie.

Milieu nitrique. Nous avons appliqué la méthode d'échange d'ions à la détermination des constantes de dissociation de l'acide nitrique dans différents mélanges eau—acid acétique. Dans ce cas nous connaissons les constantes de dissociation du nitrate d'argent dans les mélanges eau—acide acétique déterminées par potentiométrie [48], D est mesuré et c_E et C_0 sont connus. Nous avons exploité ces résultats pour déterminer K^* et $K_{0_D}^{HNO_3}$ par approximations successives suivant la méthode décrite précédemment.

La Fig. 7 montre quelques exemples de courbes théoriques $D = f(1/C_0)$ calculées à l'aide de la relation (15), ainsi que les points expérimentaux pour les deux pourcentages d'eau étudies. Nous avons retenu les valeurs suivantes: $K^* = 6,7$ pour 8,6 et 14,4 % H_2O et $pK_{0_D}^{HNO_3} = 3,18$ pour 8,6 % H_2O et 2,15 pour 14,4 % H_2O.

On retrouve la même valeur du coefficient de sélectivité que celle obtenue en milieu perchlorique et dans l'eau pure. Nous avons supposé que K^* est indépendant de la teneur en eau des mélanges et nous avons calculé par approximations successives les constantes de dissociation de l'acide nitrique (entre 2,5 % et 25 % d'eau) à partir des mesures de D en fonction du pourcentage d'eau des mélanges eau—acide acétique—acide nitrique 0,1 N. Les résultats obtenus sont représentés sur la Fig. 8. On voit que la dissociation de l'acide nitrique devient très faible dans les mélanges riches en acide acétique.

TABLEAU 1

Valeurs de la constante $pK_{0_D}^{AgClO_4}$ et du coefficient de sélectivité K^* dans les mélanges eau—acide acétique

% H_2O	K^*	$pK_{0_D}^{AgClO_4}$ (échange d'ions)	$pK_{0_D}^{AgClO_4}$ [a] (potentiométrie [48])
3,7	6,3	3,10	3,01
7,0	6,6	2,31	2,27
10,5	7,0	1,76	1,75
14,3	7,5	1,42	1,37
19,1	6,4	0,86	0,86

[a] Valeurs interpolées.

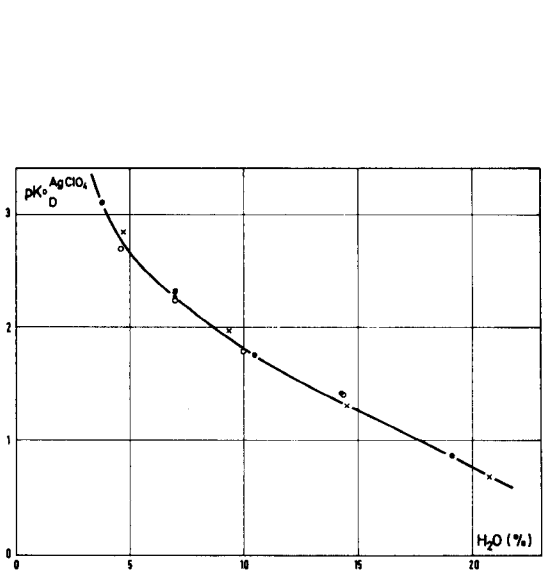

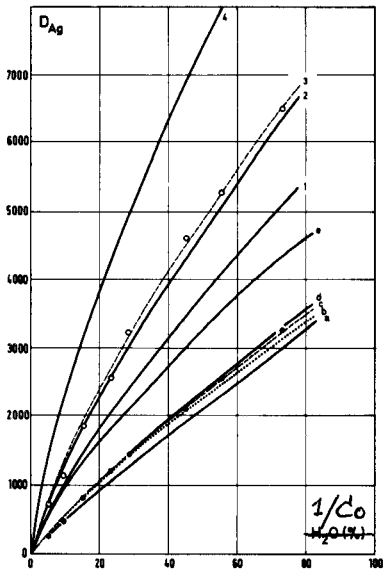

V. Ph.
22 June
1977

Fig. 6. Variation de $pK_{0_D}^{AgClO_4}$ en fonction du pourcentage d'eau des mélanges eau—acide acétique. • Déterminé par échange d'ions. ○ Déterminé par potentiométrie [48]. x Déterminé par potentiométrie en présence d'acide perchlorique [48].

Fig. 7. Variation théorique de D_{Ag} en fonction de $1/C_0$. Mélanges eau—acide acétique—acide nitrique: 8,6 % H_2O, ○ points expérimentaux; (1) $pK_0 = 3{,}0$ $K^\star = 6{,}7$ (2) $pK_0 = 3{,}10$ $K^\star = 7{,}3$ (3) $pK_0 = 3{,}18$ $K^\star = 6{,}7$ (4) $pK_0 = 3{,}5$ $K^\star = 6{,}7$.
14,4 % d'eau, • points expérimentaux; (a) $pK_0 = 2{,}0$ $K^\star = 7{,}0$ (b) $pK_0 = 2{,}18$ $K^\star = 6{,}4$ (c) $pK_0 = 2{,}16$ $K^\star = 6{,}7$ (d) $pK_0 = 2{,}12$ $K^\star = 7{,}0$ (e) $pK_0 = 2{,}5$ $K^\star = 6{,}7$.

Nous avons voulu voir si les valeurs de $K_{0_D}^{HNO_3}$ que nous avons trouvées vérifiaient la relation établie par Denison et Ramsey [57] et Gilkerson [58]

$$\log K_0 = k - \frac{Ne^2}{2{,}3\, aRT}\,\frac{1}{\epsilon}$$

où a est la distance minimum d'approche des ions, e la charge de l'électron, N le nombre d'Avogadro, R la constante des gaz parfaits, T la température absolue, ϵ la constante diélectrique et k une constante. Dans les mélanges eau—dioxane il a été montré que la constante k était négligeable [57, 59].

La variation de $pK_{0_D}^{HNO_3}$ en fonction de l'inverse de la constante diélectrique des mélanges eau—acide acétique est représentée sur la Fig. 9. On voit que les valeurs obtenues vérifient la relation précédente. A partir de la valeur de la pente de la droite nous avons recalculé la distance minimum d'approche des ions H^+ et NO_3^-. Nous avons trouvé une valeur égale à 4,7 qui est proche de celle que nous avions utilisée dans nos calculs, égale à 5,2, et que l'on trouve dans la littérature [60].

A l'aide de la droite $pK_{0_D}^{HNO_3} = f(1/\epsilon)$ nous avons calculé par extrapolation le pK de l'acide nitrique dans l'acide acétique pur. Nous avons trouvé une

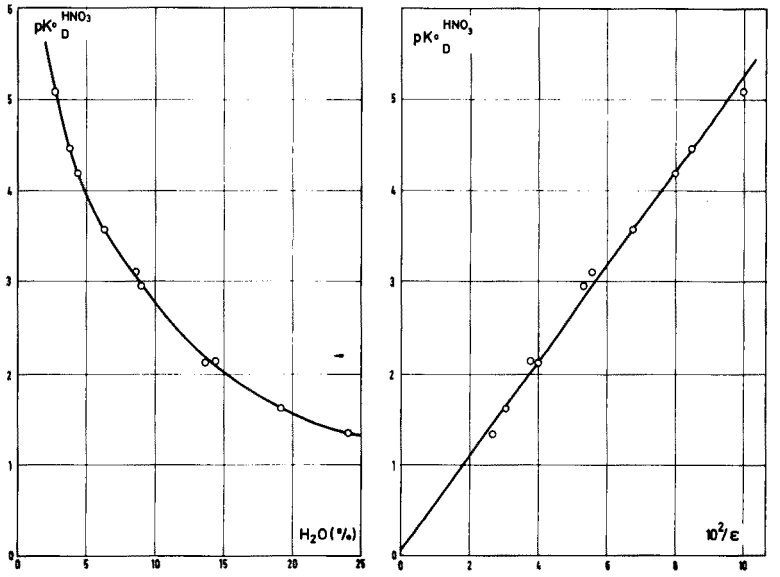

Fig. 8. Variation de $pK_{oD}^{HNO_3}$ en fonction du pourcentage d'eau des mélanges eau—acide acétique.

Fig. 9. Variation de $pK_{oD}^{HNO_3}$ en fonction de l'inverse de la constante diélectrique des mélanges eau—acide acétique (valeurs des constantes diélectriques d'après [61] et [62]).

valeur égale à 8,5 qui est assez proche de la valeur 9,4 trouvée par Izmailov [51] par conductimétrie et par Kolthoff et Bruckenstein [52], par spectrophotométrie dans l'acide acétique pur.

CONCLUSION

L'étude effectuée montre que la méthode d'échange d'ions peut être appliquée à la détermination des constantes de dissociation d'un acide connaissant les constantes de dissociation d'un sel et réciproquement. Cette méthode revient à remplacer la détermination d'une constante d'un équilibre par celle d'un autre plus facilement mesurable, suivie de l'étude de l'échange d'un élément métallique entre une résine échangeuse d'ions et une solution acide. En outre, on peut corriger les coefficients de partage des éléments de l'effet des réactions en solution et atteindre les constantes d'échange des ions.

L'application de cette méthode conduit à des calculs longs et complexes mais présente l'intérêt de pouvoir être utilisée pour déterminer des constantes de dissociation d'acides et de sels dans les solvants de faible constante diélectrique, déterminations quelquefois difficiles à réaliser par une autre méthode. Elle pourra être utile, en particulier, pour l'étude de la dissociation des sels des métaux alcalins dans les mélanges hydro-organiques.

Nous ne pensons pas possible d'étendre la méthode d'échange d'ions à

l'étude de la dissociation des sels d'éléments divalents. En effet, il faudrait établir une expression du coefficient de partage valable pour ces éléments et, compte tenu du grand nombre d'espèces en solution, on prévoit que cette expression sera très compliquée et, sans doute, inexploitable.

En outre, les éléments divalents sont souvent électroactifs et d'autres méthodes que l'échange d'ions permettent d'étudier la dissociation de leurs sels.

Ce travail a été réalisé grâce à l'aide matérielle du Commissariat à l'Energie Atomique et à l'aide scientifique de M. le Professeur B. Trémillon (Université Pierre-et-Marie Curie) que les auteurs tiennent à remercier.

BIBLIOGRAPHIE

1 F. Helfferich, Ion Exchange, McGraw-Hill, New York, 1962, pp. 507—518.
2 O. Samuelson, Ion Exchange Separations in Analytical Chemistry, Wiley, New York, 2ème éd., 1963, pp. 138—148.
3 B. Trémillon, Les séparations par les résines échangeuses d'ions, Gauthier-Vilars, Paris, 1965, pp. 120—142.
4 G. J. Moody et J. D. R. Thomas, Analyst, 93 (1968) 557.
5 J. L. Pauley, D. D. Vietti, C. C. Ou-Yang, D. A. Wood et R. D. Sherrill, Anal. Chem., 41 (1969) 2047.
6 F. W. E. Strelow, C. R. Van Zyl et C. J. C. Bothma, Anal. Chim. Acta, 45 (1969) 81.
7 R. P. Bhatnagar, R. G. Trivedi et Y. Bala, Talanta, 17 (1970) 249.
8 S. Sethi et R. S. Rai, Metals Miner. Rev., 9 (1970) 26.
9 R. G. Trivedi et R. P. Bhatnagar, Vijnana Parishad Anusandhan Patrika, 15 (1972) 121.
10 L. I. Dodova, Dokl. Bolg. Akad. Nauk, 24 (1971) 1199.
11 B. N. Zagorchev, L. I. Dodova et N. G. Todorova, Dokl. Bolg. Akad. Nauk, 24 (1971) 1207.
12 B. N. Zagorchev, L. I. Dodova et N. G. Todorova, Dokl. Bolg. Akad. Nauk, 24 (1971) 1373.
13 A. Lasztity et T. A. Belyavskaya, Proc. Anal. Chem. Conf., 3rd, 1 (1970) 59.
14 I. K. Tsitovich, Zh. Anal. Khim., 26 (1971) 1908.
15 L. G. Shishkova, Dokl. Bolg. Akad. Nauk, 25 (1972) 1525.
16 J. G. Jones et J. D. R. Thomas, Talanta, 19 (1972) 961.
17 J. Korkisch et M. M. Khater, Talanta, 19 (1972) 1654.
18 K. W. Cha, S. J. Kim et K. C. Park, Daehan Hwahak Hwoejee, 17 (1973) 434.
19 A. Lasztity, I. P. Alimarin et T. A. Belyavskaya, Magy. Kem. Foly., 80 (1974) 434.
20 B. Zagorchev, B. Balushev et N. Todorova, God. Vissh. Khimikotekhnol. Inst., Sofia, 15 (1968, pub. 1972) 235.
21 B. Zagorchev, B. Balushev et N. Todorova, God. Vissh. Khimikotekhnol. Inst., Sofia, 15 (1968, pub. 1972) 243.
22 M. Simek, Collect. Czech. Chem. Commun., 39 (1974) 3284.
23 M. Simek, Chem. Zvesti, 28 (1974) 343.
24 M. Simek, Chem. Zvesti, 28 (1974) 349.
25 E. I. Kazantsev et A. V. Plyusnin, Izv. Vyssh. Ucheb. Zaved., Khim. Khim. Tekhnol., 17 (1974) 300.
26 T. A. Belyavskaya, G. D. Brykina et T. F. Shugaeva, Vestn. Mosk. Univ., Khim., 15 (1974) 315.
27 G. L. Starobinets, L. V. Novitskaya et L. I. Sevost'yanova, Zh. Fiz. Khim., 42 (1968) 1098.

28 T. A. Belyavskaya, G. D. Brykina et L. B. Isaeva, Vestn. Mosk. Univ., Khim., 12 (1971) 468.
29 G. D. Brykina, L. B. Isaeva et T. A. Belyavskaya, Radiokhimiya, 14 (1972) 515.
30 S. Sharma, R. P. Bhatnagar, Vijnana Parishad Anusandhan Patrika, 16 (1973) 89.
31 F. W. E. Strelow, C. H. S. W. Weiner et T. N. Van Der Walt, Talanta, 21 (1974) 1183.
32 J. M. Peters et G. Del Fiore, J. Chromatogr., 108 (1975) 415.
33 V. L. Gutsanu, A. N. Pushnyak, P. K. Migal et Le Van Cuong, Izv. Vyssh. Ucheb. Zaved., Khim. Khim. Tekhnol., 17 (1974) 691.
34 S. A. Mechkovskii, Prevrashch. Kompleks. Soedin. Deistviem Sveta, Radiats. Temp., (1973) 134.
35 V. P. Leshchenko et O. D. Kurilenko, Fiz. Khim. Mekh. Liofil'nost Dispersnykh Sist., 2 (1971) 136.
36 K. A. Boni et H. A. Strobel, Z. Phys. Chem. (Frankfurt am Main), 87 (1973) 169.
37 N. Renault, N. Deschamps et I. N. Bourrelly, Anal. Chim. Acta, 64 (1973) 19.
38 S. K. Jha, F. De Corte et J. Hoste, Anal. Chim. Acta, 62 (1972) 163.
39 B. Balushev, B. Zagorchev et K. Chakrov, Dokl. Bolg. Akad. Nauk, 27 (1974) 511.
40 M. Qureshi et K. Husain, Anal. Chem., 43 (1971) 447.
41 M. Qureshi et K. Husain, Anal. Chim. Acta, 57 (1971) 387.
42 G. E. Janauer, H. E. Van Wart et J. T. Carrano, Anal. Chem., 42 (1970) 215.
43 R. Smits, P. Van Der Winkel, D. L. Massart, J. Juillard et J. P. Morel, Anal. Chem., 45 (1973) 339.
44 A. Waksmundzki et Z. Hubicki, Ann. Univ. Mariae Curie-Sklodowska, Sect. AA, 26/27 (1971) 181.
45 J. Devynck et B. Trémillon, Bull. Soc. Chim. Fr., (1967) 685.
46 Y. Coïc, Thèse, Lyon (1970).
47 G. D. Brykina, T. A. Belyavskaya et L. E. Romanovskaya, Vestn. Mosk. Univ., Khim., 14 (1973) 697.
48 A. R. Rodriguez et C. Poitrenaud, Analusis, 3 (1975) 491.
49 F. W. E. Strelow, Anal. Chem., 32 (1960) 1185.
50 A. M. Shkodin, Zh. Fiz. Khim., 34 (1960) 1625.
51 N. A. Izmailov, Zh. Fiz. Khim., 24 (1950) 321.
52 I. M. Kolthoff et S. Bruckenstein, J. Amer. Chem. Soc., 78 (1956) 1.
53 Yu. Ya. Fialkov et Yu. Ya. Borovikov, Ukr. Khim. Zh., 30 (1964) 119.
54 F. Le Ber, Thèse, Paris (1970).
55 S. Kilpi et E. Lindell, Ann. Acad. Sci. Fennicae, Sér. A II, 136 (1967) 3.
56 O. D. Bonner et L. L. Smith, J. Phys. Chem., 61 (1957) 326.
57 J. J. Denison et J. B. Ramsey, J. Amer. Chem. Soc., 77 (1955) 2615.
58 W. R. Gilkerson, J. Chem. Phys., 25 (1956) 1199.
59 J. C. James et J. G. Knox, Trans. Faraday Soc., 46 (1950) 254.
60 J. Kielland, J. Amer. Chem. Soc., 59 (1937) 1975.
61 A. N. Campbell et J. M. T. M. Gieskes, Can. J. Chem., 42 (1964) 1379.
62 Yu. Ya. Borovikov et Yu. Ya. Fialkov, Elektrokhimiya, 1 (1965) 1106.

Analytica Chimica Acta, 87 (1976) 141—148

ÉTUDE D'ÉQUILIBRES EN SOLUTION À L'AIDE DES ÉCHANGEURS D'IONS
II DÉTERMINATION DES CONSTANTES DE DISSOCIATION DES PERCHLORATES ALCALINS DANS LES MÉLANGES EAU—ACIDE ACÉTIQUE—ACIDE PERCHLORIQUE

A. R. RODRIGUEZ et C. POITRENAUD

Institut National des Sciences et Techiques Nucléaires de Saclay B.P. n° 6, 91190 Gif-sur-Yvette (France)

(Reçu le 26 mars 1976)

RÉSUMÉ

Les constantes thermodynamiques de dissociation des perchlorates de lithium, de sodium, de potassium, de rubidium et de césium dans les mélanges eau—acide acétique—acide perchlorique ont été déterminées par une méthode d'échange d'ions. Pour cela les coefficients de partage des éléments alcalins ont été mésurés dans les mélanges eau—acide acétique—acide perchlorique de teneur en eau variable (4 à 100 % en poids) et de teneur en acide perchlorique constante. Dans quelques mélanges de teneur en eau constante et inférieure à 20 % (en poids), la variation de ces coefficients de partage avec la concentration d'acide perchlorique a été étudiée. Tous les résultats obtenus ont été exploités afin de déterminer les constantes de dissociation des perchlorates alcalins et les coefficients de sélectivité des ions alcalins et hydrogène dans les mélanges hydro-organiques étudiés.

SUMMARY

The thermodynamic dissociation constants of lithium, sodium, potassium, rubidium and cesium perchlorates in water—acetic acid—perchloric acid mixtures have been determined by an ion-exchange method. The distribution coefficients of alkaline elements have been measured in water—acetic acid—perchloric acid mixtures containing a variable quantity of water (4—100 % by weight) and a constant amount of perchloric acid. The variation of these distribution coefficients with perchloric acid concentration has been studied in various mixtures containing a constant amount of water (less than 20 % w/w). The results have been used to determine the dissociation constants of alkaline perchlorates and the selectivity coefficients of alkaline ions and hydrogen ion in the aqueous organic mixtures studied.

L'addition d'un solvant organique à une solution aqueuse d'un sel métallique modifie la constante diélectrique du milieu et la solvatation des ions dissous. La composition du mélange a un effet considérable sur les coefficients de partage de cations métalliques entre une résine échangeuse d'ions et une solution acide de leurs sels.

Les méthodes classiques d'étude de complexes par échange d'ions permettent d'obtenir des renseignements sur les réactions en solution entre les cations

échangés et les anions présents. Nous avons établi [1] une relation théorique entre le coefficient de partage d'un élément monovalent entre une résine échangeuse de cations et un mélange hydro-organique et les différents paramètres dont il dépend (concentration de l'acide en solution, constantes de dissociation de l'acide et du sel, coefficient de sélectivité des ions échangés). La méthode consiste à étudier la variation des coefficients de partage des cations en fonction des concentrations des espèces en solution et en déduire des constantes des réactions chimiques.

L'object du travail a été d'appliquer cette méthode à la détermination des constantes de dissociation des perchlorates de lithium, de sodium, de potassium, de rubidium et de césium dans les mélanges eau—acide acétique connaissant les constantes de dissociation de l'acide perchlorique dans les mêmes mélanges [2, 3].

La méthode d'échange d'ions est la seule qui, à notre connaissance, permette de mesurer les constantes de dissociation d'un sel d'un métal alcalin dans une aussi grande gamme de mélanges hydro-organiques. La méthode potentiométrique serait peut-être applicable à l'aide des nouvelles électrodes indicatrices d'ions alcalins, à condition, toutefois, que celles-ci fonctionnent dans les mélanges eau—solvant organique choisis. La conductimétrie permet de déterminer ces constantes mais elle ne peut pas être utilisée pour des mélanges hydro-acétiques contenant plus de 5 % d'eau dans lesquels la dissociation du solvant est très importante [4].

Il y a peu d'études sur la dissociation de sels de métaux alcalins dans les mélanges hydro-acétiques. Seules les constantes de dissociation du perchlorate de sodium dans les mélanges de teneur en eau 5 et 9 % ont été déterminées par Wiberg et Evans [5] par coductimétrie.

PARTIE EXPERIMENTALE

L'échangeur d'ions était la résine Bio-Rad AG50W-X8, 50—100 mesh, mise sous forme H^+ après plusieurs cycles d'échange H^+—Na^+.

L'acide acétique utilisé était un produit R.P. Prolabo, contenant entre 0,05 et 0,3 % d'eau. L'acide perchlorique, le perchlorate de lithium, le perchlorate de sodium et l'acétate de potassium étaient des produits R.P. Prolabo, le carbonate de rubidium et l'acétate de césium étaient des produits Merck.

Les mélanges hydro-acétiques ont été préparés par pesée.

Le lithium a été dosé par spectrophotométrie d'absorption atomique (Techtron AA-4). Le sodium, le potassium, le rubidium et le césium ont été dosés par la mesure de la radioactivité des traceurs ^{24}Na, ^{42}K, ^{86}Rb et ^{137}Cs réalisée par spectrométrie—γ à l'aide d'un scintillateur NaI(Tl) relié à un sélecteur multicanaux.

Les coefficients de partage ont été déterminés comme précédemment [1]. Dans la solution en contact avec la résine nous avons ajouté une quantité d'élément métallique non actif pour avoir une concentration totale d'environ 10^{-3} M.

RESULTATS EXPERIMENTAUX, EXPLOITATION ET DISCUSSION

Nous avons déterminé les coefficients de partage du lithium, du sodium, du potassium, du rubidium et du césium entre une résine échangeuse de cations et un mélange hydro-organique. La Fig. 1 montre la variation des coefficients de partage de ces éléments en fonction du pourcentage d'eau des mélanges eau—acide acétique—acide perchlorique 0,1 M.

Toutes les courbes de variation des coefficients de partage des métaux alcalins présentent un maximum qui se déplace vers les pourcentages plus riches en eau dans l'ordre croissant des rayons cristallographiques des ions. Le déplacement du maximum de ces courbes semble dépendre de la solvatation des ions. En effet, la tendance à être solvaté par l'eau dépend de la taille de l'ion et diminue dans l'ordre $Li^+ > H^+ > Na^+ > K^+ > Rb^+ > Cs^+$.

On peut remarquer aussi que la courbe de variation du coefficient de partage de l'ion qui a le plus tendance à être solvaté, le lithium, présente un maximum dans les mélanges riches en acide acétique où le liquide qui imbibe la résine est plus riche en eau que la phase extérieure [6]. Par contre, le maximum de la courbe de variation du coefficient de partage du césium qui a moins tendance à être solvaté par l'eau, est situé dans la zone de pourcentages plus riches en eau, où les compositions des solutions intérieures et extérieures à la résine sont voisines.

Nous avons aussi étudié la variation du coefficient de partage des métaux alcalins en fonction de la concentration totale de l'acide perchlorique dans plusieurs mélanges hydro-acétiques de teneur en eau constante et inférieure à 20 %. Les Figs. 2 à 4 montrent quelques exemples de courbes de variations

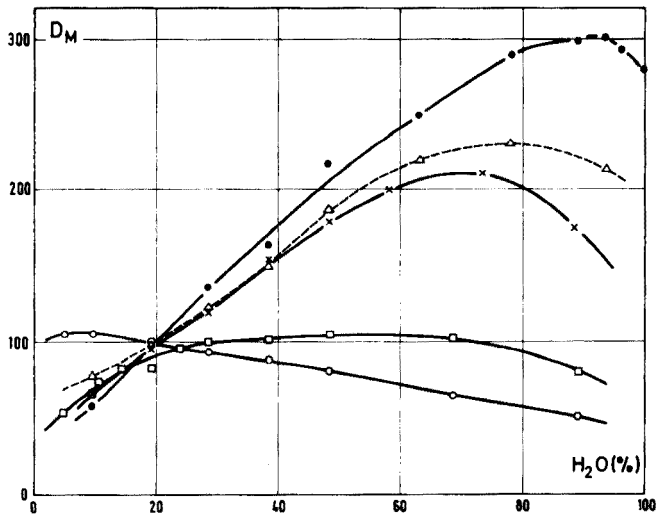

Fig. 1. Variation de D_M en fonction du pourcentage d'eau des solutions. Mélanges eau—acide acétique—acide perchlorique 0,1 M. (○) Li, (□) Na, (×) K, (△) Rb, (●) Cs.

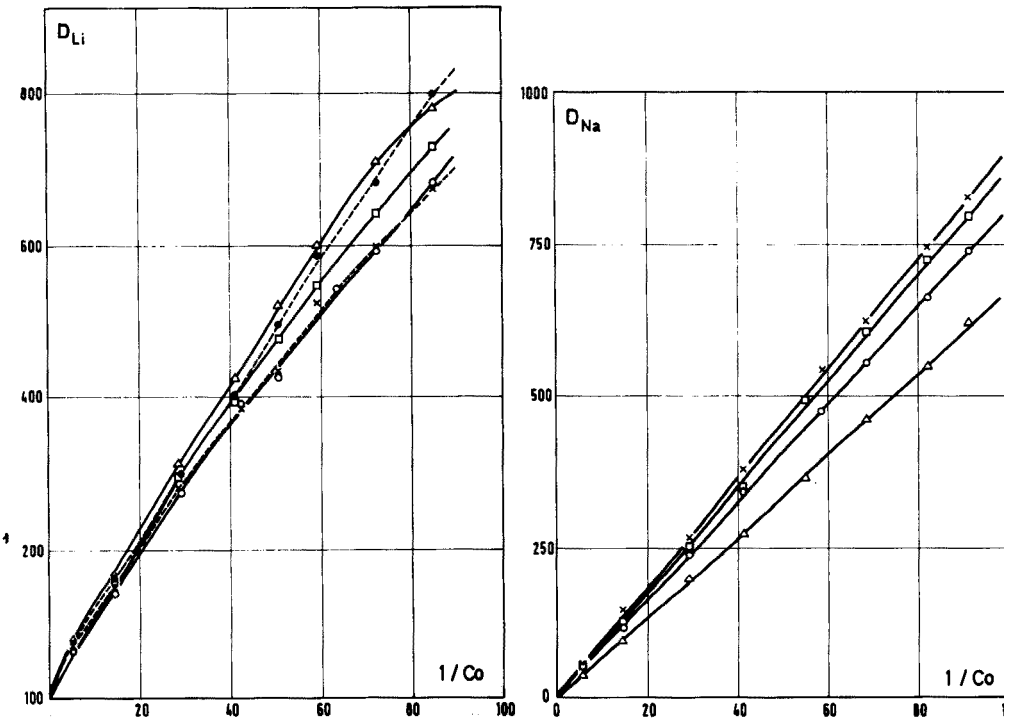

Fig. 2. Variation de D_{Li} en fonction de l'inverse de la concentration d'acide perchlorique. Mélanges eau—acide acétique à : (•) 4,7 % d'eau, (△) 7,0 % d'eau, (□) 9,5 % d'eau, (X) 14,5 % d'eau et (○) 19,2 % d'eau.

Fig. 3. Variation de D_{Na} en fonction de l'inverse de la concentration d'acide perchlorique. Mélanges eau—acide acétique à : (△) 4,7 % d'eau, (○) 9,5 % d'eau, (□) 14,4 % d'eau et (X) 19,2 % d'eau.

de D_M en fonction de l'inverse de la concentration, C_0 de l'acide perchlorique. De l'allure de ces courbes on peut déduire des renseignements sur les valeurs des constantes de dissociation des perchlorates des alcalins par rapport à celles de l'acide perchlorique comme nous l'avons fait dans le cas des sels d'argent [1].

Dans le cas du lithium on observe que la courbe de variation du coefficient de partage en fonction de $1/C_0$ présente une concavité vers le bas (Fig. 2). Ceci permet de prévoir que dans ces mélanges hydro-acétiques les constantes de dissociation du perchlorate de lithium sont plus grandes que les constantes de dissociation de l'acide perchlorique.

Pour le sodium, on remarque que D_{Na} présente une variation linéaire avec $1/C_0$ à tous les pourcentages d'eau étudiés dans les mélanges eau—acide acetique (Fig. 3). On ne peut trouver une variation linéaire que si les constantes de dissociation du perchlorate de sodium et de l'acide perchlorique sont voisines [1].

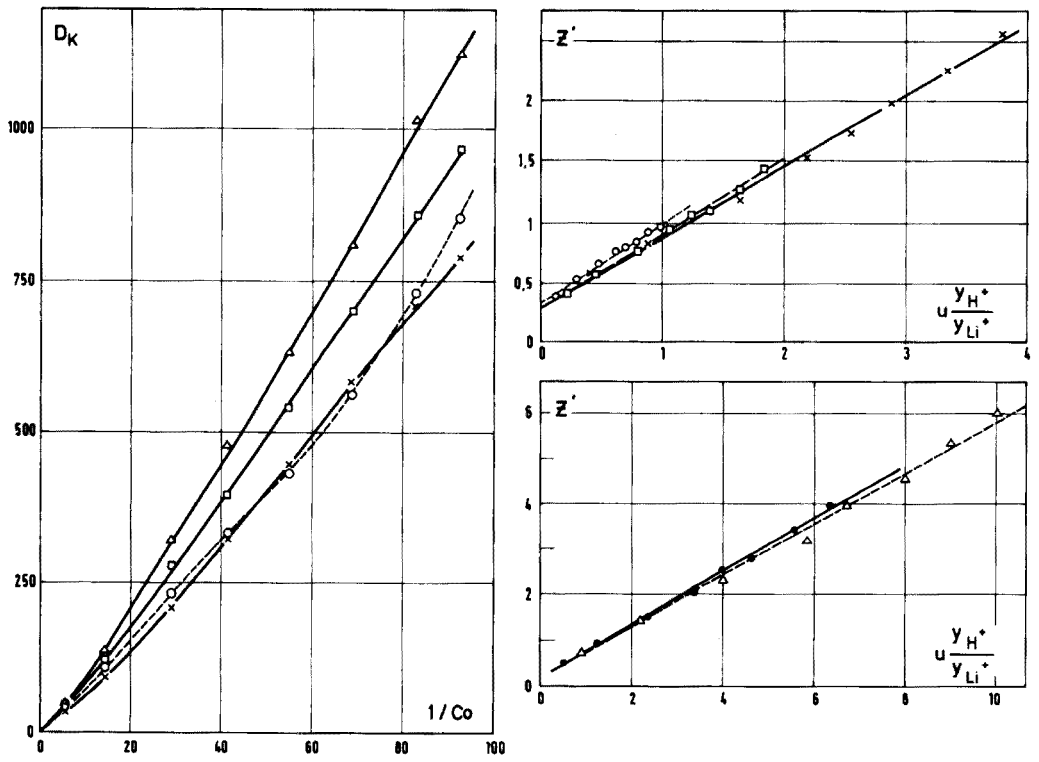

Fig. 4. Variation de D_K en fonction de l'inverse de la concentration d'acide perchlorique. Mélanges eau—acide acétique à : (×) 4,7 % d'eau, (○) 9,5 % d'eau, (□) 14,4% d'eau et (△) 19,2 % d'eau.

Fig. 5. Variation de Z' en fonction de $u\, y_{H^+}/y_{Li^+}$. Mélanges eau—acide acétique à: (○) 4,7 % d'eau, (□) 7,0 % d'eau, (×) 9,5 % d'eau, (●) 14,4 % d'eau et (△) 19,2 % d'eau.

La courbe de variation du coefficient de partage du potassium en fonction de $1/C_o$ n'est pas linéaire, elle présente une concavité vers le haut (Fig. 4). Des courbes d'allures analogues sont observées dans le cas du rubidium et du césium. On peut donc prévoir que les constantes de dissociation des perchlorates de potassium, rubidium et césium sont plus petites que les constantes de dissociation de l'acide perchlorique dans les mélanges étudiés.

Exploitation des courbes expérimentales

De l'ensemble des mesures expérimentales concernant le partage des éléments alcalins, nous avons déduit les constantes de dissociation de leurs perchlorates dans les mélanges eau—acide acétique—acide perchlorique.

Nous connaissons les constantes de dissociation de l'acide perchlorique dans ces mélanges et nous avons exploité nos résultats à l'aide de l'expression (19) établie précédemment [1]. Nous avons obtenu des variations linéaires

de Z' en fonction de $u\ y_{H^+(s)}/y_{M^+(s)}$. La Fig. 5 montre quelques droites obtenues dans le cas du perchlorate de lithium. Les valeurs trouvées pour les coefficients de sélectivité des ions M^+ et H^+ et les pK de dissociation des perchlorates des métaux alcalins dans différents mélanges eau—acide acétique sont regroupées dans le Tableau 1, où nous avons fait aussi figurer les pK de

TABLEAU 1

pK de dissociation des perchlorates de métaux alcalins et coefficients de sélectivité des ions M^+ et H^+ dans les mélanges eau—acide acétique

% H_2O	$LiClO_4$		$NaClO_4$		$KClO_4$		$RbClO_4$		$CsClO_4$		$HClO_4$
	K^*	pK_{o_D}	K^*	pK_{o_D}	K^*	pK_{o_D}	K^*	pK_{o_D}	K^*	pK_{o_D}	pK_{o_D}[c]
4,7	1,5	2,54	1,6	2,94	2,9	3,18	3,1[a]	3,32[a]	2,9[b]	3,28[b]	2,80
7,0	1,7	1,99									2,30
9,5	1,7	1,61	1,6	1,86	2,2	2,09	2,4	2,20	3,1	2,38	1,90
14,4	1,7	0,91	2,0	1,50	2,4	1,61	2,9	1,56	3,2	1,92	1,46
19,2	1,8	0,41	1,7	0,91	3,0	1,51	3,2	1,21	3,6	1,70	1,18

[a] Valeurs à 4,9 % d'eau.
[b] Valeurs à 4,8 % d'eau.
[c] Valeurs interpolées (d'après [3]).

dissociation de l'acide perchlorique dans les mêmes mélanges.

Nous avons représenté sur la Fig. 6 la variation des pK de dissociation des perchlorates de métaux alcalins en fonction du pourcentage d'eau des mélanges eau—acide acétique. Ces courbes montrent l'influence du pouvoir dissociant de ces mélanges. Dans les mélanges riches en acide acétique la dissociation ionique des sels est faible et devient de plus en plus importante lorsque le pourcentage d'acide acétique diminue.

Nous avons comparé dans le Tableau 2 les valeurs moyennes du coefficient de sélectivité des ions H^+ et M^+ dans des mélanges eau—acide acétique de teneur en eau inférieure à 20 % et celles déterminées par Bonner et Smith [7] dans l'eau pure.

On remarque que les valeurs moyennes que nous avons trouvées dans les mélanges eau—acide acétique sont du même ordre de grandeur que celles mesurées dans l'eau. En particulier, les valeurs obtenues des coefficients de sélectivité des ions Na^+ et H^+, K^+ et H^+ et Rb^+ et H^+ sont assez proches de celles de la littérature. De toute façon, on retrouve le même ordre d'affinité des métaux alcalins dans les mélanges eau—acide acétique et dans l'eau.

Les valeurs de pK de dissociation des perchlorates des métaux alcalins ont été portées en fonction de l'inverse de la constante diélectrique des mélanges hydro-acétiques (Fig. 7). On trouve des variations linéaires ce qui prouve que les valeurs déterminées vérifient la relation établie par Denison et Ramsey [8] et Gilkerson [9]

$$\log K_0 = k - \frac{Ne^2}{2{,}3\,aRT}\,\frac{1}{\epsilon} \qquad (4)$$

où a est la distance minimum d'approche des ions, e la charge de l'électron, N le nombre d'Avogadro, R la constante des gaz parfaits, T la température absolue, ϵ la constante diélectrique et k une constante.

A partir de la pente de la droit $pK_{oD}^{MClO_4} = f(1/\epsilon)$ nous avons recalculé la distance minimum d'approche des ions. Les valeurs obtenues pour les ions Li^+, Na^+, K^+, Rb^+, Cs^+, avec l'anion ClO_4^-, égales respectivement à 5,5; 5,9 ; 5,9; 5,4 ; 7,2 , sont en bon accord avec celles que l'on trouve dans la littérature comprises entre 2 et 8 Å [10].

Les valeurs que nous avons trouvées des constantes de dissociation du

TABLEAU 2

Valeurs des coefficients de sélectivité des ions alcalins et hydrogène

Echange	$K^{\star}$ moyen (nos résultats)	K_H^M (d'après [7])
H^+—Li^+	1,7	0,79
H^+—Na^+	1,7	1,56
H^+—K^+	2,6	2,28
H^+—Rb^+	2,9	2,50
H^+—Cs^+	3,2	2,56

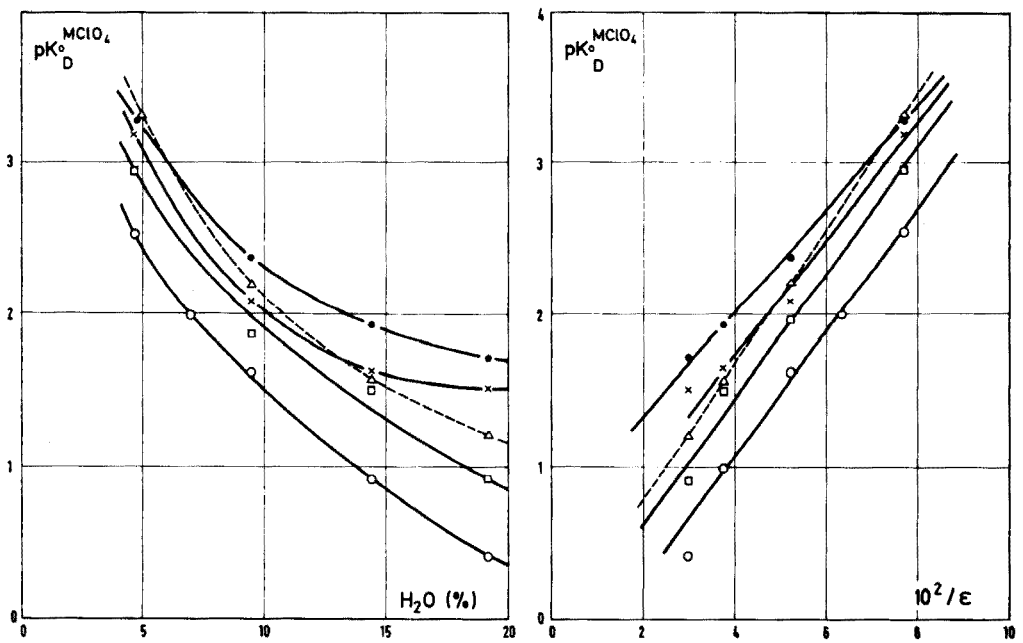

Fig. 6. Variation de $pK_{oD}^{MClO_4}$ en fonction du pourcentage d'eau des solutions, Mélanges eau—acide acétique. (○) $LiClO_4$, (□) $NaClO_4$, (×) $KClO_4$, (△) $RbClO_4$, (●) $CsClO_4$.

Fig. 7. Variation de $pK_{oD}^{MClO_4}$ en fonction de l'inverse de la constante diélectrique des mélanges eau—acide acétique. (○) $LiClO_4$, (□) $NaClO_4$, (×) $KClO_4$, (△) $RbClO_4$, (●) $CsClO_4$.

perchlorate de sodium dans les mélanges eau—acide acétique à 5 et 9 % d'eau sont assez différentes de celles obtenues par Wiberg et Evans [5] dans ces mêmes mélanges par conductimétrie. Eux-mêmes signalent l'imprécision de leurs résultats due à certaines hypothèses qui ont été faites relatives aux coefficients d'activité des espèces, aux constantes diélectriques et à la dissociation des mélanges hydro-acétiques.

Ce travail a été réalisé grâce à l'aide matérielle du Commissariat à l'Energie Atomique et à l'aide scientifique de M. le Professeur B. Trémillon (Université Pierre-et-Marie Curie) que les auteurs tiennent à remercier. Ils sont aussi reconnaissants à M. N. Deschamps (Laboratoire d'Analyse par Activation—Pierre Süe) d'avoir mis à leur disposition les appareils de son laboratoire et à Mme N. Jafrezic de l'aide qu'elle leur a apportée pour la réalisation des analyses par activation.

BIBLIOGRAPHIE

1 A. R. Rodriguez et C. Poitrenaud, Anal. Chim. Acta, 00 (1976) 000.
2 F. Le Ber, Thèse, Paris (1970).
3 A. R. Rodriguez et C. Poitrenaud, Analusis, 3 (1975) 491.
4 R. Godard, Thèse C.N.A.M., Paris (1973).
5 K. B. Wiberg et R. J. Evans, J. Amer. Chem. Soc., 80(1958) 3019.
6 A. R. Rodriguez et C. Poitrenaud, J. Chromatogr., 121 (1976) 104.
7 O. D. Bonner et L. L. Smith, J. Phys. Chem., 61 (1957) 326.
8 J. J. Denison et J. B. Ramsey, J. Amer. Chem. Soc., 77 (1955) 2615.
9 W. R. Gilkerson, J. Chem. Phys., 25 (1956) 1199.
10 J. Kielland, J. Amer. Chem. Soc., 59 (1937) 1975.

Analytica Chimica Acta, 87 (1976) 149—155

ANALYTISCHE EIGENSCHAFTEN VON HYDROPHILEN GLYKOLMETHACRYLAT—GELEN MIT CHEMISCH GEBUNDENER SALICYLSÄURE

Z. SLOVÁK, S. SLOVÁKOVÁ und M. SMRŽ

Forschungsinstitut für reine Chemikalien, Lachema, 62133 Brno (Czechoslovakia)

(Eingegangen am 12. April 1976)

ZUSAMMENFASSUNG

Hydrophile Glykolmethacrylat-Gele mit über Azogruppen gebundener Salicylsäure weisen ein hochselektives Verhalten gegenüber Fe^{3+} und Al^{3+} auf. Bei pH-Werten über 2,5 wird die durch die Komplexbildung bevorzugte Sorption von Schwermetallen von einem unspezifischen Ionenaustausch auf Grund der Dissoziation der Karboxylgruppe der Salicylsäure begleitet. Das Sorptionsvermögen für Schwermetallionen beträgt über 0,35 mMol g^{-1}. Es wurden die Verteilungskoeffizienten von 14 Metallionen in Abhängigkeit von pH bestimmt; in günstigen Fällen erreichen sie Werte über 10^4. Die Sorptionsgleichgewichte stellen sich innerhalb von 2 min ein. Es wurden chromatographische Trennungen von Metallen in μg-Mengen durchgeführt.

SUMMARY

Hydrophilic glycolmethacrylate gel with salicylic acid chemically bound via the side-chain azo groups, shows high selectivity for Fe^{3+} and Al^{3+} ions. Above pH 2.5, the enhanced sorption of heavy metals by complex formation is accompanied by nonspecific ion-exchange arising from dissociation of the carboxyl group of salicyclic acid. The sorption capacity for heavy metals exceeds 0.35 mmol g^{-1}. Distribution coefficients for 14 metal ions as a function of pH are given; under suitable conditions, some values exceed 10^4. Sorption equilibrium is achieved within 2 min. The chromatographic separation of metals in microgram amounts is discussed.

In der vorigen Mitteilung [1] haben wir über die Eigenschaften von hydrophilen Glykolmethacrylat-Gelen mit gebundenem 8-Hydroxychinolin (Spheron-Oxin) berichtet. Diese chelatbildenden Austauscher sind u.a. durch eine ungewöhnlich hohe Einstellungsgeschwindigkeit der Sorptionsgleichgewichte ausgezeichnet. Da der Austauscher nur die aktiven Oxingruppen enthält, erfolgt die Sorption von Kationen ausschliesslich durch Komplexbildung. Falls jedoch die zur Komplexbildung befähigte Gruppierung in neutralen oder in schwach sauren Lösungen dissoziieren kann (z.B. alle Chelatationsaustauscher, die Karboxylgruppen enthalten), wird die selektive Sorption von einem nichtselektiven Ionenaustausch begleitet, und man kann das Verhalten des Materials nicht an Hand der Angaben über die Komplexbildung in wässrigen Lösungen voraussagen. Die bisher meist benutzte Beurteilung der Selektivität nach dem Sorptionsvermögen (d.h. bei Bedingun-

gen eines Metallüberschusses im Vergleich zum Austauscher) führt besonders in diesen Fällen zu keiner überzeugenden Aussage (vgl. z.B. [2]).

Nachen die Selektivität und die Einstellungsgeschwindigkeit der Sorptionsgleichgewichte bei Spheron-Oxin im Blick auf eine spätere analytische Anwendung untersucht worden sind [1], beschäftigten wir uns in dieser Arbeit mit analogen Polymeren, die eine sorptionsfähige Gruppierung der Salicylsäure enthalten.

EXPERIMENTELLER TEIL

Chemikalien und Geräte

Glykolmethacrylat-Gel mit Salicylsäure, die durch Azokupplung an eine Seitenkette des Polymers gebunden ist (Spheron-Salicyl, Lachema, Brno); Gehalt 0,63 mÄquiv. Salicylsäure pro 1 g trockene Probe, berechnet aus Ergebnissen der Elementaranalyse (ex N). Porenweite des Ausgangsgels Spheron (Lachema), als Molekulargewicht eines Dextranstandards bei der Ausschlussgrenze ausgedrückt: 10^6. Korngrösse 40—63 μm.

Glycin/HCl-Pufferlösungen enthielten NaCl zur Einstellung der Ionenstärke. Azetatpufferlösungen mit bestimmter Na^+-Konzentration (meistens 0,02 M) wurden durch Ansäuren berechneter Mengen von Natriumazetat mit Essigsäure bei gleichzeitiger pH-Messung hergestellt. Bei niedrigeren pH-Werten wurde eine berechnete Menge NaCl in 0,1 M oder 0,2 M Essigsäure bzw. in Azetatpufferlösungen gelöst.

Modell 303 Perkin-Elmer Atomabsorptionsspektralphotometer, UV-VIS Spektralphotometer CF-4 (Optica Milano) und pH Meter 26 (Radiometer Copenhagen). Chromatographische Apparatur [1] zur Trennung von Kationen mit A.A.S. als Detektor. Kolonne: Glas, ϕ 4 mm, Länge 110 mm.

Bestimmung von Metallkonzentrationen

Mit Ausnahme von Y^{3+} und La^{3+} wurden alle Bestimmungen mit Hilfe der Atomabsorptionsspektroskopie (A.A.S.) durchgeführt (Arbeitsbedingungen nach Angaben des Geräteherstellers).

Zur Bestimmung von Y^{3+} oder La^{3+} wurden 5 ml Glycin-Pufferlösung pH 2,28 in einem 10 ml Messkolben vorgelegt, 1 ml Probelösung und 1 ml Reagenzlösung (1.10^{-3} M Lösung Arsenazo III in Wasser) zugefügt und mit Wasser aufgefüllt. Die Auswertung erfolgte mit Hilfe einer Eichkurve, die Resultate wurden durch Analysen von Standardzugaben überprüft.

Titrationskurven

Spheron-Salicyl (300 mg) wurde mit 10 ml frisch ausgekochtem dest. Wasser bzw. einer hiermit hergestellten 1 M NaCl-Lösung versetzt, und nach Zugabe von 0,05 bis 0,3 ml 1M NaOH wurde das Gemisch 60 min geschüttelt. Anschliessend wurde jeweils der pH-Wert gemessen, Abb. 1.

Sorptionsisothermen, Verteilungskoeffizienten, Einstellungsgeschwindigkeit der Gleichgewichte

Bei allen Versuchen war das Verhältnis von Spheron-Salicyl zur Lösung 1:100 (50 mg/5 ml). Nach Ende der festgesetzten Schütteldauer (60 min bei der Untersuchung von Isothermen und Verteilungskoeffizienten) wurden die restlichen Metallonzentrationen, bei der Ermittlung von Verteilungskoeffizienten zusätzlich auch der pH-Wert der Lösung bestimmt.

Die Sorptionsisothermen (Abb. 2) wurden für Fe^{3+} und Cu^{2+} in 0,1 M Azetatpuffer pH 5, für Fe^{3+} ausserdem in 0,1 M Essigsäure (pH 2,8) untersucht.

Die Zusammensetzung der Ausgangslösungen bei der Bestimmung von Verteilungskoeffizienten K_d ist aus Tab. 1. ersichtlich. Die Werte von K_d wurden laut Definition $[Me]_s(w/v)/[Me]_l$ (w/w) berechnet.

Die Sorptionsgeschwindigkeit wurde in 0,1 M Azetatpufferlösungen (pH 5 für Fe^{3+}, pH 4 für Cu^{2+}) sowie in einer 0,05 M HCl-Lösung (Fe^{3+}) untersucht: Nach Zugabe von 50 μg Metall zu einer Suspension von 50 mg Spheron-Salicyl in 5 ml Lösung wurde jeweils eine bestimmte Zeit lang geschüttelt. Unmittelbar anschliessend wurden mit einer Pipette etwa 2 ml Lösung durch ein aufgesetztes Mikrofilter zur Analyse entnommen.

Trennversuche

Die chromatographische Arbeitsweise wurde früher ausführlich beschrieben [1]. Die Sorption von Kationen (Cr^{3+}, Ni^{2+}, Fe^{3+}) erfolgte aus 0,1 M Azetatpuffer pH 5. Danach wurde die Kolonne mit 0,2 M Essigsäure so lange ausgewaschen, bis die durch Natrium hervorgerufene Gelbfärbung der Flamme nachliess. Dann wurden verdünnte HCl-Lösungen (siehe Abb. 6) zur Elution benutzt. Sowohl die Sorptions- als auch Elutionsgeschwindigkeit betrug 0,15 ml min^{-1} entsprechend 1,2 ml cm^{-2} min^{-1}.

ERGEBNISSE UND DISKUSSION

Die Auswahl der Auswertungskriterien—pH-Abhängigkeit der Verteilungskoeffizienten, Sorptionsvermögen und Einstellungsgeschwindigkeit der Sorptionsgleichgewichte—sowie die Methoden ihrer Ermittlung konnten von den Untersuchungen an Spheron-Oxin [1] übernommen werden. Auf Grund des identischen Gerüstes und der gleichen Seitenkette kann man bei Spheron-Salicyl die gleiche entscheidende Rolle der Zugänglichkeit der Funktionsgruppen beim Sorptionsprozess wie beim Oxinderivat erwarten, so dass sich entsprechende Versuche erübrigten.

Das Verhalten von Spheron-Salicyl ist im Vergleich zu Spheron-Oxin komplizierter, da man mit einer Dissoziation der Karboxylgruppe rechnen muss ($pK \simeq 2{,}97$ in wässriger Salicylsäurelösung [3]). In Abb. 1 werden die Titrationskurven von Spheron-Salicyl gezeigt. Die weiter unten beschriebene pH-Abhängigkeit der Verteilungskoeffizienten K_d lässt sich mit der beobachteten Dissoziation bei pH > 2,5 (Abb. 1, Kurve 2) gut in Zusam-

menhang bringen. Eine quantitative Auswertung beider Titrationen (Abb. 1) führte zu dem gleichen Ergebnis 0,56 mÄquiv g^{-1}. Ein Vergleich mit dem Resultat der Elementaranalyse (0,63 mÄquiv g^{-1}) deutet auf eine sehr gute Zugänglichkeit der funktionellen Gruppen in wässrigen Suspensionen des Ionenaustauschers. Spheron-Salicyl hat eine ähnliche hydrolytische Beständigkeit wie Spheron-Oxin; es ist in neutralen und mittelstark sauren Lösungen stabil.

Der Verlauf der Sorptionsisothermen (Abb. 2) zeigt, dass bei günstigem pH-Wert bereits kleine Metallmengen in der Lösung eine Sättigung des Austauschers bewirken. Im Anfangsbereich der Isothermen sind die Verteilungskoeffizienten von der Sättigung des Austauschers durch das gleiche Metall weitgehend unabhängig. Das gemessene Sorptionsvermögen für Schwermetallionen (0,38 mMol $Cu^{2+}g^{-1}$ in einer verhältnismässig konzentrierten Pufferlösung von pH 5, Abb. 2, Kurve 3) nähert sich der durch die Titration festgestellten Konzentration von Karboxylgruppen. Auf einen ähnlichen Wert deutet das Verhalten von Fe^{3+}in 0,1 M Essigsäure (Kurve 2). Die hohe Sorption von etwa 1,2 mMol Fe^{3+} g^{-1} in Azetatpuffer pH 5 (Kurve 1) könnte durch eventuelle Bindung mehrkerniger Azetatokomplexe, z.B. von $[Fe_3(OH)_2(CH_3COO)_6]^+$, deren Existenz bekannt ist, erklärt werden.

Mit Rücksicht auf einen möglichen nichtselektiven Ionenaustausch musste die genaue Ionenzusammensetzung der Lösungen bei der Bestimmung von Verteilungskoeffizienten kontrolliert werden. Für die meisten Schwermetalle sowie für Ca^{2+} und Mg^{2+} wurden Pufferlösungen benutzt, die nur Essigsäure

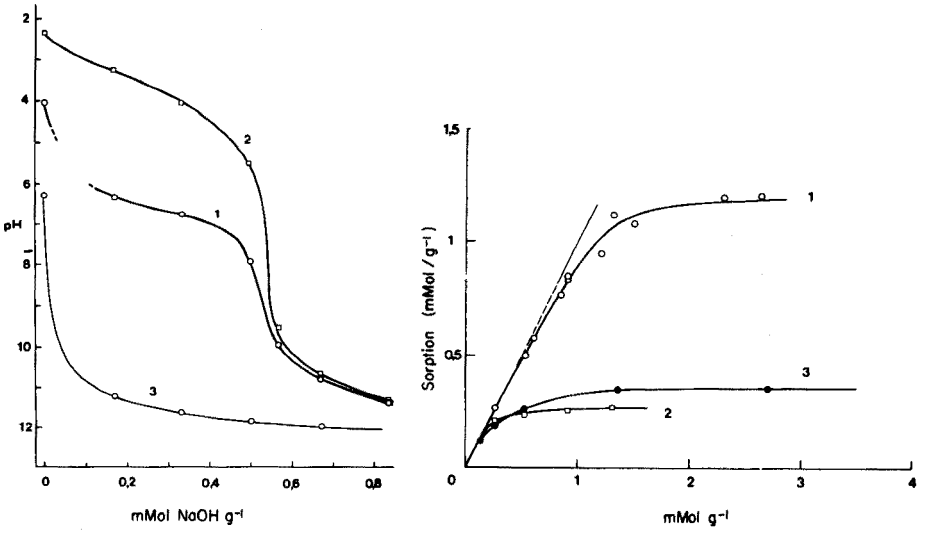

Abb. 1. Titrationskurven von Spheron-Salicyl. 300 mg Austauscher in 10 ml. (1) H_2O; (2) 1 M NaCl; (3) Blindversuch (H_2O).

Abb. 2. Sorptionsisothermen. 50 mg Austauscher in 5 ml. (1) Fe^{3+} bei pH 5. (2) Fe^{3+}in 0,1 M Essigsäure (pH 2,8). (3) Cu^{2+} bei pH 5.

und Natriumazetat bei konstanter Na^+-Ionen-Konzentration (0,02 M) enthielten. Die gleiche Natriumkonzentration wiesen Lösungen auf, in welchen die dreiwertigen Kationen (La^{3+}, Y^{3+}, Cr^{3+}) sorbiert wurden. Die in Abb. 3 dargestellten Abhängigkeiten zeigen die Abnahme der Sorption von Schwermetallen auf Grund einer nichtselektiven Konkurrenz-Austauschreaktion: Die Werte von log K_d sinken linear mit dem Logarithmus der wachsenden Na^+-Konzentration mit einem Proportionalitätsfaktor von 1. Bei unseren Versuchsbedingungen (Abb. 3) betrug die Austauschkapazität des in 1 l Gemisch befindlichen Spheron-Salicyls etwa 6 mMol (entsprechend log $c = -2{,}2$).

Die pH-Abhängigkeiten der log K_d-Werte bei einer definierten Lösungszusammensetzung (Tab. 1) drücken die Selektivität des Ionenaustauschers für die einzelnen Kationen aus (Abb. 4). Eine besonders hohe Selektivität wurde für Fe^{3+} und—weniger deutlich—für Al^{3+} beobachtet. Hier überwiegt offensichtlich die Chelatbildung bei der Sorption, was mit den höchsten bekannten Werten der Stabilitätskonstanten der Salicylsäure-Komplexe [3,4] von Fe^{3+} (log K_1 = 16) und Al^{3+} (log K_1 = 14) im Einklang ist. Eine hohe Stabilität weisen aber auch die Kupferkomplexe auf (log K_1 = 10,6). Die Salicylsäurekomplexe von Mn^{2+}, Co^{2+}, Zn^{2+} und Ni^{2+} sind in wässrigen Lösungen dagegen schwächer und etwa gleich stabil (K_1 etwa um 4—5 Grössenordnungen kleiner als bei Cu^{2+}). Trotzdem werden alle genannten zweiwertigen Metalle bei pH-Werten über 3 gemeinsam sorbiert, und gewisse Unterschiede kann man lediglich in den K_d-Werten feststellen (vgl. Abb. 4). Der Ionenaustausch wird in diesem Gebeit zum vorherrschenden Sorptionsmechanismus, was

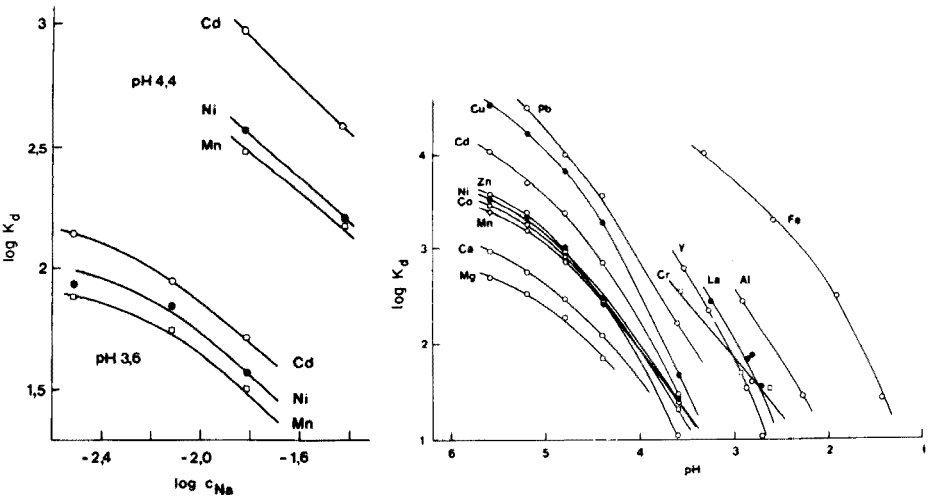

Abb. 3. Abhängigkeit der Verteilungskoeffizienten von der Na^+-Konzentration. Azetatpufferlösungen pH 3,6 und 4,4.

Abb. 4. pH-Abhängigkeit der Verteilungskoeffizienten. Ionenstärke (Na^+) 0,02, für Al^{3+} 0,05, für Fe^{3+} 0,1.

TABELLE 1

Bedingungen bei der Bestimmung von Verteilungskoeffizienten

Metall	Ausgangskonz. ($\cdot 10^{-3}$ M)	Puffer	$[Na^+]$(M)	Bemerkung
Fe^{3+}	0,18	Glycin/HCl/NaCl	0,1	
Al^{3+}	0,37	Glycin/HCl/NaCl	0,05	
Cr^{3+}	0,19	NaAc/HAc/NaCl	0,02	
La^{3+}	0,07	NaAc/HAc/NaCl	0,02	
Y^{3+}	0,11	NaAc/HAc/NaCl	0,02	
Co^{2+}	0,17	NaAc/HAc	0,02	Co^{2+}, Pb^{2+} gemeinsam
Pb^{2+}	0,05	NaAc/HAc	0,02	sorbiert
Cd^{2+}	0,09	NaAc/HAc	0,02	Cd^{2+}, Mn^{2+}, Ni^{2+}
Mn^{2+}	0,08	NaAc/HAc	0,02	gemeinsam sorbiert
Ni^{2+}	0,17	NaAc/HAc	0,02	
Cu^{2+}	0,06	NaAc/HAc	0,02	Cu^{2+}, Zn^{2+} gemeinsam
Zn^{2+}	0,06	NaAc/HAc	0,02	sorbiert
Ca^{2+}	0,21	NaAc/HAc	0,02	Ca^{2+}, Mg^{2+} gemeinsam
Mg^{2+}	0,41	NaAc/HAc	0,02	sorbiert

auch die bevorzugte Sorption der dreiwertigen Kationen Y^{3+}und La^{3+} erklärt, die in wässrigen Lösungen nur schwache Komplexe mit Salicylsäure bilden ($\log K_1$ (La) = 2,6).

Die hohen Werte der Verteilungskoeffizienten (in günstigen Fällen $> 10^4$) ermöglichen eine erfolgreiche Anwendung von Spheron-Salicyl sowohl zu analytischen als auch zu präparativen Zwecken, z.B. die Abtrennung von dreiwertigem Eisen aus praktisch beliebigen Lösungen.

Die Einstellungsgeschwindigkeit der Sorptionsgleichgewichte bei Spheron-Oxin hängt in einigen Fällen von der Natur des sorbierten Kations ab [5]. Spheron-Salicyl sorbiert sowohl Eisen (bei Spheron-Oxin der langsamste Vorgang) als auch Kupfer gleich schnell, unabhängig von der Lösungszusammensetzung. Die Einstellung des Sorptionsgleichgewichts an Spheron-Salicyl innerhalb von 2 min bei einem Verhältnis Sorbens: Lösung 1:100 in allen untersuchten Fällen (Abb. 5) lässt vermuten, dass die eigentliche Gleichgewichtseinstellung noch schneller ist und dass der Transport der sorbierbaren Kationen zu den Gelpartikeln (d.h. das Mischen) in diesem Fall zum geschwindigkeitbestimmenden Vorgang wird.

Trotz der im Vergleich zum Oxin-Derivat geringeren Selektivitätsunterschiede kann man auch Spheron-Salicyl mit Vorteil zu chromatographischen Trennungen verwenden. Als Beispiel sei hier die schnelle Trennung kleiner Metallmengen wie 50 μg Ni und 10 μg Cr sowie je 10 μg Ni, Cr und Fe angeführt (Abb. 6). Die Sorption erfolgte aus Lösungen mit einem relativ

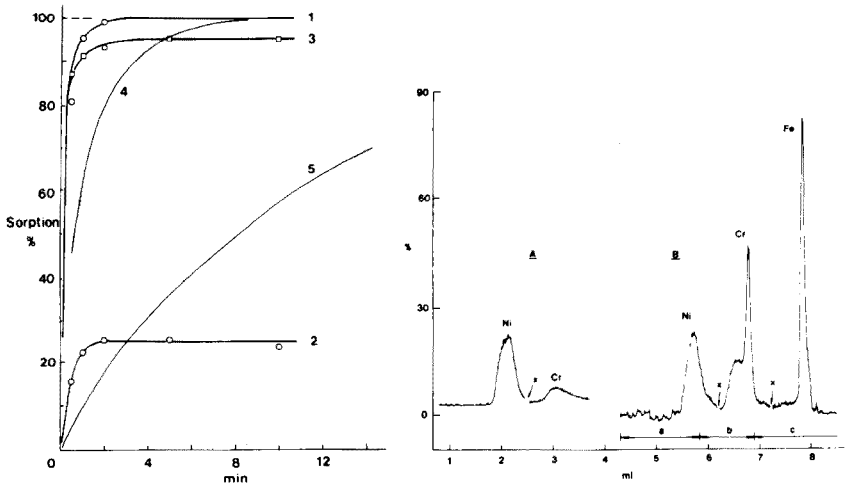

Abb. 5. Sorptionsgeschwindigkeit. (1) bis (3) Spheron-Salicyl; (4), (5) Spheron-Oxin. (1) und (4) Fe^{3+} bei pH 5; (2) und (5) Fe^{3+} in 0,01 M HCl; (3) Cu^{2+} bei pH 4.

Abb. 6. Detektion von chromatographischen Trennungen mittels A.A.S. (A) Trennung von 50 µg Ni und 10 µg Cr, Elution mit 0,01 M HCl. (B) Trennung von je 10 µg Ni, Cr, Fe; auf die Kolonne wurde gegeben: 0,01 M HCl (Abschnitt a), 0,05 M HCl (b), 1 M HCl (c). Im Teil (B) 3× Skalendehnung bei A.A.S. x Zeitpunkt des lampenwechsels und der Einstellung neuer Arbeitsbedingungen bei A.A.S.

hohen Natriumgehalt bei einem pH-Wert, bei dem auch Na^+ sorbiert wird. Vor der eigentlichen chromatographischen Elution musste das gebundene Natrium aus der Kolonne mit 0,2 M Essigsäure ausgewaschen werden. Ausser der Indikation mit Hilfe einer Flamme kann man das Ende des Auswaschens der Kolonne an einem plötzlichen Sinken des pH-Wertes unter 3 feststellen. Es zeigte sich,dass scharfe Elutionspeaks nur bei einer Frontalelution bei einer sprunghaften Erhöhung der Säurekonzentration erhalten werden (vgl. Abb. 6, Teil A und Teil B). Eine Gradientenelution könnte sich in einigen Fällen als vorteilhaft erweisen.

LITERATUR

1 Z. Slovák, S. Slováková und M. Smrž, Anal. Chim. Acta, 75 (1975) 127.
2 F. Vernon und H. Eccles, Anal. Chim. Acta, 72 (1974) 331.
3 L. G. Sillén und A. E. Martell, Stability Constants of Metal-ion Complexes, The Chemical Society, London, 1964.
4 L. Havelková und M. Bartušek, Collect. Czech. Chem. Commun., 34 (1969) 3772.
5 Z. Slovák und J. Toman, Z. Anal. Chem., 278 (1976) 115.

Analytica Chimica Acta, 87 (1976) 157—162

SYNTHESIS, ION-EXCHANGE PROPERTIES AND ANALYTICAL APPLICATIONS OF IRON(III) ANTIMONATE

J. P. RAWAT and D. K. SINGH

Department of Chemistry, Aligarh Muslim University, Aligarh, U.P. (India)

(Received 13th April 1976)

SUMMARY

Iron(III) antimonate is readily synthesized and shows excellent thermal and chemical stability. Distribution coefficients for 27 ions are presented. The separation possible include Mg—Sr, Al—Ga, Y—La, Mg—Cd—Zn, and Th—Sm.

Interest in inorganic ion-exchangers has increased greatly in recent years [1, 2]; they are often superior to ion-exchange resins in thermal stability and differential selectivity, and phosphates, arsenates, and antimonates are very stable chemically. Titanium-based exchangers [3] and the antimonates of tantalum, titanium and tin [4] have been discussed. There have been studies of iron-based exchangers [5—7], but iron antimonate has not been studied so far. This paper summarizes studies made on iron(III) antimonate, which can be synthesized under various conditions. The composition, chemical and thermal stability, reproducibility, K_d values, and break-through capacity have been determined and some important analytical separations have been achieved.

EXPERIMENTAL

Apparatus

Measurements were made with an Elico pH meter model L1-10, and a Bausch and Lomb Spectronic 20 spectrophotometer. An electric temperature-controlled SICO shaker was used.

Reagents

Iron(III) nitrate (B.D.H., India) and antimony pentachloride (B.D.H., England) were used. The latter was diluted with 4 M HCl to obtain the desired concentration. All other reagents were of AnalaR grade.

Iron(III) antimonate was prepared by mixing 0.1 M solutions of iron(III) nitrate and antimony pentachloride as outlined in Table 1. The pH was adjusted by adding ammonia solution dropwise. After 24 h the product was filtered, washed with demineralized water (pH 6) and dried at 40 °C. The

TABLE 1

Synthesis and properties of iron(III) antimonate
(The Fe(III):Sb(V) volume ratio was 2:1, except for sample 2 where the ratio was 3:1)

Sample	pH for prepn.	Properties		
		Colour	Ion-exchange capacity (meq g^{-1})	Composition Fe:Sb
1	0	Brown	0.82	1:2.41
1(a)[a]	0	Brown	0.82	1:2.40
2	0	Brown	0.81	1:2.15
3	1	Dark brown	0.43	1:1.52
4	2	Dark brown	0.22	2.04:1
5	3	Dark brown	0.20	—
6	6	Dark brown	0.19	—
7	9	Dark brown	0.11	—

[a]Sample dried at 100 °C.

product broke into small particles when immersed in water, and was converted to the H^+ form by treatment with 2 M nitric acid for 24 h with occasional shaking and renewal of the acid. The samples were dried at 40 °C.

Procedures

Ion-exchange capacity. A column containing 1 g of the exchanger in the H^+ form on a glass wool plug was prepared in a burette, and 400 ml of 1 M electrolyte was passed through the column. The effluent was collected and titrated with standard sodium hydroxide solution.

Composition. The well-powdered material (500 mg) was dissolved in 20 ml of hot 12 M hydrochloric acid. Antimony was precipitated as sulphide and determined [8] titrimetrically with potassium iodide; the iron was determined with potassium dichromate [8].

Chemical stability. The exchanger (0.5 g) was shaken with 50 ml of the solution concerned at 30 ± 2 °C for 6 h. Iron and antimony were determined spectrophotometrically with 1,10-phenanthroline and rhodamine B respectively [9].

Reproducibility of synthesis. The synthesis of sample 1(a) was repeated five times; the products were analyzed for iron and antimony, and the ion-exchange capacity with 1 M $NaNO_3$ was also determined. The molar ratio of Fe:Sb ranged from 1:2.41 to 1:2.47 and the exchange capacity from 0.81—0.83 meq g^{-1}.

Ion-exchange potentiometric titrations. Potentiometric titrations of sample 1(a) were performed with 0.1 M solutions of lithium hydroxide, sodium hydroxide, and potassium hydroxide in the presence of their respective salts [10].

Break-through capacity. The break-through capacity [11] of iron(III) antimonate (H^+-form) was determined for four divalent cations. The break-through capacity for Cd^{2+} was determined at three different temperatures by preparing the column inside a condenser and circulating water of the desired temperature. The break-through capacity was also determined for different column lengths and flow rates.

Distribution studies. The distribution coefficients were determined [12] by a batch process after equilibrium had been attained by shaking the metal ion solution with the exchanger (H^+) for 6 h at 30 ± 2 °C. The cation in solution was determined by EDTA titration and values of K_d were calculated from $K_d = 50\ (I - F)/0.5F$, where I is the volume of EDTA required by the original solution and F is the volume required after equilibrium. The total volume of the solution was 50 ml; the amount of the exchanger used was 0.5 g.

Separations. For separation studies an iron(III) antimonate (H^+-form) column, 2.5 cm long and 3.9 mm diam. was used. The flow rate in all the separations was about 0.18 ml min^{-1}.

RESULTS AND DISCUSSION

The ion-exchange capacities and the compositions of the samples of iron(III) antimonate are presented in Table 1. Samples 1, 1(a) and 2 show the maximum capacity and are closely similar in composition. In the synthesis of iron(III) antimonate, increased pH results in decreased ion-exchange capacity; the products prepared at pH values greater than one contain less antimony. The effect of the drying temperature on the ion-exchange capacity was studied; the results, shown in Fig. 1, indicate that this ion-exchanger can be used up to 200 °C without loss in ion-exchange capacity; above 200 °C there is a decrease in ion-exchange capacity but the decrease is much less than in the other antimonates (Fig. 1). The results of chemical

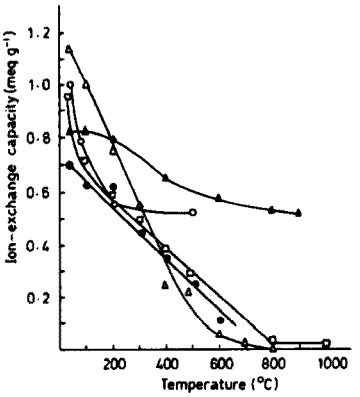

Fig. 1. Ion-exchange capacity of various antimonates as a function of drying temperature. • Ti—Sb; ○ Sn—Sb; □ Ta—Sb; △ Al—Sb; ▲ Fe—Sb.

stability measurements (Table 2) indicate that the product formed at lower pH is more stable than that formed at higher pH. Sample 1(a) was studied subsequently in detail because of its superior chemical and thermal stability.

Analysis (Table 1) gave the molar ratio of 1:2.4 for Fe:Sb in sample 1(a), and the data for all the samples show that the ion-exchange capacity decreases as the Fe:Sb ratio increases. These trends are similar to those for aluminium antimonate [13].

The results of pH titrations with different alkalies in the presence of their respective salts indicate that iron(III) antimonate in the H^+ form behaves as a weak monoprotic acid (Fig. 2). The total ion-exchange capacity is 1.5 meq g^{-1}, calculated at the neutralization point. This gives the maximum number of replaceable counter-ions and is independent of the nature of the cation.

For column operation, the break-through capacity of iron(III) antimonate for four metal ions is given in Fig. 3. The capacity increases with temperature and column length. The column behaviour of iron(III) antimonate is similar to that shown by other inorganic ion-exchangers. The break-through capacity is related to K_d values (Table 3) and plots of break-through capacity against log K_d are linear for different electrolytes.

The ion-exchange column capacity, measured in terms of the hydrogen ion liberation capacity, shows the customary increase with increase in atomic radii; the values obtained ranged from 0.80 meq g^{-1} for lithium to 1.33 meq g^{-1} for barium.

To study the analytical potentialities the distribution coefficients of 27 metal ions in five systems were determined; the results are shown in Table 3. Separations were tried for the pairs of cations for which the separation factor, K_d (A)/K_d (B) > 8. Those successful experimentally are reported in Table 4.

TABLE 2

Chemical stability of iron(III) antimonate

Sample	Solubility mg/50 ml									
	H_2O		1 M HNO_3	6 M HNO_3	2 M HCl		2 M H_2SO_4		0.1 M NaOH	
	Fe	Sb	Fe[a]	Fe[a]	Fe	Sb	Fe	Sb	Fe	Sb
1	0.00	5.25	0.04	0.14	0.18	9.74	1.12	18.26	0.00	26.34
1(a)	0.00	4.60	0.00	0.13	0.11	9.17	0.83	16.62	0.00	26.28
2	0.00	5.25	0.05	0.19	0.19	10.06	1.25	18.65	0.00	26.42
3	0.04	6.85	0.10	0.25	0.35	12.09	4.46	20.07	0.06	28.56
4	—	—	0.25	—	3.07	15.22	6.07	15.33	0.11	20.20
1[b](200°C)	—	—	0.00	0.06	0.06	73.05	0.06	36.52	—	—
1[b](400°C)	—	—	0.00	0.05	0.03	97.40	0.03	36.65	—	—
1[b](600°C)	—	—	0.00	0.01	0.01	100.56	0.00	40.17	—	—

[a]No antimony was found.
[b]Sample 1 dried at the temperature indicated.

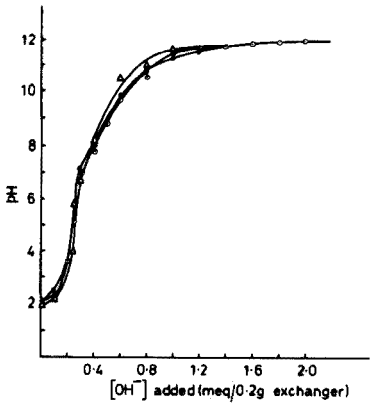

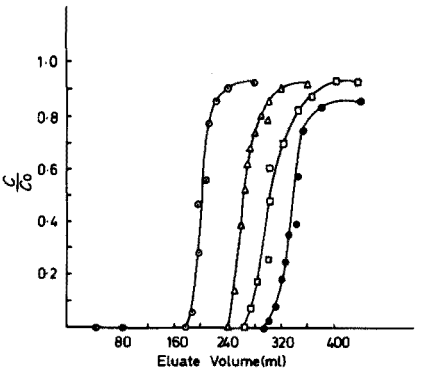

Fig. 2. pH titration curves for iron(III) antimonate (H^+) with added salt. • 0.1 M LiOH + 0.1 M LiCl; ○ 0.1 M NaOH + 0.1 M NaCl; △ 0.1 M KOH + 0.1 M KCl.

Fig. 3. Break-through curves for different cation solutions (0.02 M each). Column diameter 9 mm, length 11.3 cm; flow rate, 1 ml min^{-1}; particle diameter, 0.14—0.29 mm. ⊙Mg^{2+}; △ Ca^{2+}; □ Ba^{2+}; • Cd^{2+}.

TABLE 3

K_d values for iron(III) antimonate

Cations	K_d values, ml g^{-1}				
	0.1 M NH_4NO_3 + 0.1 M HNO_3	0.5 M HNO_3	0.1 M NH_4NO_3	0.5 M NH_4NO_3	1 M NH_4NO_3
Zn^{2+}	74.0	65.7	1126.6	335.0	248.0
Cd^{2+}	165.7	1760.0	990.0	3620.0	2385.0
Mg^{2+}	10.6	18.0	44.8	14.2	1.1
Mn^{2+}	35.5	40.0	281.8	133.3	40.0
Pb^{2+}	604.0	403.0	4300.0	402.8	340.0
Ba^{2+}	297.8	496.0	472.5	297.8	198.8
Sr^{2+}	104.8	116.8	324.0	116.8	96.2
Ca^{2+}	34.4	29.2	400.0	52.8	40.0
Dy^{3+}	T.A.[a]	148.0	T.A.	224.0	124.0
Y^{3+}	T.A.	266.0	T.A.	97.8	86.6
La^{3+}	T.A.	T.A.	T.A.	T.A.	2800.0
Pr^{3+}	T.A.	1010.0	T.A.	T.A.	2120.0
Tm^{3+}	810.0	355.0	T.A.	506.6	65.4
Sm^{3+}	T.A.	680.0	T.A.	1070.0	870.0
Tb^{3+}	T.A.	416.0	T.A.	416.0	115.0
Ho^{3+}	T.A.	138.0	1090.0	116.4	211.0
Gd^{3+}	T.A.	260.3	T.A.	1473.3	1073.0
Nd^{3+}	T.A.	680.0	T.A.	2240.0	2040.0
Ga^{3+}	147.6	463.0	T.A.	785.7	287.5
Zr^{4+}	T.A.	T.A.	T.A.	T.A.	T.A.
Cu^{2+}	T.A.	232.7	T.A.	2340.0	1210.0

TABLE 3 (continued)

Cations	K_d values, ml g^{-1}				
	0.1 M NH_4NO_3 + 0.1 M HNO_3	0.5 M HNO_3	0.1 M NH_4NO_3	0.5 M NH_4NO_3	1 M NH_4
In^{3+}	T.A.	106.6	T.A.	2380.0	520.0
Al^{3+}	T.A.	60.0	240.0	38.7	0.0
Ni^{2+}	480.0	64.5	624.0	228.2	90.0
Hg^{2+}	T.A.	170.6	T.A.	712.0	238.3
V^{5+}	10.0	174.0	—	—	95.7
Th^{4+}	22.6	84.8	—	—	84.0

[a]T. A. = Total adsorption.

TABLE 4
Separations achieved

Sample	Mixture	Eluant	Eluate (ml)	Amount loaded (μg)	Amount recovered (μg)
1	Mg^{2+}	0.5 M NH_4NO_3	70	170.13	165.45
	Sr^{2+}	0.5 M NH_4NO_3—0.1 M HNO_3	80	718.48	728.99
2	Al^{3+}	1 M NH_4NO_3	80	146.78	145.70
	Ga^{3+}	1 M HNO_3	70	418.32	401.59
3	Y^{3+}	0.5 M NH_4NO_3—0.1 M HNO_3	90	320.07	309.30
	La^{3+}	1 M NH_4NO_3—0.5 M HNO_3	80	644.56	644.56
4	Mg^{2+}	0.5 M NH_4NO_3	40	84.58	84.58
	Zn^{2+}	0.5 M HNO_3	40	113.76	117.84
	Cd^{2+}	1 M NH_4NO_3—0.5 M HNO_3	50	409.13	404.64
5	Th^{4+}	0.5 M NH_4NO_3—0.1 M HNO_3	80	426.95	422.31
	Sm^{3+}	1 M NH_4NO_3—0.5 M HNO_3	90	351.93	354.64

The authors are grateful to Prof. W. Rahman for providing research facilities. One of us (D. K. Singh) thanks C.S.I.R., India, for financial assistance.

REFERENCES

1 V. Vesely and V. Pekarek, Talanta, 19 (1972) 219.
2 H. F. Walton, Anal. Chem., 46 (1974) 398R.
3 M. Qureshi, N. Zehra, S. A. Nabi and V. Kumar, Talanta, 20 (1973) 609.
4 M. Qureshi, J. P. Gupta and V. Sharma, Anal. Chem., 45 (1973) 1901.
5 J. P. Rawat and P. S. Thind, Can. J. Chem., 54 (1976) 1892.
6 V. Kourim, J. Rais and B. Million, J. Inorg. Nucl. Chem., 26 (1964) 1111.
7 V. G. Kuznetsov, Z. V. Popova and G. B. Seifer, Zh. Neorg. Khim., 15 (1970) 2710.
8 N. H. Furman, Standard Methods of Chemical Analysis, 6th edn., Vol. 1, Van Nostrand, New York, 1962.
9 E. B. Sandell, Colorimetric Determination of Traces of Metals, Interscience, New York, 1959.
10 N. E. Topp and K. W. Pepper, J. Chem. Soc., (1949) 3299.
11 J. Inczedy, Analytical Applications of Ion Exchangers, Pergamon Press, 1966, p. 126.
12 J. P. Rawat and S. Q. Mujtaba, Can. J. Chem., 53 (1975) 2586.
13 J. P. Rawat and J. P. Singh, Chromatographia, (Communicated).

Analytica Chimica Acta, 87 (1976) 163—175

A CHEMILUMINESCENCE PHOTOMETER FOR TRACE CHROMIUM(III) DETERMINATIONS

S. D. HOYT* and J. D. INGLE, Jr.

Department of Chemistry, Oregon State University, Corvalis, OR 97331 (U.S.A.)

(Received 8th May 1976)

SUMMARY

The design of a simple chemiluminescence photometer is described. The sample is injected into a spectrophotometric cell containing the reagents, and the resultant chemiluminescence peak is recorded along with the peak height and peak area. The instrument includes a temperature-controlled cell holder with stirring capabilities. The determination of p.p.b. levels of chromium(III) is described. Chromium(III) enhances the chemiluminescence reaction of luminol and hydrogen peroxide in basic solutions. Useful calibration curves are obtained from $4 \cdot 10^{-9}$ to 10^{-4} M Cr(III); $5 \cdot 10^{-10}$ M is the detection limit. Chromium(III) is determined in natural water samples and NBS Orchard Leaves.

Chemiluminescence analysis is attractive for trace metal determinations and recent reviews [1—3] attest to its growing popularity. The instrumentation is simple, detection limits are low, the dynamic range for analysis is often large, and the technique is selective for certain metal oxidation states. Some metal ions enhance particular chemiluminescent reactions and the chemiluminescence produced can often be related to the concentration of the metal ion. The most important limitation is that several metal ions may enhance the same reaction so that separation or masking is required for real samples. Analytical procedures based on activation of the luminol—H_2O_2 reaction have been developed for Cu [4], Mn [5], Co [6], V [7], Fe [8], Cr [9], Ce [10], Hg [11], and Th [12]. Masking with EDTA is useful [9] in the determination of chromium(III), because the Cr(III)—EDTA complex is formed slowly at ambient temperatures, and chromium can be determined by rapid measurements. This procedure has been used in the determination of chromium(III) in water and biological samples at p.p.b. levels [9, 13]. Few other analytical techniques possess the necessary detection limit for these trace levels.

The designs of different chemiluminescence instruments vary primarily in the technique for mixing the sample and reagents. The three types of sample modules which have been developed are a discrete sampling system [14, 15], a flow system [9], and a centrifugal analyzer [16]. With the dis-

*Present Address, Victor Valley College, Victorville, CA 92392

crete sampling system all reagents except the analyte are placed in a reaction cell in front of a photomultiplier tube (PMT). A lid is placed over the reaction cell, the analyte solution is injected into the reaction cell with a syringe, and the resulting photon peak is continuously monitored. This approach is used in commercial bioluminescence instruments and could be carried out with stopped-flow mixing.

In the flow cell system [9], the reactants (e.g. luminol, H_2O_2) and the samples are pumped by a motor-driven syringe system. The sample is injected into the blank stream. After the reactants enter the cell, they are mixed by a nitrogen flow. The light emission is measured by a PMT attached to a chart recorder. The output of the PMT represents the integrated light intensity between the time the reactants enter the cell and when they leave the cell.

The centrifugal fast analyzer [16] is basically a rotor with 15 cuvettes on the outside and two sample chambers connected to each cuvette. The chromium(III) samples or standards and the peroxide are placed in one chamber and the luminol—EDTA solution in the other. Rotation mixes the reactants, and the signal from each cuvette is observed as it passes the PMT; a PDP 8/I controls the data collection. A comparison of the three methods is shown in Table 1.

This paper is concerned with the design of a versatile discrete-sampling chemiluminescence photometer. The instrument is applied to the p.p.b. and sub-p.p.b. determination of chromium(III) with luminol and hydrogen peroxide in basic solutions. The reaction and instrumental conditions for analysis and for reduction of interferences have been optimized. The potential of the

TABLE 1

Comparison of chemiluminescence sampling methods

Discrete sampling system	Flow system	Centrifugal analyzer
Versatile readout system	Peak area measurement	Versatile readout system
Small sample	Larger sample	Small sample
External magnetic stirring	Internal stirring by gas bubbles	External stirring by rotor
Thermostated cell holder	More difficult to use thermostated holder	Difficult to use thermostated cell holder
Complicated electronics (if peak detector or integrator is used)	Simple electronics	Computer electronics
No multi-sample capability	Simple to make repetitive measurements on one sample	Multi-sample analysis capability
Simple instrumentation that can be portable	Complex flow cell and syringe system (not easily portable)	Complex instrument (not easily portable)
Low cost	Moderate cost	High cost
Sample cell easily modified for samples requiring O_2	Can be used with O_2	Difficult to use for samples requiring O_2

technique for determining chromium(III) is demonstrated by a calibration curve from 10^{-9}—10^{-4} M and a detection limit of $5 \cdot 10^{-10}$ M.

INSTRUMENTATION AND METHODS

The chemiluminescence photometer is based on the discrete sampling system, which was chosen because a simple, rugged instrument for field work was required. The main advantages of the discrete sampling system over the flow system are that: (a) it requires a smaller sample volume; (b) a more versatile electronics system which measures the instantaneous signal, the peak height, and the peak area can be used; and (c) changing the sample loop after measurements of real samples [9, 13] is avoided.

Some of the advantages of the proposed system over previous discrete sampling units include temperature control for the sample cell, a large light-tight compartment to allow room for modifications to the cell holder, high light-collection efficiency, compatibility with a monochromator, a magnetic stirrer, a cooled PMT housing to reduce dark current noise, and a versatile electronics system. The three essential parts of the instrument are the sample compartment, the cooled PMT housing, and the electronics readout system.

Sample compartment

The box-form housing was constructed from milled aluminum plates (Fig. 1) held together with 6-32 machine screws. The inside edges of the box were sealed with a black rubber compound to prevent light leaks. The sample compartment was divided into an upper (main) compartment and a lower (motor) compartment. The photomultiplier opening was designed to be compatible with a Heath model EU-700 monochromator so that chemiluminescence spectra could be obtained. Water and gas (if needed) enter the motor compartment through four bulkhead swagelock fittings (h) attached to the back plate and flow through 0.25-in. copper tubing to a second set of four bulkhead fittings when entering the main sample compartment. Access to the sample compartment is through adjustment ports (f) which have screw plate covers with felt gaskets. The lid (i) has a swagelock fitting (e) with a septum for injection of the sample.

The sample cell holder, machined from brass, was thermostated by water circulating through holes (l) drilled in the block. Copper tubing was sealed into the holes with epoxy resin and connected to the bulkhead swagelock connectors by Tygon tubing. Thermostated water was circulated by a Haake model FJ temperature bath and pump. This cell holder is unusual because the cell is surrounded on three sides by the cell holder since there is no need for an excitation window. The 1-cm square glass sample cell is held in position (g) of the holder by movable block (k) which keeps the cell in thermal contact with the holder.

The holder is attached to a movable carriage (o) which provides a 0.75-in. adjustment in height and can accommodate different holders and cells. Four

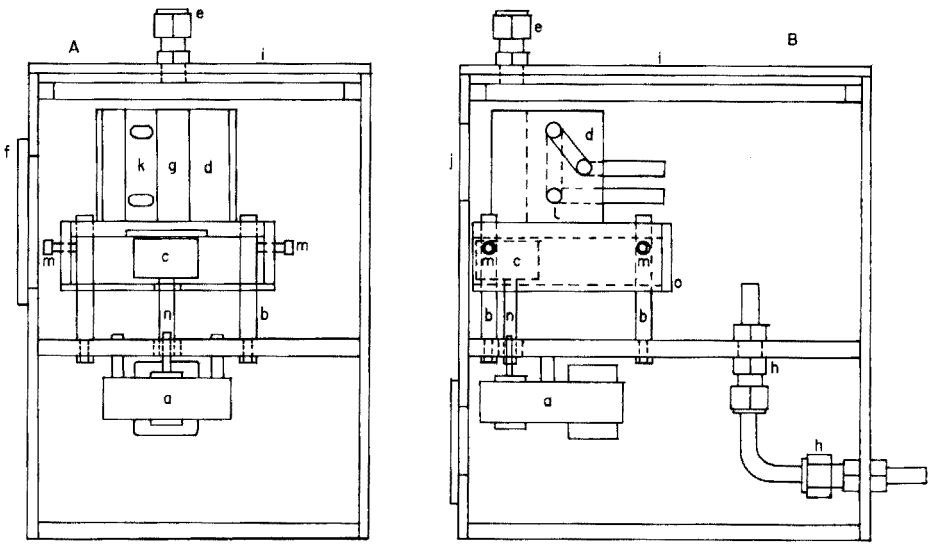

Fig. 1. Diagram of Sample Module. A. Front View. B. Side View. (a) Stirring motor. (b) Carriage supports (steel). (c) Stirring magnet (Alnico). (d) Sample cell holder (brass). (e) Swagelock injection port (brass). (f) Access port and cover (aluminum). (g) Sample cell (glass). (h) Bulkhead swagelocks (brass). (i) Sample module lid (aluminum). (j) PMT window. (k) Movable cell block (brass). (l) Water circulator holes. (m) Adjustment screws 8-32 (steel). (n) Stirring motor shaft (steel). (o) Movable carriage (aluminum).

set screws (m) hold the carriage in position. To reach the screw, adjustment plate (f) must be removed. The cell holder is held to the carriage by two brass screws on the top of the holder which allows it to be removed for cleaning.

Stirring magnet (c) is connected to a motor with a hollow brass shaft, held in position with a set screw so that it can be adjusted with the height of the carriage. The speed is controlled by an external Variac. For stirring a special teflon-coated stirring bar designed for the 1-cm square cell (Bel-Art F-37150) was driven by a small induction motor. The front panel is connected to the PMT housing.

Cooled photomultiplier housing

The design and construction of the cooled photomultiplier housing used with this chemiluminescence apparatus was discussed recently [17]. The housing consists of a light-tight compartment in which nitrogen gas cooled by liquid nitrogen is circulated to cool the PMT, a PMT socket and appropriate dynode resistors and electrical connectors, and a shutter mechanism. The PMT photocathode is 1.5-in. from the front face of the sample cell, for high light collection efficiency.

Electronics

The photocurrent from the PMT (RCA Model C-31025C, with Keithley Model 244 power supply) was amplified and converted to a voltage by the current amplifier. The signal from the amplifier was monitored and modified by different types of circuitry and readout devices as shown in Fig. 2, in order to ascertain the optimal arrangement. A Tektronix Model 564B storage scope, a Heath Model SR-255B chart recorder, and a Fluke Model 8000A digital voltmeter were used. The integrator was constructed from an operational amplifier (Function Modules 380J) wired in the standard configuration with a 100 K input resistor and 5 μF feedback capacitor [18]. Shorting of the feedback capacitor and connection of the input to the current amplifier was accomplished with mercury-wetted relays controlled by switches on the front panel of the integrator.

Comparison of the instantaneous chemiluminescence signal recorded on a storage scope to that recorded on the chart recorder indicate that the chart recorder response was slow enough to attenuate the signal by up to 25 % and that the attenuation depended on the signal level. Because of this, some other way of measuring the peak height was required.

A peak detector based on a design by Piepmeier [19] was constructed to provide a means of accurately measuring the peak height without the use of a storage scope. The circuit diagram was identical to that presented earlier [19] except that the output of the current amplifier was connected directly to point B, R_3 = 100 K, R_5 = 0, R_6 = 10 K, C_3 = 1 μF, D_1 and D_2 were IN457 diodes, and the OA's were Analog Devices A504J. Actual chromium chemiluminescence peaks were simultaneously recorded on the storage scope and peak detector to test the peak detector performance.

Solutions

All solutions were made with double-distilled water from a Corning Water still (model AG-3), attached to the house-distilled water. All chemicals were

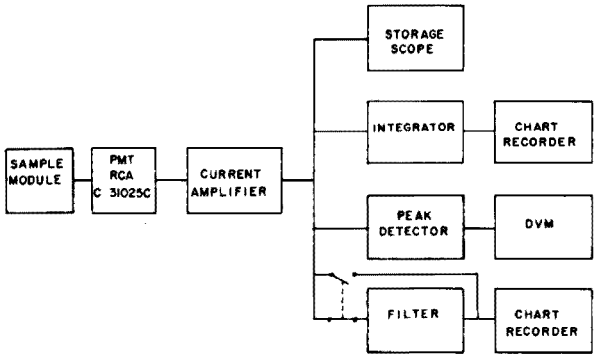

Fig. 2. Block diagram of photometer

analytical-reagent grade or better as specified. The final pH of all solutions was adjusted by adding either 0.5 M NaOH or 1 M HCl with a buret while monitoring with a micro-pH electrode and the Chemtrix digital pH meter (model 60).

Luminol stock solution, 10^{-3} M. Luminol (0.1772 g; 5-amino-2, 3-dihydro-1,4-phthalazinedione, Eastman) was dissolved in water and 1 ml of 0.5 M NaOH in a 1-l volumetric flask. No recrystallization was required. For the $8 \cdot 10^{-5}$ M luminol working solution 16 ml of the 0.001 M solution was diluted to 1 l in a volumetric flask with 100 ml of 10^{-2} M EDTA, 500 ml of 0.10 M $NaHCO_3$ buffer, and about 5 ml of 0.5 M NaOH to adjust the pH to 11.0.

Hydrogen peroxide $1.2 \cdot 10^{-1}$ M. 30 % Hydrogen peroxide (16 ml) and 100 ml of 10^{-2} M EDTA were diluted to 1 l after adjusting the pH to 4.0 with about 1 ml of 1 M NaOH.

Chromium(III) stock solution (10^{-3} M). Chromium nitrate (0.4001 g; Baker and Adamson reagent grade) was dissolved in 1 l of water. Standard Cr(III) solutions were made by appropriate dilutions. The pH was adjusted to 4.0 with about 1 ml of 1 M HCl to minimize hydrolysis.

The stabilities of 0.25 N hydrogen peroxide and $8 \cdot 10^{-5}$ M luminol solutions were studied for 5 days. There was no noticeable decrease in the peroxide concentration. The luminol solution provided an initial increase in chemiluminescence signal on the first day and then remained stable.

Injection procedures

With the shutter closed and the lid off the sample module, luminol solution was put into the reaction cell with a 1-ml Eppendorf pipet followed by the hydrogen peroxide from a 0.5-ml Eppendorf pipet. The lid was replaced, the shutter opened, and the integrator or peak detector set to the run position. Chromium(III) solution (0.5 ml) was injected rapidly in a reproducible manner with a 0.5-ml Hamilton gas-tight syringe (a platinum needle should be used at low concentrations to prevent contamination). The signals were recorded and then the shutter was closed. The lid of the sample compartment was removed and the solution removed by suction with a disposable pipet connected to a vacuum aspirator bottle. The cell was rinsed twice with 3 ml of double distilled water in a polyethylene wash bottle, before another sample was injected. Figure 3 shows the difference between the background, blank, and analyte signals at lower concentrations. The chromium and blank peaks appear on top of the background reaction. At concentrations below 10^{-7} M, the blank signal must be subtracted from the total signal to obtain the signal from chromium(III) in the sample.

OPTIMIZATION

To take full advantage of the procedure, the reagent concentrations, reaction conditions, and instrumental variables must be optimized, to give the maximum signal to background ratio (S/B or S/N). Three measure-

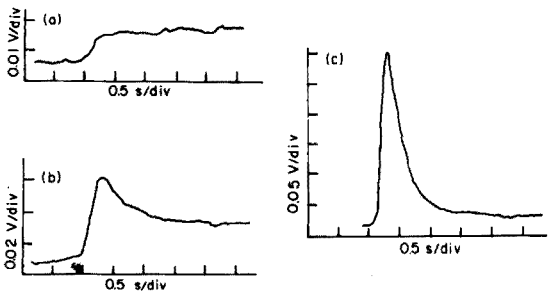

Fig. 3. Scope tracings. (a) Background (H_2O_2 + luminol); gain 10^9. (b) Blank (H_2O_2 + luminol + distilled water); gain 10^9. (c) Analyte (H_2O_2 + luminol + 10^{-6} M Cr); gain 10^6.

ments were made for each condition or concentration and the mean value was calculated. The effect of reagent concentration on the background signal was also studied; 5 measurements were taken if the standard deviation was high. The final optimum conditions (Table 2) agree reasonably well with previous data [9] except that a higher pH was optimal.

Luminol and hydrogen peroxide concentrations

The luminol optimization curves for the peak height, peak area, and peak background reaction signal versus luminol concentration are shown in Fig. 4. The concentration axis is labeled in final cell luminol concentration which is 2/5th of the initial concentration. The data on the luminol-background reaction signal appears to follow the luminol—Cr curve closely, and hence there is no optimum luminol concentration for maximum S/B.

The optimum final cell concentration for both peak height and peak area measurements is $8 \cdot 10^{-5}$ M luminol. For the peak area measurements, lower luminol concentrations are not advantageous because the analysis time is increased. Figure 4 clearly illustrates that optimum conditions depend upon the mode of readout. The peak signal decreases at lower luminol concentra-

TABLE 2

Optimum conditions

Reagent	Peak height	Peak area
Luminol[a]	$8 \cdot 10^{-5}$ M	$8 \cdot 10^{-5}$ M
Hydrogen peroxide[a]	10^{-1} M	10^{-2} M
Luminol pH	12.0	11.0
Cell temperature	as high as possible	24 °C
$NaHCO_3$ buffer	0.05 M	0.05 M
EDTA	10^{-3} M	10^{-3} M
Cr(III)	10^{-6}—10^{-5} M	10^{-7}—10^{-5} M

[a]Final cell concentration.

tions because the reaction is slower, which yields a broader peak, so that peak height is not proportional to peak area.

The bending off of both curves above 10^{-4} M appears to coincide with the Cr(III)—luminol complex formation postulated by Seitz et al. [9]. However, since the background reaction without chromium exhibits the same behavior, this justification is suspect.

The hydrogen peroxide optimization curves for chromium and the background are shown in Fig. 5. The concentrations reported are final cell concentrations which are 1/5th the initial concentration. The optimum value for peak area is 10^{-2} M and for peak height is 10^{-1} M. A concentration of $3 \cdot 10^{-2}$ M was chosen as a compromise optimum value for peak height and peak area measurements because at higher concentrations, the background signal increases significantly.

pH optimization curves for the chromium reaction exhibited a broad maximum as reported previously [9]. The background reaction peak remained constant above pH 10.5. The optimum pH value for peak height is 12.0 and for peak area is 11.0. For subsequent measurements, a pH of 11.0 was used unless only peak height measurements were made, in which case the pH was changed to 11.2. The above pH values are the pH of the luminol buffer solution and not the final pH of the reaction mixture.

Cell temperature

The temperature dependence of the signal was studied by varying the cell temperature. For low temperatures, a coil of copper tubing inserted in an

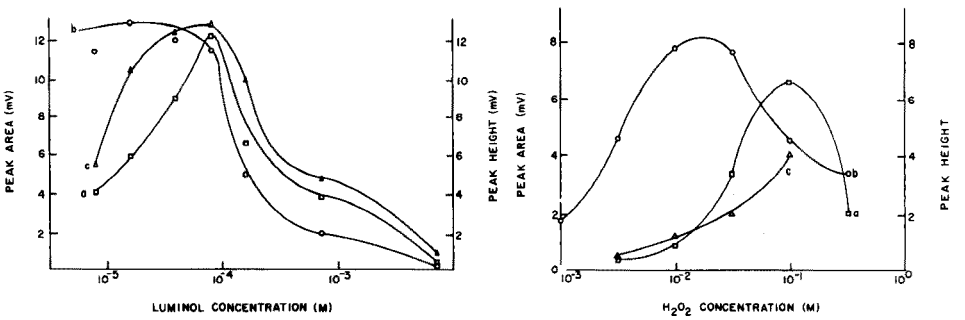

Fig. 4. Luminol concentration optimization. (a) Cr peak height. (b) Cr peak area. (c) Background peak height. Conditions: 1 ml of luminol (variable concn.) with 10^{-2} M EDTA, 0.05 M $NaHCO_3$ buffer, and pH 11.0; 0.5 ml of $2 \cdot 10^{-3}$ M H_2O_2 (final cell concn.) with 10^{-2} M EDTA, and pH 4.0; 1 ml of $5 \cdot 10^{-7}$ M Cr(III) (final cell concn.), pH 3.5; gain 10^6 V/A. Background studies done with 0.5 ml H_2O_2 injected into 1 ml of luminol; gain 10^8 V/A.

Fig. 5. Hydrogen peroxide optimization (a) Cr peak height. (b) Cr peak area. (c) Background peak height. The conditions were the same as for Fig. 4, except that 1 ml of $8 \cdot 10^{-5}$ M luminol (final cell concn.) was used, and the H_2O_2 concentration was varied.

ice bath was connected between the cell holder and temperature bath. The temperature in the cell was measured by placing a thermometer in the cell, which was filled with water, and allowing it to equilibrate. The Cr(III) solutions were pre-cooled in a water bath for the low temperature measurements, and the luminol and hydrogen peroxide solutions were allowed to equilibrate in the cell before the measurement.

Figure 6 shows the results for the peak height and peak area optimization. The optimum temperature for peak area measurements is about room temperature (24 °C) while for the peak height measurements the signal continually increases with temperature over the measurement region. For convenience a temperature of 25 °C was selected. The improvement of the signal with higher temperatures is probably caused by the increased rate of the chemiluminescence reaction. The leveling off with the peak area measurements is probably caused by a decrease in the quantum efficiency.

Buffer solutions

Three buffers commonly used for the pH range 10—11 were tested. The 0.05 M buffers chosen were sodium hydrogencarbonate ($pK_2 = 10.33$), boric acid ($pK = 9.23$), and sodium dihydrogenphosphate ($pK_2 = 7.21$, $pK_3 = 12.32$). Seitz et al. [9] chose boric acid even though it is not an optimum buffer for the pH 11.0 region. The buffers were compared at the pH values of 10.0 and 11.0. A pH 11.0 $NaHCO_3$ buffer was finally chosen because it provided a larger peak area signal than the other buffers. The final pH after mixing with the other reagents is 10.3 because of the acidic behavior of hydrogen peroxide.

EDTA

Seitz et al. [9] proposed 10^{-2} M EDTA for masking potential interfering ions. Although the Cr—EDTA complex forms very slowly, analyses must be run before any significant complex formation. The time dependence of the signal on EDTA concentration for 10^{-5} M Cr is shown in Fig. 7. The value at zero time is that obtained if no EDTA is added. For 10^{-3} M and 10^{-4} M EDTA, there is an initial increase in signal when EDTA is added, and then the curve levels off. For 10^{-2} M EDTA, the peak area and peak height signals decrease rapidly with time so that the time of analysis after addition of EDTA is critical. Clearly 10^{-2} M EDTA is not suitable and 10^{-3} M EDTA was chosen.

Blank

EDTA was added to different distilled water samples to determine what was causing the blank signal. House-distilled water gave a blank signal over twice as large as that from the double-distilled water. After an initial measurement of untreated distilled water, EDTA was added to mask metal ions. The blank peak produced by the double-distilled water is soon eliminated by the EDTA addition which suggests that the blank signal is due to trace contaminants in the distilled water. The improvement in the house-distilled water is not as good.

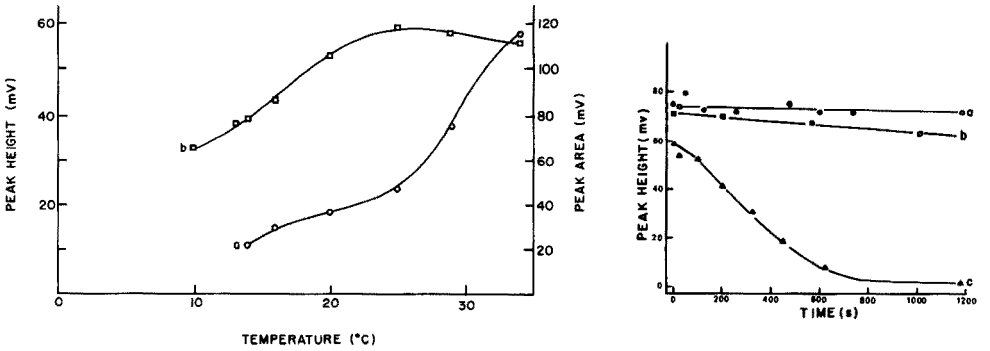

Fig. 6. Cell temperature optimization. (a) Peak height. (b) Peak area. Conditions: $5 \cdot 10^{-7}$ M Cr(III) with optimal reagent concentrations.

Fig. 7. EDTA reaction with 10^{-5} M Cr(III). △ 10^{-2} M EDTA. □ 10^{-3} M EDTA. ○ 10^{-4} M EDTA. Conditions: $5 \cdot 10^{-7}$ M Cr(III) with optimal reagent concentrations.

RESULTS AND DISCUSSION

Chromium(III) calibration curve

Solutions with Cr(III) concentrations from 10^{-4} M to 10^{-10} M were analyzed to determine the dynamic range of analysis. Measurements were made for peak height and peak area without EDTA, and for peak height with solutions containing EDTA. The results shown in Fig. 8 illustrate the remarkable dynamic range of the technique.

To test the reproducibility of the calibration curve the same points were run one day later; the points were then 24 % lower, but the shapes of the curve were identical. The plot with EDTA added (see Fig. 8A) falls 4.2 % lower than that for solutions run without EDTA; the lower signal is caused by some Cr(III)—EDTA complex formation.

The log—log plot for the peak height measurements is linear from 10^{-5} to 10^{-8} M with a slope of 1.33. The average relative standard deviation for peak height measurements without EDTA is 4.4 %, and with EDTA it is 3.1 %. The fact that the chemiluminescence signal is proportional to $[Cr(III)]^{1.33}$ is difficult to explain; Seitz [20] has indicated that such behavior has been observed. The non-linearity at higher concentrations is due to the precipitation of $Cr(OH)_3$ which could be seen when a $3 \cdot 10^{-3}$ M Cr(III) solution was injected.

The peak area data for Cr(III) without EDTA addition are shown in Fig. 8B. The curve has about the same shape as the peak height curve, but deviates at the low end, because of the difficulty of measuring the peak area on top of a large background signal at low concentrations. For the peak area log—log calibration curve, the linear region is 10^{-7}—10^{-5} M, the slope is 1.17, and the average relative standard deviation is 6.0 % for all points but 2.8 % for points above $3 \cdot 10^{-7}$ M.

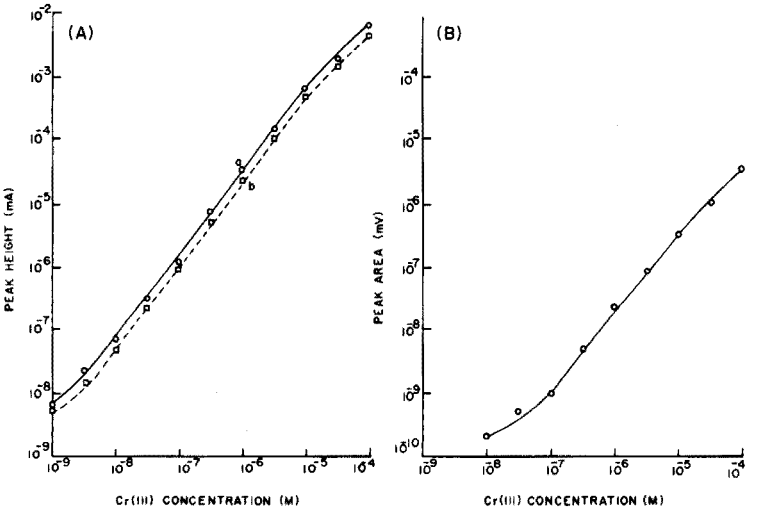

Fig. 8(A). Peak height calibration curve. (a) Without EDTA. (b) With EDTA, 10^{-3} M. (B) Peak area calibration curve.

The peak area was normally taken as the integrator output after it had reached a constant value. For the lowest Cr(III) concentrations, the integrator output did not reach a constant value because of the background reaction, so that the integrator output after 1 min of reaction was used. The peak area measurements provided no better precision, and peak height measurements were preferred, since they are faster and can be used at lower Cr(III) concentrations.

The theoretical detection limit, defined as the concentration producing a signal twice the standard deviation of a blank measurement, is $4 \cdot 10^{-10}$ M, or about 0.05 p.p.b. In practice, concentrations lower than 10^{-9} M could not be measured because of non-linearities at lower concentrations, which result in a practical detection limit [21] of about 10^{-9} M.

Interferences

EDTA was added to the Cr(III) solutions just before analysis to prevent metal ion interferences. To test the effectiveness of the EDTA, 10^{-6} M solutions of common metal ions which catalyze the luminol—peroxide reaction were tested with a $3 \cdot 10^{-7}$ M Cr(III) solution.

Of the solutions tested, Fe(III), Fe(II), and Co(II) interfered even with the addition of EDTA, whereas the Cu(II) interference was eliminated. The results agree with the data of Seitz et al. [9], and with information on the destruction of EDTA with H_2O_2 [22]. Other ions which interfere at high levels are SO_4^{2-}, NH_4^+, SO_3^{2-}, and NO_2^-, all of which decrease the signal. Sulfite and nitrite destroy the hydrogen peroxide. Any other chemicals which decompose hydrogen peroxide also interfere.

Since Fe and Co still interfere, the chromium in real samples was determined by the difference between the signal after addition of EDTA and the signal after heating the sample—EDTA solution for 4 min near boiling [9] to force the EDTA—Cr complexation to completion. The EDTA was added to the sample by injecting 100 μl of 0.1 M EDTA into 10 ml of sample.

Digestion and pH adjustment

The chemiluminescence technique measures only free chromium(III) so that any complexes must be destroyed by dry ashing or wet digestion. After acid digestion of samples, the pH was adjusted to between 2.0 and 4.0 with sodium hydroxide. Ammonia solution was first used because it has lower levels of trace metal contamination than any other strong base, but ammonia totally inhibited the chemiluminescence reaction.

Analysis of natural water samples

To measure the uncomplexed chromium(III) in natural water samples, organic material in the sample need not be destroyed. Four Willamette River water samples were gathered at various locations. The pH of the river water was about 7 so it was adjusted to pH 3.5 with HCl. The Cr(III) concentrations in the four samples averaged 1.2 p.p.b.

A tap water sample was analyzed similarly; the signal was below the lowest standard (1 p.p.b.) and the concentration was estimated to be 0.6 p.p.b.

Determination of biological samples

For determination of p.p.b. concentrations of chromium(III) in biological samples, an acid digestion was used. A 5:2 nitric—perchloric acid mixture from EM Suprapur acids was used. The sample and nitric acid were refluxed in test tubes on a Technicon block digester for about 1.5 h. The perchloric acid was added and heated to fumes at 230 °C. The samples were then removed, cooled, and adjusted to pH about 3.0 as described earlier.

To test the digestion procedure and the technique, NBS standard reference Orchard Leaves were analyzed. The Cr(III) concentration was found to be 2.2 p.p.m. which compares favorably with the accepted value of 2.3 p.p.m. The relative standard deviation for ten samples was 20 %. The large relative standard deviation probably resulted from the digestion procedure. Seitz et al. [9] postulated that the holes in the block digester must be within 2 °C in order to get a low standard deviation; on the Technicon block digester the variation is much larger.

Acknowledgement is made to the NSF (Grant No. MPS7520055) for partial support of this research.

REFERENCES

1 W. R. Seitz and M. P. Neary, Anal. Chem., 46 (1974) 188A.
2 U. Isaacson and G. Wettermark, Anal. Chim. Acta, 68 (1974) 339.
3 W. R. Seitz and D. M. Hercules, in Chemiluminescence and Bioluminescence, M. J. Cormier, D. M. Hercules, and J. Lee, (Eds.), Plenum Press, New York, 1973, pp. 427—449.
4 A. K. Babko and N. M. Lukovskaya, Zh. Anal. Khim., 17 (1962) 50.
5 I. E. Kalinishenko, Ukr. Khim. Zh., 35 (1964) 755.
6 A. K. Babko, N. M. Lukovskaya, Zavod. Lab., 29 (1963) 404.
7 A. K. Babko and N. M. Lukovskaya, J. Anal. Chem. USSR, 20 (1965) 1153.
8 W. R. Seitz and D. M. Hercules, Anal. Chem., 44 (1972) 2143.
9 W. R. Seitz, W. W. Suydam, and D. M. Hercules, Anal. Chem., 44 (1972) 957.
10 J. Bognar and L. Sipos, Mikrochim. Ichnonal. Acta, 56 (1963) 1066.
11 L. I. Dubovenko and T. A. Bogoslovskayu, Ukr. Khim. Zh., 37 (1971) 1057.
12 L. I. Dubovenko and Chan Ti Huu, Ukr. Khim. Zh., 35 (1969) 957.
13 R. T. Li and D. M. Hercules, Anal. Chem., 46 (1974) 916.
14 H. A. Neufeld, C. J. Conklin and R. D. Towner, Anal. Biochem., 12 (1965) 303.
15 A. K. Babko, L. V. Markova, and N. M. Lukovskaya, Zh. Anal. Chim., 23 (1968) 401.
16 J. L. Bowling, J. A. Dean, G. Goldstein, and J. M. Dale, Anal. Chim. Acta, 76 (1975) 47.
17 S. D. Hoyt and J. D. Ingle, Jr., Anal. Chem., 48 (1976) 232.
18 H. V. Malmstadt, C. E. Enke and S. R. Crouch, Control of Electrical Quantities in Instrumentation, W. A. Benjamin, Menlo Park, 1975, pp. 57—58.
19 E. H. Piepmeier, Appl. Spectrosc., 26 (1972) 100.
20 W. R. Seitz, personal communication, 1976.
21 J. D. Ingle, Jr. and R. L. Wilson, submitted to Anal. Chem.
22 D. D. Perrin, Masking and Demasking of Chemical Reactions, Wiley-Interscience, New York, 1970, p. 56.

Analytica Chimica Acta, 87 (1976) 177—184

COMPLEXES OF MORIN AND QUERCETIN WITH BORIC ACID AND OXALIC ACID IN ACETIC ACID MEDIUM. FLUORIMETRIC DETERMINATION OF BORON

L. PSZONICKI and W. TKACZ

Institute of Nuclear Research, 03-195 Warsaw 91 (Poland)

(Received 12th March 1976)

SUMMARY

The binary and ternary fluorescent complexes of morin or quercetin with boric acid and oxalic acid in an anhydrous acetic acid medium are described. The physico-chemical and spectral properties and chemical composition of these complexes have been established. The ternary complexes are suitable for fluorimetric determinations of boron. The limits of detection are 0.1 ng B ml^{-1} and 0.3 ng B ml^{-1}, for the morin and quercetin complexes, respectively, and calibration graphs are linear up to 10 μg B ml^{-1}.

Murata and Yamauchi [1] described a fluorimetric determination of boron based on the Taubock test; the fluorescence intensity was measured for an acetone solution of the boron—morin complexes formed by evaporation of the test solution containing morin and an excess of oxalic acid and heating the residue at 100 °C. The formation and properties of this type of complex have been studied in detail and structural formulae have been suggested [2, 3]. However, their preparation is inconvenient analytically and strict standardization of the procedure is necessary for reproducible results.

Hörhammer and Hänsel [4] described the formation of solid flavone—boric acid fluorescent complexes in glacial acetic acid in the presence of oxalic acid. The possibility of using this method of complex formation for analytical purposes seemed worth investigating. In this paper, the formation of two types of flavone—boric acid complex (a binary flavone—boric acid complex and a ternary flavone—boric acid—oxalic acid complex) directly in anhydrous acetic acid is discussed. The composition and chemical structure of these complexes as well as their analytical properties have been investigated.

EXPERIMENTAL

Apparatus

A home-made spectrofluorimeter [5] and a Unicam SP-700 spectrophotometer were used for scanning the uncorrected fluorescence spectra and absorption spectra. A Spekker H-760 photometer with a special fluorimetric photomultiplier attachment [5] was used to measure the fluorescence intensity. The primary filter was a Kodak filter No. 1 (Hg-line 436 nm) and the secondary filter a Kodak No. 4. Fluorescence intensities were measured against a fluorescent standard. A Hilger and Watts Uvispec spectrophotometer was used to measure absorption at fixed wavelengths. Silica cells (1.00 cm) were used. A Techniprot type WT microbalance was used. Silica apparatus was used where possible.

Reagents

For the boric acid stock solution (0.1 mg B ml^{-1}), 57.2 mg of analytical-grade boric acid was dissolved in anhydrous acetic acid and the solution diluted to 100 ml.

Analytical-grade oxalic acid was recrystallized twice from small volumes of quartz-redistilled water, dried at 105 °C, and powdered. For the morin (T. Schuchardt) and quercetin (Koch-Light) stock solutions (1 mg ml^{-1}), 100 mg of reagent, dried at 105 °C, was dissolved in anhydrous acetic acid and the solution diluted to 100 ml.

The fluorescence standard was a $1 \cdot 10^{-6}$ M solution of 3-aminophthalimide in 0.05 M sulphuric acid.

Glacial acetic acid (analytical grade, POCh) was distilled and the 117—119 °C fraction was collected. To prepare anhydrous acetic acid, 2 kg of the glacial acetic acid and 20 ml of acetic anhydride were boiled under reflux for at least 15 h; the acetic acid was then distilled and the 117—118 °C fraction was collected (yield 90 %). The acid was stored in a silica bottle fitted with a calcium chloride guard tube.

Preparation of complexes

Ternary complexes in anhydrous acetic acid solution were prepared as follows: 1 ml of boric acid solution in anhydrous acetic acid (0.005—0.2 μg B) was placed in a 25-ml volumetric flask, 1 ml of flavone stock solution was added and the solution was diluted to about 3 ml. Then 10 mg of oxalic acid was added and the solution was left in a stoppered flask for 20 min to develop a yellowish-green colour. The flask was filled to the mark with anhydrous acetic acid and the solution was ready for measurement. A blank was prepared similarly.

The binary complex in anhydrous acetic acid was prepared in the same way, but oxalic acid was not added.

To prepare the solid complexes, 1.5 g of flavone was dissolved in 70 ml of boiling anhydrous acetic acid, cooled and filtered. The filtrate was heated

to boiling under reflux. Then a hot solution (about 100 °C) of 1.5 g of boric acid in 30 ml of anhydrous acetic acid (or for preparation of the ternary complex, 1.5 g of boric acid and 1.5 g of oxalic acid in 30 ml of anhydrous acetic acid) was added, and the solution was kept boiling under reflux for 30 min. Next day, the solution was filtered, and the precipitate was washed five times with 15 ml of boiling anhydrous acetic acid and then with boiling chloroform to remove the acetic acid. The precipitate was dried for 4 h at 60 °C.

RESULTS

Effect of solvent

The possibility of direct formation of the fluorescent complexes was investigated for solutions in formic acid, glacial and anhydrous acetic acid, propionic acid, normal and anhydrous dioxane, anhydrous diethyl ether, acetone and ethanol. Only dioxane and simple aliphatic acids gave positive results, and acetic acid was chosen as the most convenient. In dioxane only the ternary complex is formed when the solution is boiled; evaporation of about half the solution gives more efficient complex formation and better reproducibility. In glacial acetic acid two complexes are formed: the binary boric acid—morin complex and the ternary boric acid—morin—oxalic acid complex. More efficient complex formation is possible by heating the mixture; the fluorescence intensity of the ternary complex is then much higher but reproducibility is poor.

The best conditions for direct complex formation in solution are found with anhydrous acetic acid. Both types of complex are formed at room temperature. The fluorescence intensity increases quickly, reproducibility is good, and the order of addition of reactants is unimportant. Anhydrous acetic acid was therefore chosen as the optimal medium and used in all further investigations.

Optimal conditions for complex formation

Pure solid complexes were prepared in order to investigate their properties and chemical composition. The preparation was based on the Hörhammer—Hänsel procedure [5] with some modifications. In anhydrous acetic acid at high temperatures, oxalic acid decomposes quickly, but if the solution contains at least an equivalent amount of boric acid, there is no decomposition; the optimal procedure is given above.

When the complexes are formed in anhydrous acetic acid solution, the binary and ternary complexes are formed directly after mixing of the reactants. The fluorescence intensity increases quickly, attains its maximum after some minutes and is then stable for about 60 min. With boron concentration on the p.p.m.-level, the speed of reaction is proportional to the concentration of the reactants. With a large excess of flavone (for the binary complex) or flavone and oxalic acid (for the ternary complex), the reaction is quantitative for boron.

The optimal excess of flavone depends on the volume of the solution. Under the conditions described in Experimental, the dependence of the fluorescence intensity on the excess of morin is shown in Fig. 1; the plot for quercetin is similar.

The optimal excess of oxalic acid is difficult to determine because of its decomposition in anhydrous acetic acid. Under the given conditions, the optimal amount is about 10 mg, which must be added directly as the solid to avoid decomposition.

Properties of the complexes

The binary morin complex is very finely crystalline, brown in colour and stable on storage. The ternary morin complex is a very fine powder, dark yellow in colour and stable on storage. The binary quercetin complex is dark yellow and finely crystalline. On storage, the colour changes through yellow-green to green-grey, and the odour of acetic acid appears. The ternary quercetin complex is finely crystalline (rhomboid), brown-red in colour and stable on storage.

All the solid complexes are readily soluble in acetone, alcohols and dioxane, less soluble in acetic acid, diethyl ether and water, and insoluble in benzene, chloroform and carbon tetrachloride. The dissolved complexes decompose slowly. Initially, the solution shows intense fluorescence and the characteristic maximum, but these disappear eventually and the maximum of the free flavone appears.

The ternary complexes in acetic acid decompose to the binary complexes. The presence of about 1 % of oxalic acid in the solution prevents degradation of the ternary complexes and improves their solubility considerably. Degraded ternary complexes can be reformed by addition of an excess of oxalic acid.

None of the complexes has a stable melting point; they decompose on heating with evolution of acetic acid.

Spectral characteristics

Figure 2 shows the absorption spectra of the binary (curve 2) and ternary (curve 3) morin complexes, and that of free morin (curve 4). Both the binary and ternary complex spectra are obtained from solutions containing equimolar amounts of boric acid and morin. Under such conditions, the complexes are in equilibrium with the free reactants, and the spectra show the maximum of free morin also. Curve 1 presents the uncorrected fluorescence spectrum of the ternary complex excited with the Hg 436-nm line, which does not excite fluorescence in free flavones. The fluorescence spectrum of the binary complex coincides exactly with that of the ternary complex but the intensity is about ten times lower. The spectra for the quercetin complexes are similar but the bonds in the regions around 450 nm and 270 nm are less intense. The spectral maxima for both types of complex are listed in Table 1. The fluorescence maximum for all the complexes occurs at 505 nm.

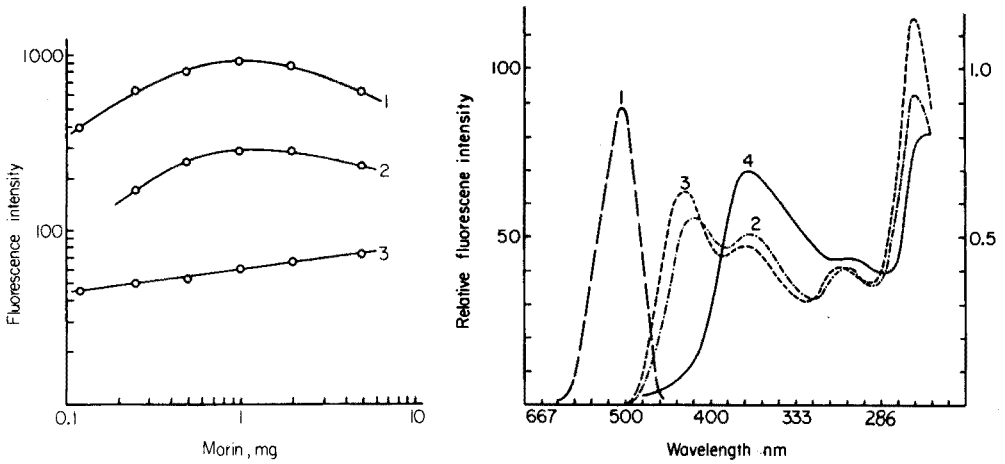

Fig. 1. Effect of the amount of morin on the complex fluorescence for various quantities of boron. (1) 0.5 μg; (2) 0.2 μg; (3) blank.

Fig. 2. Absorption and fluorescence spectra of the morin complexes. 1. Fluorescence spectrum of ternary complex. 2. Absorption spectrum of binary complex. 3. Absorption spectrum of ternary complex. 4. Absorption spectrum of morin. Boron, 5.4 μg; morin, 150 μg; oxalic acid, 10 mg.

TABLE 1

Spectral maxima of complexes

Species	λ_{max} (nm)	Species	λ_{max} (nm)
Morin	361	Quercetin	373
Morin binary complex	411	Quercetin binary complex	427
Morin ternary complex	425	Quercetin ternary complex	443

In the presence of excess of flavone, boron is fixed quantitatively in the complex and the fluorescence intensity is proportional to boron concentration up to 10 ng ml^{-1}. The limit of fluorimetric detection is 0.1 ng ml^{-1} for the morin ternary complex, and 0.3 ng ml^{-1} for the quercetin complex. The reproducibility of the fluorescence intensity is good; the relative standard deviation for eleven identical solutions containing 10 ng B ml^{-1} was 8 %.

Chemical composition of the complexes

The chemical composition of the solid complexes was investigated by elemental analysis, and the most probable formulae were calculated (Table 2). The molar ratios of boric acid and flavone were determined by spectrophotometric and spectrofluorimetric titrations. The results of the titration for the morin ternary complex (Fig. 3a) indicate that the molar ratio of boric acid to morin is 1 : 1. Further addition of the titrant enhances the

TABLE 2

Results of elemental analysis

Complex	Found		Calculated		Suggested mole ratio[a]	Molecular formula
	% C	% H	% C	% H		
Binary morin	49.9	3.4	50.2	3.7	1:1.1	$C_{17}H_{15}O_{11}B$
Ternary morin	48.5	3.4	49.5	3.1	1:1:1.1	$C_{19}H_{14}O_{13}B$
Binary quercetin	46.5	4.1	44.8	3.8	1:2.2	$C_{19}H_{19}O_{15}B_2$
Ternary quercetin	48.2	3.0	49.5	3.1	1:1:1.1	$C_{19}H_{14}O_{13}B$

[a]Flavone:boric acid:oxalic acid. acetic acid.

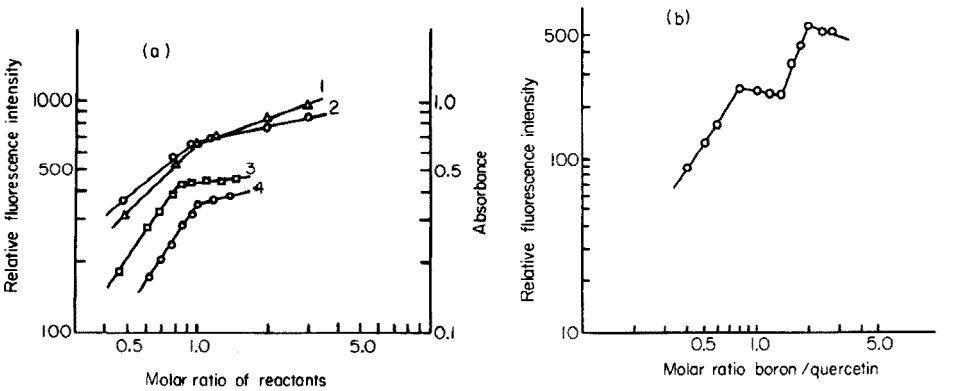

Fig. 3. (a) Composition of ternary morin complex by the molar ratio method. 1. Spectrophotometric titration of 15 μg of morin by boron. 2. Spectrophotometric titration of 0.54 μg of boron by morin. 3. Fluorimetric titration of 30 μg of morin by boron. 4. Fluorimetric titration of 0.54 μg of boron by morin. Absorbance measured at 425 nm; path length, 10 mm. (b) Composition of binary quercetin complex by the molar ratio method. Titration of 60 μg of quercetin by boron.

fluorescence, which indicates that at the equivalence point the complex is in equilibrium with the free reactants. Analogous titration results were obtained for the morin binary complex and the quercetin ternary complex. Only the curve for the quercetin binary complex (Fig. 3b) is anomalous, indicating that the molar ratio of boric acid to quercetin is 2:1 when excess of boric acid is present. All these results agree well with the elemental analyses in Table 2. The solid complexes, precipitated from anhydrous acetic acid also contain acetic acid in the molar ratio 1:1 to all the complex molecules except the binary quercetin complex for which the ratio is 2:1.

DISCUSSION

All the data presented show clearly that two types of flavone–boric acid complex may be formed directly in anhydrous acetic acid media. Even small amounts of water affect this reaction and reduce its efficiency. The free

reactants are more soluble in acetic acid than the complexes are, so that the complexes are easily precipitated. The results obtained for the chemical composition and the spectral characteristics indicate that the complexes formed are of the same type as the ternary complexes formed in the dry residue on heating at 100 °C, which have been used for fluorimetric boron determinations [6].

The fact that the solid ternary complexes decompose during dissolution in anhydrous acetic acid but reform on addition of excess of oxalic acid indicates that the oxalic acid is linked to the strongly positive boron atom rather than to the nucleophilic oxygen atoms of the flavone as suggested by Hörhammer and Hänsel [4].

On the basis of these results the following structural formulae are proposed:

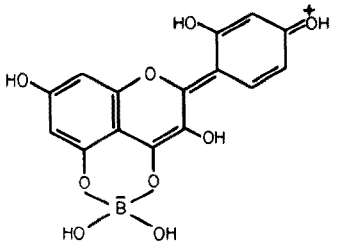

Binary complex of morin

I

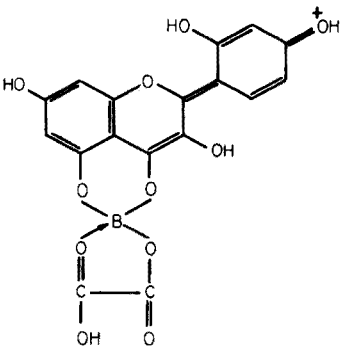

Ternary complex of morin

II

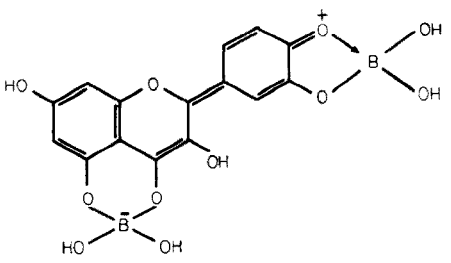

Binary complex of quercetin

III

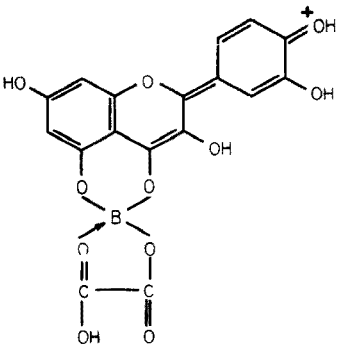

Ternary complex of quercetin

IV

Depending on the properties of the solution, boric acid may exist in the ortho or meta form, or there may be an equilibrium mixture. There are no

data on the form of boric acid in anhydrous acetic acid, and the elemental analyses are not precise enough to allow a definitive statement that only the ortho form is present. Both forms may be present in the binary complexes. For the ternary complexes this difference has no significance because in both cases the final formula must be the same.

From the point of view of fluorimetric analysis for boron, the ternary complexes are particularly interesting. In the presence of the flavone and oxalic acid, boron reacts quantitatively and the solution has a very intense fluorescence.

REFERENCES

1 A. Murata and F. Yamauchi, J. Chem. Soc. Jpn., Pure Chem. Sect., 79 (1958) 231.
2 L. Pszonicki and W. Tkacz, Chem. Anal. (Warsaw), 15 (1970) 809, 1097.
3 W. Tkacz and L. Pszonicki, Chem. Anal. (Warsaw), 16 (1971) 535.
4 L. Hörhammer and R. Hänsel, Arch. Pharm., 288 (1955) 315.
5 L. Pszonicki, Chem. Anal. (Warsaw), 12 (1967) 431, 375.
6 J. Dabrowski and L. Pszonicki, Chem. Anal. (Warsaw), 16 (1971) 51.

Analytica Chimica Acta, 87 (1976) 185—191

THE EFFECT OF MIXED AQUEOUS SOLVENT SYSTEMS ON THE FLUORESCENCE OF INDOLES AND AROMATIC AMINO ACIDS AND THEIR METABOLITES

P. M. FROEHLICH* and M. YEATS

Trace Analysis Research Centre, Department of Chemistry, Dalhousie University, Halifax, Nova Scotia B3H 4J3 (Canada)

(Received 22nd April 1976)

SUMMARY

The fluorescence of a number of indoles, tyrosine, tryptophan and some of their metabolites is greater in ethanol—water and DMSO—water systems than in pure water. This enhancement suggests that analytical procedures which include detection via fluorescence should be performed in mixed aqueous solvent systems where possible. The addition of non-aqueous solvents is believed to diminish the formation of exciplexes between the excited state of the fluorophore and water, and hence increases the fluorescence quantum yield. The magnitude of the increment depends on the nature of the groups attached to the aromatic ring as well as on the aliphatic side-chain in the case of the amino acid metabolites. The enhancement is especially large in metabolites with several OH groups, e.g. L-Dopa, and is believed to be due to the competition of the various polar groups on the fluorophore for the water molecules in the micro-environment.

The fate of the excited singlet states of aromatic amino acids and their metabolites is dependent on environmental effects such as the composition of the solvent and temperature [1—4]. As an example, the fluorescence quantum yield of tryptophan in aqueous solution decreases with increase in temperature [4] and is considerably higher in ethylene glycol than in water [5]. McGuire and Feldman [5] have shown that the excited singlet states of tryptophan and tyrosine interact with water to form excited state complexes (exciplexes); such a process competes with the radiative process and leads to a diminution of the fluorescence intensity.

Fluorescence of the aromatic amino acids and their metabolites is of especial interest because many of the analytical procedures for these compounds depend on the measurement of their native luminescence. Similarly, the determination of many compounds is effected via the preparation of a fluorescent derivative. Since the formation of such exciplexes results in a decrease in the fluorescence intensity, the choice of some other solvent is desirable. While this is feasible in many situations, it is difficult for aqueous samples (e.g. of serum, protein hydrolysates, and urine).

*Present address for correspondence: Department of Chemistry, North Texas State University, Denton, Texas 76203, U.S.A.

This paper reports a study of the effect of mixed aqueous solvents (ethanol—water and dimethylsulfoxide—water) on the fluorescence of tyrosine and tryptophan and some of their metabolites. The results indicate that fluorescence intensities are sensitive to the composition of the solvent: the addition of ethanol or DMSO to water leads to higher fluorescence intensities. The luminescence of fluorescent derivatives, e.g. fluorescamine derivatives of amino acids and peptides, is likewise dependent on the composition of the solvent; the addition of DMSO to water enhances the fluorescence.

EXPERIMENTAL

Apparatus

Fluorimetric measurements were obtained with an Aminco-Bowman spectrophotofluorimeter equipped with a Hanovia 901C Xe lamp and a Hammamatsu 1P21 photomultiplier. The cell housing was maintained at 25 ± 0.2 °C by a constant temperature bath (Haake Instrument Co., Saddle Brook, N.J.).

Ultra-violet spectra were obtained with a Bausch and Lomb Model 505 spectrophotometer and absorption data were obtained with a Unicam model SP500 spectrophotometer.

Reagent and Chemicals

Dimethylsulfoxide (ACS grade), and acetone (ACS grade) were obtained from Fisher Scientific Co., Fairlawn, N.J. Ethanol was purified by the Mg/I_2 process [6]. U.v. spectra were taken of each sample of solvent to ensure the absence of impurities absorbing at longer wavelengths than the fluorophores; such impurities might lead to energy transfer or other interference phenomena. Attempts were not made to dry the solvents rigorously as the small quantities of water contained therein (DMSO contains 0.06 % H_2O) would not effect the results. All water was doubly distilled from a glass still and used on the day of distillation.

Amino aids, metabolites, and enzymes were obtained from Sigma Chemical Co. Fluorescamine (Roche Diagnostics, Nutley, N.J.) was used as received.

Method of data collection

A stock solution of the fluorophore of interest was prepared; this was diluted with water and solvent to produce solutions containing the same quantity of the fluorophore in solutions of varying solvent composition. The concentration of the fluorophore in each run was below the self-quenching region (in most runs, the fluorophore concentrations were ca. $1 \cdot 10^{-5}$ M). The absorbance of each solution was recorded to ensure that it remained constant as the solvent composition was changed. Samples were stored in the dark and used within two hours of preparation.

The relative fluorescence intensity data was obtained for each solution by

comparing the maximum peak height of the fluorescence spectrum with the corresponding peak height of the fluorophore in water. Although small changes in λ_{max} of ca. 3—5 nm were observed as the solutions became less aqueous, the fluorescence intensities were compared at λ_{max} for each solution. The small error (ca. 1—2 %) introduced in approximating the relative fluorescence intensity in this fashion rather than using the integrated area of the fluorescence spectrum will not effect the overall conclusions. When small absorbance changes were observed as the composition of the solvent changed, the relative fluorescence intensity was corrected to reflect these changes.

Fluorescamine derivatives were prepared as described previously [7]. The composition of the solvent was altered by replacing part of the buffer system [8] with non-aqueous solvent.

RESULTS AND DISCUSSION

The changes in fluorescence intensity observed with change in the composition of the solvent may be seen in Fig. 1. Similar data was obtained for a number of indoles, tyrosine and tryptophan, and some of their metabolites: Some of the data for compounds of biological and clinical interest are included in Table 1. The fluorescence of fluorescamine derivatives of amines, amino acids and peptides is also higher in mixed DMSO—water solvent systems than in water (Table 2).

The enhancement of the fluorescence as the solvent system is altered will be discussed in terms of the analytical implications. Additionally, consideration of the interaction between the excited singlet and solvent molecules leads to an understanding of the nature of the excited state.

The data clearly suggest that it should be possible to develop more sensitive analytical procedures for compounds which fluoresce (or can be converted into fluorescent derivatives) by consideration of the solvent system. Several

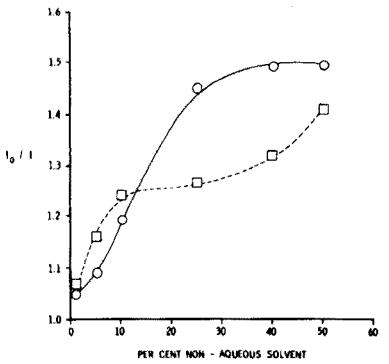

Fig. 1. Relative fluorescence intensity of indole in mixed solvent systems.
○ DMSO □ Ethanol

TABLE 1

Relative fluorescence intensities in mixed solvents[a]

	% Ethanol (v/v)					% DMSO (v/v)				
	1	5	10	25	50	1	5	10	25	50
Indole	1.05	1.09	1.19	1.45	1.45	1.07	1.16	1.24	1.27	1.39
5-Hydroxyindole	1.04	1.14	1.30	1.74	2.00	1.06	1.27	1.46	1.69	1.77
5-Methoxyindole	1.03	1.08	1.30	1.46	1.68	1.10	1.15	1.25	1.48	1.58
Indole-3-acetic acid	1.02	1.00	1.00	1.14	1.07	1.00	1.04	1.16	1.21	1.31
5-Hydroxyindole-3-acetic acid	1.05	1.11	1.26	1.33	1.62	1.02	1.15	1.40	1.51	1.73
5-Methoxyindole-3-acetic acid	1.06	1.08	1.10	1.14	1.36	1.02	1.10	1.15	1.22	1.45
Tryptophan	1.04	1.06	1.03	1.08	1.10	1.00	1.03	1.06	1.18	1.52
Tryptamine	1.00	1.03	0.89	0.70	0.64	1.00	1.00	1.02	1.01	0.98
5-Hydroxytryptamine	1.03	1.09	1.27	1.31	1.36	1.02	1.06	1.07	1.29	1.38
5-Methoxytryptamine	1.03	1.08	1.08	1.24	1.43	1.00	1.05	1.10	1.28	1.42
5-Hydroxytryptophan	1.04	1.09	1.21	1.30	1.49	1.02	1.09	1.17	1.31	1.42
Tyrosine	1.02	1.18	1.16	1.22	1.46	1.00	1.03	1.02	1.09	1.24
L-Dopa	1.16	1.32	1.36	2.36	2.73	1.12	1.32	1.58	1.88	2.03
6-Hydroxydopa	1.07	1.20	1.36	1.91	3.22	1.10	1.26	1.50	3.52	5.75
Noradrenalin	1.01	1.16	1.31	1.68	1.99	1.02	1.05	1.09	1.27	1.22
Adrenalin	1.08	1.12	1.36	1.84	2.24	1.07	1.18	1.28	1.28	1.32
3-Aminotyrosine	1.02	1.05	1.20	1.28	1.50	1.02	1.04	1.08	1.25	2.00
p-Aminophenylalanine	1.04	1.15	1.22	1.48	1.72	1.06	1.27	1.50	2.11	2.87
3-Methoxytyrosine	1.04	1.17	1.23	1.41	1.54	1.00	1.04	1.09	1.16	1.22

[a]All measurements are relative to the fluorescence of the compound in pure water. Experimental error = ± 5 %. Data taken from duplicate runs.

TABLE 2

Relative fluorescence intensity of fluorescamine derivatives in DMSO/water solvent systems[a]

Amine	30 % DMSO (v/v)	50 % DMSO (v/v)
Alanine	1.38	1.88
Aniline	1.73	2.33
Chymotrypsin	1.28	1.48
Tryptophan	2.18	2.77
Serine	1.39	2.02

[a]All measurements are relative to the fluorescence of the derivative in pure water. Experimental error = ± 5 %. Data taken from duplicate runs.

fluorimetric assays (e.g. the procedure for tryptophan developed by Duggan and Udenfriend [9]) involve the measurement of native luminescence after the fluorophore is isolated in an analytically useful form. If ethanol or DMSO could replace water in one (or more) of the isolation steps, the fluorescence intensity of the tryptophan would be higher. Similarly, the large increase in the luminescence of a derivative in mixed aqueous solvents suggest that it may be useful to add the derivatizing reagent or buffer system in non-aqueous solvents rather than in water, when possible.

Inspection of the relative fluorescence intensity data leads to several correlations: (i) the fluorescence intensity increases as the solvent is made less aqueous in all cases except tryptamine — the only compound with a β-ethylamino group as the only group appended to the ring; (ii) the increase in fluorescence intensity is related to the number of hydroxyl groups attached to the ring (see 6-hydroxydopa vs. dopa vs. tyrosine); (iii) the increase in fluorescence intensity as the solvent is made less aqueous is smaller for methoxy derivatives than for hydroxy derivatives (see 5-methoxyindole vs. 5-hydroxyindole).

These results can be discussed with respect to the various deactivation pathways available to the excited singlet state. Ricci [10] has shown that k_f, the rate of fluorescence of tryptophan and tryptamine, is fairly insensitive to the nature of the solvent, hence the change in fluorescence quantum efficiency is probably due to changes in the rate of non-radiative transitions. Considerable evidence exists that water interacts with the excited state of the compounds of interest in this study [5]. The formation of excited state complexes provides an additional pathway for the decay of the excited state, hence reducing the fluorescence quantum yield. In polar solvents where hydrogen bonding may stabilize the exciplex, the complex is usually not fluorescent, and the fluoresence quantum yield is lower [11, 12]. Since the fluorescence quantum yields of the compounds of interest here are higher in non-aqueous polar solvents (e.g. ethanol, ethylene glycol) it is not unreasonable to suggest either that exciplexes do not form in these solvents, or, if they do form, that they are weaker than exciplexes derived from water. However, it is necessary to note the effect of small portions of potential quenchers in a given solvent. Walker et al. [13] have shown, for example, that n-butanol can form an exciplex with indole in n-pentane, and Longworth [14] has suggested that an exciplex forms between isopropanol and 1,2-dimethylindole in 3-methylpentane. In contrast, Feitelson [3] has found that the addition of ethanol slightly enhances the fluorescence of tyrosine and *o*-methyltyrosine in water. This might indicate either that alcohols do not form complexes with these excited states, or that fewer or weaker exciplexes form, hence more excited states fluoresce.

The data and correlations (i)—(iii) will now be considered in terms of the micro-environment of the excited state. The general enhancement of the fluorescence in mixed DMSO—water and mixed ethanol—water solutions might be due to the decreased concentration of water in the immediate vicinity of the excited state; both DMSO and ethanol are likely to form

exciplexes less effectively than water, so that a higher fluoresence intensity is achieved. The fluorescence intensity of tryptamine decreases as the fraction of the non-aqueous solvent increases, possibly because of enhancement of intramolecular quenching by the β-NH_2 group on the side-chain, when fewer hydrogen-bonded amine groups are present. Excited state complexation by the NH_2 group is well documented [15—17] and intramolecular-$N(CH_3)_2$ quenching has been reported for *N,N*-dimethylaminoethylnaphthalene [18].

A consideration of the micro-environment of the excited state is also useful in the understanding of the fluorescence data for the compounds which have hydroxyl groups. There are several sites in the excited state which are polar and might compete to interact with water, e.g. the OH group, the aromatic ring, and the substituents on the aliphatic chain. If it is assumed that water preferentially associates with the —OH and the substituents on the side-chain since they are more polar than the aromatic rings, then as the concentration of water decreases, there is a decrease in the number of water molecules in the region of the aromatic nucleus, fewer exciplexes form, and the fluorescence intensity increases. This effect is most apparent with polyhydroxy compounds such as adrenalin, L-dopa and 6-hydroxydopa. The enhancement in fluorescence arising from the aromatic hydroxyl group is paralleled by the aromatic amino group—presumably for similar reasons. The enhancement in fluorescence appears to occur with both the hydroxy and methoxy species (cf. 5-methoxy and 5-hydroxyindole; 5-methoxy and 5-hydroxytryptamine; 5-methoxy and 5-hydroxyindole acetic acid) and is greater for the hydroxyl species in each case, thus suggesting that hydrogen bonding is at least part of the interaction present.

The nature of the group(s) appended to the aliphatic chain is important in the enhancement effects. The effect of the NH_2 group discussed above is quite noticeable in the series noradrenalin (terminal CH_2NH_2 group), adrenalin (terminal CH_2NHCH_3 group) and L-dopa (terminal $CH(COO^-)NH_3^+$ group). The fluorescence enhancement is greatest with the amino acid and least with the primary amine; these results are likewise observed with 5-hydroxytryptamine and 5-hydroxytryptophan.

The present data indicate that in some cases DMSO enhances the fluorescence to a greater extent than the corresponding ethanol solution while the reverse is true in other cases. It does not seem possible to make any broad generalizations, although DMSO enhances luminescence to a greater extent than ethanol when a carboxylic acid group (as opposed to a zwitterionic $-COO^-$) is present, and the fluorescence enhancement is greater in DMSO for compounds with aromatic amine groups.

The choice of the ideal solvent system for fluorescence analysis appears to depend on the structural features of the fluorophore and the effect of the solvent system on the micro-environment of the excited state. The use of mixed solvent systems enhances the fluorescence intensity of a number of compounds of analytical interest, as well as the fluorescence of a useful

derivative for primary amines. The design of new fluorimetric procedures should therefore include a consideration of the use of mixed aqueous solvent systems.

We thank the National Research Council of Canada for support of this work.

REFERENCES

1 D. V. Bent and E. Hayon, J. Am. Chem. Soc., 97 (1975) 2599, 2606, and 2612.
2 J. Feitelson, Isr. J. Chem., 8 (1970) 241.
3 J. Feitelson, Photochem. Photobiol., 9 (1969) 401.
4 E. P. Kirby and R. F. Steiner, J. Phys. Chem., 74 (1970) 4480.
5 R. McGuire and I. Feldman, Photochem. Photobiol., 18 (1973) 119.
6 A. I. Vogel, A Textbook of Practical Organic Chemistry, J. Wiley, New York, 1956, p. 167.
7 S. Stein, P. Böhlen, J. Stone, W. Dairman and S. Udenfriend, Arch. Biochem. Biophys., 155 (1973) 203.
8 P. M. Froehlich and T. D. Cunningham, Anal. Chim. Acta, 84 (1976) 427.
9 D. E. Duggan and S. Udenfriend, J. Biol. Chem., 223 (1956) 313.
10 R. W. Ricci, Photochem. Photobiol., 12 (1970) 67.
11 M. Goldman and E. L. Wehry, Anal. Chem., 42 (1970) 1178.
12 J. A. Otterstedt, J. Chem. Phys., 58 (1973) 5716.
13 M. S. Walker, T. W. Bednar and R. Lumry, J. Chem. Phys., 45 (1968) 3455; 47 (1967) 1020.
14 J. W. Longworth, Photochem. Photobiol., 7 (1968) 587.
15 D. Schulte-Frohlinde and R. Pfefferkorn, Ber. Bunsenges. Phys. Chem., 72 (1968) 330.
16 T. R. Evans, J. Am. Chem. Soc., 93 (1971) 2081 and references therein.
17 J. Tournon, E. Kuntz and M. Ashraf El-Bayoumi, Photochem. Photobiol., 16 (1972) 425.
18 E. A. Chandross and H. T. Thomas, Chem. Phys. Lett., 9 (1971) 393.

Analytica Chimica Acta, 87 (1976) 193—199

EXTRACTION AND SPECTROPHOTOMETRIC DETERMINATION OF GALLIUM WITH 4-(2-PYRIDYLAZO)RESORCINOL

M. ŠIROKI and M. J. HERAK

Laboratory of Analytical Chemistry, Faculty of Science, The University of Zagreb, Strossmayerov trg 14, 41000 Zagreb (Yugoslavia)

(Received 5th March 1976)

SUMMARY

A sensitive and selective spectrophotometric determination of gallium is described. It is based on extraction of gallium from 3 M hydrochloric acid solution as a chloro-complex into 1,2-dichlorobenzene and exchange of the chloro ligand with 4-(2-pyridylazo)resorcinol (PAR); the final association complex of Ga—PAR with tetraphenylarsonium ions is measured in the organic phase. The absorption maximum occurs at 510 nm and the effective molar absorptivity is $(8.2 \pm 0.3) \cdot 10^4$ l mol^{-1}cm^{-1}. Beer's law is obeyed over the range 0.2—2 p.p.m. of gallium. Few ions interfere.

Many chromogenic agents have been used for the spectrophotometric determination of gallium. 4-(2-Pyridylazo)resorcinol (PAR, H_2R) [1, 2] is very sensitive, but it is inselective, forming coloured complexes with several metal ions. Addition of tetraphenylarsonium- or tetraphenylphosphonium chloride allows the Ga—PAR complex to be quantitatively extracted into chloroform and similar solvents [3]. Since many metal—PAR complexes are extracted only slightly or not at all, the selectivity of the PAR method for gallium can be increased appreciably by extraction and measurements in the organic phase. However, the PAR complexes of a few metal ions that usually accompany gallium are also extracted, causing large interferences [4—7].

In the present paper a selective and sensitive extraction—spectrophotometric method is described. It is based on the extraction of gallium as a chloro complex from hydrochloric acid solution; the chloride is then exchanged with PAR, and the resulting Ga—PAR complex is determined spectrophotometrically in the organic phase.

EXPERIMENTAL

Apparatus and reagents

A Beckman spectrophotometer Model DU-2 was used. ^{67}Ga was measured with a well-type scintillation counter (NaI/Tl) from Ekco Electronics.

Analytical-grade reagents and deionized water were used. Chloroform contained 0.5 % ethanol. Tetraphenylarsonium- and tetraphenylphosphonium

chloride (Fluka) were dissolved in water and/or in chloroform. The monosodium salt of PAR (Merck) was dissolved in water. The acetate buffer pH 6 was 0.4 M.

^{67}Ga from the Institute "Ruđer Bošković", Zagreb, was used in chloride form.

Standard solution of gallium (0.01 M). Fuse gallium oxide with potassium hydrogensulfate, dissolve the melt in 1 M HCl and, to remove the sulfates, precipitate gallium with ammonia. Centrifuge, wash and dissolve the precipitate in 6 M HCl. Standardize gravimetrically with cupferron, and prepare more dilute solutions as required.

Determination of the distribution ratio

Radiometric measurements were used. The organic solvent and the aqueous solution (5 ml), containing the gallium—chloro or gallium—PAR complex, were shaken mechanically for 15 min. After phase separation, an aliquot (1 ml) of each phase was counted. The distribution ratio (D_{Ga}) was calculated by dividing the counts/100 s of the organic and aqueous phase.

Recommended procedure for gallium

Into a separating funnel, pipette 1,2-dichlorobenzene (5 ml) and add an aliquot of hydrochloric acid solution, containing 1—10 μg of gallium. Add an aqueous solution of tetraphenylarsonium- or tetraphenylphosphonium chloride (1 ml of 0.02 M), followed by water or hydrochloric acid to adjust the solution to 3 M in HCl. Shake for 2 min and separate the phases. Remove the organic phase into a 50-ml conical flask containing an aqueous solution of PAR (2 ml of 0.001 M), tetraphenylarsonium- or tetraphenylphosphonium chloride (0.5 ml of 0.02 M) and acetate buffer pH 6 (2.5 ml). Shake mechanically for 5 min. Separate the phases by centrifugation and measure the absorbance of the organic phase at 510 nm in 1-cm cells, against a reagent blank.

RESULTS AND DISCUSSION

The determination of gallium in an organic phase, following extraction of Ga—PAR complexes, is more selective than the method based on direct measurement in the aqueous solution. However, metal ions such as iron(III), vanadium(V), cobalt(II) and copper(II), still interfere even in trace amounts, since their PAR complexes are also easily extracted. The selectivity can be improved remarkably if the Ga—PAR complex is prepared from the previously extracted gallium—chloro complex. The relatively simple and fast two-stage extraction procedure developed does not require stripping of gallium into an aqueous solution. In brief, gallium is extracted from 3 M hydrochloric acid solution with Ph_4AsCl or Ph_4PCl into 1,2-dichlorobenzene or chloroform. The organic phase is contacted with a buffered aqueous solution of PAR so that the chloride is replaced by PAR, and the absorbance of the organic phase

is measured. The reactions involved can be presented

$$[GaCl_4]^-_{aq} + [Ph_4X]^+ \xrightarrow{3\ M\ HCl} [Ph_4X]\,[GaCl_4]_{org}$$

$$[Ph_4X]\,[GaCl_4]_{org} + 2\ HR^-_{aq} \xrightarrow{pH\ 5\text{—}6} [Ph_4X]\,[GaR_2]_{org} + 2\ H^+ + 4\ Cl^-$$

where X = As or P, and HR and R refer to ionic forms of 4-(2-pyridylazo)-resorcinol (H_2R). Similar principles have been utilized by Bansho and Umezaki [8], but the extraction mechanism and working details described here are quite different.

Gallium is extracted initially by the method of Finston and Rahaman [9], with 1,2-dichlorobenzene as solvent and Ph_4AsCl as extractant. Chloroform is a better solvent for the Ga—PAR complex than 1,2-dichlorobenzene, whereas 1,2-dichlorobenzene is better for the Ga—chloro complex (Table 1).

Effect of hydrogen ion and ligand concentration

The extraction of the gallium—chloro and gallium—PAR complexes was studied with different hydrogen ion, chloride and PAR concentrations. Maximal extraction of the Ga—PAR complex was achieved over the pH region 4—7 (Fig. 1A, curve 1, and Fig. 1B, curves 2—4), in which range the 1:2 Ga:PAR complex [1—3] is stable in the aqueous solution (Fig. 1B, curve 1). The best reproducibility was obtained with the buffered medium at pH 5—6.

Optimal concentrations of the H^+ and Cl^- ion in the extraction stage involving the Ga—chloro complex are 3 M (Fig. 2). At least a five-fold excess of PAR is needed for quantitative formation of the Ga—PAR complex. No essential difference was found whether 1,2-dichlorobenzene or chloroform was used as solvent.

TABLE 1

Extraction of gallium—chloro and gallium—PAR complexes
(Ga = $1 \cdot 10^{-5}$ M, HCl = 3 M, $(C_6H_5)_4XCl$ = $1 \cdot 10^{-2}$ M, PAR = $1 \cdot 10^{-4}$)

Solvent	$(C_6H_5)_4AsCl$		$(C_6H_5)_4PCl$	
	D_{Ga}	% E	D_{Ga}	% E
Ga—chloro complex				
1,2-Dichlorobenzene	585	99.6	482	99.6
Chloroform	19	95.2	16	94.1
Chloroform—acetone (5 + 1)	34	97.1	34	97.1
Ga—PAR complex				
1,2-Dichlorobenzene	14	93.5	15	93.8
Chloroform	114	99.3	126	99.4
Chloroform—acetone (5 + 1)	108	99.2	114	99.3

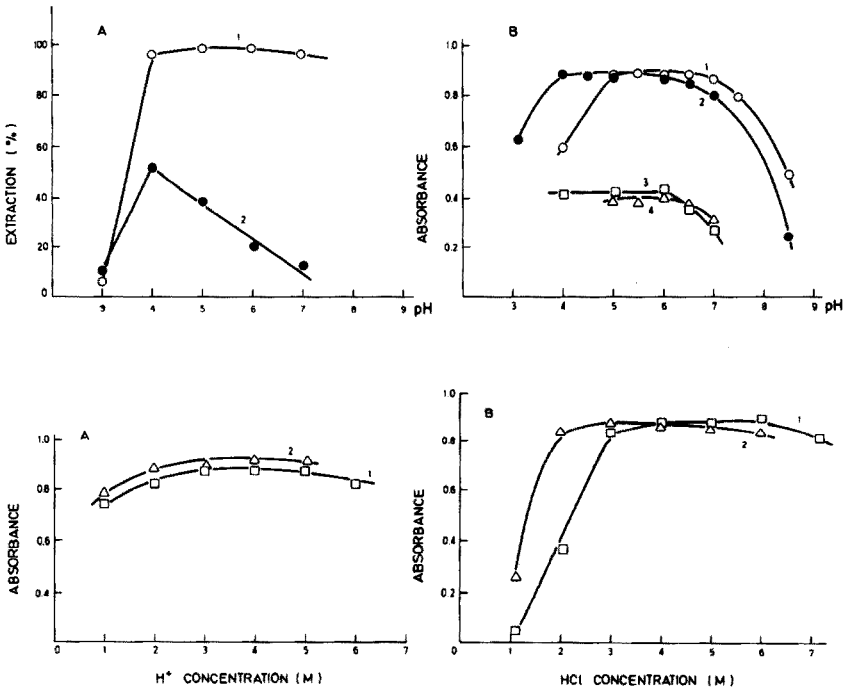

Fig. 1. (top) The effect of pH. A, The extraction of $1 \cdot 10^{-5}$ M gallium from buffered aqueous solution pH 6: (1) with $1 \cdot 10^{-3}$ M Ph_4AsCl in chloroform, (2) with chloroform alone. The extraction was followed radiometrically. B, The absorbance of $1 \cdot 10^{-5}$ M Ga—PAR complex: (1) in aqueous solution (at λ_{max} = 505 nm), (2) in chloroform phase obtained by extraction from the aqueous solution containing Ph_4AsCl (at λ_{max} = 510 nm), (3) and (4) in the organic phase obtained by the two-stage extraction procedure with chloroform and 1,2-dichlorobenzene, respectively (absorbance values divided by 2).

Fig. 2. Effect of hydrogen ion (A) and chloride (B) concentration on the extraction of the gallium—chloro complex from $1 \cdot 10^{-5}$ M gallium. For (A), the chloride concentration was constant (6 M). Curves 1, chloroform. Curves 2, 1,2-dichlorobenzene.

Optimal extractant concentration

Different extractant concentrations were required to achieve maximal absorbance readings with the two organic solvents studied. A much higher concentration of extractant was needed for the Ga—chloro complex extraction with chloroform than with 1,2-dichlorobenzene (Fig. 3, curves 1 and 2). Analysis of both organic phases for the tetraphenylarsonium cation [10] showed that more extractant was extracted into chloroform than into 1,2-dichlorobenzene. This indicates more pronounced co-extraction of chloride along with the gallium—chloro complex, into chloroform.

To reach maximal absorbance of the final extract, an excess of tetraphenylarsonium cation is also required in the second extraction stage. The

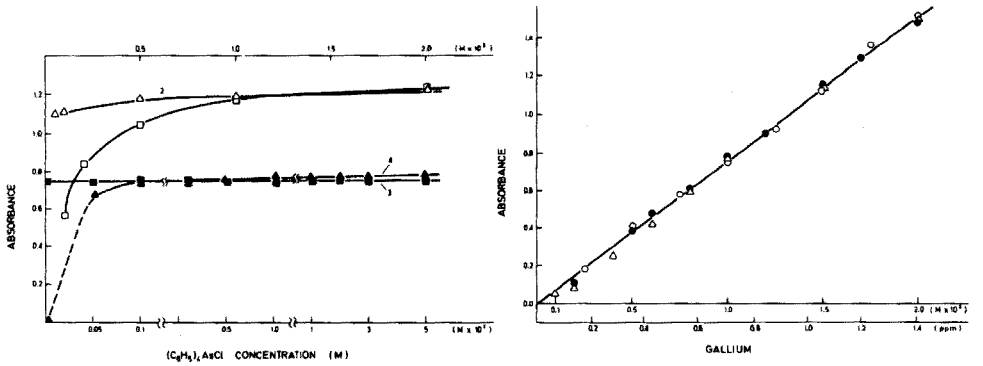

Fig. 3. The effect of extractant concentration. (1) and (2) Dependence of absorbance on the concentration of Ph_4AsCl in extraction of the gallium—chloro complex (upper abscissa), with chloroform and 1,2-dichlorobenzene, respectively. (3) and (4). Effect of Ph_4AsCl on the Ga—PAR formation and extraction stage (lower abscissa) with chloroform and 1,2-dichlorobenzene, respectively.

Fig. 4. Calibration graph. ○, Extraction of Ga—PAR complex from aqueous solution with chloroform. ●, The two-stage procedure with chloroform. △, The two-stage procedure with 1,2-dichlorobenzene.

concentration of tetraphenylarsonium cation present in the organic phase after extraction of the Ga—chloro complex, is large enough when chloroform is used, but not when 1,2-dichlorobenzene is used (see curves 3 and 4, Fig. 3). Therefore with 1,2-dichlorobenzene, more extractant is needed in the second extraction.

When the concentration of tetraphenylarsonium- or tetraphenylphosphonium chloride was above 0.01 M in the first extraction stage and above 0.001 M in the second, nearly identical absorbance values were obtained with both solvents (Fig. 4).

Equilibrium for both systems was achieved after 2 min of shaking. Nearly complete extraction of gallium was achieved by a single extraction in both stages with phase volume ratios of 1:1.

Beer's law, sensitivity and reproducibility

The calibration graph (Fig. 4) is linear over the range 0.2—1.5 p.p.m. of gallium in the measured solution. The effective molar absorptivity of the coloured extract at 510 nm is $(8.2 \pm 0.3) \cdot 10^4$ l mol^{-1} cm^{-1}.

The reproducibility expressed as relative standard deviation is about ± 4 % for $5 \cdot 10^{-6}$—$2 \cdot 10^{-5}$ M Ga and about ±10 % at lower concentrations. The results obtained with very low gallium concentrations tend to be low.

The effect of foreign ions

The effect of foreign ions on the determinations of gallium by the proposed two-stage extraction method is shown in Table 2. Most of the cations studied

TABLE 2

Effect of foreign ions
(Ga = $1 \cdot 10^{-5}$ M, $(C_6H_5)_4AsCl$ = $1 \cdot 10^{-2}$ M, HCl = 3 M, PAR = $1 \cdot 10^{-4}$ M, acetate buffer pH 5.5. Absorbance measured against reagent blank.)

Ion	Ion:Ga (molar)	*A* at 510 nm		Ion	Ion:Ga (molar)	*A* at 510 nm	
		$C_6H_4Cl_2$	$CHCl_3$			$C_6H_4Cl_2$	$CHCl_3$
—	—	0.838	0.781	Nb(V)	10	0.810	0.758
Al(III)	1000	0.841	0.761		100	0.840	0.772
	10000	0.843	0.810	Co(II)	10	0.823	0.770
Ca(II)	1000	0.839	0.758		100	0.853	0.795
	10000	0.840	0.866	Ni(II)	10	0.853	0.772
Mg(II)	1000	0.842	0.743		100	0.828	0.783
	10000	0.837	0.775	Zn(II)	10	0.713	0.690
Mn(II)	100	0.847	0.737		100	0.738	0.790
	1000	0.838	0.758	Cu(II)	1	0.840	0.743
Fe(III)	100	0.840[a]	0.785[a]		10	0.838[c]	1.040
	1000	0.860[a]	0.838[b]		100	0.848[c]	0.942[c]
	10000	0.820[b]	0.980[b]	Cd(II)	10	0.840	0.739
Cr(III)	100	0.850	0.780		100	0.860	0.799
	1000	0.858	0.898	Pb(II)	10	0.830	0.790
Ti(IV)	10	0.840	0.724		100	0.840	0.771
	100	0.810	0.826	Ag(I)	10	0.820	0.680
Zr(IV)	10	0.830	0.671		100	0.870	0.730
	100	0.850	0.672	Hg(II)	1	0.841	0.751
V(V)	10	0.873[a]	0.871[a]		10	1.060	0.855
	100	0.862[a]	0.841[a]	Sn(II)	1	0.840	0.732
					10	0.605	0.252
SO_4^{2-}	1000	0.843	0.789	CrO_4^{2-}	10	0.850	0.820[a]
	10000	0.848	0.800		100	0.850	0.894[a]
NO_3^-	1000	0.850	0.751	MnO_4^-	10	0.865	0.875[a]
Br^-	10	0.830	0.791		100	0.851[a]	0.724[a]
	100	0.810	0.820	$C_2H_3O_2^-$	1000	0.830	0.770
I^-	10	0.810	0.781		10000	0.820	0.838
	100	0.800	0.780	$C_4H_4O_6^{2-}$	100	0.775	0.787
SCN^-	10	0.800	0.868		1000	0.700	0.864
	100	0.790	0.871		10000	0.590	0.927
MoO_4^{2-}	10	0.830	0.735	$C_2O_4^{2-}$	100	0.820	0.788
	100	0.810	0.760		1000	0.296	0.710
WO_4^{2-}	10	0.749	0.831		10000	0.042	0.635
	100	0.750	0.831				

[a]and [b]Ascorbic acid added before the first extraction stage (0.02 and 0.06 M, respectively). [c]0.005 M KCN added in the second extraction stage.

do not interfere when 1,2-dichlorobenzene is used as the solvent. Interferences of Fe(III) and V(V) can be eliminated by addition of ascorbic acid to the aqueous solution and allowing the system to stand for 10 min, before the first extraction. Interference of copper is eliminated by addition of cyanide

in the second extraction stage. The interference of chlorine formed in the hydrochloric acid solution on addition of strong oxidizing anions such as MnO_4^- and CrO_4^{2-} can also be eliminated with ascorbic acid. Hg(II) and Zn(II) interfere if present in a ten-fold excess, and Sn(II) interferes above the molar ratio 1:1. Of the anions studied, only tungstate and large amounts of oxalate and tartrate interfere. With chloroform, the interferences are more pronounced than with 1,2-dichlorobenzene, which is therefore the preferred organic solvent.

The authors are grateful to M. Koren and M. Ognjenović for carrying out numerous analyses.

REFERENCES

1 K. Hagiwara, M. Nakane, V. Osumi, E. Ishii and Y. Miyake, Jpn. Anal., 10 (1961) 1379; Chem. Abs., 56 (1962) 14917 b.
2 M. Hniličkova and L. Sommer, Z. Anal. Chem., 193 (1963) 171.
3 M. Široki and M. J. Herak, J. Inorg. Nucl. Chem., in press.
4 M. Široki and C. Djordjević, Anal. Chim. Acta, 57 (1971) 301.
5 M. Široki, Lj. Marić, Z. Štefanac and M. J. Herak, Anal. Chim. Acta, 75 (1975) 101.
6 Lj. Marić, M. Široki and M. J. Herak, J. Inorg. Nucl. Chem., 37 (1975) 2309.
7 M. Široki, Lj. Marić, M. J. Herak and C. Djordjević, Anal. Chem., 48 (1976) 55.
8 K. Bansho and Y. Umezaki, Bull. Chem. Soc. Jpn., 40 (1967) 326.
9 H. L. Finston and M. S. Rahaman, Mikrochim. Acta, (1969) 78.
10 M. Široki and Lj. Marić, Anal. Chim. Acta, 79 (1975) 265; Z. Anal. Chem., 276 (1975) 371.

Analytica Chimica Acta, 87 (1976) 201—208

DÉTERMINATION POTENTIOMÉTRIQUE ET SPECTROPHOTOMÉTRIQUE DE L'ÉCHELLE DE pH DANS L'ACIDE FORMIQUE

M. BREANT

Equipe de Recherche C.N.R.S. n° 100 associée à l'I.N.S.A. de Lyon, Laboratoire de Chimie Industrielle et Analytique, Bâtiment 401, 69621 Villeurbanne (France)

C. BEGUIN et C. COULOMBEAU

Equipe de Recherche associée C.N.R.S. n° 478, Laboratoire de Cinétique et Dynamique Moléculaires, C.E.R.M.O., Université de Grenoble I, B.P. 53, 38041 Grenoble (France)

(Reçu le 5 mai 1976)

RÉSUMÉ

A partir de mesures spectrophotométriques et potentiométriques, nous avons déterminé la constante d'autoprotolyse de l'acide formique puis, dans ce solvant, les constantes acide—base caractéristiques des acides bromhydrique, chlorhydrique, méthanesulfonique, *p*-toluènesulfonique, sulfurique II, trifluoroacétique, picrique et benzoïque.

SUMMARY

Spectrophotometry and potentiometry have been used to determine the self-ionization product of formic acid and the acidity constants of hydrobromic, hydrochloric, methanesulfonic, *p*-toluenesulfonic, sulfuric, trifluoroacetic, picric and benzoic acids in formic acid.

L'interprétation des réactions de solvolyse de fluorures de benzoyle à différents pH dans l'acide formique [1] nécessite la connaissance des équilibres acide—base dans ce solvant. Les données de la littérature n'étant pas toujours concordantes [2], nous nous sommes proposés de déterminer les limitations basique et acide de l'échelle de pH dans le solvant (recherche des acides forts et des bases fortes) puis, les constantes d'acidité d'un certain nombre de couples acide—base utilisés au cours des réactions de solvolyse et pour lesquelles aucune valeur n'a été publiée. Nous avons également comparé l'échelle de pH obtenue à celles établies dans l'eau et dans divers autres acides.

Les méthodes de travail que nous avons mises en oeuvre sont la potentiométrie à l'électrode de verre à remplissage de mercure et la spectrophotométrie à l'aide d'indicateurs colorés.

MÉTHODE POTENTIOMÉTRIQUE

Recherche d'une électrode indicatrice

Les travaux antérieurs concernant des mesures potentiométriques dans l'acide formique indiquent que l'électrode à quinhydrone [3, 4] et dans certains cas l'électrode de verre [5, 6] ont un comportement satisfaisant et reproductible bien que la deuxième perde sa sensibilité au cours du temps. L'électrode à hydrogène est presque [7] unanimement rejetée pour son manque de reproductibilité et de stabilité [3, 4, 8]. Nous avons néanmoins effectué quelques mesures avec l'électrode à hydrogène et constaté qu'elle n'était effectivement ni stable ni reproductible, ce que nous avons attribué aux variations de concentrations consécutives au départ de solvant entrainé par le courant d'hydrogène plutôt qu'à la présence d'oxyde de carbone [4] également entrainé par l'hydrogène. Nous avons finalement utilisé l'électrode de verre à remplissage de mercure proposée dans le diméthylsulfoxyde par Richtie et Uschold [9] et testée dans le diméthylacétamide [10], la *N*-méthylpyrrolidone [11], le glycol [12] et le méthanol [13] par les chercheurs de l'E.R. 100. Dans l'acide formique, nous avons constaté que la réponse de l'électrode était stable et reproductible.

Recherche d'un acide fort et d'une base forte

D'après les données de la littérature [14] l'acide trifluorométhanesulfonique serait complètement dissocié dans l'acide formique. Nous nous sommes assurés de ce fait en vérifiant que ses solutions dans l'acide formique obéissaient à la loi de Nernst: $E = E_0 + 0{,}058 \log [H^+]$. Nous avons maintenu la force ionique constante et égale à 0,1 M par addition de perchlorate de lithium. La pente des droites $E = f(\log [CF_3SO_3H])$ obtenues dans ces conditions est de 0,065 V par unité de pH. Ce résultat confirme que l'acide trifluorométhanesulfonique est fort dans l'acide formique. (Il ne parait pas décomposer trop vite l'acide formique.)

Les travaux antérieurs font mention de plusieurs bases fortes [3, 6, 15] dans l'acide formique. Nous avons retenu la diéthylamine et vérifié que ses solutions obéissaient à la loi de Nernst: la pente des droites: $E = f(\log [Et_2NH])$ est effectivement de 0,058 V par unité de pH.

L'étendue de l'échelle de pH peut être déterminée par potentiométrie à condition de tracer rapidement, l'une à la suite de l'autre, les deux droites de Nernst en milieu acide puis en milieu basique afin que la réponse de l'électrode de verre puisse être considérée comme constante au cours des deux manipulations. En milieu acide l'extrapolation à $[CF_3SO_3H] = 1$ M conduit à un potentiel de 1,172 V correspondant à pH 0. En milieu basique l'extrapolation à $[Et_2NH] = 1$ M conduit à un potentiel de 0,810 V. L'étendue de l'échelle est donc égale à 0,362 V. On remarque que la réponse de l'électrode n'est pas la même en milieu acide (0,065 V/un. log) qu'en milieu basique (0,058 V/un. log), phénomène constaté également dans d'autres solvants [11].

Si nous utilisons la pente moyenne 0,061 V/un. log nous obtenons une

échelle de 5,9 unités et si nous utilisons la valeur théorique de 0,058 V/un. log nous obtenons une échelle de 6,2 unités, valeur proposée par la littérature [3, 6, 7, 15, 16].

La corrélation entre l'échelle de pH déterminée dans l'acide formique et celles déterminées dans d'autres acides peut être effectuée à partir du coefficient d'activité de transfert du proton de l'eau à l'acide formique. Nous avons estimé cette grandeur par la méthode de Strehlow [17], procédé qui nécessite la connaissance du potentiel standard du couple H_2/H^+ dans l'acide formique. Nous avons déjà indiqué que nous n'avions pu vérifier le fonctionnement de l'électrode à hydrogène dans l'acide formique. Nous avons dû nous contenter d'une seule mesure, rapide, en milieu acide: pour $[CF_3SO_3H] = 0{,}44$ N nous avons obtenu $E = 0{,}217$ V/ECS dans l'acide formique, soit 0,012 V/Fc/Fc^+. En admettant que l'électrode suit la loi de Nernst, nous en déduisons, pour $[CF_3SO_3H] = 1$ M: $E^0_{H_2/H^+} \# +0{,}032$ V/Fc/Fc^+. Dans l'eau, ce potentiel est égal à —0,396 V. D'où

$$p\gamma^{HCOOH}_{H_2O}(H^+) = -(0{,}032 + 0{,}396)/0{,}058 = -7{,}4$$

Comme on pouvait le prévoir, le proton est moins solvaté par l'acide formique que par l'eau. La valeur $p\gamma^{HCOOH}_{H_2O}(H^+)$ obtenue permet de fixer (Fig. 1) la position relative des domaines de pH caractéristiques des acides formique, acétique et trifluoroacétique par rapport à l'eau. Nous constatons que le domaine de pH utilisable dans l'acide formique se situe entièrement en milieu superacide.

Détermination des constantes d'acidité de quelques couples acide—base

La méthode consiste à doser les acides par une base forte, la diéthylamine ou la pipéridine et les bases par l'acide trifluorométhanesulfonique. La réaction est du type $HA + B \rightarrow HB^+ + A^-$. E étant la valeur du potentiel mesuré à intensité nulle nous étudions par exemple sa variation en fonction de l'addition de la base B à la solution de l'acide HA. Avant le point équivalent

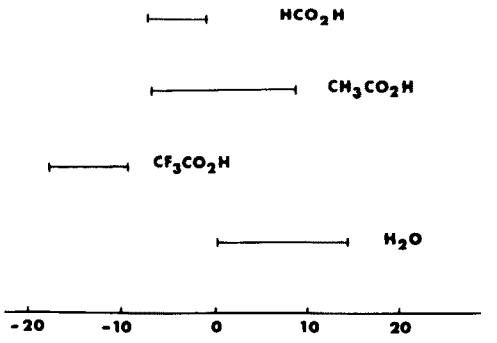

Fig. 1. Comparaison des domaines de pH accessibles dans l'eau, l'acide acétique, l'acide trifluoroacétique et l'acide formique, comparaison effectuée à partir de l'hypothèse de Strehlow.

nous avons en solution les espèces HA, A^- et HB^+, le potentiel pris par l'électrode indicatrice sera $E = E_1 + 0{,}058 \log [HA]/[A^-]$. Au point équivalent tout l'acide HA a été dosé par la base B. Si x représente la fraction de base ajoutée, au point équivalent $x = 1$ et au point $x = 0{,}5$ la moitié de l'acide HA a été dosé donc $[HA] = [A^-]$, le potentiel de demi-neutralisation mesuré en ce point permet en se reportant aux courbes d'étalonnage, de connaître le pH de la solution, nous avons alors $pH = pK_{HA/A^-}$. Après la point équivalent le potentiel, donc le pH, est fixé par l'excès de base forte. Un raisonnement analogue permet d'exploiter les courbes de dosage d'une base B par l'acide HA.

Le dosage de l'acide méthanesulfonique par la diéthylamine est donné à titre d'exemple (Fig. 2) et l'ensemble des résultats obtenus est consigné dans le Tableau 1.

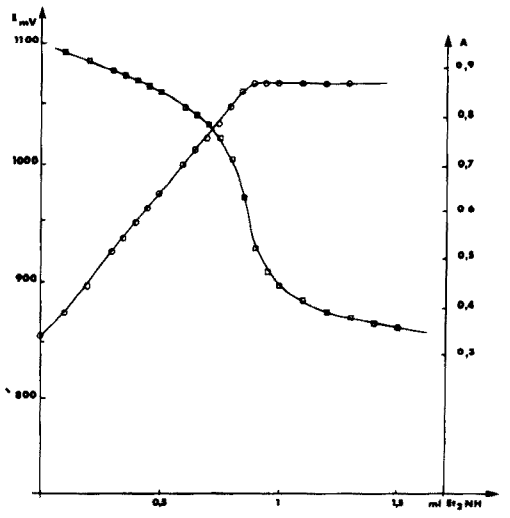

Fig. 2. Dosage de l'acide méthanesulfonique par la diéthylamine; □ potentiel de l'électrode de verre; ○ absorbance des solutions.

TABLEAU 1

Comparaison des constantes d'acidité obtenues par spectrophotométrie (S) et par potentiométrie (P).

Composé	S	P	Littérature
Acide bromhydrique	0,30	$0{,}5_5$	
Acide chlorhydrique	1,45	1,4	1,23 [6]; 1,4 [16]
Acide methanesulfonique	1,60	1,6	
Acide *p*-toluenesulfonique	1,60	$1{,}7_5$	0,73 [6]
Acide sulfurique II	4,35	$4{,}2_5$	4,7 [15]
Acide trifluoracétique	4,60	4,7	
Acide picrique	4,85	4,9	
Acide benzoïque	4,90	$4{,}9_5$	
Erreur	±0,05	±0,1	

MÉTHODE SPECTROPHOTOMÉTRIQUE

Le principe général de la méthode ayant été exposé en détail dans une publication récente [18], nous n'indiquerons ci-après que la marche suivie dans le cas particulier de l'acide formique.

Le début de l'échelle de pH (milieu acide fort) est établi à partir des résultats obtenus par potentiométrie: l'acide trifluorométhanesulfonique s'étant révélé entièrement dissocié dans l'acide formique, ses solutions normale, décinormale, centinormale tamponnent le milieu à pH 0, 1 et 2. Nous avons d'abord sélectionné un indicateur coloré I_1 virant dans cette zone de pH (0—2) l'*o*-nitrodiphénylamine, et mesuré, en fonction de l'acidité du milieu, l'absorbance de ses solutions au maximum d'absorption de la forme basique I. La relation $pH = pK_{I_1} + \log [I]/[IH^+]$ conduit à la constante pK_{I_1} de l'indicateur. Nous avons alors suivi la neutralisation de l'acide méthanesulfonique par la pipéridine (ou la diéthylamine) tout d'abord à l'aide de l'*o*-nitrodiphénylamine, ensuite à l'aide du vert de bromocrésol (I_2). La formule $pK_A = pK_I + \log [I]/[IH^+]$, dans laquelle les concentrations sont relevées à la demi-neutralisation de l'acide méthanesulfonique conduit à la constante pK_A de cet acide, connaissant pK_{I_1}, puis à pK_{I_2} connaissant pK_A.

Le même procédé permet de passer de pK_{I_2} à la constante du couple acide benzoïque/benzoate, puis de cette constante à celle du bleu de bromothymol I_3. Le virage de ce dernier indicateur ayant lieu en milieu base forte (diéthylamine, pipéridine) on atteint le produit d'autodissociation pK_i du solvant en relevant la concentration de base correspondant à la demi-neutralisation du bleu de bromothymol. En effet, nous avons alors la relation

$$pH = pK_{I_3} = pK_i - \log [\text{base forte}]_{1/2\ \text{neutralisation}}$$

Choix des indicateurs: Nous avons testé les "indicateurs de Hammett" [15] susceptibles de virer dans l'acide formique. Le spectre d'absorption de la *p*-nitraniline est très proche de la barrière du solvant et nous n'avons pu faire de mesures précises. L'*o*-nitraniline n'est pas stable en milieu basique dans l'acide formique et la dinitro-2, 4-aniline vire en milieu trop acide pour permettre un démarrage correct de l'échelle. Nous avons finalement sélectionné — expérimentalement — l'*o*-nitrodiphénylamine. En ce qui concerne les deux autres indicateurs, nous avons mis à profit la remarque que les sulfones phtaleïnes (bleu de thymol, rouge de crésol, rouge de chlorophénol . . . etc.) possèdent deux virages en milieu aqueux, les pK_I correspondants différant de six unités environ [19]. Nous avons donc pensé que le vert de bromocrésol et le bleu de bromothymol pour lesquels on n'observe qu'un virage dans l'eau (pK_I: 4,6 et 6,8 respectivement) devaient posséder un deuxième virage en milieu superacide. Compte tenu du décalage entre les échelles de pH dans l'eau et l'acide formique on pouvait espérer observer le virage du vert et du bleu respectivement en milieux neutre et basique dans l'acide formique, ce que l'expérience a vérifié.

Résultats et discussion

La Fig. 2 met en évidence le type de courbes obtenues au cours des

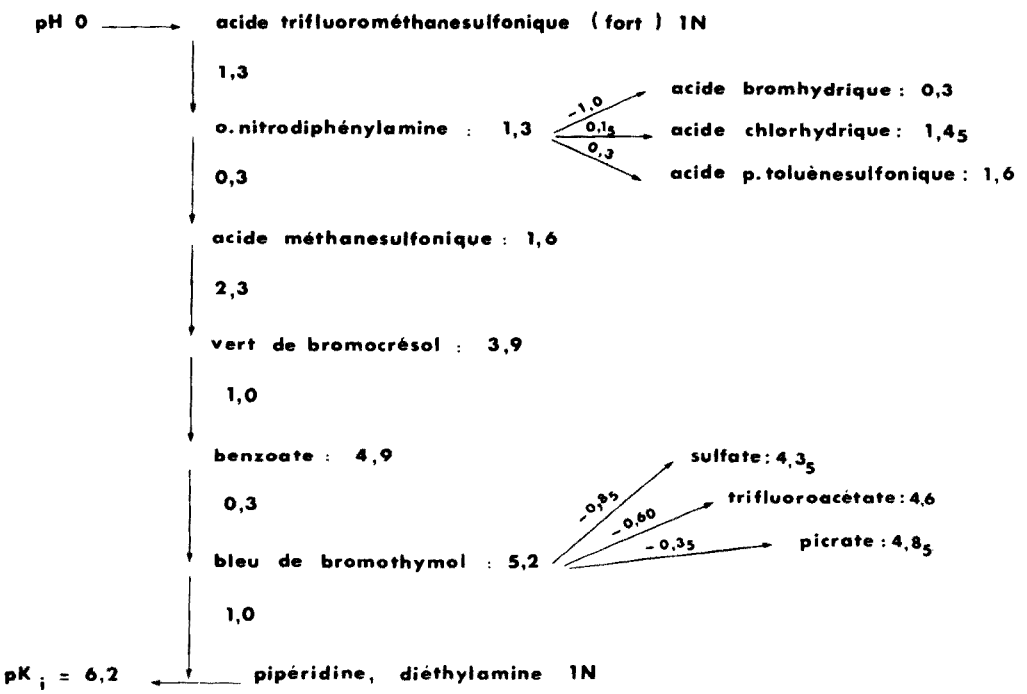

Fig. 3. Détermination spectrophotométrique de l'échelle de pH dans l'acide formique.

dosages et l'ensemble des valeurs obtenues est rassemblé dans la Fig. 3: les flèches indiquent l'ordre des déterminations, le chiffre en regard, les écarts entre les pK_I et les pK_A, et les constantes acide—base qui en découlent figurent à la suite de chaque composé. Ces valeurs ont été reportées dans le Tableau 1, en regard de celles obtenues par potentiométrie. Nous constatons une remarquable concordance entre les résultats obtenus par spectrophotométrie et ceux découlant des mesures potentiométriques.

PARTIE EXPÉRIMENTALE

Produits

Les indicateurs utilisés sont de marque Aldrich et Merck. Les acides chlorhydrique et bromhydrique sont des gaz, produits de Matheson. Les acides trifluorométhanesulfonique et méthanesulfonique ont été fourni par Fluka, la diethylamine et la pipéridine par Carlo Erba et les autres produits par Prolabo.

Le trifluoroacétate et le picrate de lithium sont préparés à partir des acides correspondants et de carbonate de lithium. Après recristallisation dans l'eau, ils sont séchés par un séjour prolongé dans une étuve à 100 °C (trifluoroacétate) et à 150 °C (picrate) [20].

L'acide *p*-toluenesulfonique a été recristallisé dans l'éther éthylique puis séché sous pression réduite avec une pompe à palette puis dans un dessicateur en présence d'anhydride phosphorique; il fond à 92 °C. Même après ce traitement il s'agit toujours du monohydrate.

L'acide formique est distillé sur une colonne à remplissage de spires de verre de 2 mm de diamètre et munie d'un manteau argenté sous vide de 1 m de hauteur. Il est recueilli à l'abri de la lumière et utilisé immédiatement après distillation.

Appareils et mode opératoire

Les bases sont titrées par l'acide trifluorométhanesulfonique, les acides par la diéthylamine ou la pipéridine. Les réactifs sont utilisés sans dilution et introduits dans la solution à l'aide de seringues à micromètre Gilmont (0,2 ou 2 ml).

Nous avons suivi l'absorption de la forme basique de l'*o*-nitrodiphénylamine 10^{-4} M à 435 nm, celle de la forme basique du vert de bromocrésol à 440 nm (la forme acide rose, 555 nm, absorbe peu) et celle de la forme acide du bleu de bromothymol 2.10^{-5} M à 555 nm (la forme basique jaune absorbe peu). (Le vert de bromocrésol étant très peu soluble dans l'acide formique, nous avons introduit le produit solide directement dans la cellule de mesure si bien que sa concentration n'est pas connue avec précision.)

L'absorbance des solutions est enregistrée à l'aide d'un spectrophotomètre Beckman modèle 24 S ou DBT ou ACTA MVI. Les différences de potentiel sont mesurées à l'aide d'un millivoltmètre Tacussel Minisis ou Orion Modèle 701.

Les mesures potentiométriques sont suivies en relevant la réponse d'une électrode de verre à remplissage de mercure Tacussel (ayant préalablement trempée 3 ou 4 jours dans l'acide formique; il est nécessaire par ailleurs de la retremper dans l'eau périodiquement pendant quelques jours puis dans l'acide formique sinon elle perd sa sensibilité) par rapport à une électrode de référence Ag/AgCl/KCl dans l'acide formique reliée à la solution étudiée par une jonction liquide d'acide formique saturé en perchlorate de lithium. Le potentiel de demi-vague anodique relatif à l'oxydation du ferrocène mesuré par rapport à cette électrode est reproductible et égale à +0,205 V. Le dosage est suivi conjointement par potentiométrie et par spectrophotométrie. On utilise pour cela une cuve à circulation placée dans le spectrophotomètre et reliée à une cellule pouvant recevoir de façon étanche les deux électrodes servant à la potentiométrie, une seringue Gilmont pour l'addition des réactifs et un tube de desséchant. La circulation de la solution est assurée par une minipompe d'introduction Jobin et Yvon. Les tuyaux reliant les deux cellules et la minipompe sont en polychlorure de vinyle. La localisation du point équivalent ($x = 1$) est utilisée pour le dépouillement des courbes spectrophotométriques.

Nous remercions le Centre National de la Recherche Scientifique pour son aide dans le cadre de la RCP n° 279 (Influence des solvants non aqueux sur les réactions ioniques).

BIBLIOGRAPHIE

1 C. Béguin, C. Coulombeau et S. Hamman, Résultats non publiés.
2 Mises au point A. I. Popov dans J. J. Lagowski (Ed.), The Chemistry of Non-Aqueous Solvents, Vol. 3, Academic Press, London, 1970, p. 340; G. Charlot et B. Trémillon, Les Réactions Chimiques dans les Solvants et les Sels Fondus, Gauthier-Villars, Paris, 1963, p. 207.
3 L. P. Hammett et N. Dietz, J. Am. Chem. Soc., 52 (1930) 4795.
4 A. I. Popov et J. C. Marshall, J. Inorg. Nucl. Chem., 19 (1961) 340.
5 M. Gutterson et T. S. Ma, Mikrochim. Acta, (1960) 1.
6 A. M. Shkodin, N. A. Izmailov et N. P. Dzyuba, Zh. Obshch. Khim., 20 (1950) 1999; 23 (1953) 27; Zh. Anal. Khim., 6 (1951) 273.
7 L. M. Mukherjee, J. Am. Chem. Soc., 79 (1957) 4040.
8 V. A. Pleskov, Zh. Fiz. Khim., 20 (1940) 153.
9 C. D. Richtie et R. E. Uschold, J. Am. Chem. Soc., 89 (1967) 1721.
10 M. Bréant et J. Georges, Talanta, 20 (1973) 916.
11 M. Dupin et J. P. Terrat, J. Electroanal. Chem. Interfacial Electrochem., 35 (1972) 261.
12 M. Collard, Résultats non publiés.
13 J. L. Mouton, D.E.A. de Chimie Analytique, Lyon, 1972.
14 R. N. Haszeldine et J. M. Kidd, J. Chem. Soc., (1953) 4228.
15 L. P. Hammett et A. J. Deyrup, J. Am. Chem. Soc., 54 (1932) 4239.
16 H. I. Schlesinger et A. N. Martin, J. Am. Chem. Soc., 36 (1914) 1589.
17 H. M. Koepp, H. Wendt et H. Strehlow, Z. Elektrochem., 64 (1960) 483.
18 M. Bréant, A. Auroux et M. Lavergne, Anal. Chim. Acta, 83 (1976) 49.
19 E. Bishop, Indicators, Pergamon Press, Oxford, 1972.
20 O. Silberrad et H. A. Phillips, J. Chem. Soc., 93 (1907) 474.

Analytica Chimica Acta, 87 (1976) 209—210

Short Communication

ELECTRONIC ABSORPTION OF HYDROXIDE IONS

W. SZAFRANSKI

Distillation Product Industries, Division of Eastman Kodak, Rochester, N.Y. (U.S.A.)

P. ZUMAN

Department of Chemistry, Clarkson College, Potsdam, N.Y. (U.S.A.)

(Received 9th June 1976)

Little attention has been paid to the electronic absorption in the u.v. region of simple anions containing only σ-bonds. It has been reported [1] that aqueous 1 M sodium hydroxide solutions in the region between 230 and 300 nm showed an absorbance 37 % higher than that of water. The absorbance below 200 nm was followed with a vacuum spectrograph and an absorption band with a maximum at 186 nm, log ϵ ca. 3.7, was reported [2]. Similar information on the existence of electronic absorption can be drawn from reports on the photochemical generation of hydrated electrons, which in solutions of alkali or alkaline earth hydroxides was reported to take place in the ultraviolet region [3] and more specifically [4] at 185 nm.

The above information has not become widely known, and it has been commonly assumed that absorption by hydroxide ions lies outside the scope of commercial spectrophotometers. In the course of an investigation of the hydration—dehydration equilibria of carbonyl compounds, u.v. absorption of the geminal diol anion was observed. To interpret the electronic transition involved, a simple model system for anions containing only σ-bonds was sought. This, together with the observation that the "cut-off" of spectra in alkali hydroxide solutions shifts to longer wavelengths with increasing hydroxide concentration led us to investigate the absorption spectra in aqueous solution of lithium, sodium, and tetramethylammonium hydroxides.

Spectra of solutions containing 10^{-4}—10^{-3} M alkali hydroxide show a gradual increase in absorbance below 215 nm with decreasing wavelength. The shape of the spectrum resembles that of a "foot" of an absorption band with a maximum between 180 and 190 nm. The absorbance at 205 nm and 210 nm was a linear function of hydroxide concentration over the range 0—$1.4 \cdot 10^{-3}$ M. The plot was identical for solutions of lithium, sodium, and tetramethylammonium hydroxide, indicating that the absorbance is a function of the hydroxide ion concentration only. Together with the fact that the absorbance for different preparations of sodium hydroxide was identical, this rules out the possibility of the absorption resulting from an impurity.

As $4 \cdot 10^{-4}$ M solutions of hydroxide ion gave an absorbance of ca. 0.2 at 205 nm it is possible to estimate that the molar absorptivity in the region of the absorption maximum will be of the order of 10^4 l mol^{-1}. Attempts are being made to obtain a better approximation of the wavelength of the absorption maxima and the molar absorptivities by means of a multiparametric fitting procedure [5].

The order of magnitude of the molar absorptivity seems to rule out the possibility of a $n \rightarrow \sigma^*$ transition; a $\sigma \rightarrow \sigma^*$ transition and photolysis seem to be more plausible.

Qualitatively similar absorption spectra for alkoxides, hydrogen sulfide anion, selenides, and tellurides are also being studied, as is the relationship between the spectra of these anions and those of corresponding molecules — which for the negatively charged species occur invariably at longer wavelength.

This work was carried out in partial fulfillment of the M.S. program of W.S., kindly supported by Distillation Product Industries, Division of Eastman Kodak.

REFERENCES

1 J. Cluzet and T. Kofman, Compt. Rend. Soc. Biol., 103 (1930) 783.
2 H. Ley and B. Arends, Z. Phys. Chem. (B), 6 (1929) 240.
3 M. S. Matheson, W. A. Mulac and J. Rambani, J. Phys. Chem., 67 (1963) 2613.
4 J. Jortner, M. Ottolenghi and G. Stein, J. Phys. Chem., 66 (1962) 2029, 2037, 2042.
5 L. Meites, private communication (1975).

Analytica Chimica Acta, 87 (1976) 211—213

Short Communication

THE APPLICATION OF AN ION-EXCHANGE RESIN—GRAPHITE PASTE ELECTRODE IN COMPLEXIMETRIC TITRATIONS

R. KURODA and N. YOSHIKUNI

Laboratory for Analytical Chemistry, Faculty of Engineering, University of Chiba, Yayoi-cho, Chiba (Japan)

(Received 15th August 1975)

Wyllie and Patnode [1] were the first workers to embed ion-exchange resins in an inert binder to achieve robust membranes. The most extensive studies have been made by Pungor et al. [2—4] who attempted to prepare ion-exchange resin electrodes based on silicone rubber for the determination of SO_4^{2-}, Cl^-, OH^-, H^+, K^+, Zn^{2+} and Al^{3+}. More recent work on heterogeneous membrane electrodes involving ion-exchange resins has been reviewed by Koryta [5]. In this communication, a new cation-exchange resin—graphite paste electrode is described. This type of electrode is selective only to ions of different valency and not to individual ions. However, the electrode has some of the advantages of Růžička's selectrode [6, 7] and is very easily made. The cation-exchange resin (Ba^{2+})—graphite paste electrode can be used to follow the titration of a variety of metals by addition of EDTA and back-titration with a standard Ba^{2+} solution.

Experimental

The sensing material was a graphite paste prepared by mixing cation-exchange resin Dowex 50W,X-8 (Ba^{2+}-form, < 200 mesh, air-dried), commercial graphite powder and Nujol in the proportion of 1 : 1 : 1.1 (weight ratio). A 5-mm thick layer of the paste was packed into one end of a glass tube (3.0-mm i.d.). A platinum wire was inserted into the paste and secured through two rubber plugs. Before use, the electrode was conditioned for 24 h by soaking in 10^{-3} M $BaCl_2$ solution; it was also stored in this solution when not in use. Potential measurements were made at 25 °C with an Orion Research Ionalyzer (Model 801); an Orion single-junction saturated reference electrode (Model 90-01) was used. A Corning Model 12 Research pH Meter was used for the potentiometric titrations.

Results and discussion

The paste electrode gave a linear response for E vs. $\log a_{Ba}$ over the molarity range 10^{-5}—10^{-2} M Ba^{2+} with a slope of 24.5 mV/decade at 25 °C; this is less than the theoretical Nernstian slope. In this molarity range, the

equilibrium potential was established within 1 min; further study showed that decreasing the proportion of Nujol (1 : 1 : 0.5) yielded stable potentials within 30 s. The electrode gave stable potential readings for 3—5 days after its construction, and then the potential shifted by about + 1.5 mV a day, although the slope remained constant. Daily calibration is essential. The resin in the barium form was used, because of the high ion-exchange distribution coefficient of Ba^{2+} and of low hydrolysis tendency of the resin in that form. The selectivity coefficients were measured by the fixed interference method. The K_{ij} values, defined as $K_{ij} = a_i/a_j^{2/y}$, (where i is the primary ion (Ba^{2+}), j the interferent and y the charge of the interferent), were 3 for Li^+, 10 for Na^+, 40 for K^+, 83 for Rb^+, 2300 for Cs^+, 70 for NH_4^+, 0.36 for Mg^{2+}, 0.57 for Ca^{2+}, 0.52 for Sr^{2+}, 0.29 for Zn^{2+}, 0.62 for Cd^{2+}, 0.94 for Cu^{2+}, and $2 \cdot 10^4$ for H^+. The electrode can therefore be used only for simple barium salt solutions if direct potentiometric measurements are made.

Complexiметric titrations

The stability constant of the barium—EDTA chelate is as low as $10^{7.76}$, among the lowest of the metal—EDTA chelates. Therefore, free EDTA in the presence of more stable metal—EDTA chelates can be titrated safely with Ba^{2+} ions. Lack of adequate metal indicators for Ba^{2+} has not warranted the back-titration of many metals with barium(II) solutions. Resin paste electrodes can be used for the back-titration of individual metal ions in excess of EDTA with standard Ba^{2+} solutions. A direct plot of E vs. ml is not beneficial in the presence of the interfering Na^+ ions, which come from EDTA and the NaOH added to achieve an appropriate pH in the back-titrations. The E vs. ml curve is linear only if $a_{Ba} < K \cdot a_{Na}^2$. In this case the indicator electrode potential is approximated by $E = E_0 + (S/2) \ln K \cdot a_{Na}^2 + (S/2)\ a_{Ba}/K \cdot a_{Na}^2$, where S corresponds to RT/F, K is the selectivity coefficient for Na^+, and the other symbols have the usual meanings. The restricted addition of standard Ba^{2+} solution as well as the factor $1/K \cdot a_{Na}^2$ will result in a low potential change after the equivalence point.

Gran plots permit better location of the equivalence points. In the presence of interfering Na^+ ions the following equation should give the basis for the Gran plot

$$(V_0 + V)\ 10^{2E/2.3S} = C(V - V_e)\ 10^{2\epsilon/2.3S} + K\ \frac{m^2}{V_0 + V} \cdot 10^{2\epsilon/2.3S},$$

where $\epsilon = E_0$ + reference electrode potential + junction potential, C and V are the concentration and added volume, respectively, of the standard Ba^{2+} solution, V_0 the starting volume (sample + EDTA added + NaOH added to adjust pH), V_e the volume of the standard Ba^{2+} solution added to obtain the equivalence point, and m the amount (mmol) of Na^+ ion present. In the present titration system, m is constant and $V_0 \gg V$, so that the second term of the right-hand side of the equation can be assumed to be nearly constant. Extrapolation of the straight line described by the experimental points $[V, (V_0 + V), 10^{2E/2.3S}]$ meets the term $K m^2\ 10^{2\epsilon/2.3S}/(V_0 + V)$

for a value $V = V_e$. A typical titration curve is shown in Fig. 1. The other results for metals chosen arbitrarily are listed in Table 1. The mathematical treatment is general, being applicable to other cases, where the potentiometric titrations must be performed in the presence of interfering ions responding to the indicator electrode.

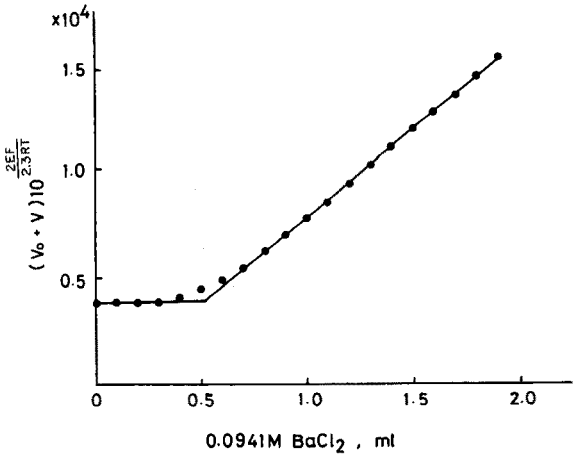

Fig. 1. Back-titration of 0.0500 mmol Zn^{2+} in excess of EDTA with 0.0941 M $BaCl_2$ solution. EDTA added: 0.1010 mmol.

TABLE 1

Titrations

(All starting volumes were 100 ml. To the metal ion solution, 10.0 ml of 0.0101 M EDTA and an appropriate amount of 0.1 M NaOH were added and diluted to 100 ml (V_0). The solution was titrated with 0.0941 M $BaCl_2$ with increment volumes of 0.010 ml. The total mmole of Na^+ present ranged from 0.4 to 1.6 depending on the acidity of the stock solution. Boiling for 5 min before the titration for Al^{3+}, Cr^{3+} and Mn^{2+} ensured complete chelation.)

Ion	Added (mg)	Found (mg)	pH	Ion	Added (mg)	Found (mg)	pH
Al^{3+}	1.55	1.57	10.3	Zn^{2+}	3.27	3.27	10.1
Ca^{2+}	2.00	2.05	11.8	Ba^{2+}	2.58	2.58	11.1
Cr^{3+}	2.29	2.26	11.0	Ba^{2+}	12.9	12.9	11.8
Mn^{2+}	2.98	3.02	11.4	Pb^{2+}	10.4	10.2	11.0
Cu^{2+}	4.14	4.07	10.3				

REFERENCES

1 M. R. Wyllie and H. W. Patnode, J. Phys. Chem., 54 (1950) 204.
2 E. Pungor, K. Toth and J. Havas, Hung. Sci. Instrum., 3 (1965) 2.
3 E. Pungor, J. Havas and K. Toth, Acta Chim. Hung., 41 (1964) 239.
4 E. Pungor and J. Havas, Acta Chim. Hung., 50 (1966) 77.
5 J. Koryta, Ion-Selective Electrodes, Cambridge University Press, Cambridge, 1975.
6 J. Růžička and C. G. Lamm, Anal. Chim. Acta, 53 (1971) 206; 54 (1971) 1.
7 J. Růžička, C. G. Lamm and J. C. Tjell, Anal. Chim. Acta, 62 (1972) 15.

Analytica Chimica Acta, 87 (1976) 215—219

Short Communication

A MICROSAMPLING CUP SYSTEM FOR USE IN ATOMIC ABSORPTION SPECTROMETRY WITH A NITROUS OXIDE—ACETYLENE FLAME*

M. KAHL, D. G. MITCHELL, G. I. KAUFMAN and K. M. ALDOUS

Division of Laboratories and Research, New York State Department of Health, New Scotland Avenue, Albany, NY 12201 (U.S.A.)

(Received 12th April 1976)

Various atomic absorption procedures for analyzing microsamples have been developed; these include flameless devices such as the graphite furnace, carbon rod, carbon filament and tantalum strip atomizers, and the Delves microsampling cup with flame atomization [1]. For routine use with high sample throughput, the microsampling cup—flame technique has several important advantages compared with flameless atomization devices: (a) sample preparation can be carried out away from the spectrometer; (b) samples can be wet- or dry-ashed in the cup, which reduces contamination problems and improves efficiency; and (c) the spectrometric measurement process is rapid, typically 8—15 s per measurement.

Use of the microsampling cup technique with a nitrous oxide—acetylene flame rather than an air—acetylene flame greatly increases the number of determinable elements [2]. With such an arrangement, Ag, Cd, Cu, Pb and Zn can be determined without significant interference effects in several "difficult" matrices [3]. This is a distinct advantage over flameless techniques, which are very interference-prone.

There are two major instrumental problems with the use of the nitrous oxide—acetylene flame in a microsampling cup—flame atomization instrument: the possibility of an explosive flashback is a significant hazard, particularly with a hot absorption tube located over the burner head; and cups, cup-holding loops and absorption tubes cannot always satisfactorily withstand the hot flame and its associated thermal shock. This communication describes an instrument system that overcomes these problems. It successfully incorporates the nitrous oxide—acetylene flame in a microsampling cup—flame apparatus suitable for routine analysis of aqueous microsamples.

Instrument design

The instrument system (Fig. 1) consists of a burner, a silicon carbide absorption tube, a molybdenum loop to hold molybdenum cups and a

*Presented in part at the Pittsburgh Conferences on Analytical Chemistry and Applied Spectroscopy, March 4—8, 1974 and March 3—7, 1975.

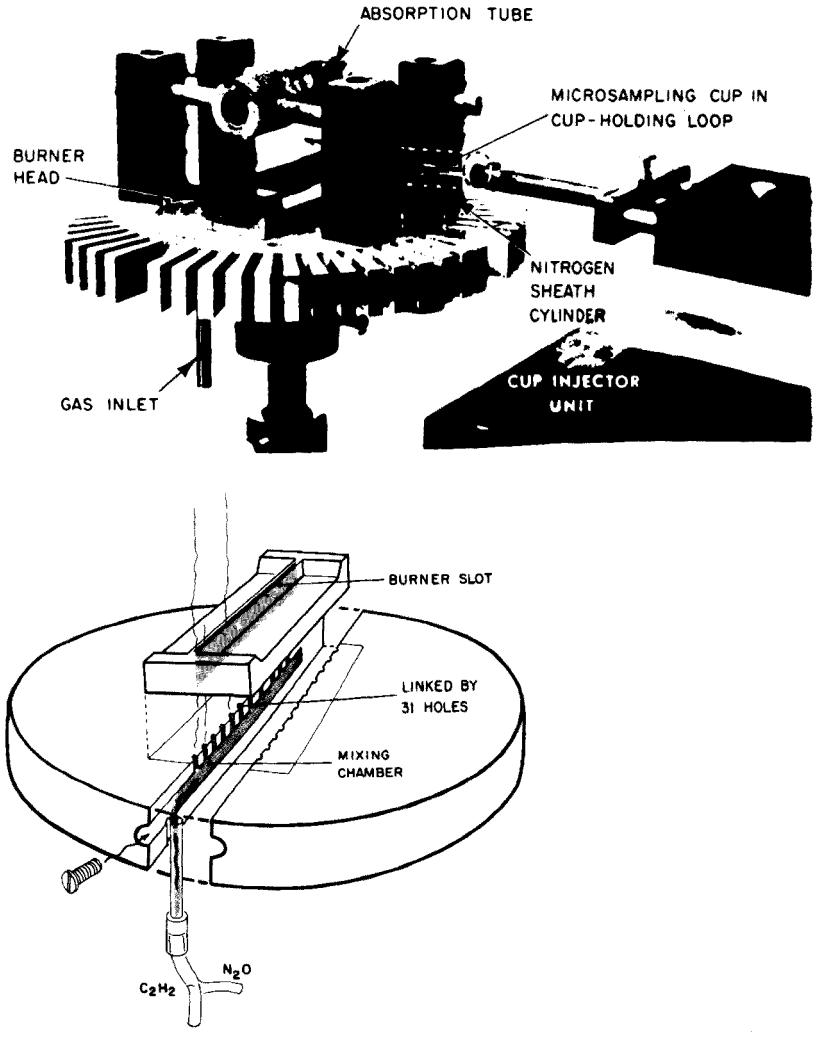

Fig. 1(a). Burner-injector system. (b) Schematic view of the burner head.

nitrogen sheath cylinder in which the cups can be cooled without oxidation. A very stable bench-mounted cup injector unit is used to feed sample cups to the flame.

Burner. The burner (Fig. 1b) was constructed from type 316 stainless steel. Fuel and oxidant are fed via a Y-connector to a small volume (0.9-cm^3) mixing chamber. The gas mixture passes through a row of 31 holes (0.66-mm diameter) to a 0.38 × 57-mm burner slot which is sharply beveled to promote air entrainment into the flame and to minimize carbon buildup. This system provides mixing sufficient to produce a uniform laminar flame.

Flashback problems have been minimized in three ways. (a) A flame trap is built in. The diameter of the holes (0.66 mm) through which mixed gases are fed to the burner slot is very close to the quenching distance, 0.5 mm, for the nitrous oxide—acetylene flame [4]. Furthermore, the 31-hole flame trap has a total area of 10.6 mm^2, compared with the 21-mm^2 burner slot. Thus, even if the gas velocity at the exit slot drops sufficiently to allow the flame to propagate inside the burner, it must then drop another 50 % before the flame can reach back into the mixing chamber. (b) As a heat sink, an aluminum mounting block (15-cm diameter, 1.25-cm thick) is fitted to the burner head. (c) The volume of mixed gases is minimized by having a total burner volume of about 2 cm^3 from the Y-connector to the exit slot, i.e. <1 % of the mixed gas volume of a conventional nebulizer burner. The severity of any flashback will thus be greatly reduced.

Absorption tube. Alumina absorption tubes mounted on ceramic bridges [2, 3] cannot long withstand the thermal shock of the hot flame, even when heated gradually by first burning an air—acetylene flame for 10 min. They have been replaced by a 50-mm × 9.5-mm i.d. × 19-mm o.d. silicon carbide tube mounted on two 100-mm × 4.8-mm silicon carbide rods.

Cups and loops. Holed cups fabricated from 0.13-mm molybdenum plate and geometrically similar to the holed nickel cups reported earlier [5] are supported by triangular loops fabricated from 3-mm × 0.38-mm molybdenum ribbon.

Nitrogen sheath. At the temperatures reached in the nitrous oxide—acetylene flame, molybdenum cups and loops oxidize rapidly in air with evolution of copious white fumes. This causes nonspecific absorption on subsequent injections. In addition, the cup surface is corroded and cup life is limited to about 20 injections. This problem was solved by withdrawing the cup into an atmosphere of nitrogen. Nitrogen fed at ca. 3 l min^{-1} to the 5 × 1.8-cm diameter cylinder (Fig. 1) adequately protects the cup from oxidation and extends cup life to at least 50 injections. To conserve nitrogen gas, flow is controlled by a solenoid valve (No. 82615, Automatic Switch Co., Florham Park, NJ, USA) with a 0—10-s timing circuit (ABTI-120-1010, Sensitrol Inc., Albion, IL, USA).

Cup-injector unit. A heavy (8-kg) stable cup injector is firmly clamped to the bench. It is fitted with a microswitch to control the solenoid valve of the nitrogen sheath.

Standards. ACS reagent-grade salts were used to prepare aqueous standards for the metals listed in Table 1.

Instrument operation

The burner-absorption tube unit is mounted on the nebulizer chamber of an atomic absorption spectrometer (Varian-Techtron Model AA5) and optically aligned by conventional burner position controls. A cup is placed in the cup-holding loop and located about 1 mm below the entrance hole of the absorption tube. The timing circuit is set to open the solenoid valve for

TABLE 1

Detection limits[a] obtained with the microsampling cup nitrous oxide—acetylene flame system

Element	Wavelength (nm)	Detection limit		Optimum gas flow (l min^{-1})	
		$\mu g\ l^{-1}$	ng	N_2O	C_2H_2
Ag	328.1	0.4	0.08	4.7	2.8
As	193.7	40.0	8.0	1.9	1.2
Au	242.8	5.0	1.0	3.8	2.4
Bi	223.1	7.0	0.35	3.8	2.4
Cd	228.8	0.05	0.01	3.8	2.4
Co	240.7	25.0	5.0	5.6	3.5
Cr	357.9	100.0	20.0	5.2	3.3
Cu	324.7	3.0	0.6	5.2	3.3
Li	670.7	8.4	1.6	5.2	3.3
Mn	279.5	5.0	1.0	5.2	3.3
Ni	232.0	50.0	10.0	5.6	3.3
Pb	217.0	0.5	0.1	3.8	2.4
Sb	217.6	30.0	6.0	3.8	2.4
Se	196.0	10.0	2.0	1.47	0.9
Sn	286.3	200.0	40.0	5.2	3.3

[a]Defined as the concentration which produces a peak absorbance signal equal to the peak-to-peak noise of the baseline.

6 s when the cup is withdrawn from its position under the tube. Gas flow rates are set at 3—4 l min^{-1} for nitrous oxide and at 3 l min^{-1} for acetylene, and the nitrous oxide—acetylene flame is ignited without first burning an air—acetylene flame. Before use, cups are burned off for about 15 s or until the absorption baseline returns to zero at the analytical wavelength.

Up to 100 μl of sample standard is pipetted (20, 50 or 100-μl Eppendorf pipette) into the cup, dried and then injected into the flame. Both peak and integrated absorbance are measured.

Instrument performance

Flashback. Many attempts were made to induce flashback. The nitrous oxide—acetylene flame was operated at many different flow rates, including very low flow rates, and the two gases were turned off in various sequences. All attempts failed except when both gases were switched off rapidly and simultaneously, which resulted in a fairly gentle pop rather than a typical explosive bang.

Effect of absorption tube position on sensitivity. A volatile (Cd), a moderately volatile (Ag) and a less-volatile (Co) element were studied. The absorption tube was located 12, 14, 17 or 25 mm above the burner, and solutions giving about 50 % absorption were analyzed. A slightly fuel-rich flame was used. At nitrous oxide flow rates of 3—6 l min^{-1}, sensitivity increased with decreasing tube heights, reaching a maximum at 12 mm. This

is as close to the burner as practicable, and the tube was located in this position for all later experiments.

Effect of gas flow rates on sensitivity. The effect of gas flow rates was investigated by varying the nitrous oxide rates over the range 1—6 l min^{-1}, with the acetylene flow rate about 60 % of the oxidant flow rate. For highly volatile elements such as selenium, sensitivity increased with decreasing flow rates. Less volatile elements such as cobalt required maximum flow rates, and moderately volatile metals such as silver showed maximum sensitivity at intermediate flow rates (Table 1).

Detection limits and precision data. Detection limits were obtained for elements with holed cups and at their respective optimum gas flow rates (Table 1). Precision data were obtained for two representative elements, Co and Pb, at the ca. 50 % absorption level. The relative standard deviations were 6.7 % for both metals at concentrations of 0.5000 $\mu g\, l^{-1}$ and 0.025 $mg\, l^{-1}$, respectively.

Discussion

The instrument system described has been working satisfactorily for over two years. It is convenient and reliable, and gives good detection limits for a wide range of metals in aqueous solutions. The fact that sensitivity increases with decreasing tube height in flame suggests that the tube should be placed as close as practicable to the burner. The major remaining challenge is to identify cup materials which can withstand acids and high-temperature oxidation. Such materials would allow sample digestion in the cup and eliminate the need for the nitrogen sheath.

This project was supported in part by NIH research grant number 5 RO1 GM20431-02 awarded by the Institute of General Medical Sciences, PHS/DHEW.

REFERENCES

1 H. T. Delves, Analyst (London), 95 (1970) 431.
2 D. G. Mitchell, A. F. Ward and M. Kahl, Anal. Chim. Acta, 76 (1975) 456.
3 A. F. Ward, D. G. Mitchell and K. M. Aldous, Anal. Chem., 47 (1975) 1656.
4 K. M. Aldous, B. W. Bailey and J. M. Rankin, Anal. Chem., 44 (1972) 191.
5 A. F. Ward, D. G. Mitchell, M. Kahl and K. M. Aldous, Anal. Chem., 20 (1974) 1199.

Analytica Chimica Acta, 87 (1976) 221—225

Short Communication

DETERMINATION OF TRACE QUANTITIES OF SILICON IN HIGH-PURITY ZIRCONIUM

P. JAGAM

Neutron Activation Laboratory, Geology Department, Dalhousie University, Halifax (Canada)

D. S. MURTY

Physics Department, Saint Mary's University, Halifax (Canada)

(Received 22nd April 1976)

In a study of the 14-MeV neutron activation products of zirconium enriched in ^{96}Zr (86.4 %), it became necessary to consider the possibility of ^{28}Al activity being produced by a $^{28}Si(n,p)$ reaction from a silicon impurity in the sample. Since only 40 mg of the enriched zirconium sample was available, a nondestructive method of analysis for silicon was essential. In addition, it was considered worthwhile to obtain natural samples of zirconium from different manufacturers to study the variation of the silicon content.

The $^{28}Si(n,p)^{28}Al$ reaction with 14-MeV neutrons has been extensively used in the determination of major and minor quantities of silicon in iron [1], steel [2] and rocks [3, 4], but there is little information about trace quantities. The present communication reports a non-destructive method developed for the zirconium matrix.

Experimental

Apparatus. 14-MeV neutrons were produced by the $^{3}H(d,n)\,^{4}He$ reaction with a Kaman Nuclear A-711 neutron generator operated at 120 kV with an estimated flux of 10^9 n cm^{-2} s^{-1}. A pneumatic transfer system and a dual-axis rotator assembly were used for irradiation of samples in conjunction with a programmed electronic timer. A sample and a standard could be simultaneously irradiated. At the end of the irradiation, both samples were simultaneously returned to the load port with a delay of 5 s, and then transferred manually to two ORTEC 40-cm^{-3} Ge(Li) detectors of the right-angle dipstick variety. Counting could be commenced with a minimum delay of 30 s from the end of the irradiation time.

The detectors were housed in a rectangular lead castle (36 × 62 × 46-in.) with 2 in. of lead all around, and arranged back to back so as to separate the active volumes by 48 in.; a 2-in. thick lead wall separated the detectors within the castle.

The detectors were connected to a Nuclear Data Model 50/50 4096-channel analyzer, equipped with two a.d.c.'s, a two-parameter a.d.c. control and two live-time clocks. The gating signals provided by the clocks were used to count the clock-times separately for the two detectors during the analyzer live-time period for a first-order dead-time correction wherever necessary.

Nuclear data. The pertinent nuclear data are summarized in Table 1. The important reactions are the $^{90}Zr(n,2n)^{89m}Zr$ and $^{28}Si(n,p)^{28}Al$ reactions.

Sample preparation. Seven samples of zirconium were obtained from different manufacturers; three were in oxide form and four in metallic form. Two of the metal samples were machined carefully to give turnings suitable for packing in the polyethylene sample holders (3/8 in. diameter, 1.5 in. long). The ZrO_2 sample enriched in ^{96}Zr was first packed in 1-mil polythene and then packed centrally in the sample holder.

Preliminary considerations. For a 3-g 100 % SiO_2 standard, an irradiation of 150 s, a delay of 60 s, and a count of 300 s gave an average sensitivity of 0.09 counts/p.p.m. on one detector and 0.12 counts/p.p.m. on the other. The samples were counted at 3/8 in. from the face of the detector, the distance being controlled by a 3/8-in. thick perspex absorber. A delay time of 60 s was chosen to minimize the dead-time effects and any interference from the 8-s ^{16}N activity produced by fast neutron reaction with oxygen in the samples.

Since only traces of silicon were present in the samples, cyclic irradiation and counting were necessary to accumulate sufficient counts under the full energy 1778.9-keV ^{28}Al peak. Since the ^{28}Al half-life is 2.243 min, a cycle time of 30 min was chosen to allow for complete decay of the activity in the standard. The standards were 100 % silica and were previously calibrated against international geochemical standards. The known calibration is considered to be accurate to 0.1 % absolute.

TABLE 1

Fast neutron reactions on silicon and zirconium which produce prominent γ-peaks

Reaction	Half-life [5]	γ-ray energy (keV) abundance [5]
$^{90}Zr(n,p)^{90m}Y$	3.19 h	202.4(9.7 −1), 479.3(9.1 −1)
$^{90}Zr(n,\alpha)^{87m}Sr$	2.81 h	388.4(8.25 −1)
$^{90}Zr(n,2n)^{89m}Zr$	4.18 min	587.8(1.00) 1507.4(7.2 −2)
$^{90}Zr(n,2n)^{89}Zr$	78.5 h	511(β^+), 909.2(1.00) 1712.9(7.7 −3)
$^{94}Zr(n,p)^{94}Y$	19.4 min	919.2(7.357 −1)
$^{92}Zr(n,p)^{92}Y$	3.53 h	934.5(1.372 −1)
$^{28}Si(n,p)^{28}Al$	2.243 min	1778.9(1.000)

Procedure. The sample and standard were simultaneously irradiated in the dual-axis rotator for 150 s. After 60 s, they were counted simultaneously in the live-time mode for a period of 300 s, the samples always being on the more efficient detector. A second count with a delay of 15 min was also accumulated for 300 s to observe the decay of the activity. To facilitate the accumulation of both the counts, the data from each count were stored separately on a cartridge tape unit during the experimental run. Each run consisted of 20 cycles. At the end, an on-line computer was used to add the 20 individual spectra from the sample to obtain a cumulative total spectrum for final analysis.

A typical spectrum thus obtained is shown in Fig. 1. The peak areas at 1507.4 and 1778.9 keV are directly proportional to the amounts of zirconium and silicon, respectively. The peak areas were determined by using SAMPO program [6] and a CDC 6400 computer system.

Results and discussion

The dual-axis rotator arrangement for irradiation permits the use of the silica standard as a flux monitor as well as a comparator for silica determination. From the calibration constants of the two detectors, the counts under the peak at 1778.9 keV from the SiO_2 standard are used for a direct calculation of silicon in each sample by simple proportion. The results obtained together with the values quoted by the manufacturers are given in Table 2. The values of the ratio of the 1778.9 to 1507.4-keV peak areas are included in Table 2, to show the variation of silicon relative to zirconium, with Zr as an internal monitor in the different samples.

The silicon values (Table 2) show good agreement for Zircaloy-2, which is SRM 360a (N.B.S.) with a certified value based on the molybdenum blue

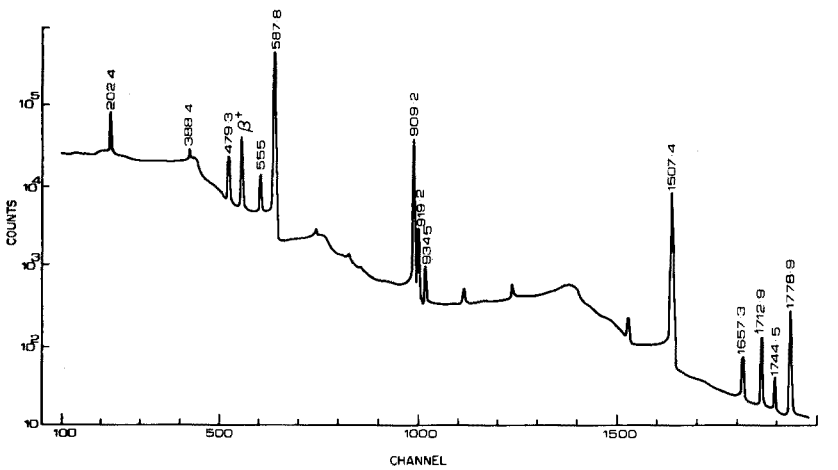

Fig. 1.

TABLE 2

Results for silicon present (as p.p.m. Si)

Material	Supplier	Quoted values[a]	This work	Ratio of $\frac{1778.9}{1507.4} \times 10^2$
$^{96}ZrO_2$	O.R.N.L.	0.01 %	3050	13.8
ZrO_2	Johnson-Matthey	10—20	247	7.95
ZrO_2[a]	Spex Ind., N.J.	100—300	108 ± 11	3.49
Zr	Spex Ind., N.J.	<30	99	2.11
Zircaloy-2	N.B.S.	51	60 ± 5[b]	1.45
Zirconium	N.B.S.	(30)	139	2.83
Zirconium	Materials Research Corp., N.Y.	2	25 ± 2[c]	0.54

[a]Manufacturer's data from spectrochemical, photometric and mass spectrographic methods. [b]Three determinations. [c]Two samples.

photometric method. The other quoted values are semiquantitative general ranges obtained by various methods. Except for the Spex ZrO_2, our values are several times higher than the reported ranges. The following checks were made to see if a high bias could be introduced by the system or the method itself.

Because of the high energy of the γ-ray from the standard, interference between the two sections of the lead castle must be ruled out. In a test run, the standard was irradiated and counted as before, while the other detector simply recorded the background; this test clearly ruled out the possibility of interference. Similarly, the contribution from the blank was also ruled out in a separate run with an unused blank. A so-called soiled-blank test was made to see how much silica a blank picked up because of dust in the system; a regularly used, well worn blank was measured, but even this test yielded only an effective contribution of about 3 p.p.m. Si.

Another possibility is an interference reaction contributing to the 1778.9-keV peak either directly by the same activity being produced or by the emission of a γ-ray of this energy from another activity. The absence of this peak in the second count spectrum, recorded with 15-min delay, indicated that the activity has a short half-life ($\ll$ 15 min); from the compilation of Bowman and MacMurdo [5], it can be concluded that this activity is indeed due to the $^{28}Si(n,p)^{28}Al$ reaction.

An interfering reaction that can produce the same activity is $^{31}P(n,\alpha)^{28}Al$, but the manufacturer's data do not include phosphorus, except for the zirconium from Materials Research Corp., for which a value of less than 0.1 p.p.m. is quoted (mass spectrometry). In the system used here 2 g of phosphorus was found to be approximately equal to 1 g of silicon in terms of

producing ^{28}Al activity. If phosphorus were the interfering impurity, it would have to be present in even higher quantities than the silicon reported. However, even these levels of phosphorus are around the lower limits of detection for spectrographic analysis, in most of the samples. The enriched sample of $^{96}ZrO_2$ (ORNL) has a detailed report on at least 35 elements to 0.01 %, but phosphorus was not included. Therefore, it can reasonably be concluded that there is no high bias in the values reported here from phosphorus interference.

The authors are grateful to Professor G. K. Muecke for providing a sample of Specpure zirconium, and for his encouragement in this work.

REFERENCES

1 R. Van Grieken, A. Speecke and J. Hoste, J. Radioanal. Chem., 6 (1970) 385.
2 R. Van Grieken, R. Gijbels, A. Speecke and J. Hoste, Anal. Chim. Acta, 43 (1968) 381.
3 K. Huysmans, R. Gijbels and J. Hoste, Talanta, 20 (1973) 843.
4 D. M. Bibby, Anal. Chim. Acta, 79 (1975) 125.
5 W. W. Bowman and K. W. MacMurdo, At. Data Nucl. Data Tables, 13 (1974) 89.
6 J. T. Routti and S. G. Prussin, Nucl. Instrum. Methods, 72 (1969) 125.

Analytica Chimica Acta, 87 (1976) 227—231

Short Communication

DETERMINATION OF EUROPIUM AND DYSPROSIUM IN ROCKS BY NEUTRON ACTIVATION AND HIGH-RESOLUTION x-RAY SPECTROMETRY

P. VOLDET

Department of Mineralogy, University of Geneva, 13 rue des Maraîchers, 1211-Geneva-4 (Switzerland)

W. HAERDI

Department of Mineral, Analytical and Applied Chemistry, University of Geneva, 30 quai E. Ansermet, 1211-Geneva-4 (Switzerland)

(Received 30th April 1976)

Neutron activation analysis has been used in the determination of various rare-earth elements in rocks for a number of years. The present communication describes a rapid method for the simultaneous determination of europium and dysprosium in rocks. The short half-life isotopes ^{152m}Eu ($t_{1/2}$, 9.3 h) and ^{165}Dy ($t_{1/2}$, 2.36 h), and an experimental AGN-201-P reactor with a nominal thermal neutron flux of 10^9 n cm^{-2} s^{-1} were used.

The rare-earth elements must be separated from the other elements present in rocks before neutron activation. The essential purpose of the separation when short half-life isotopes are employed is to obtain the same matrix for different types of rocks and standards for the measurements of activity by high-resolution x-ray spectrometry. The analytical method proposed is based on a gravimetric separation of the rare-earth group [1], and on a chromatographic method of concentration of the group described by Ryabukhin et al. [2].

Experimental

Standards. Solutions (100 μg ml^{-1}) of Eu and Dy were prepared by dissolving the appropriate weighted quantities of the oxides (Fluka p.a.) in dilute nitric acid.

Procedure. The separation involved the following steps: (1) decomposition of 1g of rock powder by acid attack with HF, HNO_3 and H_2SO_4 in the conventional way; (2) ammoniacal precipitation and filtration of the hydroxides; (3) dissolution of the precipitate in dilute HCl, evaporation of the solution, and dissolution of the residue in 5 ml of 0.1 M HCl; (4) chromatography. For chromatography, the solution was passed through a Dowex 50W-X8 cation-exchange column (100-200 mesh, 16 mm diam., 120 mm long, pre-equilibrated with 4 M HCl), at a flow-rate of about 1 ml min^{-1}. The rare-earth

elements were eluted with 4 M HCl. This column chromatography allows the separation of micro amounts of rare-earth elements from the large amounts of iron, aluminium, magnesium, calcium, and other elements.

This study was carried out for different rocks, the elution being tested initially with a radioactive tracer, ^{152,154}Eu. Figure 1 shows an elution curve of europium. The recovery was 99—100 %.

After the chromatography, the eluate was evaporated after addition of 1 mg of Ca carrier. The residue was dissolved in 5 ml of 0.1 M HCl, 2 ml of a saturated oxalic acid solution was added, and the oxalates were precipitated with ammonia solution (1 + 2) at pH 5.0. After filtration of the oxalates on a circle (diam. 2 cm) of S and S 589^3 paper, the paper was dried and sealed in thin polyethylene foil.

The standards (5 μg Eu, 5 μg Dy and 5 μg Eu + 5 μg Dy) were prepared by precipitation of the oxalates as described above after the addition of 1 mg of Ca carrier.

Irradiation and counting. Samples and standards were irradiated for 30 min in the AGN-201-P reactor at a thermal neutron flux of 10^9 n cm^{-2} s^{-1}. After a cooling time of 5—200 min, each sample was counted for 500 s with a Ge detector (Seforad; 200 mm^2 in area and 7 mm in depth). The signals from the detector were passed through a preamplifier (Seforad SR 200) and an amplifier with pulse stretcher (Seforad SR 300). The resulting pulses were analysed by a 4096-channel Zoomax SEIN analyzer (2048 channels were used in this counting). The resolution of the system for the 5.9-keV Mn Kα x-ray (from ^{55}Fe) and the 122-keV ^{57}Co peak is 225 and 520 eV, respectively. It was calibrated at 0.06 keV per channel.

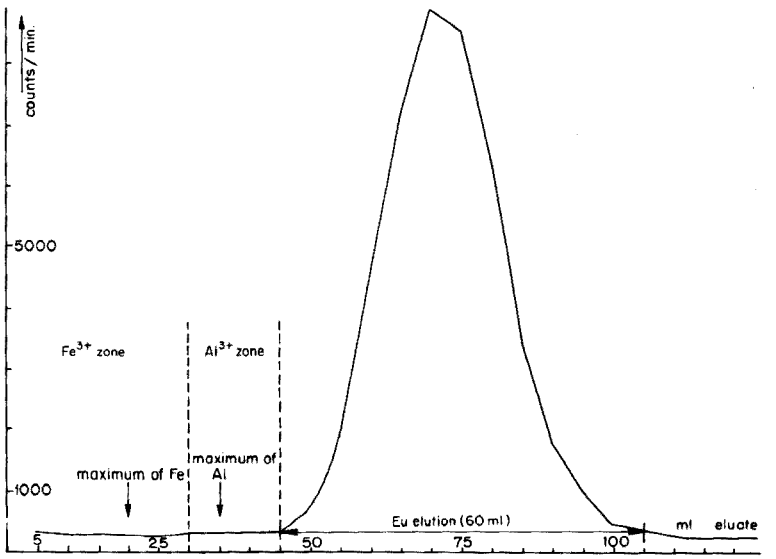

Fig. 1. Elution curve of europium.

For the determination of ^{152m}Eu, the Sm Kα x-rays at 39.52, 40.13 keV and 45.40 keV were measured; for ^{165}Dy, the Ho Kα x-rays at 47.53 and 53.87 keV were measured.

Results and discussion

The method described allows the determination of a minimum amount of about 0.2 p.p.m. of Eu and Dy in rocks. The precision (of the order of 5—10 %) is limited principally by the accuracy of the measurement method. The other rare earths do not interfere in the method employed (Fig. 2).

This method was applied to various geological standards. The data obtained for Eu and Dy are given in Table 1 and are compared with previous results; the agreement is generally good. The method described has the following advantages: (1) absence of interferences by the use of x-ray spectrometry with a Ge detector instead of γ-ray spectrometry [7]; (2) speed of irradiation and measurement time, since the waiting period of 3—4 weeks necessary in the usual instrumental method (measurement of ^{152}Eu) is eliminated.

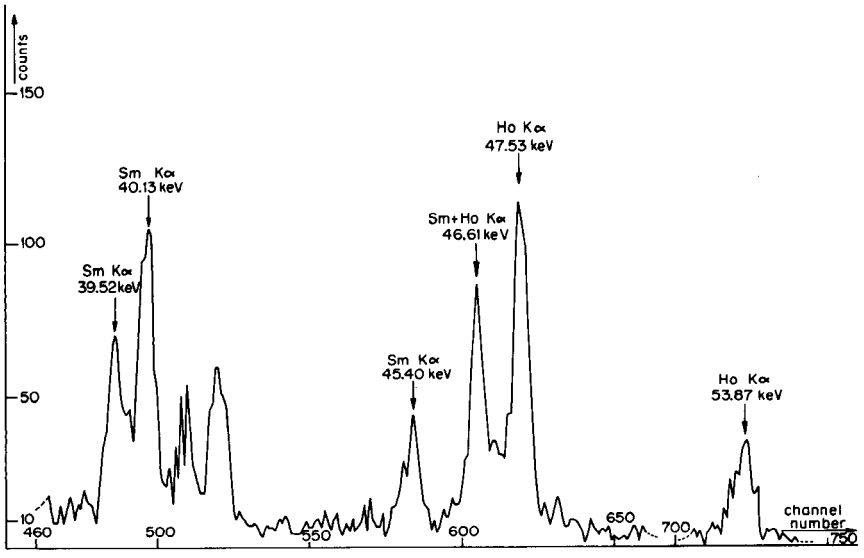

Fig. 2. Partial x-ray spectrum of grandiorite GSP-1 irradiated for 30 min, recorded 50 min after the irradiation.

TABLE 1

Comparison of results with literature data

Rock	References	Eu (p.p.m.)	Dy (p.p.m.)
Andesite	Flanagan [3]	1.7	3.5
AGV-1[a]	Hooker et al. [4]	1.54—1.7	3.55—3.5
	This work	1.72	4.28
Basalt	Flanagan [3]	1.94	6.3
BCR-1[a]	Hooker et al. [4]	1.89—1.94	6.3—6.35
	This work	1.90	6.34
Granite	Flanagan [3]	1.5	2.6
G-2[a]	Hooker et al. [4]	1.34—1.5	2.11—2.6
	This work	1.24	2.48
Granodiorite	Flanagan [3]	2.4	5.4
GSP-1[a]	Hooker et al. [4]	2.23—2.21	5.52—5.45
	This work	2.68	5.82
Granite	Certified value	2	17
NIM-G[b]	Jackson and Strelow [5]	0.39	15.8
	This work	0.45	16.28
Syenite	Certified value	0.4	0.6
NIM-S[b]	Jackson and Strelow [5]	0.24	0.30
	This work	0.36	0.63
Lujavrite	Certified value	2	n.d.[c]
NIM-L[b]	Jackson and Strelow [5]	1.0	1.9
	This work	1.26	3.72
Norite	Certified value	0.6	n.d.
NIM-N[b]	Jackson and Strelow [5]	0.67	1.1
	This work	0.69	1.93
Pyroxenite	Certified value	0.2	n.d.
NIM-P[b]	Jackson and Strelow [5]	0.12	0.48
	This work	0.25	1.21
Dunite	Certified value	0.06	n.d.
NIM-D[b]	Jackson and Strelow [5]	0.0032	0.019
	This work	<0.1	<0.1
Syenite	Abbey et al. [6]	2.2—2.9	n.d.
SY-2[c]	This work	2.74	27.3
Syenite	Abbey et al. [6]	14—18	n.d.
SY-3[c]	This work	20	125
Gabbro	Abbey et al. [6]	1.4	n.d.
MGR-1[c]	This work	2.4	4.6

[a]U.S.G.S. International geological standards.
[b]NIMROC geochemical reference materials, South African Bureau of Standards, Pretoria. The samples NIM-G, S, L. N, P and D had, respectively, the serial numbers SARM-[1-6]-1/329. The certified values are taken from SARM 1-6 (1974). Location details are given in ref. 1.
[c]Not determined.
[d]Canadian rock samples for use as certified reference materials, Geological Survey of Canada, Ottawa.

We thank Professor R. Beeler, in charge of the reactor of the Faculty of Sciences, University of Geneva, and Mr. E. Burgener, the operator of this equipment. We are also grateful to Professor F. Jaffé, Department of Mineralogy, University of Geneva, for a critical review of the manuscript.

REFERENCES

1 P. Voldet and W. Haerdi, Anal. Chim. Acta, 72 (1974) 111.
2 V. A. Ryabukhin, N. S. Stroganova, N. G. Gatinskaya and A. N. Ermakov, Zh. Anal. Khim., 28 (1973) 2166.
3 F. J. Flanagan, Geochim. Cosmochim. Acta, 37 (1973) 1189.
4 P. J. Hooker, R. K. O'Nions and R. J. Pankhurst, Chem. Geol., 16 (1975) 189.
5 P. F. S. Jackson and F. W. E. Strelow, Chem. Geol., 15 (1975) 303.
6 S. Abbey, A. H. Gillieson and G. Perrault. Report MPR/MSL 75-132 (TR).
7 M. Mantel and S. Amiel, J. Radioanal. Chem., 16 (1973) 127.

Analytica Chimica Acta, 87 (1976) 233—237

Short Communication

SPECTROPHOTOMETRIC DETERMINATION OF NICKEL BY OXIDATION OF THE NICKEL(II)—NIOXIME COMPLEX WITH HEXACYANOFERRATE(III) IN SODIUM HYDROXIDE MEDIUM

C. GONZALEZ PEREZ, L. POLO DIEZ and A. SANCHEZ PEREZ
Department of Analytical Chemistry, University of Salamanca, Salamanca (Spain)
(Received 23rd April 1976)

Nickel can be determined spectrophotometrically with various vic-dioximes as chromogenic reagents [1]. Two types of methods have been developed: those based on extraction of the nickel(II) precipitate into an organic solvent, usually chloroform, with measurement of the absorbance in the extract; and those based on the intense red colour produced in alkaline solutions in the presence of oxidizing reagents. The oxidation of the nickel(II)—dimethylglyoxime complex was first studied by Feigl [2]; for the colorimetric determination of nickel, bromine has been widely used as the oxidant, but the red colour fades with time, so that many other oxidants have been examined. After some disagreement in the literature, it seems certain [3] that nickel is present in this soluble complex as Ni(IV).

Nioxime (cyclohexane-1,2-dionedioxime) has not been used extensively as a colorimetric reagent for nickel. Johnson and Simmons [4] obtained a red colour after oxidation with bromine, but preferred to stabilize the nickel(II)—nioxime complex with gum arabic. Both types of procedure have been used spectrophotometrically [5—7]. The present communication describes a spectrophotometric study of the soluble red nickel—nioxime complex obtained from nickel(II) solutions in presence of an excess of nioxime in sodium hydroxide medium, with hexacyanoferrate(III) as the oxidizing agent. Optimal conditions for determination of nickel, and interferences from elements commonly encountered in steels are considered.

Experimental

Reagents and apparatus. All the chemicals used were reagent grade, except nioxime, which was synthesized [8]. A stock solution (0.10 M) of nickel nitrate was standardized by the gravimetric dimethylglyoxime method. A Unicam SP1800 spectrophotometer equipped with a Unicam AR 25 linear recorder and 1.0-cm glass cells was used.

Preliminary experiments. The oxidation of nickel(II) by air in alkaline medium in the presence of nioxime is slow; attempts were made to find a suitable oxidizing reagent to increase both rate of reaction and stability of the

complex obtained. The characteristic absorption band of the complex at 460 nm was used in studying the effects of some oxidants. With air, the maximum absorbance (A_{max}) is obtained after about 3 h and the stability of the colour is quite good; with $(NH_4)_2S_2O_8$, the A_{max} values are lower and the colour fades rapidly, especially for large $(NH_4)_2S_2O_8$ concentrations; with $NaBiO_3$, the A_{max} values are obtained after about 90 min, but the absorbance then decreases with time; with Br_2 in high concentrations the red colour is obtained rapidly but also fades quite rapidly; using lower concentrations of Br_2 the colour is more stable. The best results were obtained with $K_3Fe(CN)_6$.

Procedure for spectrophotometric determination of nickel. Transfer an aliquot containing nickel(II) in the range 30—400 μg to a 50-ml volumetric flask which contains a solution of 4 g of sodium hydroxide, dissolved and cooled previously, and 6 mg of nioxime. Then add a solution containing 10 mg of potassium hexacyanoferrate(III) and finally dilute to the mark with distilled water. After 15 min, measure the absorbance at 460 nm using water as reference.

Results and discussion

The concentration of hexacyanoferrate(III) affects both the rate of development of the colour and the maximum absorbance, as shown in Fig. 1. The stability of the colour is quite good and the optimum concentration is about six times greater than the nickel(II) concentration. The increase in absorbance in the absence of hexacyanoferrate is also shown (air is of course present); the absorbance of these solutions stays unchanged for weeks.

The effect of sodium hydroxide concentration on the absorbance of different solutions is shown in Fig. 2. With increasing sodium hydroxide con-

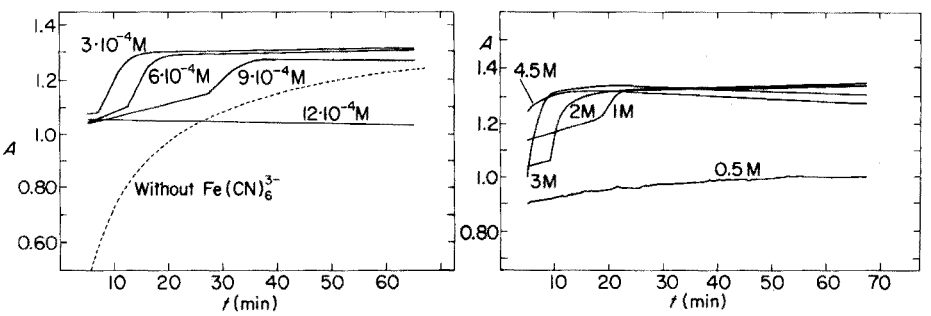

Fig. 1. The influence of the potassium hexacyanoferrate(III) concentration on the absorbance as a function of the time. [Ni(II)] = $1.0 \cdot 10^{-4}$ M, [Nioxime] = $6.0 \cdot 10^{-4}$ M, [NaOH] = 1.5 M; λ = 460 nm.

Fig. 2. The influence of the sodium hydroxide concentration on the absorbance as a function of the time. [Ni(II)] = $1.0 \cdot 10^{-4}$ M, [Nioxime] = $6.0 \cdot 10^{-4}$ M, [$K_3(Fe(CN)_6)$] = $6.0 \cdot 10^{-4}$; λ = 460 nm.

centrations above 3 M, the stability of the colour decreases; about 2 M was taken as the optimum.

Figure 3 shows the effect of nioxime concentration on the rate of development and on the stability of the red colour. Maximum colour development is faster when the amount of nioxime is increased. A mole ratio of at least 6:1 (nioxime: Ni(II)) is necessary to obtain both maximum absorbance and rapid development, but the maximum absorbance is not affected by ratios up to at least 20:1.

The colour of the complex is stable at temperatures in the range 17—40 °C. At 50 °C, the absorbance decreases gradually up to 60 min; at 62 °C the complex decomposes rapidly, probably because of an increased rate of reaction between nickel in higher oxidation states and the other components in the solution, especially hydroxide. Room temperature was therefore used in all cases.

Beer's law and precision. Beer's law was obeyed over the range $1 \cdot 10^{-5}$—$15 \cdot 10^{-5}$ M. The molar absorptivity is about 13,600 l mol^{-1} cm^{-1} at 460 nm.

The reproducibility was estimated from the results of ten sample solutions, each with a final Ni(II) concentration of $1.0 \cdot 10^{-4}$ M. A mean absorbance of 1.397 was found; the standard deviation and the relative standard deviation were $5 \cdot 10^{-3}$ and 0.36 %, respectively.

Interferences. The effects of elements commonly found in steels were studied. First, the influence of iron(III) in a 30:1 mole ratio, (Fe III:Ni II) was considered. Maximum absorbance values cannot be obtained after filtering off the iron hydroxide precipitate because of adsorption phenomena; this interference was avoided by using tartrate as masking agent. In the presence of tartrate the red colour develops more slowly, probably owing to competitive reactions between nioxime and tartrate for nickel, but eventually the same maximum absorbance values as in the absence of iron are obtained after

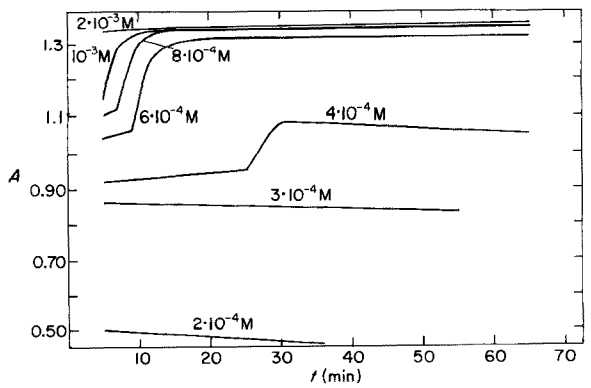

Fig. 3. The influence of the nioxime concentration on the absorbance as a function of the time. [Ni(II)] = $1.0 \cdot 10^{-4}$ M, [NaOH] = 2 M, [$K_3(Fe(CN)_6$] = $6.0 \cdot 10^{-4}$ M; λ = 460 nm.

about 4 h. Beer's law is obeyed in the same nickel concentration range as in the absence of iron.

The effects of other ions, in the presence of iron, were then studied. Table 1 shows that Al, P, W, V, Si and Mo do not interfere in the mole ratio 10:1 (element:nickel); Cr(III) and Cr(VI) may be present in a mole ratio not higher than 2:1. In the presence of Mn, Cu, or Co, an excess of nioxime is necessary because these ions consume the reagent; 0.6:1, 0.6:1 and 0.2:1 mole ratios for Mn, Cu and Co, respectively, are tolerable. With Ti small positive errors are obtained, probably because of titanium hydroxide precipitation.

One of us (C. G. P.) is indebted to the "Fundación Juan March" for a Fellowship.

TABLE 1

Study of interferences on the determination of nickel (5.15 μmol) in the presence of iron (0.15 mmol) and tartaric acid (3.3 mmol) (Volume = 50 ml; [Nioxime] = 0.04 mmol; $[K_3(Fe(CN)_6)]$ = 0.03 mmol

Concentration mmol/50 ml								
Al	P, W, V, Mo or Si	Cr(III)	Cr(VI)	Mn	Cu	Co	Ti	Ni(II) Found (μmol)
0.05								5.25
	0.05							5.15
		0.05						5.65
		0.03						5.32
		0.01						5.27
			0.05					5.40
			0.03					5.32
			0.01					5.27
				0.05				5.80
				0.05[a]				5.95
				0.03[a]				5.62
				0.01[a]				5.42
				0.003[a]				5.10
					0.05			5.62
					0.05[a]			5.40
					0.003[a]			5.15
						0.05		0.03
						0.05[a]		7.00
						0.03[a]		6.35
						0.003[a]		5.30
						0.001[a]		5.20
							0.05	5.30

[a][nioxime] = 0.15 mmol/50 ml.

REFERENCES

1 See, e.g. E. B. Sandell, Colorimetric Determination of Traces of Metals, 3rd edn., Interscience, New York, 1959.
2 F. Feigl, Ber. Deut. Chem. Ges., 57B (1924) 758.
3 D. G. Davis and E. A. Boudreaux, J. Electroanal. Chem., 8 (1964) 434.
4 W. C. Johnson and M. Simmons, Analyst (London), 71 (1946) 554.
5 R. C. Ferguson and C. V. Banks, Anal. Chem., 23 (1951) 448.
6 E. A. Johnson and E. J. Newman, Analyst (London), 81 (1956) 318.
7 M. Karvanek, Prum. Potravin, 15 (1964) 282; Sb. Vys. Sk. Chem. Technol. Praze, Ekon. Rizeni Chem. Prum., 23 (1969) 13.
8 C. C. Hach, C. V. Banks and H. Diehl. Organic Syntheses, Vol. 4, J. Wiley, New York, 1963, p. 229.

Analytica Chimica Acta, 87 (1976) 239—242

Short Communication

PHOTOMETRIC DETERMINATION OF TOTAL LANTHANIDES AFTER EXTRACTION SEPARATION

J. MUSIL

Metalworks, Mníšek pod Brdy (Czechoslovakia)

J. DOLEŽAL

Department of Analytical Chemistry, Charles University, Prague (Czechoslovakia)

(Received 28th April 1976)

A basic characteristic of the lanthanide group is the chemical similarity of the individual members. Consequently, data on the total lanthanide content often suffices in practical problems, particularly when all the lanthanides behave similarly, e.g. in the production of alloy steels, or when the ratio of the individual members is constant (e.g. in geochemistry).

Photometric determination of the sum of the lanthanides requires a reagent (e.g. arsenazo-III) with equal sensitivity for the individual members [1—3]. As with other reagents for individual lanthanides arsenazo-III also generally requires prior separation of lanthanides from the matrix. Co-precipitation with oxalates or fluorides is tedious; rare earth elements can be extracted as complexes with salicyclic acid at pH 5 into a number of organic solvents [4, 5]. This separation is affected by large amounts of iron which must be removed, e.g. by extraction as the chloro complex, before this method can be used analytically.

Experimental

Samples and solutions. All chemicals were of p.a. quality. Arsenazo-III (Lachema, Prague) was used as received.

For the standard solutions of La, Ce and Pr, dissolve La_2O_3, CeO_2 and Pr_6O_{11} in 12 M HCl, and standardize the solutions complexometrically. Prepare the oxides of praseodymium or lanthanum by igniting the chlorides at 900 or 1000 °C, respectively; prepare CeO_2 by ignition of ammonium hexanitratocerate at 550 °C. Prepare a complete lanthanide solution from the mixed metals.

Before use, saturate the methyl isobutyl ketone (MIBK) with hydrogen chloride by shaking for 2 min with (1 + 1) HCl. Prepare 1 M salicylate buffer by dissolving 70 g of salicyclic acid in 480 ml of 1 M NaOH, and adjust to pH 5.0 with 2 M NaOH.

Norwegian silicates with certified individual rare earth element contents (determined by neutron activation analysis and mass spectrometry) and samples of non-alloy steel containing lanthanides, were used.

(a) Alloy steels with low concentrations of alloying elements. (lanthanide contents of 0.002—0.05 %): Dissolve the sample (0.2 g) in 10 ml of 12 M HCl with the addition of 1 ml of 15 % H_2O_2. Evaporate the solution to dryness and dissolve the residue in 5 ml of HCl (1 + 1); add 0.5 ml of H_2O_2 and boil the mixture for about 1 min. After cooling, add 10 ml of 12 M HCl, transfer the solution to a separatory funnel, and dilute with 5 ml of water. Extract iron with 20 ml of MIBK by shaking for 2 min, wash the extract with 2 ml of HCl (1 + 1), evaporate the combined aqueous phases to dryness on a water bath and dissolve the residue in 1 ml of HCl (1 + 1). Add ca. 0.2 g of ascorbic acid and 10 ml of salicylate buffer, followed by NH_4OH (1 + 1) dropwise to redissolve the precipitated salicylic acid; add a further 10 ml of the same buffer. Dilute the solution in the separatory funnel to 30 ml and extract with 20 ml of MIBK for 2 min. Back-extract the lanthanides with two 10-ml portions of 0.01 M HCl for 1 min, transfer the combined back-extracts to a 50-ml volumetric flask, and add gradually 2 ml of aqueous 2.5 % ascorbic acid, 3 ml of aqueous 5 % thiourea, 5 ml of aqueous 1 % sulphosalicylic acid and 5.0 ml of 0.04 % arsenazo-III solution. Dilute the mixture to the mark with 0.01 M HCl and measure the absorption at 655 nm with reference to a blank solution.

(b) Silicates soluble in acids (10^{-2} % lanthanides). Evaporate the sample (0.1 g) to dryness in a platinum dish with acid (10 ml of HF + 2 ml of H_2SO_4, 1 + 1). Remove fluorides carefully with two further evaporations with 4 ml of H_2SO_4 (1 + 1). Dissolve the final residue in 5 ml of HCl (1 + 1), transfer into a beaker, and follow procedure (a).

(c) Analysis of slate. Follow procedure (b), except that the residue after the second evaporation is fused with $K_2S_2O_7$. Dissolve the melt in 5 ml of HCl (1 + 1) and follow procedure (a).

Results and discussion

The dependence of the absorbance on the pH was studied with pure solutions. The application of the arsenazo-III—lanthanide system [6] was broadened by the addition of masking agents, sulphosalicylic acid (masking aluminium), thiourea (masking traces of Cu, Ni and Co) and ascorbic acid which masked traces of Fe and ensured the trivalency of lanthanides. The effect of pH in the presence of these materials is shown in Fig. 1. At pH 2, the masking ability decreases; measurements were therefore carried out at pH 1.9 (readily adjusted by the addition of 0.01 M HCl solution). The resulting pH of the photometric solutions (followed potentiometrically) was 1.95 ± 0.03 (without correction).

The salicylate extraction from 1 M salicylate buffer at pH 5.0 was studied at a phase volume ratio of H_2O:MIBK = 3:2. On shaking in a separatory funnel, equilibrium is attained after 1.5 min; the total extraction was 99.5 %. The results are valid for the individually studied lanthanides, for artificial mixtures, and for a complete lanthanide mixture. Trivalency, which is important for the extraction of Ce and Pr, can be established by preliminary

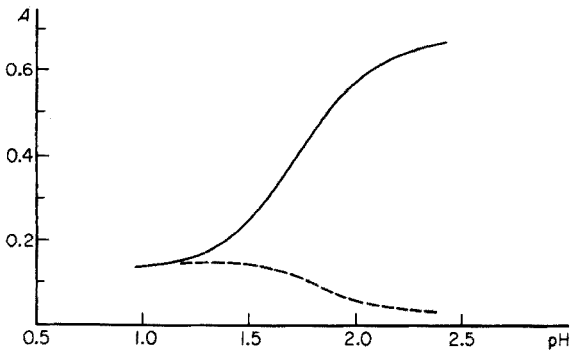

Fig. 1. Dependence of the absorbance of 0.05 mg of lanthanides on pH: —— blank: –––– (for conditions, see text).

reduction with boiling peroxide. The back-extraction of the lanthanides with 0.01 M HCl was studied similarly. This operation is also essentially quantitative under the conditions given above.

The analysis of artificial mixtures showed that the extraction of iron as the chloro complex does not involve the loss of lanthanides.

The calibration curve is linear up to a concentration of 1.6 $\mu g\ ml^{-1}$ of lanthanides. The improved linearity (cf. ref. 1) may arise from the presence of the additional reagents which stabilize the dissociation equilibria in the solution. The complete procedure and the colorimetric procedure alone gave individual points lying on the same straight calibration plot; this shows that, for construction of the calibration curve, the colorimetric process is sufficient and the extraction separation can be omitted. For calibration it is desirable to use mixtures of lanthanides that approximate in content to the individual elements in the test material, but deviations from this ideal do not lead to substantial errors, as the molar absorptivities of the individual lanthanides and of lanthanum are practically identical. The absorbance of the solution is constant in daylight for 100 min.

Interferences. Determination of the sum of the lanthanides is not affected by the presence of an equal amount of Mo, a 5-fold excess of Cr and Ni, or a 2-fold excess of Mn; the separation performed is adequate to eliminate interference from the other elements found in low concentrations in normal and alloy steels. With high Cr and Ni contents, the separation is not complete; consequently the method is not suitable for steels with high concentrations of alloying elements. Yttrium reacts identically to the lanthanides throughout the entire procedure and interferes.

Accuracy and precision. The accuracy of the results was verified with artificial mixtures, by the standard addition method, and with silicate reference standards. With steels, the ratio of cerium to total lanthanides was also used to test the accuracy of the procedure. The cerium content was determined photometrically with *o*-tolidine [7]. A constant value was

obtained for this ratio, indicating that the results are not subject to a systematic error (Table 1). The relative standard deviation was 7.5 % for a lanthanide content of 0.01 %.

TABLE 1

Results

Exp.	Sample	Content (%)		Found[b] (%)
		Ln	Ce	Ln
(1)	0.2 g spectral Fe	0	—	0
(2)	as (1) + 0.05 mg (La + Pr)	0.025	—	0.026
(3)	as (1) + 0.05 mg Ce	0.050	—	0.051
(4)	Steel A	—	0.023	0.030
(5)	Steel A + 0.10 mg CLM[a]	—	—	0.081
(6)	Steel B	—	0.051	0.065
(7)	Larvikite (silicate ASK-1) [8]	0.060	—	0.059
(8)	Slate (ASK-2) [8]	0.019	—	0.019

[a]CLM = complete lanthanide mixture. [b]Calibration with a Ce + La + Pr mixture (6 + 3 + 1).

REFERENCES

1 S. B. Savvin, Talanta, 8 (1961) 673,
2 P. K. Spitsyn and V. S. Schvarev, Zh. Anal. Khim., 26 (1971) 1313.
3 H. Onishi and C. V. Banks, Talanta, 10 (1963) 399.
4 N. S. Poluektov, Tr. Kom. Anal. Khim. Akad. Nauk. SSSR, 14 (1963) 154.
5 B. N. Sudanikov, V. A. Zaitsev and J. G. Pucchov, Nauchn. Dokl. Vyssh. Shk. Khim. Khim. Tekhnol., (1959) No. 1, 80.
6 V. G. Gorjushina, S. B. Savvin and E. V. Romanova, Zh. Anal. Khim, 18 (1963) 1340.
7 D. Blazejak-Diteges, Z. Anal. Chem., 251 (1970) 11.
8 Reported Concentration Values for Minor and Trace Elements ASK-1, ASK-2 and ASK-3, Analytisk sporelement kosmite Norden, Oslo 1975.

Analytica Chimica Acta, 87 (1976) 243—246

Short Communication

SEPARATION AND SPECTROPHOTOMETRIC DETERMINATION OF AZIDE

E. A. NEVES, E. DE OLIVEIRA and L. SANT'AGOSTINO

Instituto de Química da Universidade de São Paulo, Cidade Universitária, c. post. 20780, São Paulo (Brazil)

(Received 4th March 1976)

Azide ions form complexes with several metal cations and this has been used for the colorimetric determination of several cations in aqueous medium [1—7]. Conversely, azide can be determined with iron(III) reagents [8—11]. Azide can be determined colorimetrically with carbon disulphide [12], but this procedure is kinetic dependent, and this class of product is unstable [13].

The present communication reports an azide determination with copper(II) ions, in which CuN_3^+ is formed quantitatively. Although the sensitivity is not markedly better than that of the iron(III) method, the proposed method is based on superior spectral characteristics since at the λ_{max} (375 nm) there is no reagent absorption; moreover, the pH conditions are less critical. A separation method is described for the recovery of azide as the volatile hydrazoic acid. This separation procedure should make it possible to determine azide by various electrometric methods.

Experimental

Apparatus and reagents. A Beckman DU spectrophotometer and 10-mm silica cells were used. A.R. or C.P. reagents were used. Sodium azide (Merck) was purified by dissolving in water, filtering and precipitating with ethanol. Standard solutions were prepared from the anhydrous salt; working solutions were prepared as needed by dilution.

The distillation apparatus consisted of a large test tube (5-cm diam., 20-cm high) with a sidearm packed with glass wool to prevent carryover of spray. A rubber stopper carried the nitrogen inlet tube drawn out to a fine tip to provide regular bubbles, and a separating funnel for the introduction of hydrogen sulphate solution. From the sidearm, a right-angled tube with a medium pore filter at the tip led to the absorber, which was a 10-ml conical flask with a sidearm at the base fitted with two small bulbs angled upwards.

Procedures. In the absence of interfering ions, pipette 1.0 ml of acetate buffer solution (1 M sodium acetate—0.1 M acetic acid) into a 10-ml volumetric flask, add an aliquot (up to 3 ml) of the aqueous test solution, mix, add 5 ml of 0.92 M copper nitrate solution (containing 10^{-3} M HNO_3) and

dilute to the mark with water. Measure at 375 nm against a copper—acetate buffer blank. Prepare a calibration graph similarly.

In the presence of interfering ions, use the distillation apparatus. Mix a volume of the test solution with 2.0 ml of standard 1.00 M sodium hydroxide in the distillation tube, add 10 drops of the 30 % hydrogen peroxide, stir, wait for at least 3 min and then add 3 ml of freshly prepared alkaline tin(II) solution. (1.6 % (w/v) $SnCl_2$ solution in 0.2 M HCl treated with 1 M NaOH until the tin(II) hydroxide precipitate dissolves.) Place 5 ml of saturated potassium hydrogensulphate in the funnel and 5.00 ml of 0.300 M sodium hydroxide in the absorber, and connect up the apparatus. Transfer the contents of the funnel to the tube, and pass nitrogen for 20 min (about 2 bubbles/s). Add 5.00 ml of 0.330 M acetic acid to the absorption solution, mix and add 5.00 ml of 1.38 M copper nitrate containing 10^{-3} M HNO_3. Measure the absorbance at 375 nm and calculate the azide content from a calibration plot established in the same way.

Results and discussion

Effect of reaction conditions. When a fixed azide concentration ($2 \cdot 10^{-4}$ M) was treated with increasing concentrations of copper(II), the absorbance at 375 nm became constant with copper(II) concentrations above 0.1 M. A concentration of 0.46 M was used in the final method to ensure reproducibility. Under these conditions Beer's law was followed; but the addition of sodium acetate (0.01 M) improved the sensitivity. Probably some azide remained as undissociated hydrazoic acid in the absence of sodium acetate; more than 0.1 M acetate decreased the absorbance, probably because of anion competition. After the separation of azide by distillation into an alkaline absorbent, acetic acid was used for neutralization; a high acetate ion concentration resulted from this procedure. In tests on $2 \cdot 10^{-4}$ M azide in the presence of 0.1 M sodium acetate, free acetic acid in the range $5 \cdot 10^{-2}$—2.10^{-3} M did not affect the absorbance, and Beer's law was still obeyed. Neither copper(II) nor acetate buffer concentration were critical parameters for the direct determination of azide in absence of interfering agents but free acetic acid decreased the sensitivity somewhat at the 10^{-2} M level. Under the recommended conditions, the molar absorptivity was about 1600 l mol^{-1} cm^{-1}.

Separation of azide. Azide was volatilized from acidic solution as hydrazoic acid, which was transferred with a flow of nitrogen and recovered in a sodium hydroxide solution. For displacement of azide, a saturated potassium hydrogensulphate solution gave the best results. The bubbling rate of nitrogen was not critical. To check the efficiency of the transference, two concentrations of sodium hydroxide absorption solution were tested with and without cooling; the results are shown in Table 1. Comparison with direct measurements showed that 99.4 % of azide was recovered in 0.300 M sodium hydroxide at room temperature, after a bubbling time of 20 min. The use of an ice bath was unnecessary.

For the separation method, a Ringbom plot indicated an optimal range of

TABLE 1

Effect of bubbling time on the recovery of 5.00 ml of sodium azide ($5.0 \cdot 10^{-4}$ M) in two different hydroxide concentrations, with and without cooling

[NaOH] = 0.10 M[a]		[NaOH] = 0.30 M[a]		[NaOH] = 0.30 M	
Time (min)	% Recovery	Time (min)	% Recovery	Time (min)	% Recovery
5	79.0	5	78.4	5	79.2
10	86.0	10	81.8	10	85.0
15	97.5	15	93.2	15	97.8
20	99.2	20	95.2	20	99.4
30	98.0	30	99.6	30	98.8
40	75.4	40	98.8	40	96.8
60	46.0	60	86.8	60	90.0

[a] Absorption vessel immersed in an ice bath.

0.085—0.55 mM or 3.6—23 μg ml^{-1} for azide. At 90 % transmittance, the limiting azide concentration was 0.029 mM or 1.2 μg ml^{-1}. The precision of the method was tested by 20 measurements of two azide concentrations; for 4.00 μg ml^{-1} and 21 μg ml^{-1}, the absorbances were 0.151 and 0.795, respectively, with standard deviations of 0.0016 in both cases.

Effect of diverse ions. Anions like CN^-, SO_3^{2-}, $S_2O_3^{2-}$, $S_4O_6^{2-}$, S^{2-}, I^-, Cl^-, Br^-, SCN^-, interfere in the direct procedure by reacting with copper(II) to form complexes or precipitates. Nitrite oxidizes azide to nitrogen in acidic medium, as do several other oxidants, e.g. MnO_4^-, $Cr_2O_7^{2-}$, IO_3^- or ClO_3^-. Some anions like chloride interfere only in concentrations higher than 0.1 M.

The separation of azide, as described above, eliminates many potentially interfering ions, except for oxidants and those anions which are carried over, with hydrazoic acid, e.g. cyanide and some sulphur anions.

Many cations interfere in the direct reaction of azide with copper(II) by competition and formation of precipitates, or weak or strong complexes. In fact, azide must often be determined in strong inert complexes, e.g. of platinum(IV), or in sparingly soluble salts, e.g. $Pb(N_3)_2$. In such cases, HN_3 evolution may be retarded.

The effects of interfering ions were examined at two azide concentrations (4 and 21 μg ml^{-1}); 500 times these concentrations of interfering agents was added in each experiment, and the azide was separated and determined as described. Oxidizing agents such as NO_2^-, MnO_4^- and CrO_4^{2-} ($Cr_2O_7^{2-}$) virtually destroyed the azide ions. The anions CN^-, SO_3^{2-}, $S_2O_3^{2-}$, $S_4O_6^{2-}$, S^{2-} and I^- caused negative errors of 0.5—2 %, when the azide concentration was 21 μg ml^{-1}, and negative errors up to 10 % for 4 μg ml^{-1} azide. The cations Ni^{2+}, Co^{2+}, Cd^{2+}, Mn^{2+}, Cu^{2+}, Zn^{2+}, Cr^{3+}, Fe^{3+}, NH_4^+, Al^{3+} (added as nitrates) did not interfere in the azide separation and determination; mercury(I) and the chloro complexes of Pt(IV) and Pd(II) caused 4 % low results for azide at 4 μg ml^{-1} but the error was negligible at 21 μg ml^{-1}.

All the above-mentioned interferences were eliminated by previous treatment of the test solution with alkaline hydrogen peroxide and subsequent elimination of the excess with $Sn(OH)_3^-$. Azide ions show exceptionally high resistance to oxidizing agents in alkaline media; even permanganate has no effect. Under such conditions CN^-, SCN^-, NO_2^- and all the sulphur anions mentioned are oxidized. Platinum, gold, palladium and silver ions are reduced to the metals by alkaline hydrogen peroxide. When a strong acid is added to displace the hydrazoic acid, oxidants in the test solution and those formed by interaction with hydrogen peroxide in alkaline medium e.g. IO_3^-, $MnO(OH)_2$, CrO_4^{2-}, $Co(OH)_3$, can destroy hydrazoic acid. The addition of excess of tin(II) to the alkaline solution eliminates the excess of hydrogen peroxide. When the solution is acidified, tin(II) reacts preferentially with any remaining oxidants. The treatment with alkaline hydrogen peroxide did not affect the azide concentration. Checks on the determination of 4 μg ml^{-1} azide in the presence of 500-fold amounts of strong interferences such as NO_2^-, MnO_4^- and CrO_4^{2-}, showed that recovery of azide was complete.

This work was supported by the FAPESP and CNPq Foundations, to whom the authors are greatly indebted.

REFERENCES

1 F. G. Sherif and A. M. Awad, Anal. Chim. Acta, 26 (1962) 235; J. Inorg. Nucl. Chem., 24 (1962) 179.
2 B. K. S. Nair, L. H. Prabhu and D. G. Vartak, J. Sci. Ind. Res., 203 (1961) 487.
3 P. Senise and O. E. S. Godinho, J. Inorg. Nucl. Chem., 23 (1970) 3641.
4 P. Senise, J. Am. Chem. Soc., 81 (1959) 4196.
5 P. Senise and E. A. Neves, J. Inorg. Nucl. Chem., 34 (1972) 1923; 33 (1971) 351.
6 H. K. El-Shamy and M. F. Nassar, J. Inorg. Nucl. Chem., 16 (1960) 124.
7 G. Saini and G. Ostacoli, J. Inorg. Nucl. Chem., 8 (1958) 346.
8 C. E. Robertson and C. M. Austin, Anal. Chem., 29 (1957) 854.
9 Y. Mizushima and T. Sekine, Rep. Gov. Chem. Ind. Res. Inst. Tokyo, 50 (1955) 255.
10 R. M. Wallace and E. K. Dukes, J. Phys. Chem., 65 (1961) 2094; Anal. Chem., 33 (1961) 242.
11 A. Anton, J. G. Dodd and A. E. Harvey Jr., Anal. Chem., 32 (1960) 1209.
12 G. S. Johar, Talanta, 19 (1972) 1461.
13 E. A. Neves and D. W. Franco, J. Inorg. Nucl. Chem., 36 (1974) 3851.

Analytica Chimica Acta, 87 (1976) 247—250

Short Communication

THE SPECTROPHOTOMETRIC DETERMINATION OF SULFATE, CHLORIDE AND FLUORIDE IN PLANT MATERIALS

W. LIKUSSAR, H. RABER, H. HUBER and D. GRILL

Institute für Pharmazeutische Chemie, Anorganische und Analytische Chemie sowie für Anatomie und Physiologie der Pflanzen, Universität Graz, A-8010 Graz (Österreich)

(Received 13th May 1976)

In environmental control, comprehensive knowledge of SO_2 and/or SO_3 incorporation by plants in areas of industrial smog is of great importance [1]. This is also true for fluorides, usually hydrogen fluoride, the main component of fumes emitted from aluminium smelting plants. A further important air pollutant of anthropic origin is chloride, usually as hydrogen chloride. Even damage to plants by common salt may be important. Since flora in overcrowded industrial regions is often affected simultaneously by these three pollutants, the determination of sulfate, chloride and fluoride is of importance; the extent of damage to biological materials for compensation claims is usually estimated on the results of chemical analyses. The procedures used should therefore be simple, rapid and suitable for serial analyses.

The methods proposed so far tend to be costly and time-consuming, particularly in the mineralization of plant materials [2—5]. To avoid these difficulties, the Schöniger combustion [6] has been applied in determination of sulfate [7], chloride [8, 9] or fluoride [10—12]. The combination of the Schöniger combustion and elimination of interfering cations by adding an ion-exchange resin directly to the solutions has given satisfactory results [7, 9, 12].

This communication describes a technique for the simultaneous determination of sulfate, chloride and fluoride. The spectrophotometric methods for sulfate and chloride by Bertolacini et al. [13] and for fluoride by Quentin et al. [14], were modified, improved and adapted to this problem.

Experimental

Fluoride reagent solution. Pulverize 103 mg of lanthanum nitrate hexahydrate (Merck 5326) and 100 mg of alizarin-3-methylamino-*N,N*-diacetic acid dihydrate (Merck 1010) in a mortar and mix with 10 ml of buffer solution (18.9 g of acetic acid (100 %) and 25.2 g of sodium acetate trihydrate in 1 l of water). Transfer this solution to a 1 -l volumetric flask, add an additional 90 ml of buffer solution and 500 ml acetone (Merck 14) and dilute to the mark with water.

Apparatus. Schöniger combustion flasks (1 l) with platinum gauzes or

clamps were used. A Zeiss PMQ 3 spectrophotometer was used with 1.000 and 5.000-cm silica cells.

Recommended general procedure. Pipet 20.0 ml of hydrogen peroxide solution (3 %) into a dry Schöniger flask. For the combustion, wrap homogenized plant material dried at 105 °C, up to a weight of 100 mg, into an eighth part of a filter paper (Macherey-Nagel MN 640 d, ash-free, 12.5-cm diam.). Fill the flask with pure oxygen and burn the sample. After the absorption of the resulting gases (30 min) add about 0.2 g of swollen cation-exchange resin (Dowex 50W-X8, 20-50 mesh, Na^+-form) superficially dried previously between filter paper. Shake the flask for about 2 min.

Procedure for the determination of sulfate. Transfer 10.0 ml (or a smaller aliquot) of the absorption solution containing 25—300 μg of sulfate to a 50-ml volumetric flask. Add 5 ml of aqueous 0.05 M potassium hydrogenphthalate solution and 25 ml of ethanol. After the addition of about 0.1 g of barium chloranilate (Merck 2363), dilute to the mark with distilled water, and stir with a magnetic stirrer for about 25 min. Filter the solution through dry dense paper filter into a 1.000-cm silica cell after discarding the first portion. Measure the absorbance of the clear solution at 332 nm against a reagent blank. Calculate the SO_3 content from a calibration graph prepared with standard sulfate solutions. The molar absorptivity (ϵ) is $1.82 \cdot 10^4$ l mol^{-1} cm^{-1}.

Procedure for the determination of chloride. Transfer 10.0 ml (or a smaller aliquot) of the absorption solution containing 50—1000 μg of chloride to a 50-ml volumetric flask. Add 5 ml of 0.5 M nitric acid and 25 ml of methyl Cellosolve (ethylene glycol monomethyl ether). After the addition of about 0.1 g of mercury(II) chloranilate (Merck 2364) dilute to the mark with distilled water and stir magnetically for about 25 min. Filter through dry dense filter paper into a 1.000-cm silica cell after discarding the first portion. Measure the absorbance at 332 nm as described for sulfate. The molar absorptivity is $2.13 \cdot 10^3$ l mol^{-1} cm^{-1}.

Procedure for the determination of fluoride. Transfer 10.0 ml (or a smaller aliquot) of the absorption solution containing 0.5—5 μg of fluoride to a 50-ml volumetric flask. Add 25 ml of the fluoride reagent solution, dilute to the mark with distilled water, and leave for 15 min. Then measure the absorbance in a 5.000-cm cell at 620 nm vs. a reagent blank. Calculate the fluoride content of the sample from a calibration graph prepared with standard sodium fluoride solution. The molar absorptivity is $1.29 \cdot 10^4$ l mol^{-1} cm^{-1}.

Results and discussion

Statistical data for the determinations of sulfate, chloride and fluoride in simple test solutions were reported earlier [7, 9, 12] as well as the removal of interfering cations.

To investigate the mutual influences of the three anions in the three determinations, test solutions containing a definite amount of the anion to be determined and a large excess of the two other anions were analyzed.

The results in Table 1 show that the relative errors can be tolerated, inasmuch as the amounts added are related only to extreme compositions of plant materials. The relative errors are negligible when the concentrations of the test solution are in the range usually found in spruce needles (Table 1, sample 1). The relative standard deviations ranged from 1.4 to 7.8 % with five determinations in each case.

The validity of the proposed method was then tested for matrices corresponding to plant materials. To simulate such conditions, concentrated standard solutions of the three anions were added directly to a plant sample (spruce needles of known composition) from a 100-μl Hamilton pipet. The effect of interfering ions, the mutual influence of the three anions, and possible losses during the combustion were thus checked. The results are listed in Table 2. The recoveries are satisfactory and in good agreement with results obtained from pure test solutions. The relative standard deviation was slightly increased and ranged from 3.4 to 8.6 % (five determinations).

The method is suitable for minimum contents of 500 p.p.m. of sulfate, 1000 p.p.m. of chloride and 10 p.p.m. of fluoride at a weight of dry sample of 100 mg.

TABLE 1

Mutual influences in the determination of sulfate, chloride and fluoride

Sample	Sulfate (calc. as SO_3)			Chloride			Fluoride		
	Giv. (μg ml^{-1})	Fnd. (μg ml^{-1})	Rel. err. (%)	Giv. (μg ml^{-1})	Fnd. (μg ml^{-1})	Rel. err. (%)	Giv. (μg ml^{-1})	Fnd. (μg ml^{-1})	Rel. err. (%)
1	4.0	4.06	+ 1.5	4.00	3.96	− 1.0	0.0400	0.0402	+0.5
2	1.0	1.17	+17.0	20	—		5	—	
3	4.0	4.38	+ 9.5	20	—		5	—	
4	6.0	6.44	+ 7.3	20	—		5	—	
5	50	—		1.00	0.872	−12.8	5	—	
6	50	—		10.0	9.34	− 6.6	5	—	
7	50	—		20.0	18.6	− 7.0	5	—	
8	50	—		50	—		0.0200	0.0192	−4.0
9	50	—		50	—		0.0400	0.0412	+3.0
10	50	—		50	—		0.1000	0.1076	+7.6

TABLE 2

Recovery of sulfate, chloride and fluoride from spruce needles

Sample	Sulfate			Chloride			Fluoride		
	Added (p.p.m.)	Found	Rec. (%)	Added (p.p.m.)	Found	Rec. (%)	Added (p.p.m.)	Found	Rec. (%)
1	0	2530	—	0	940	—	0	56.0	—
2	2000	4610	101.8	0	931	99.0	0	55.8	99.6
3	0	2550	100.8	1000	1930	99.5	0	56.0	100.0
4	0	2510	99.2	0	925	98.4	50.0	105.3	99.3
5	2000	4480	98.9	1000	1890	97.4	50.0	104.6	98.7

REFERENCES

1 K. Garber, Luftverunreinigungen und ihre Wirkungen, Geb. Borntraeger-Verlag, Berlin, 1967.
2 A. Seuthe, Glüeckauf, 75 (1939) 409, 909.
3 H. Jäger and L. Steubing, Angew. Bot., 44 (1970) 209.
4 W. Oelschläger and M. Kirchgessner, Landwirtsch. Forsch., 13 (1960) 64.
5 W. Oelschläger and W. Wöhlbier, Forschungsber. Dt. Forschungsgemeinschaft, 14 (1968) 6.
6 W. Schöniger, Mikrochim. Acta, (1955) 123.
7 H. Raber, W. Likussar and D. Grill, Toxicol. Environ. Chem. Rev., in print.
8 S. E. Allen, Chemical Analyses of Ecological Materials, Blackwell, Oxford, 1974.
9 W. Likussar, H. Huber, H. Raber and D. Grill, Mikrochim, Acta, in print.
10 D. A. Levaggi, W. Oyung and M. Feldstein, J. Air. Poll. Contr. Ass., 21 (1971) 277.
11 W. Kronberger and G. Halbwachs, IX. Intern. Arbeitstg. fortsl. Rauchschadenssachverst., Marianske Lazne CSSR, 1974.
12 H. Raber, H. Huber, W. Likussar and D. Grill, Angew. Botanik, in print.
13 R. J. Bertolacini and J. E. Barney II, Anal. Chem., 29 (1957) 281.
14 K. E. Quentin and A. Rosopulo, Z. Anal. Chem., 241 (1968) 241.

Analytica Chimica Acta, 87 (1976) 251—253

Short Communication

THE PREPARATION OF FORMAZIN STANDARDS FOR NEPHELOMETRY

E. W. RICE

Pathology Department, Allentown Hospital Association, Allentown, PA 18102 (U.S.A.)

(Received 26th April 1976)

One of the persistent basic problems of nephelometry and turbidimetry concerns selection of reference and instrument calibration standards. Currently, the most widely adopted primary standard [1] consists of aqueous suspensions of "formazin", proposed in 1926 by Kingsbury et al. [2]. This substance, an insoluble condensation product of uncertain composition [3], is prepared by mixing solutions of hexamethylenetetramine and hydrazine sulfate. Turbidities of working standards carefully prepared from a stock suspension are reproducible to about ±1 %. The stock is stable for several months but more dilute working suspensions made by diluting the stock with water may be stable for less than a week, depending on their concentration and also on how often the settled formazin is resuspended. Preparations left undisturbed for long periods tend to be less stable than those which are mixed occasionally.

Directions for synthesizing a formazin stock suspension standard are as follows [1]: Prepare an aqueous 1.000 % (w/v) solution of hydrazine sulfate, and an aqueous 10.00 % (w/v) solution of hexamethylenetetramine, and clarify both solutions by filtering through a 0.45-μm membrane filter; mix exactly equal volumes of the two solutions, stopper the container and allow to stand undisturbed at room temperature (25 ± 3 °C) for 24 h. During this interim the colorless solution becomes turbid and a stable amorphous white precipitate of formazin slowly appears. This stock suspension has an assigned value of 4000 formazin turbidity units (4000 FTU). Working suspensions are prepared by accurate dilution of this well-mixed stock standard with membrane-filtered distilled water.

These accepted instructions tacitly assume that weaker suspensions of formazin made by diluting the stock with water elicit the same output signal from a nephelometer as would identical suspensions prepared with a diluent consisting of the clear filtered supernatant fluid of a stock preparation.

This communication presents experimental data showing that FTU readings of working standard formazin suspensions prepared with water, in fact, average about 8 % higher than the theoretically correct FTU values of comparable standards diluted with supernatant stock solution.

Experimental

Apparatus. A Hach-Model 2424 Clinical Nephelometer (Hach Chemical Company, Ames, Iowa) with an inserted "0—100 %" meter card, readable to ±0.5 % of the full scale was employed. The nephelometer was operated on "sensitivity 100" without a light filter and in conjunction with acid-washed 13 × 100 mm disposable glass culture tube-cuvettes.

Reagents and standards. Three stock standard formazin suspensions (4000 FTU) were prepared as described above and working standard suspensions with calculated values of 160, 100, 80, 40, and 10 FTU were accurately made from each stock by diluting with water, membrane-filtered stock fluid, and 5.00 % (w/v) hexamethylenetetramine in 0.2 % (v/v) sulfuric acid solution, respectively (see Table 1). (Thus, a total of 45 standards were prepared.) Additional standards stronger than 160 FTU were not evaluated.

Procedures. The nephelometer was set at 0 % with filtered distilled water and the turbidity of each of the thoroughly mixed standards determined against one of the "stock fluid-diluted" 160 FTU standards adjusted to 100 %. The FTU values of the standards therefore equalled "% scale reading × 1.6".

Results and discussion

The very precise nephelometric linear responses of standard formazin suspensions reported in the literature were confirmed: no set of triplicates varied more than 1 % scale reading, irrespective of the diluent used. Table 1 summarizes the experimental data and shows that working formazin standard suspensions prepared by the generally prescribed manner of diluting a stock 4000 FTU preparation with water, average a + 8 % error compared with suspensions made properly with a diluent of stock fluid. It was established subsequently that acidified hexamethylenetetramine solution may be used alternatively as an equally accurate diluent. This particular solution was investigated as a diluent because it constituted the initial milieu of the combined reagents (minus hydrazine) and simulates the final stock formazin suspension fluid mixture of excess hexamethylenetetramine and sulfuric acid. It is more convenient to prepare than the filtered stock fluid.

TABLE 1

Experimental FTU values of formazin nephelometry standards

Diluent	FTU values[a]				
1 Stock fluid	160.0	100.5	80.5	40.0	10.0
2 Acidified hexamethylenetetramine	160.0	100.5	80.5	40.0	10.0
3 Water	169.0	109.0	88.0	44.0	10.5

[a]Each figure is mean of 3 preparations.

In addition, it became fortuitously evident that formazin suspensions made with either acidified hexamethylenetetramine solution or stock fluid are more stable than the conventional water-diluted preparations. Some of the latter aqueous formazin standard suspensions begin to aggregate as fine threads and clumps within a week. In contrast, all suspensions diluted with either acidified hexamethylenetetramine or stock fluid gave constant FTU values for at least a month after their preparation.

Recently, very stable aqueous suspensions of uniform polystyrene latex spheres have become commercially available as secondary nephelometry and turbidimetry standards. The exact nephelometric "FTU rating" of all such preparations depends on the wavelength of the light scattered. The stated FTU rating of latex standards should also contain the wavelength of light used in establishing the values. At present, this information is not supplied. For example, Table 2 shows the actual FTU equivalency of one latex "100 FTU standard" obtained when various Corning filters were used in the nephelometer. The large variances combine both the effects of wavelength plus errors incurred by the commercial latex standard having been calibrated against a formazin suspension prepared (presumably) with water instead of with stock fluid.

The universal efficacy of latex standards depends largely on their careful ultimate calibration against accurate formazin suspensions, prepared by the techniques mentioned here. Once the correct FTU ratings of latex suspensions are established, they can serve as useful and very stable secondary daily instrument calibration standards and they need to be verified only periodically against formazin suspensions.

TABLE 2

FTU Equivalence of a "100 FTU latex nephelometry standard" vs. color of light scattered (Corning filters were used)

	Red	Orange	Yellow	Green	Blue	Indigo	Violet	None
FTU rating[a]	106	120	126	130	139	142	143	123

[a]Compared with a valid 100 FTU formazin standard.

REFERENCES

1 Standard Methods for the Examination of Water and Wastewater, 13th edn., American Public Health Association, New York, 1971, pp. 350—356.
2 F. B. Kingsbury, C. P. Clark, C. Williams and A. L. Post, J. Lab. Clin. Med., 11 (1926) 981.
3 M. Mashima, Bull. Chem. Soc. Jpn., 39 (1966) 504.

Analytica Chimica Acta, 87 (1976) 255—257

Short Communication

COMPLEX FORMATION AND FLUORESCENCE PART V. THE WATER-SOLUBLE COMPLEX OF BERYLLIUM(II) AND 8-QUINOLINOL-5-SULFONATE

J. A. BISHOP

Department of Chemistry, Cedar Crest College, Allentown, PA 18104 (U.S.A.)

(Received 22nd January 1976)

The formation constants of most of the complexes of cations with 8-quinolinol-5-sulfonic acid have been determined [1—4], and the effect of changes in pH and oxidation state on fluorescent complexes have been studied [2, 5, 6]. Complexes with beryllium(II) have not been studied previously.

Experimental

Samples of 8-quinolinol-5-sulfonic acid (10^{-3}—10^{-4} M) in the absence and presence of Be(II) of about the same molarity were titrated with 0.1 M NaOH from a microburet. A Fisher Acumet expanded scale meter, model 320 was used to measure pH. Fluorescence measurements were made as the titration progressed on aliquots transferred to a cuvet with a dropper, the sample being replaced in the titration vessel after each measurement. Fluorescence was measured with either a Farrand spectrofluorimeter or a Turner fluorimeter model 110, at λ ex = 365 nm and λ em = 520 nm.

The 8-quinolinol-5-sulfonic acid solutions were adjusted to the pH of a $BeSO_4$ solution of the same molarity before making the solution up to 100 ml in a dry beaker. When the $BeSO_4$ solutions were added to the complexing agent solution before making up to 100 ml, the pH dropped slightly, indicating complex formation. In all cases the initial volume was 100 ml and the temperature was 24 ± 1 °C.

Solutions (ca. 10^{-2} M) were prepared from 8-quinolinol-5-sulphonic acid (Eastman Kodak Co.) and from $BeSO_4 \cdot 4H_2O$ (Fisher Chemical Co.). Working solutions were prepared from these by dilution.

Discussion

The curves shown in Fig. 1 are typical of the results obtained, regardless of the ratio of 8-quinolinol-5-sulfonate (L) to Be(II) used. At point A on curve I, the end-point of the titration of the mixture of HCl and H_2L is HL. Through complex formation this point shifts to point B on curve II when Be(II) is present. The increased volume of NaOH can be used to calculate the value of the formation complex [7] if the only reaction (omitting valences)

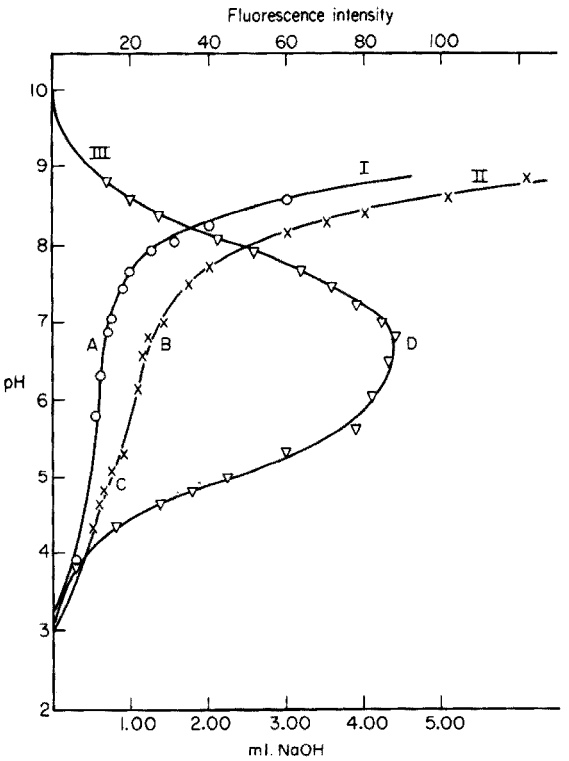

Fig. 1. Titration of HCl + H_2L and HCl + H_2L + Be(II) with NaOH; ○ pH vs. ml. of NaOH for HCl + H_2L. × pH vs. ml. of NaOH for HCl + H_2L + Be(II). ▽ pH vs. fluorescence for HCl + H_2L + Be(II).

is Be + HL ⇌ BeL + H (1). Simpson and Vallee have studied ZnL_n complexes by this method [8]. With Be(II), however, the cation is present as a mixture of hydroxy complexes, and at least one additional equilibrium is involved $2Be(OH) \rightleftharpoons Be_2(OH)_2$ (2), so that a direct calculation is difficult. Perkins has pointed out that Be(II) complexes hydrolyze at pH 7 and above [9].

The volume of NaOH corresponding to the distance between points A and B indicates that a 1:1 complex is formed. It was decided to calculate the value of the first formation constant (K_1) from the drop in pH (point A to point C) for the volume of NaOH required to reach the end-point of the titration of Curve I. Below pH 5 Be(II) is essentially in the Be^{2+} form (ignoring hydration) and reaction (1) is applicable, the equilibrium expression being

$$K = [BeL]\,[H]/[Be]\,[HL] = K_1K_{HL} \qquad (3)$$

where K_{HL} is the ionization constant of the acid HL. The increase in [H] shown by the pH drop is equal to [BeL], and [H] in eqn. (3) is [H] as determined by the pH of point C.

The average value of log K_1 for six determinations was 5.46 (s = 0.17). When the log K_1 values for MgL, CaL, SrL and BaL were plotted against r^3 a straight line was produced, and its projection to the r^3 value for beryllium gave a value of ca. 5.4 for log K_1. The values of r (the covalent radius) were taken from Sanderson [14]. For some other complexes, values of K_1 are in the order Be > Mg > Ca [11].

The fluorescence peak of Curve III in Fig. 1 rises slightly with increase in the L/Be ratio, but remains at the same pH. The decrease in fluorescence, as the solution becomes basic, probably results from the beryllium in the complex being titrated in a manner similar to the H in HL, with the formation of $BeOH^+$, $Be_2(OH)_2^{2+} \cdots Be_n(OH)_m$, etc; alternatively it may result from the formation of BeLOH, $Be_2L_2OH_2$, in which the two beryllium ions are linked by the two OH ions, and the beryllium is linked to L by Be—O—L bonds.

An attempt to use a mole ratio plot [2] at pH 7 was not successful, presumably because of hydrolysis.

REFERENCES

1 I. C. Sillen, A. E. Martell and E. Hogfeldt, Stability Constants, Supp. No. 1, Spec. Pub. No. 25, The Chemical Society, London, 1971.
2 J. A. Bishop, Anal. Chim. Acta, 53 (1971) 456; 63 (1973) 305.
3 P. Souchay and M. Cadiot-Smith, Compt Rend. Acad, Sci. Ser. C., 271 (1970) 173.
4 T. Fulle Soldi, C. Bertoglio Riolo and G. Spini, Ann. Chim. (Rome), 59 (1965) 1031; 60 (1970) 836.
5 D. E. Ryan and B. K. Pal, Anal. Chim. Acta, 44 (1969) 1031; 47 (1969) 35; 48 (1969) 227.
6 R. von Slageren, G. den Boef and W. E. van der Linden, Talanta 20 (1973) 739.
7 M. Calvin and K. W. Wilson, J. Am. Chem. Soc 67 (1945) 2003.
8 R. T. Simpson and B. I. Vallee, Inorg. Chem., 8 (1969) 1185.
9 D. G. Perkins, Biochem J., 51 (1950) 87; 55 (1953) 469.
10 R. T. Sanderson, Chemical Periodicity Reinhold Pub. Co. New York (1960) p. 26.
11 P. Lingaiah and E. V. Sundaram, J. Ind. Chem. Soc., 48 (1971) 961.

Analytica Chimica Acta, 87 (1976) 258

ERRATA

A. Colombo, Systematic Errors in Vacuum and Inert Gas Fusion Analysis for Oxygen in Metals, *Anal. Chim. Acta*, 81 (1976) 397—407.

On p. 400, line 7 : for alkaline earth metals, read alkali metals.
On p. 401, line 32 : delete under (a).
On p. 403, line 3, and in footnote (c) to Table 1 : for ref. [10], read ref. [11].

R. F. Sanzolone and T. T. Chao, Atomic Absorption Spectrometric Determination of Copper, Zinc, and Lead in Geological Materials, *Anal. Chim. Acta*, 86 (1976) 163—168.

On p. 164, the second sentence of *Apparatus and calibration* should read: The air pressure was 45 p.s.i. (meter reading 4.0) and the acetylene pressure 10 p.s.i. (meter reading of 1.2 for Cu and Zn, and 0.2 for Pb) in all cases.

Mercury Analysis Working Party of the Bureau International Technique du Chlore, Standardization of Methods for the Determination of Traces of Mercury Part II. Determination of Total Mercury in Materials Containing Organic Matter, *Anal. Chim. Acta*, 84 (1976) 231—257.

On page 255, under *Method 3*, Lab. No. 6 should read 7^{b}.

Quadrupole Mass Spectrometry and its Applications

edited by **PETER H. DAWSON,** National Research Council of Canada.

1976. xxii + 350 pages. US $49.75/Dfl. 129.00. ISBN 0-444-41345-6

This is the first comprehensive account of quadrupole mass spectrometry. While its many contributors provide a broader-than-usual viewpoint, it is, nevertheless, a systematic text. It begins with simple qualitative descriptions of the mass filter, the monopole, the quadrupole ion trap and related time-of-flight spectrometers. It proceeds to an exploration of their particular advantages, disadvantages and applications. Experimental design and performance is discussed in detail. The theoretical treatment includes computational design techniques such as the recently developed utilisation of phase-space dynamics. Although there have been countless routine applications of quadrupole mass spectrometry, there are an unusual number of individualized applications in both science and technology which require specially designed or modified instruments. This book will therefore be of interest and value to many users for whom a knowledge of quadrupole design, performance and limitations may be essential.

ELSEVIER SCIENTIFIC PUBLISHING COMPANY

P.O. Box 211, Amsterdam, The Netherlands

Distributor in the U.S.A. and Canada:
ELSEVIER/NORTH-HOLLAND, INC.,
52 Vanderbilt Ave., New York, N.Y. 10017

The Dutch guilder price is definitive. US $ prices are subject to exchange rate fluctuations.

(Continued from page 4 of cover)

Contents

Short Communications

PRINTED IN THE NETHERLANDS

CONTENTS

(continued on inside page of the cover)